ISOLATION, CHARACTERISTATION AND SCREENING OF NEW ZEALAND ALPINE ALGAE FOR THE PRODUCTION OF SECONDARY METABOLITES IN PHOTOBIOREACTORS

A thesis submitted in fulfilment of the requirements

for the Degree of

Doctor of Philosophy in Chemical and Process Engineering

University of Canterbury

By

KISHORE GOPALAKRISHNAN

Department of Chemical and Process Engineering,

University of Canterbury,

Christchurch, New Zealand

2015

DEDICATED TO MY BELOVED FATHER

MR GOPALAKRISHNAN SUBRAMANIAN.

ABSTRACT

This inter-disciplinary thesis is concerned with the production of polyunsaturated fatty acids (PUFAs) from newly isolated and identified alpine microalgae, and the optimization of the temperature, photon flux density (PFD), and carbon dioxide (CO_2) concentration for their mass production in an airlift photobioreactor (AL-PBR). Thirteen strains of microalgae were isolated from the alpine zone in Canyon Creek, Canterbury, New Zealand. Ten species were characterized by traditional means, including ultrastructure, and subjected to phylogenetic analysis to determine their relationships with other strains. Because alpine algae are exposed to extreme conditions, and such as those that favor the production of secondary metabolites, it was hypothesized that alpine strains could be a productive source of PUFAs. Fatty acid (FA) profiles were generated from seven of the characterized strains and three of the uncharacterized strains.

Some taxa from Canyon Creek were already identified from other alpine and polar zones, as well as non-alpine zones. The strains included relatives of species from deserts, one newly published taxon, and two probable new species that await formal naming. All ten distinct species identified were chlorophyte green algae, with three belonging to the class Trebouxiophyceae and seven to the class Chlorophyceae. Comparative study between the distribution of algae at Canyon Creek and Mount Philistine, another alpine region in New Zealand where algal distribution was studied in detail, revealed that algal distribution patterns in the New Zealand alpine zone are complex, with some taxa apparently widely distributed and others range restricted or rare (with the caveat that very few sites have been studied in detail). At least some of the differences between the two sites could be accounted for by geographic differences, resulting in contrasting environmental conditions such as rainfall.

As hypothesized, alpine strains isolated from the Canyon Creek were rich in PUFAs. Eight among the ten strains have PUFA proportions higher than monounsaturated fatty acids and saturated FAs. In a comparison of FA profiles of Scenedesmaceae species from a hot environment (Algerian Sahara) with the Scenedesmaceae species from Canyon Creek, the latter revealed a much greater degree of unsaturation. In addition, the Canyon Creek strains contained some FAs (such as docosapentaenoic acid, DPA) that were absent from Saharan strains. Among the strains from Canyon Creek *Lobochlamys segnis* LCR-CC-5-1A was selected for optimization experiments on the basis of growth kinetics, temperature response and FA composition, of which 60% of total FAs were PUFAs. Of that 60%, the α-linolenic acid (ALA) content was 46%.

Two identical 1.5 Liter AL-PBRs were used for culturing *Lobochlamys segnis* LCR-CC-5-1A to study the effect of CO_2 concentration, PFD and temperature on specific growth velocity, production of PUFAs, omega-3 FAs and, specifically, the concentration of ALA. The concentrations of CO_2 examined in this research were 1.5, 3.0 and 4.5% in air. Similarly, the reponses of the strain to seven different PFDs, namely 38, 77, 115, 178, 210, 236 and 253 μmol m^{-2} s^{-1} and six different temperatures, 5, 10, 15, 20, 25 and 30ºC, were analyzed. The maximum specific growth velocities (μmax) of the cultures were calculated from the experimental data and the cell production rate was calculated from fitting logistic growth models to these data; the two were compared by converting the former to the latter. The significance of the tested parameters was assessed using ANOVA and Tukey tests.

The optimum conditions assessed at lab scale for maximum production of biomass, PUFAs and ALA were found to be a CO_2 concentration of 3.0%, temperature of 20°C, and PFD of 178 μmol m^{-2} s^{-1}. Increasing biomass production has the effect of maximizing PUFA production because there was no significant increase in concentration of PUFAs, omega-3 FAs,

or ALA under levels of CO_2, temperature, and PFD differing from those under which maximum growth occurred.

Acknowledgements

I would like to express my sincere gratefulness to my supervisors Dr. Gabriel Visnovsky and Dr. Phil Novis for offering me an opportunity to work as a Ph.D student. Their constant guidance and encouragement has motivated and helped me to grow as a self-determining researcher. I am extremely thankful for their massive support throughout the period of study and predominantly while I was in a critical family situation.

I sincerely acknowledge the support for the fatty acid analysis done by Dr. Jason Ryan from Callaghan Innovation. Valuable ideas and suggestions were provided by Dr. Paul Broady from School of Biological Sciences. Also I am very grateful to Dr. Phil Novis and Vicki Novis for the steps taken to improve my academic writing. I also thank Vaughan Myers for his support in Transmitting electron microscopic work, Nic Bolstridge (Landcare Research) for her lab assistance and Mike Flaws (Department of Mechanical Engineering, University of Canterbury) for his support in Scanning electron microscopic work

I would like to acknowledge the University of Canterbury (UC) for providing me with a UC Doctoral Scholarship and I wish to thank Chemical and Process Engineering technical staff, post-graduate students and administrators for their support and cooperation. Also I wish to acknowledge my friends Dr. Balaji Somasundaram, Dr. Swaminathan Detchanamurthy, Dr Kannan Subramanian, Mr Prasanna Ponnumallayan, Mr Arun Manikavasagam, Ms Charlotte Pushparajan and Mr Sakthi Priya Balaji for making me feel at home away from home.

I would like to express my deepest thanks and gratitude to my mother Mrs Leela Gopalakrishnan, my friendly brother Mr Praveen Gopalakrishnan and my affectionate sister Ms

Reshma Gopalakrishnan for their love and support. Finally, I would like to dedicate this thesis to my beloved father Mr Gopalakrishnan Subramanian.

CONTENTS

LIST OF FIGURES

LIST OF TABLES

ABBREVIATIONS

°C	Degree Celsius
µ	Growth rate
µmax	Maximum specific growth rate
AA	Arachidonic acid
ALA	α-linolenic acid
AL-PBR	Airlift photobioreactor
ALRs	airlift reactors
ANOVA	Analysis of variance
Bp	Base pairs
CCW	Counter-clockwise displaced
CO_2	Carbon dioxide
CW	Clockwise-displaced
DHA	Docosahexaenoic acid
DO	Directly opposed
DPA	Docosapentaenoic
ECL	Equivalent chain length
EPA	Eicosapentaenoic acid
EPS	Exopolysaccharides
FAME	Fatty acid methyl esters
FAs	Fatty acids

GLA	γ -Linolenic acid
GLC	Gas-liquid chromatography
HCA	Hierarchical cluster analysis
k_La	Volumetric mass transfer
LC-PUFAs	Long chain polyunsaturated fatty acids
LEDs	Light-emitting diodes
MGDG	Monogalactosyldiacylglycerol
MPB	Maximum-parsimony bootstrap
MUFAs	Monounsaturated fatty acids
NJ	Neighbour Joining
nls	Nonlinear least square
Nuc	Nucleus
PAR	Photosynthetically active radiation
PFD	Photon flux density
PFD	Photon flux density
PUFAs	Polyunsaturated fatty acids
Pyr	Pyrenoid
TAG	Triacylglycerols
Φ_1	Maximum population size

CHAPTER 1

INTRODUCTION & OVERVIEW

CHAPTER 1

INTRODUCTION & OVERVIEW

1.1 SECONDARY METABOLITES IN HUMAN HEALTH

Primary metabolites are found in all organisms. These include carbohydrates, lipids and proteins, which are involved in the fundamental biochemical reactions common to all life. Like primary metabolites, secondary metabolites are organic compounds which are produced in biological systems. However, they are not directly involved in growth or reproduction of the organism (Fraenkel 1959). The functions of most secondary metabolites are related to the organism's interaction with its environment.

Fatty acids (FAs) are important secondary metabolites because they are the building blocks of lipids, which have several functions such as membrane building (Heinz 1996), energy storage (Brasaemle 2007) and signalling (Wang 2004). The general structure of a FA is a hydrocarbon chain with a carboxyl group at one end and a methyl group at the other. There are two types of FAs: saturated and unsaturated. Unsaturated FAs have one or more double bonds in their carbon backbone; if more than one double bond occurs then the FA is regarded as a "polyunsaturated fatty acid" (PUFA). As a result of these double bonds, there are two possible geometric configurations for unsaturated FAs: *cis* and *trans*. The former refers to the situation where two hydrogen atoms are opposite each other across the double bond, with the latter referring to the alternative configuration. FAs are described by specific nomenclature, for instance 18:2n-6, which states the number of carbon atoms in the chain (18), the number of

double bonds (2) and the position of the first double bond from the methyl terminus (6). If the first double bond between carbon and carbon from the methyl terminus is at the third position then the molecule is termed an n-3 or omega 3 FA. Similarly if it is at the sixth position then it is stated as n-6 or omega 6 FA. Enzymes such as 12-desaturase and 15-desaturase are required to synthesise PUFAs; these are lacking in plant and animal cells, so these organisms are unable to synthesise "long chain polyunsaturated fatty acids" (LC-PUFAs) such as Eicosapentaenoic acid (EPA) and Docosahexaenoic acid (DHA). They can, however, produce saturated and most monounsaturated FAs.

Linoleic acid (C18:2n-6) is the FA from which all other omega-6 FAs are synthesised; similarly, α-linolenic acid (ALA) (C18:3n-3) is the parent for all the other omega-3 FAs (Clandinin *et al.* 1994). For instance, in humans the omega-6 FA arachidonic acid (AA) (C20:4n-6) is synthesized from linoleic acid. Also humans can convert ALA to the long-chain form acids EPA (20:5n-3), Docosapentaenoic acid (DPA) (25:5n-3) and DHA (22:6n-3) (Brenna 2002). These three main important long chain n-3 fatty acids have very important roles in the improvement and action of the brain, cardiovascular strength and inflammatory response. When integrated in the lipid bilayer membrane of the cells, they also play important roles in controlling the membrane eicosanoid biosynthesis, cell signalling cascade, and gene expression (Shahidi & Miraliakbari 2005)

Among the three important long chain omega 3 fatty acids, DHA (Jiang *et al.* 2004) is recognized for its benefits in cardiovascular health and neural development (Horrocks & Yeo 1999). Clinical and epidemiological studies have indicated that DHA plays an important role in the development and functioning of brain, retina, and reproductive tissues for both adults and infants (Gill & Valivety 1997). Also, it is recognised that DHA is a vital component of human

breast milk that supports the development of a baby's brain and nervous system (Singh 2005). At present DHA is available in commercial baby foods. However, in many countries fish products are banned from infant formula due to potential contamination by heavy metals such as mercury (Ratledge 2004). While several infant formulas have been enriched with up to 0.2% of DHA, it has been shown that the level of DHA in these products is not yet sufficient for correct neurodevelopment in infants (Auestad *et al.* 2001, 2003). To meet the dietary requirements for DHA, synthetic DHA is produced in the laboratory (Rubin 1991), but only DHA derived from an organic source is recommended for infant formula. Thus, to produce an infant formula containing the recommended quantity of organic DHA at a reasonable price, it is necessary to find new sources of the compound.

A number of scientific authorities such as the Department of Health, London (1991), the British Nutrition Foundation (1992), the Scientific Committee for Food (1993), and World Health Organization have specifically recommended PUFA intake levels. Table 1.1 shows the recommendations for average population intakes of unsaturated FAs by various scientific authorities.

1.2 SOURCES OF POLYUNSATURATED FATTY ACIDS

The major sources of PUFAs are plants, fish and microbes. At present, one of the most common commercial sources of LC-PUFAs is fish oil, which can contain 20-30% of these FAs. Seeds from plants that contain PUFAs like ALA are flaxseed, hempseed, butternuts, Persian walnuts, pecan nuts and hazel nuts. However, oil seeds contain a much lower proportion of PUFAs compared to fish sources.

Different ranges of PUFAs can be obtained from cryptogams (e.g. mosses and algae), bacteria, fungi, and protozoa (Ratledge & Wilkinson 1988). Initially, PUFAs were believed to be absent in bacterial membranes (Erwin & Bloch 1964), but PUFAs such as EPA and DHA are now known to be present in the membranes of deep sea bacteria, living under high pressure and low temperature (DeLong & Yayanos 1986, Nichols *et al.* 1993, Yano *et al.* 1997). High levels of DHA are produced by the bacterial species *Moritella marina*, and by the fungi *Thraustochytrium* sp. and *Entomophthora* species (Wu *et al.* 2005).

Table 1.1 Recommendations for average population intakes (% total energy) of unsaturated fatty acids by different scientific authorities

Scientific authorities	Total fat	MUFA	Omega 6 PUFA	Omega 3 PUFA	trans-FA
	(% total energy)				
Department of Health (1991)	33	12	>1.0	>0.2	<2.0
British Nutrition Foundation (1992)	27	12	3-10	0.5-2.5	<2.0
Scientific Committee for Food (1993)	-	-	2.0	0.5	-
World Health Organization (1998)	15-30	10-15	4-10	0.4-2.0	-

Divisions of algae that include representatives which produce long chain omega-3 FAs include chrysophytes, cryptophytes, dinoflagellates, chlorophytes (Cohen *et al.* 1995, Behrens &

Kyle 1996), bacillariophytes (Boswell *et al*. 1992), eustigmatophytes (Yonfmanitchai & Ward 1989) and rhodophytes (Cohen 1990).

1.2.1 ALGAE AS A SOURCE OF POLYUNSATURATED FATTY ACIDS

The use of fish as the main commercial source of omega-3 FAs has several drawbacks, the most important is that the global fishery is not a renewable source at its current level of exploitation. Overfishing the world's oceans has led to a great decline in many fish species (Myers & Worm 2003, White & Costello 2014), and the need for fishery conservation. Additionally, omega-3 FAs from fish have substantial taste, odour and stability issues in storage. The process for purifying FAs from fish oil is still complicated, resulting in retail costs of up to US$ 144 g^{-1} for 99% pure DHA and US$ 2,000 g^{-l} for 99% pure EPA (Barclay 1994). These difficulties restrict the use of fish oils as the main source of PUFAs. To overcome these difficulties, it is necessary to find other sources.

Algae are the primary synthesizers of omega-3 FAs in the aquatic food chain. Thus PUFAs are not produced by fish; instead, fish acquire them through their diet by eating zooplankton that have fed on algae (Ackman *et al.* 1964). Algae cultivation could therefore be used as a renewable and sustainable source for the production of PUFAs, providing that an economic process is developed at industrial level. Polyunsaturated fattyacids recovered from algae will not have the problems associated with taste and odour as those derived from fish. Also, the recovery process of PUFAs from microalgae is very easy (Ward & Singh 2005) when compared to the recovery process from fish (Abedi & Sahari 2014).

1.3 WHAT ARE ALGAE?

Taxonomically, algae are a heterogeneous assemblage of organisms including unicellular and multicellular forms. The former include some of the smallest eukaryotes, e.g. *Ostreococcus tauri* (Courties *et al.* 1994), and the latter include giant seaweeds over 50 metres long, e.g. *Macrocystis* (Van Den Hoek *et al.* 1995). Algae occur in fresh, marine and brackish water including extreme habitats such as snow (Weiss 1983, Duval *et al.* 2010) and hot deserts (Bell 1993). Many multicellular microalgae exhibit cellular specialization, but they lack organs which are found in land plants (which are themselves green algae in a cladistic sense; Lewis & Flechtner 2004). Algae are generally classified into more than a dozen major groups, primarily on the basis of pigment composition, storage products, ultrastructural features, and molecular genetic evidence. Cyanobacteria, which are usually regarded as an algal group, are also considered to be the extant relatives of the progenitors of the eukaryotic chloroplast (Keeling 2004). The one biochemical feature that unites organisms regarded as algae is the ability to carry out oxygenic photosynthesis (Vioque 2007).

Algae are responsible for more than half of the oxygen composition of the Earth's atmosphere as a result of photoautotrophic growth (Kasting & Siefert 2002). Marine algae are thought to have slowly proliferated over a billion years, growing photoautotrophically, and gradually changing the composition of the Earth's atmosphere until it was oxygenic, and thereby capable of supporting new types of metabolism. Evidence for this includes fossilized stromatolites (putative cyanobacterial colonies) and chemical signatures in ancient rock strata (Graham & Wilcox 2000). The ancestors of modern cyanobacteria (blue-green algae) were also the earliest terrestrial autotrophs (Horodyski & Knauth 1994).

Similar procedures that are used for the classification of land plants are used for the classification of algae into taxonomic groups. Features of algae such as flagella apparatus, cell division processes, and organelle structure and function have been studied extensively using the electron microscope, resulting in considerable modification of earlier classification schemes based on light microscopy alone. Molecular studies, particularly gene sequencing, have reinforced some of these changes (Van Den Hoek *et al*. 1995) and led to further revisions (Pröschold *et al.* 2001).

Algae are commonly divided into ten taxonomic divisions, namely Cyanophyta, Glaucophyta, Rhodophyta, Heterokontophyta (also known as Ochrophyta and Stramenopiles), Haptophyta, Cryptophyta, Dinophyta, Euglenophyta, Chlorarachniophyta and Chlorophyta. The names of the divisions and classes of algae were originally based on the color of the organism: Cyanophyta, blue green algae; Rhodophyta, red algae; Chrysophyceae, golden algae; Phaeophyceae, brown algae; Chlorophyta, green algae (Van den Hoek *et al.* 1996). These high-level classifications of algae have generally remained intact; however, ultrastructural and phylogenetic analyses have introduced major changes below this level, as noted above (Graham *et al.* 2009).

All algae documented in this thesis are members of the division Chlorophyta. Chlorophyta occur mainly in aquatic habitats (marine and freshwater), but many species have also adapted to a wide range of environments such as rocks, snowfields and tree trunks. The division contains around 500 genera and 8000 species. Subdivision into classes and orders is made according to differences in flagella length and structure, number of flagella, hairs and scales on the flagella, flagellar axoneme, arrangement of flagellar basal bodies, chloroplast features, difference in the chloroplast membranes and thylakoid arrangements, accessory

pigments, pyrenoids and the position of the pyrenoids, starch and the form of its sequestration around the pyrenoid (Van Den Hoek *et al.* 1995). The arrangement of the flagellar basal apparatus has emerged as the most evolutionarily conserved character, aligned with molecular evidence (Graham *et al*. 2009).

The commonly accepted major classes of Chlorophyta are Ulvophyceae, Trebouxiophyceae and Chlorophyceae (Leliaert *et al.* 2012) and these encompass most of the diversity in the division. Where flagellate cells occur, they have a cruciate ("cross-like") X-2-X-2 flagellar root arrangement. The flagella apparatus is classified further according to the respective position of the basal bodies when the cell is viewed from the apex; these may be directly opposed (DO), clockwise-displaced (CW), or counter-clockwise displaced (CCW). Motile cells of the Ulvophyceae and Trebouixophyceae have the CCW orientation, with DO, CW, and some other less common configurations occurring in the Chlorophyceae (Graham *et al*. 2009).

Cell division characteristics also vary among chlorophytes. Ulvophyceaen division follows closed mitosis with a persistent spindle. Trebouxiophyceae and Chlorophyceae have non persistent spindles during mitosis, but semi-closed mitosis occurs in the former and closed mitosis in the latter (Graham & Wilcox 2000).

As shown above, algal classification along with the identification of new species requires the determination of very fine scale cellular components, in addition to gene sequencing followed by phylogenetic analysis. Examples in New Zealand include the studies of Novis *et al.* (2008a), Novis & Visnovsky (2011a), Novis & Visnovsky (2012) and Gopalakrishnan *et al*. (2014), in which new taxa have been erected with the aid of ultrastructural and molecular evidence. The naming of algal species is governed by the

International Code of Nomenclature for algae, fungi, and plants (McNeill et al. 2012). The Code requires accessible type specimens and published descriptions or diagnoses that distinguish new species from those already known. Valid publication generally equates to papers in peer-reviewed scientific literature, thus attempting to ensure that decisions regarding new species are robust. In the case of algae such papers must often document fine cellular detail and the results of molecular investigation

1.4 SECONDARY METABOLITES FROM ALGAE

In general, microalgae are a significant source of uncommon and interesting secondary metabolites. Most microalgal secondary metabolites are recognized as possible sources of new compounds or potential drugs for human use (Berenbaum 1995). Secondary metabolites isolated from higher plants tend to have little variation, whereas microalgae have yielded new secondary metabolites such as nostocyclamide, nostocine A, and Fischerellin A, which are not found in higher plants or other traditional sources (Leflaive & Ten-Hage 2007). Applications such as antitumor, cholesterol-lowering, immunosuppressant, antiprotozoal, antihelminthic, antiviral and anti-ageing activities have been found from the secondary metabolites of microalgae, and many more are likely to be found (Vaishnav & Demain 2011). Therefore exploring secondary metabolites from algae is an important and fruitful field of study.

Some algal secondary metabolites are produced commercially by fermentation technology. For instance, *Chlorella* sp. produces β-1,3-glucan, which acts as a blood lipid reducer (Spolaore *et al.* 2006). *Hematococcus pluvialis* is used for production of astaxanthin, a pigment with excellent antioxidant activity (Olaizola 2000). Phaeophyceae produce alginates, which are used in the food industry (Draget *et al.* 2005).

Algal biotechnology has developed in the last decade, due to new and industrially important compounds discovered from algae. Currently, application of algae and algal products are widespread and used in several fields such as energy sources, e.g. biofuel (Craggs *et al.* 2011) which comprises hydrogen (Melis & Happe 2001), methane (Hansson 1983) and ethanol (Ueno *et al.* 1998), fertilizers (Benemann 1979); food and food additives, e.g. *Spirulina,* (Vonshak & Richmond 1988), *Dunaliella* for β-carotene production (García-González *et al.* 2005); and pollution control. Along with traditional sources, a number of algae such as *Haematococcus, Dunaliella, Chlorella,* and *Spirulina* are used for production of the industrially important products listed in Table 1.2.

Some alpine algae produce large amounts of secondary metabolites such as carotenoids, especially under low nitrogen conditions and high solar irradiance (Britton & Goodwin 1988). Carotenoids such as astaxanthin, canthaxanthine, echinenone, hydroxy-echinenone and β-carotene have been identified in chlorophytes (Kleinig & Czygan 1969, Grung *et al.* 1989, Lee & Soh 2004). β-carotene, one of the secondary metabolites, accumulates in lipid globules outside the chloroplast (Czygan 1968, Yong & Lee 1991). Nitrogen limitation induces the production of carotenoids which act as sunscreens to avoid photo-damage during high solar irradiance (Boussiba & Vonshak 1991). These carotenoids are particularly important in snow, since they can occur in abundances large enough to colour it (Hoham & Duval 2001). For instance, green, orange and reddish-orange snows are all found near penguin rookeries at Rumpa, and green and red snow near a petrel rookery at Skarvsnes, East Antarctica (Akiyama 1979).

1.4.1 POLYUNSATURATED FATTY ACIDS FROM ALPINE ALGAE

Algae from alpine regions, due to their tolerance and adaptation to low temperatures, are expected to have unique FAs and lipid composition. The algae endure an extreme environment, especially low temperatures and high irradiance, associated with a high risk of cell damage. PUFAs are implicated in protection against these extremes (Roessler 1990, Thompson 1996, Mock & Kroon 2002).

Table 1.2 Industrially important products from algae

Alga	Product
Arthrospira species	γ -Linolenic acid (GLA)
Parietochloris incisa	AA
Crypthecodinium species	DHA
Pavlova lutheri	DHA and EPA
Isochrysis galbana	DHA and EPA
Dunaliella salina	Glycerol β-Carotene
Haematococcus pluvialis	Astaxanthin
Spirulina platensis	Phycocyanin
Porphyridium cruentum	Polysaccharides

Generally there is a relatively low limit to the accumulation of PUFAs in most algae, because the production of these FAs is strictly regulated. However, certain algal species can be induced to produce high concentrations of PUFAs (Shifrin & Chisholm 1981). *Parietochloris incisa* isolated from Mt. Tateyama, Japan, was found to be rich in long chain PUFAs. This alga is also rich in triacylglycerols (TAG). During the logarithmic growth phase, the TAG reached 43%, of the total FAs, a value that increased to 77% during the stationary phase (Bigogno *et al.* 2002). In some ice algae such as *Nitzschia frigida* and *Melosira arctica* the TAG content is also high (40-50% ; Falk-Petersen *et al.* 1998). TAG-containing long chain PUFAs have the capability to support organisms to adapt to a different environment rapidly. Unfavorable conditions such as nitrogen starvation have induced production of AA in *P. incisa* to a maximum of 21% dry weight (Bigogno *et al*. 2002).

1.5 ALGAE CULTIVATION

Algae can be cultivated in a variety of systems, which can usually be classified into two major groups, as follows.

1.5.1 OPEN SYSTEMS

Algae have been cultivated in open ponds since 1950 (Borowitzka 1999). Ponds used for algal cultivation may be natural or artificial. Among the artificial ones, raceway ponds are the most common (Jiménez *et al.* 2003). In these ponds, water is forced to flow through a closed circular or oval loop channel with the help of paddles. The inoculum and nutrients are usually introduced in front of the mixing paddles and these paddles are usually driven by electric power. This circulation also prevents to a certain extent the settling of nutrients and algae to the bed of the

pond. However, this mixing is very poor from a mass transfer rate perspective, resulting in low productivity (Brennan & Owende 2010).

The method of cultivating algae in natural open ponds has advantages, such as a large area of pond that can produce a huge amount of biomass (Rodolfi *et al.* 2009). The cost of biomass production is also relatively low (Ugwu *et al.* 2008). Open ponds require only a very low amount of energy (Rodolfi *et al*. 2008) to work reasonably efficiently. For instance, the cost of producing *Dunaliella salina* used for biofuel production in an open pond system was calculated as €2.55 Kg^{-1} of dry mass (Tan 2008). However, open ponds present a number of disadvantages as well. In open ponds there is a greater risk of contamination (Pulz 2001), due to invasion by other species in the environment. Culturing of specific algae in open ponds is more feasible if the strain of interest can grow under extreme conditions, such as highly acidic, highly alkaline, or highly saline conditions, so most species (which grow under normal conditions) cannot invade the pond. *Dunaliella salina* can grow at high salinity, and *Spirulina* in high alkalinity, so these organisms can be grown as monocultures in open ponds (Borowitzka 1999).

Open pond cultivation harvests more algal biomass, but its rate is not constant throughout the year, as described by Setlik *et al.* (1970) for *Chlorella* production. Open ponds are difficult to maintain operationally at an optimum temperature (Brennan & Owende 2010). This is because they are exposed to the variation of environmental temperatures, but also due to the loss of water by evaporation. In addition, controlling light intensity to its optimum is impossible, depending on the natural day-night cycle in the area where the open pond is located (Cuaresma *et al.* 2011). Though steps have been trialled to cover ponds with plastic covers and greenhouses to maintain high temperatures, this has not resulted in a decrease in contamination (Chaumont 1993). Also,

covering a big pond is practically very challenging. For all these reasons, open pond systems are not suitable for large scale production of many algal species.

1.5.2 CLOSED SYSTEMS

Closed photobioreactor systems have important advantages over open pond systems, including (Ugwu *et al*. 2008, Xu *et al.* 2009):

- Prevention of contamination for the cultivation of monocultures, without the need for extreme conditions.
- Provision of greater control over operating conditions such as mixing, pH, light, CO_2 concentration, and temperature.
- Prevention of water evaporation.
- Reduction of CO_2 losses from out gassing.
- Higher cell concentrations can be reached.

These advantages permit the production of many valuable products, including food, complex biopharmaceuticals and health products and cosmetics.

Microalgae cultivated in photobioreactors use light as an energy source, and are typically provided with CO_2 as a carbon source. Carbon dioxide is passed into the reactor through a sparger to saturate the media (Pulz 2001). Culture media used for the growth of algae are designed specifically depending on the type on microalgae. They include other elements required in micro quantities such as nitrogen, phosphorous, hydrogen, sulphur, calcium, magnesium, sodium and potassium. Trace quantities of iron, boron, manganese, copper,

vanadium, cobalt, nickel, silicon and selenium are also required to maintain high cell growth (Suh & Lee 2003).

In bioreactors, mixing maintains the supply of nutrients to the cells, avoids settling of nutrients and microalgae, and increases the dissolution of gases (CO_2) in the liquid phase (culture media). In conventional stirred tank bioreactors an impeller is used for producing the mixing, but for algal cultivation it cannot be used in all cases, because the large shear force produced by it can result in cell damage (Barbosa & Wijffels 2004). Other disadvantages of moving part or agitator mixing inside the reactor are the generally high level of cell disturbance, the complicated sterilization requirements, and the high energy requirement for mixing. To overcome these issues, mixing in the reactor can be carried out using gas injection. This gas injection accomplishes reactor mixing, circulation and aeration. The reactors that utilise this kind of mixing are bubble column reactors and airlift reactors (ALRs).

Light from an artificial or natural source is supplied to photobioreactors so that microalgae can undergo photosynthesis. Photosynthesis is a process that converts light energy to chemical energy and stores it in the bonds of sugar molecules (Murata *et al.* 2007).

$$6CO_2+6H_2O+\text{Sunlight} \longrightarrow C_6H_{12}O_6+6O_2$$

The process involves two main stages. The molecules of the photosystem II reaction centre are excited to a higher energy state by absorbing light energy. The excited electron passes through the electron transport chain to Photosystem I. During the electron transport chain the hydrogen ions are shifted from the stroma to the thylakoid lumen. The ATP and NADPH produced from the electron transport chains are used in the Calvin Cycle (also called the “dark

reactions"). An effective photobioreactor needs to accommodate both stages of photosynthesis within the same sealed tank without causing damage due to high light intensity (a process known as photoinhibition).

In recent years new design of photobioreactors have led to increased efficiency (Degen *et al.* 2001, Morita *et al.* 2001b, Pulz 2001, Samson & Leduy 2009). Two decades ago photobioreactors were designed to produce stable isotopically labelled compounds ^{13}Carbon, ^{2}Hydrogen, and ^{15}Nitrogen (Behrens *et al.* 1989, Behrens *et al.* 1994), pigments, FAs and bioactive molecules (Kyle *et al.* 1988, Behrens 1992). In addition to the production of biomass, photobioreactors have been designed for the removal of various compounds from water (An & Kim 2000, Gaffney *et al.* 2001), production of gas vesicles in cyanobacteria, and hydrogen production (Huang & Rorrer 2002, Barahona & Rorrer 2003, Polzin & Rorrer 2003).

1.6 VERTICAL TUBULAR PHOTOBIOREACTORS

Vertical column photobioreactors may be of four types, as follows.

1.6.1 BUBBLE COLUMN PHOTOBIOREACTORS

Bubble column reactors belong to the general class of multiphase reactors. Their shape is cylindrical, with the height more than double the diameter. In a bubble column photobioreactor homogeneous cultures can be maintained. It is a closed controlled reactor with gas distributor at the bottom. Gas distribution has an important effect on the performance of a bubble column reactor. The mass and heat transfer efficiencies of a bubble column reactor are efficient and controllable. According to Luo *et al* (1999), the most important parameter relating to transport phenomena in bubble column reactor design is gas holdup. This gas holdup is proportional to the

gas velocity and the operating pressure. Maintanence and operational costs are very low because of the absence of the moving parts for mixing; mixing is carried out by the gas flow.

1.6.2 AIRLIFT PHOTOBIOREACTOR

This type of reactor works on the principle of a circular mixing pattern. It contains two tubes, a downcomer and a riser. This setup allows both the air and liquid to flow in two directions. Usually the air is injected into the riser which acts as a normal bubble column reactor; the riser receives more air than the downcomer and this creates the difference in the bulk density. Due to this density difference the fluid starts to move; the liquid in the riser moves in the upward direction and the liquid in the downcomer moves towards the bottom. The downcomer of the photobioreactor designed by Loubiere *et al.* (2008) produced a swirling motion. Compared to other types of photobioreactors, ALRs have good mass transfer rate, strong mixing without hydrodynamic sheer and relatively low power consumption.

The airlift concept of exploiting hydrostatic pressure differences resulting from gas injection into a baffled chamber containing liquid has been known for a long time. The "Pachuca Tank", used in the metallurgy industry to leach ores of gold, uranium and other metals, is probably the first example of industrial use of the principle for reactor applications (Lamont 1958). The system's property, which made it attractive for this application, was its capability of producing efficient mixing in the reacting systems without moving parts. The first clearly defined "airlift" reactor was patented by Lefrancois in 1955. Initially, the device was mainly applied to large-scale microbiological processes, such as single cell protein production. Since then, the use of these reactors has expanded to include applications in different fields.

The term ALR covers a wide range of gas-liquid or gas-liquid-solid pneumatic contacting devices that are characterized by fluid circulation in a defined cyclic pattern through channels built specifically for this purpose. In ALRs, the content is pneumatically agitated by a stream of air or sometimes other gases. In those cases, the name "gas lift reactor" has been used. In addition to agitation, the gas stream has the important function of facilitating exchange of material between the gas phase and the liquid; oxygen is usually transferred to the liquid, and in some cases reaction products are removed through exchange with the gas phase (Rubio *et al.* 1999).

The main difference between ALRs and bubble columns (which are also pneumatically agitated) lies in the type of fluid flow, which depends on the geometry of the system. The bubble column is a simple vessel into which gas is injected, usually at the bottom, and random mixing is produced by the ascending bubbles. In ALRs (Merchuk & Siegel 1988), the major pattern of fluid circulation is determined by the design of the reactor, which has a channel for gas and liquid upflow (the riser), and a separate channel for the downflow (the downcomer). The two channels are linked at the bottom and at the top to form a closed loop. The gas is usually injected near the bottom of the riser (Merchuk & Gluz 1999). The extent to which the gas disengages at the top, in the section termed the gas separator, is determined by the design of this section and the operational conditions. The fraction of the gas that does not disengage, but it is entrapped by the descending liquid and taken into the downcomer, has a significant influence on the fluid dynamics in the reactor and hence on the overall reactor performance (Merchuk & Gluz 1999).

1.7 HELICAL PHOTOBIOREACTOR

This is a type of photobioreactor which is helical in arrangement. The helical structure is usually arranged into a large cylinder or cone (Singh & Sharma 2012). These systems typically use artificial light but there are also designs based on natural light. The culture is mixed and agitated by the formation of bubbles resulting from air pumped into the tubes. Thus, the pumping rate determines the level of mixing in a helical photobioreactor. The ground surface area occupied by this kind of reactor is very low, which is one of its main advantages. The main disadvantage is the large amount of energy required for pumping the broth in the tubes when scaling up (Singh & Sharma 2012). Another disadvantage is that the deposition of cells on the internal tube surface stops the penetration of light into the tubes. The cells adhering to the internal wall surface can be resuspended by increasing the pressure of air injected into the tube, but this also increases the sheer stress on suspended cells.

The flow pattern of the liquid and air inside the reactor has an important role in the growth of the cells. The flow pattern in the reactor is calculated by the Reynolds number (Re).

$$Re = \rho v L/\mu$$

ρ – Density of the liquid (kg m^{-3})

v – Mean velocity (m s^{-1})

L – Travelling length of the liquid (m)

μ – Dynamic viscosity (kg m^{-1} s^{-1})

In this kind of reactor the Reynolds number is maintained above 2300. Lower values indicate laminar (as opposed to turbulent) flow, which leads to lower mass transfer due to the low level of mixing. Molina (2001) found that stable growth of *Phaeodactylum tricornutum* occurred under turbulent flow and not under laminar flow. Increasing the flow rate above turbulence had no

effect on the growth rate (μ). Thus the flow rate in this kind of reactor has a significant impact on the growth of algae in them. *Spirulina, Chlorella, Phaeodactylum,* and *Monodus* have been grown in this kind of reactor in indoor conditions (Chrismadha & Borowitzka 1994, Morita *et al.* 2001a) and in outdoor conditions at pilot scale level (Lu *et al.* 2002). These kind of reactors have been recommended for large scale cultivation of *Phaeodactylum tricornutum*, but with improved mass transfer to avoid the stress produced due to high levels of dissolved oxygen (Hall *et al.* 2003). In general although this type of reactor is easily scaled up, the disadvantages noted above mean that it has seldom been used to date.

1.8 FLAT PLATE PHOTOBIOREACTOR

This reactor design comprises many transparent thin panels arranged in parallel, with high surface-to-volume ratio. Aeration is achieved from the bottom of each panel. The panel's surface area is high relative to its volume, so a high amount of light can be received by a small volume of culture. Usually the light is supplied artificially, and the flat plate reactors are mounted vertically and exposed to the light source from one side. When sunlight is used as the light source, the reactors are inclined at an appropriate position to receive maximum light intensity. High photosynthetic efficiencies can reportedly be achieved by flat plate photobioreactors (Richmond 2000). The area exposed directly to the light source is called the photic zone; here, the cells reach their light saturation and photoinhibition. The amount of light received by the cells away from this photic zone decreases gradually. Under the conditions used by Janssen *et al.* (2003), light in such a rector was effective for the growth of *Chlamydomonas reinhardtii* up to a depth of 0.8 mm. The relative mass transfer rate is low in flat plate photobioreactors because the space between the plates is very low. The clearance efficiency of the dissolved O_2, which is

important to achieve a good mass transfer rate, is therefore reduced (Sierra *et al.* 2008). This is one of the main disadvantages of this kind of reactor. Also, some algae form a mat on the internal transparent walls, reducing the light intensity reaching the suspended cells, and scaling up is quite complicated because temperature control becomes very challenging (Sierra et al. 2008). Despite their apparent simplicity, few such systems have been used for mass cultivation (Tredici *et al.* 1999). The footprint of a flat plate photobioreactor is low; this is one of its major advantages. The flat plate photobioreactor can be used both in batch and continuous cultivation processes.

1.9 FACTORS AFFECTING ALGAL GROWTH AND SECONDARY METABOLITE PRODUCTION

1.9.1 STRAIN SELECTION

Many algal strains and species have been screened and studied from different environments for sustainable growth in mass cultures. A selected strain should have a promising potential for large scale production (Ramawat & Merillon 1999). Before selecting the strains, their characteristics should be well studied. The strain to be selected should have good μ and there should not be intense effect on μ and production due to slight changes in growth conditions. The optimum temperature for its growth should not be far outside ambient, to avoid large energy costs associated with scaling up. Strains should not produce any bi-products which disturb the nutrient level of media. Before scaling up to fermentation level, the details of secondary metabolites produced by the strains should be analyzed at shake flask level. This topic is introduced more thoroughly in Chapter 4.

1.9.2 LIGHT INTENSITY

Providing adequate light is necessary for an efficient and well-functioning photobioreactor. Increasing the light intensity above the saturation point may cause photoinhibition. Normally each strain has its individual point of photo inhibition, and use of flashing light is one way to overcome it. The effect of flashing lights is theoretically explained using the light and dark reactions of photosynthesis. The effect is thought to result from the fast reduction of electron acceptors, associated with the photosystem II complex, followed by their oxidation in the dark period (Kim *et al.* 2006). Photoinhibition begins to occur in *Nostoc commune* microalgae at illumination intensity above 200 μmol m^{-2} s^{-1} (Novis *et al.* 2007). During the lag phase of algal cultivation, the intensity of the light can be set below the required level and ramped upwards as the culture grows (Pulz 2001). This topic is introduced more thoroughly in Chapter 6.

1.9.3 TEMPERATURE

Temperature has a major effect on growth and survival of microalgae, and it also influences the production of secondary metabolites (Guschina & Harwood 2006). Different methods are used for controlling the temperature. Each method has its own advantages and disadvantages. For instance, use of cooling coils inside the media can provide efficient cooling, but the coil may interfere with the agitation or circulation inside the vessel. This method is efficient for cells that do not form biofilms and if they are sensitive to shear stress (only low agitation or circulation should be supplied). In another method cool water is circulated though an external jacket and this method does not have complications like coils. Thus this is one of the efficient method for mainting the temperature in the reactor. Generally a temperature probe should be

used to enable measurement of the temperature inside the photobioreactor. This topic is introduced more thoroughly in Chapter 7.

1.9.4 CARBON SOURCE

Microalgae have been grown using different carbon sources. Carbon is the most important nutrient (i.e. it is required in the greatest amount), and is usually provided in the form of CO_2. The concentration of CO_2 used varies greatly. The simplest approach is to blend CO_2 with air, for example 0.2 to 5.0% of the total gas flow (Morita *et al*. 2001b, Babcock *et al.* 2002). Carbon dioxide is converted into many organic compounds which are used for metabolic purposes and other processes involved in the cell. Carbon is the backbone of many components such as sugars, lignans, chitins, alcohols, fats, aromatic esters, carotenoids and terpenes. Moreover carbon has a major role in photosynthesis, which fixes atmospheric carbon into organic molecules. Carbon is the energy currency in cells. Care must be taken to ensure that the CO_2 input does not adversely lower the pH of the culture. Another strategy is to use CO_2 to control the pH of the culture (Delente *et al.* 1992, Babcock *et al*. 2002). This topic is introduced more thoroughly in Chapter 5.

1.9.5 OTHER NUTRIENTS

Other nutrients required are nitrogen, phosphorous, hydrogen, oxygen, sulphur, calcium, magnesium, sodium and potassium. Additional nutrients are needed in trace quantities, often micro or nano-grams per litre: iron, boron, manganese, copper, molybdenum, vanadium, cobalt, nickel, silicon and selenium (Suh & Lee 2003). If one of these does not exist in sufficient quantities, auto-inhibitory compounds may be excreted by the cells. It is difficult to specify a

chemical make-up for culturing microalgae because each strain has different requirements, and as a result the optimal composition for each strain with each medium is different. However, there are a number of defined freshwater media that are useful for growing a wide variety of algae (Stein 1973, Guillard 1975, Morel *et al.* 1975).

It is important to ensure the growth medium has sufficient macronutrients, trace elements and vitamins to maximise growth of the algae and minimise the stress imparted on them. Vitamin B_1 (thiamine), vitamin B_{12} (Cyanocobalamin) and vitamin H (Biotin) are the three vitamins usually used for culturing microalgae. Many algae need only one or two of these vitamins, but there seems to be no harm by adding a nonessential vitamin (Provasoli & Carlucci 1974). Other vitamins are also included in some recipes. For example, nicotinamide is added to the culture medium for *Phacotus lenticularis* (Schlegel *et al.* 2000).

1.10 SPECIFIC GROWTH RATE

It is essential to measure the specific growth velocity (μmax) of algae in the culturing system in order to determine optimal levels of the parameters influencing growth, such as CO_2, media composition, light, and agitation.

Counting the sum of cells per unit volume of culture is the most common method used to assess the aggregate population. Other techniques used to estimate the cell population include biomass, dry cell weight, phosphorous content, organic nitrogen content, and chlorophyll content.

In the transmitted light method the examination is done by allowing a known volume of culture to settle on a plane and the number of cells on the plane is counted under a microscope. If

they are motile they are immobilized (by heating the slide moderately) before counting (Throndsen 1995, Andersen & Throndsen 2003). A hemocytometer, which utilises rulings of known size, is often used to measure the cell concentration. A homogenised culture should be sampled to avoid inaccuracies in the cell count due to sedimentation. Lugol's iodine solution is an example of a preservative used to store cell culture samples for later enumeration. An acid solution is best to preserve flagella, but this can destroy coccolith structures, so it is highly recommended to use weak acid to avoid the damage when counting such forms (Hallegraeff *et al.* 2003).

1.11 AIMS OF THE STUDY

The aim of this study was to isolate and identify a novel alpine alga rich in PUFAs, as a potential candidate to develop a sustainable process to mass produce these PUFAs in an AL-PBR under optimal conditions.

In order to achieve this aim, the following objectives were defined:

1. To isolate pure algal strains from the New Zealand alpine zone.
2. To identify the isolated algal strains using polyphasic taxonomic techniques (morphology including ultrastructure, and molecular phylogenetic analysis).
3. To select a suitable candidate algal strain for large scale cultivation and PUFA production.
4. To design an appropriate AL-PBR for culturing the selected algal strain at larger scale.
5. To optimize the cultivation parameters affecting growth and PUFA production of the strain.

CHAPTER 2

TAXONOMY OF SCENEDESMACEAN ALPINE ALGAE FROM CANYON CREEK

CHAPTER 2

TAXONOMY OF SCENEDESMACEAN ALPINE ALGAE FROM CANYON CREEK

Note that a paper based on this chapter has been published: Gopalakrishnan *et al*. 2014. (Gopalakrishnan, K., Novis, P. & Visnovsky, G. 2014. Alpine Scenedesmaceae from New Zealand: new taxonomy. *New Zealand Journal of Botany*:1-16.).

2.1 INTRODUCTION

Freshwater green algae in the family Scenedesmaceae are well known from aquatic habitats, soils (Trainor & Hilton 1963) and cryptogram crusts (Lewis & Flechtner 2004). The genus *Scenedesmus* and its close relatives are distributed throughout the world (Prescott 1962), including Antarctica (Lesser *et al.* 2002). According to Broady *et al*. (2012) 10 species of *Scenedesmus* and 15 species of *Desmodesmus* have been identified in New Zealand.

Most genera in Scenedesmaceae form colonies in aquatic habitats, and usually as coenobia with 4–32 cells. Most of the differences in morphology that traditionally separate species in Scenedesmaceae are differing numbers of cells in the coenobia (Chodat 1926), shape of the cells (Chodat 1926), arrangement of the cells (Meyen 1829), and ornamentation of the cell wall (Chodat 1926, Hortobágyi 1969). The cell wall structure of cells possessing spines is different from that in cells lacking spines (Hegewald *et al.* 1990, Hegewald & Schnepf 1991).

Discussion about the morphological variation of Scenedesmaceae has been long-standing (Chodat 1913, Holtmann & Hegewald 1986, Hegewald *et al*. 1990, Trainor 1998). Hegewald & Silva (1988) noted 1300 species of *Scenedesmus* in the global literature at that time, but suggested that actual diversity could be as low as 30 species due to phenotypic plasticity; the same species can receive a different name in various parts of the world due to this variation, leading to an artificial inflation in the number of species in the genus. After allowing for phenotypic plasticity and the splitting up of genera, Guiry & Guiry (2013) estimated a diversity of about 430 species of *Scenedesmus* worldwide.

It is possible to identify morphological characters that are evolutionarily conserved using molecular data. For example, Hegewald & Silva (1988) proposed the sub-genera of *Scenedesmus* and *Desmodesmus* on the basis of morphological differences (mainly the presence of spines and other surface features), which was confirmed by Kessler *et al*. (1997) by analysis of 18S rDNA. As a result of modern molecular and ultrastructural study, the Scenedesmaceae now includes forms quite different from the coenobial morphotypes that originally circumscribed the family. Some unicellular taxa formerly classified as *Chlorella* are now considered to be species of *Scenedesmus* e.g. *S. rubescens* (P.J.L Dangeard) E.Kessler, M.Schafer, C.Hummer, A.Kloboucek & V.A.R.Huss and *S. vacuolatus* I.Shihira & R.W.Krauss (Huss *et al.* 1999). In addition, unicellular forms collected from desert soil belong to *Scenedesmus* according to phylogenetic analyses of 18S and ITS rDNA (Lewis & Flechtner 2004).

The genus *Scotiellopsis* traditionally included unicells with distinctive longitudinal ribs, resembling Chlorellaceae in reproductive features. However, phylogenetic study demonstrated that *Scotiellopsis* spp. formed a clade with *Scenedesmus vacuolatus*, prompting their transfer to the genus *Coelastrella* in the Scenedesmaceae (Hanagata 1998). *Coelastrella terrestris* (Reisigl)

Hegewald & N.Hanagata (as *Scotiellopsis terrestris* (Reisigl) Puncocharova & Kalina) has been found previously in the New Zealand alpine zone (Novis 2001). Similarly Novis and Visnovsky (2012) described a new monospecific genus from New Zealand, *Cryptodesmus*, from alpine soil that lacked spines and did not form coenobia in culture, but was robustly grouped with Scenedesmaceae according to phylogenetic analysis.

In this chapter I describe three strains of Scenedesmaceae isolated from the alpine zone in Canyon Creek, New Zealand. *Desmodesmus abundans* (Kirchner) E.Hegewald has been reported previously, *D. granulatus* (West & G.S.West) P.Tsarenko is a new record for New Zealand, and *Coelastrella multristriata* var. *grandicosta* is new to science. We also transfer the erroneously named *Cryptodesmus ellipsoideus*, previously isolated from the NZ alpine zone at a different site, to the genus *Coelastrella* as the result of new molecular and ultrastructural investigations.

2.2 MATERIALS AND METHODS

2.2.1 COLLECTION SITE

Sampling was carried out in upper Canyon Creek, Ahuriri Conservation Park, South Island, New Zealand (Figure 2.1). Details of the samples from which the taxa described here were isolated are given in Table 2.1.

2.2.2 COLLECTING METHOD

Each sample (approximately 1–2 g) was taken directly into a sterilised 9 ml polycarbonate test-tube with a screw-top lid by pushing the uncapped tube through the material to be sampled.

Collected samples were refrigerated overnight at the field camp and two days in the laboratory before inoculation of cultures.

2.2.3 CULTURING

Sample material was suspended in sterile water and a small volume plated on 5.5 cm diameter Petri plates containing 1.2% agarised BG-11 medium (Rippka *et al.* 1979), diluted to 10% concentration, by aseptic spread plate technique in a laminar flow hood. The agar was first prepared at double strength, washed for 5 days after autoclave sterilisation by soaking daily in fresh sterile distilled water. Media and agar were autoclaved separately, cooled to ~45°C, and recombined before pouring plates. After inoculation the Petri plates were incubated at 5–6°C with light intensity of approximately 50 µmol photons m^{-2} s^{-1} for three weeks. After 3 weeks, each distinct colony type on each plate was examined microscopically and isolated into unialgal culture by aseptic streak plate technique.

2.2.4 LIGHT MICROSCOPIC ANALYSIS

Strains were examined under a light microscope (Leica DMBL, Germany) for cell size, shape, colour, and developmental features and photographed using a digital camera system (Canon DS126271).

2.2.5 TRANSMISSION ELECTRON MICROSCOPY

Samples were fixed in 2% OsO_4, 0.1 M cocodylate buffer for 2 hours and then allowed to warm to room temperature. The samples were dehydrated by ethanol series and embedded in Spurr's resin (Spurr 1969). Specimens were sectioned using an ultramicrotome (Leica Ultracut,

Reichert–Jung, Germany), stained in 2% uranyl acetate and lead citrate for 5 min each, and examined using a Zeiss EM902 transmission electron microscope (Zeiss, Germany).

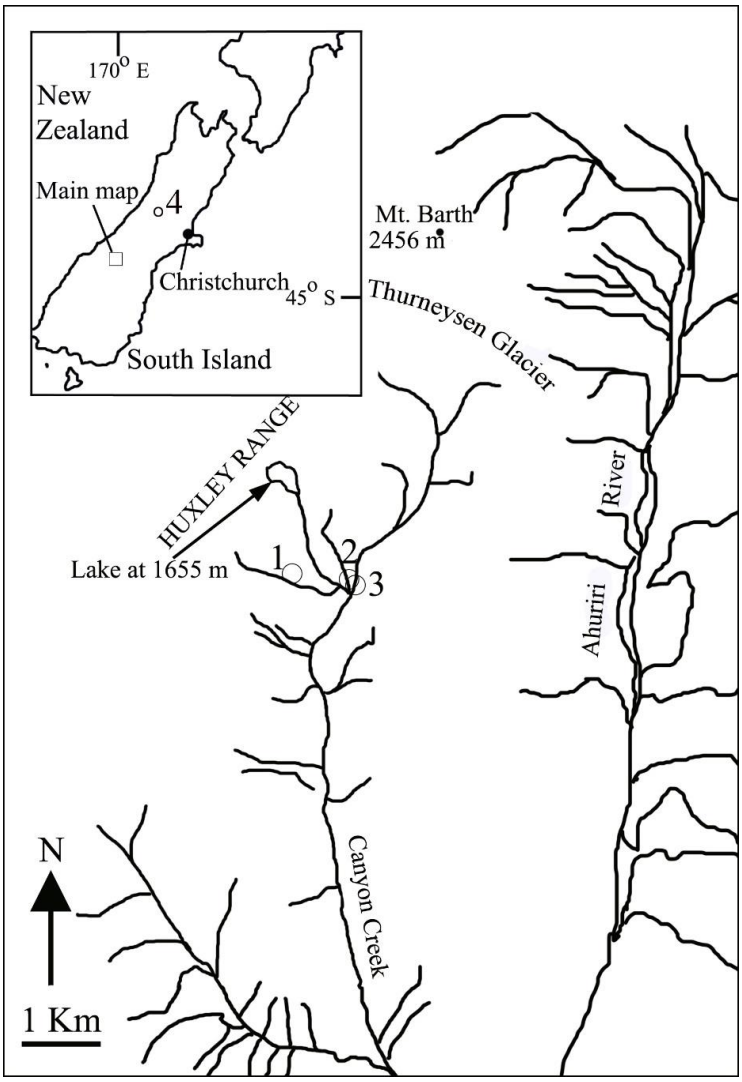

Figure 2.1 Main map shows the collection sites (1,2 & 3) of samples from which strains of Scenedesmaceae LCR-CC-11-1c-1a, LCR-CC-12-1d, LCR-CC-15-1b-1a were isolated (see also Table 2.1). The inset map shows the location of the main map and the collection site (4) of the sample from which strain LCR-CG-7 was isolated.

Table 2.1 Origins of samples taken on 16 February 2011, from which the Upper Canyon Creek strains were isolated (see also Figure 2.1). Data for *Coelastrella ellipsoidea* are from Novis & Visnovsky (2012).

Strain	Description of sample	Locality
Desmodesmus abundans LCR-CC 11-1c-1a	Scum in tarn at 1320 m altitude	44°10’43.58’’S, 169°36’6.75’’E
Coelastrella multistriata var. *grandicosta* LCR-CC 12-1d	Green filaments in tarn 1320 m altitude	44°10'43.58’’S, 169°36'6.75’’E
Desmodesmus granulatus LCR-CC 15-1b-1a	Cyanobacterial mat in tarn 1300 m altitude	44°11'14.38’’S, 169°35'15.29’’E
Coelastrella ellipsoidea LCR-CC-CG7	Alpine herbfield soil 1640 m altitude	42°53'20.189’’S, 171°32'08.460’’E

2.2.6 SCANNING ELECTRON MICROSCOPY

Cells were fixed in 3% gluteraldehyde for 8–10 h, followed by three rinses in buffer without glutaraldehyde. The samples were dehydrated in a graded ethanol series and critical point dried. Dried samples were mounted on stubs, gold coated, and viewed with a JEOL JSM 7000F field emission, high resolution SEM operated by the Department of Mechanical Engineering, University of Canterbury, Christchurch, New Zealand.

2.2.7 DNA ISOLATION AND SEQUENCING

Plates containing unialgal cultures were checked for contamination microscopically. DNA from unialgal cultures was extracted using paramagnetic-particle technology, Automated Maxwell® 16 Instruments (Promega Corporation, Madison, Wisconsin, USA), and the resulting samples processed using Zymo Clean and Concentrate columns, according to the manufacturer's instructions (Zymo Research, Irvine, CA, USA). The extracted DNA was amplified in PCR with primers for the 18S rDNA gene (Hoham *et al.* 2002) and the additional primers Coel18SF1 (5′-AGGGAAGGCAGCAGGCGCGC-3′), Coel18SR1 (5′-CCGGGACTCGGAGTCGACGT-3′), Coel18SF2 (5′-GTGGGTTCTAGCGGTCCGCC-3′) and Coel18SR2 (5′-CCGCCCGTCGCTCCTACCGAT-3′), and visualised using agarose gel electrophoresis and ethidium bromide staining. The amplified products were diluted prior to using in Big Dye Terminator 3.1 sequencing reactions, and capillary separation of the products was carried out by Landcare Research, Auckland, New Zealand. Electropherograms were checked using Sequencher 4.8 (Gene Codes Corporation, Michigan, USA).

2.2.8 PHYLOGENETIC ANALYSIS

Relationships between the algal strains were investigated by comparing the sequences with datasets of algal sequences compiled from GenBank, aligned using ClustalX 1.8 (Thompson *et al.* 1997), and checked by eye. Analyses were carried out using two methods. The first was the program MrBayes v3.1.2B4 (Ronquist & Huelsenbeck 2003), constructing a Bayesian analysis of phylogeny, using MEGA (Tamura *et al.* 2011) to select the model of DNA substitution (GTR+G+I). Two independent runs of 2.5 million generations were used; each with 4 chains and random starting trees, and a consensus tree was constructed discarding the first 500000

generations as burnin (judged from log-likelihood plots). Means of parameter estimates were compared with their associated variances to assess effective modelling and the efficiency of chain swapping was evaluated using the program output. The second method was a maximum-parsimony full heuristic bootstrap (MPB) analysis implemented in PAUP 4.0b10 (Swofford 2002), employing the following settings: branches collapsed if maximum length equals 0, DELTRAN character state optimization, and assignment of character states not observed in terminal taxa allowed at internal nodes. Nonparametric bootstrap values for nodes were calculated on the basis of 1000 resamplings.

The 18S rDNA genes of several *Coelastrella* species contain 1–4 introns (Figure 2.2). The phylogenetic analyses of *Coelastrella* were restricted to 7 intron-containing strains, with 4 strains lacking introns (2 *Coelastrella* and 2 other Scenedesmaceae) as an out-group. After ambiguously aligned regions were removed, the sequences were partitioned into exons and introns prior to Bayesian analysis. Then analyses were run with and without the introns present and the results assessed; the presence of introns strengthened some relationships and did not reduce support for others, so the datasets containing introns were used to produce the final topologies. Finally, the distribution of introns in the different strains was used (by coding intron presence/absence as binary characters) in an exhaustive parsimony search.

Two datasets of 18S rDNA sequences were compiled. The first included strains of *Desmodesmus*, and was 1826 bases long, with 258 variable sites (93 parsimony informative). The length of our *D. granulatus* sequence was 494 bases, and that of *D. abundans* was 1060 bases. The second dataset included strains of *Coelastrella*, and was 2678 bases long (including introns), with 163 variable sites (38 parsimony-informative). The length of our *C. multistriata* var. *grandicosta* sequence was 2486 bases, and that of *C. ellipsoidea* was 1776 bases.

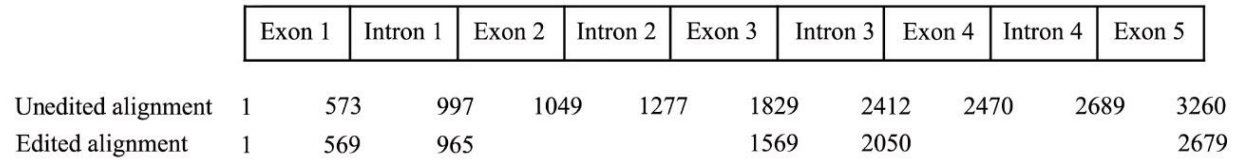

Figure 2.2 Arrangement of exons and introns in the 18S rDNA dataset of *Coelastrella* strains.

2.3 RESULTS

***Coelastrella ellipsoidea* (P.M.Novis & G.Visnovksy) K.Gopalakrishnan, P.M.Novis & G.Visnovsky (Figure 2.3)**

BASIONYM: *Cryptodesmus ellipsoideus* P.M.Novis & G.Visnovsky

REFERENCE: Novis & Visnovsky (2012) p. 18, Figure 3.

NEW ZEALAND LOCALITIES: Alpine herbfield soil, Mt Philistine, Arthur's Pass National Park.

GLOBAL DISTRIBUTION: Not found outside New Zealand to date.

DESCRIPTION:

Cells ellipsoidal to slightly irregular in shape (8–10 µm long, 6–9 µm wide; Figures 2.3A, 2.3B). Chloroplast cup shaped, parietal, with single prominent pyrenoid. Ribs on cell surface, faintly defined and difficult to detect by LM, running between poles, up to approximately 15 per cell (Figures 2.3C, 2.3D). Reproduction by formation of autospores, 2–8 cells per sporangium.

OBSERVATIONS:

The closest sequence to our strain was that of *Coelastrella* sp. F50, with a p-distance of 0.016 (exclusive of intron sequences). This is likely an artifact of the short sequence of sp. F50, since phylogenetic analysis placed the two species quite distantly (Figure 2.5). Also, sp. F50 did not contain introns, whereas *C. multistriata* var. *ellipsoidea* contained intron 1 (Figure 2.2), as did *C.* sp. KGU H001, *C. multistriata* var. *corcontica*, and *C. multistriata* var. *multistriata*. All these organisms were separated from other *Coelastrella* species by robust splits in the Bayesian analysis (Figure 2.5), although they were not collectively resolved into a clade.

Novis & Visnovsky (2012) observed very small protruberances on the cell wall of this species, visible by TEM. A new examination of the cells by SEM, showing ribs running longitudinally between poles, identified the strain as a species of *Coelastrella*, and the introns present in the 18S rDNA genes of many of these species misled the original BLAST search. Here, we correct the earlier taxonomy.

CULTURE: LCR-CG7

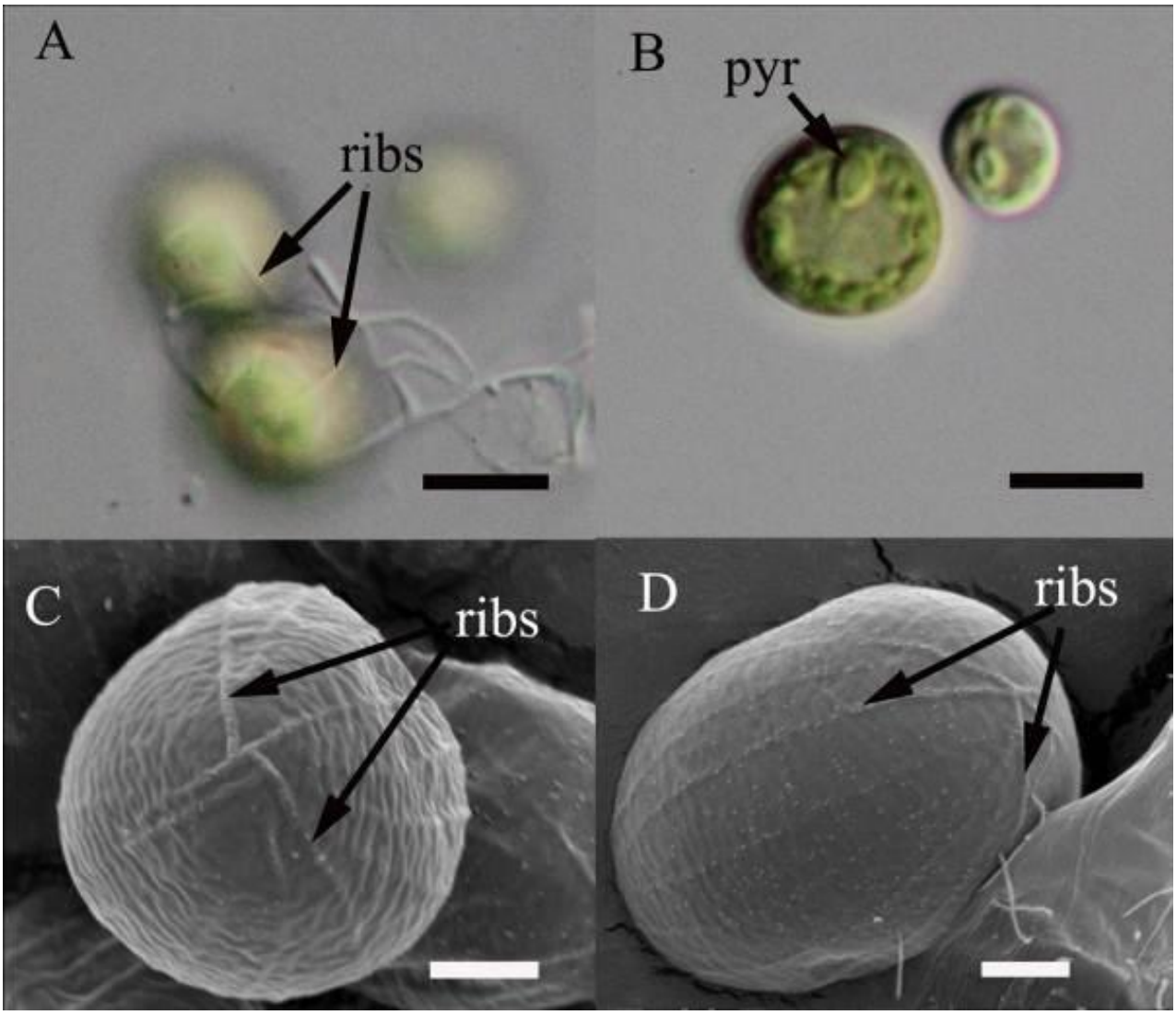

Figure 2.3 *Coelastrella ellipsoidea* (photographed from culture LCR-CG7). **A, B**, light micrographs, **D, E,** scanning electron micrographs. **A,** Fine ribs on outer surfaces of cells. **B, A** mature cell containing a pyrenoid surrounded by starch. **C, D,** Ribs run longitudinally between poles, where they anastomose. Note the finer nature of the ribs in this species compared to *Coelastrella multistriata* var. *grandicosta*. Scales: 10 µm in **A** and **B** and 1 µm in **C** and **D.**

***Coelastrella multistriata* var. *grandicosta* K.Gopalakrishnan, P.M.Novis & G.Visnovsky (Figure 2.4)**

NEW ZEALAND LOCALITIES: Upper Canyon Creek (see Table 2.1).

DESCRIPTION:

Cells ellipsoidal in shape (7–12 µm long and 6–9 µm wide). Chloroplast parietal, with single pyrenoid. Distinct longitudinal ribs (approximately 9–12 per cell) running between poles (Figures 2.4E, F). Cell wall structured in multiple layers (Figure 2.4D). Reproduction by autosporangia containing 4–8–16 daughter cells (Figure 2.4B). Mature cells produce red cytoplasmic pigment when grown on solid medium.

OBSERVATIONS:

The isolate from upper Canyon Creek differed from *Coelastrella* sp. KGU-H001 by a p-distance of 0.01. The introns present in the 18S rDNA gene (Figure 2.2) of *Coelastrella* sp. KGU-H001, *C. multistriata* var. *multistriata* strain C6-2 and *C. corcontica* strain Kalina 1967/9 differ. *Coelastrella* sp. KGU-H001 contains intron 1, var. *multistriata* and var. *corcontica* both contain introns 1 and 3, whereas var. *grandicosta* only contains intron 3. Intron 3 is alignable where present in these strains, and a 31 base deletion has occurred in var. *grandicosta* relative to the others. Phylogenetic analysis failed to resolve the relationships between these taxa (Figure 2.5).

Coelastrella multristriata var. *grandicosta* has the same cell size as var. *multistriata*, but has more pronounced ribs (Ettl & Gärtner 1995). The prominent ribs also distinguish our strain from *C. ellipsoidea* (above) and *C. corcontica* (Kalina 1987), from which it also differs

substantially in 18S rDNA sequence (0.020 p-distance for *C. ellipsoidea*). In our opinion, the similarity in the 18S rDNA sequence between this strain and other varieties of *C. multistriata* (Figure 2.5) is too high to warrant erecting a new species, but the variation is consistent with that between varieties, with a commensurate level of morphological distinctiveness. We anticipate that another new variety of *Coelastrella multistriata* could be erected to accommodate sp. KGU-H001, but morphological data do not yet seem to be available for this strain.

CULTURE: LCR-CC-12-1d

***Desmodesmus abundans* (Kirchner) E.Hegewald (Figure 2.6)**

REFERENCE: Tsarenko & John (2002) p. 420.

NEW ZEALAND LOCALITIES: upper Canyon Creek (this study), Whangamarino Swamp, Wallaceville, and Lake Rotomanuka (Etheridge 1983).

GLOBAL DISTRIBUTION: cosmopolitan.

DESCRIPTION:

Cells ellipsoidal (10–15 µm long and 5–8 µm wide) to spherical (8–15 µm diameter) in shape (Figure 2.6A). Chloroplast parietal, with clearly visible pyrenoid surrounded by a sheath of starch plates (Figure 2.6C). Ribs occur rarely (1–2 per cell) on the cell wall, and are accompanied by spines approximately 1 µm long, up to 10 per cell (Figures 2.6E, F). Coenobia not observed. Autospores produced by longitudinal division, 2–8 per sporangium (Figure 2.6B). Granular cytoplasm. Orange to red pigment droplets, sometimes copious, in aging cells.

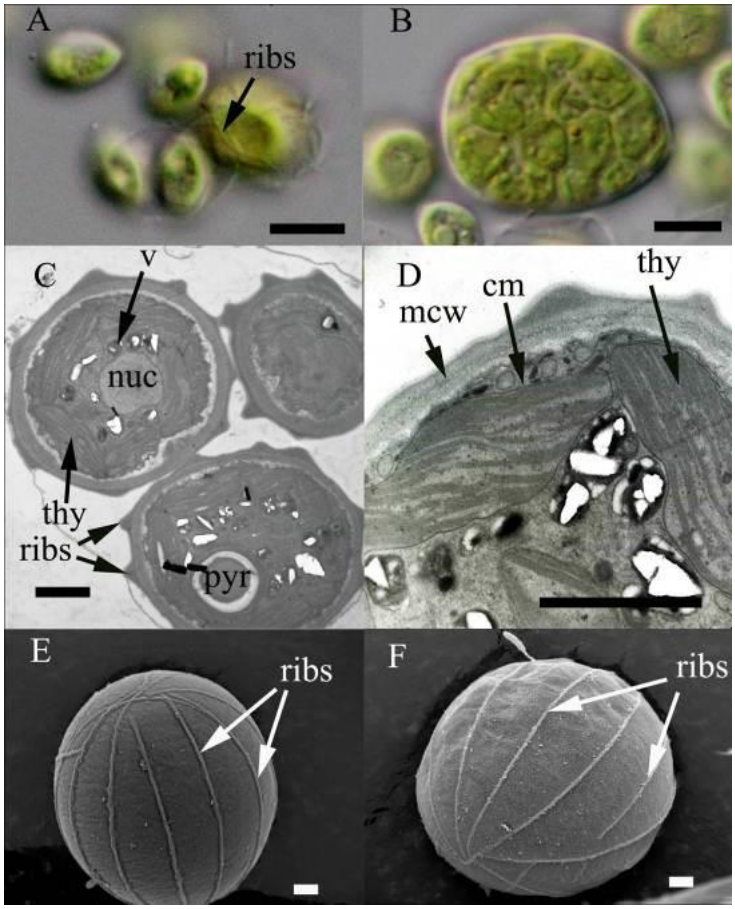

Figure 2.4 *Coelastrella multistriata* var. *grandicosta* var. nov. (Photographed from culture LCR-CC 12-1d). **A, B,** light micrographs, **C, D,** Transmission electron micrographs **E, F,** Scanning electron micrographs **A,** Ribs on cell surfaces are indicated. **B,** Autosporangium containing daughter cells. **C**, Section of daughter cells inside a sporangium showing pyrenoid (pyr), thylakoid (thy), nucleus (nuc) vesicles (v) and the ribs on the cell wall outer surfaces. The ribs are much more defined than in *C. ellipsoidea* (Figure 3 and Novis & Visnovsky 2012). **D,** Higher magnification view of one cell showing multi layered cell wall (mcw), thylakoid membranes (thy) and chloroplast membrane (cm). **E, F,** scanning electron micrograph showing longitudinal ribs, which anastomose at the poles, on the surface of two cells. Scales: 10 µm in **A** and **B,** 1 µm in **C, D, E** and **F**.

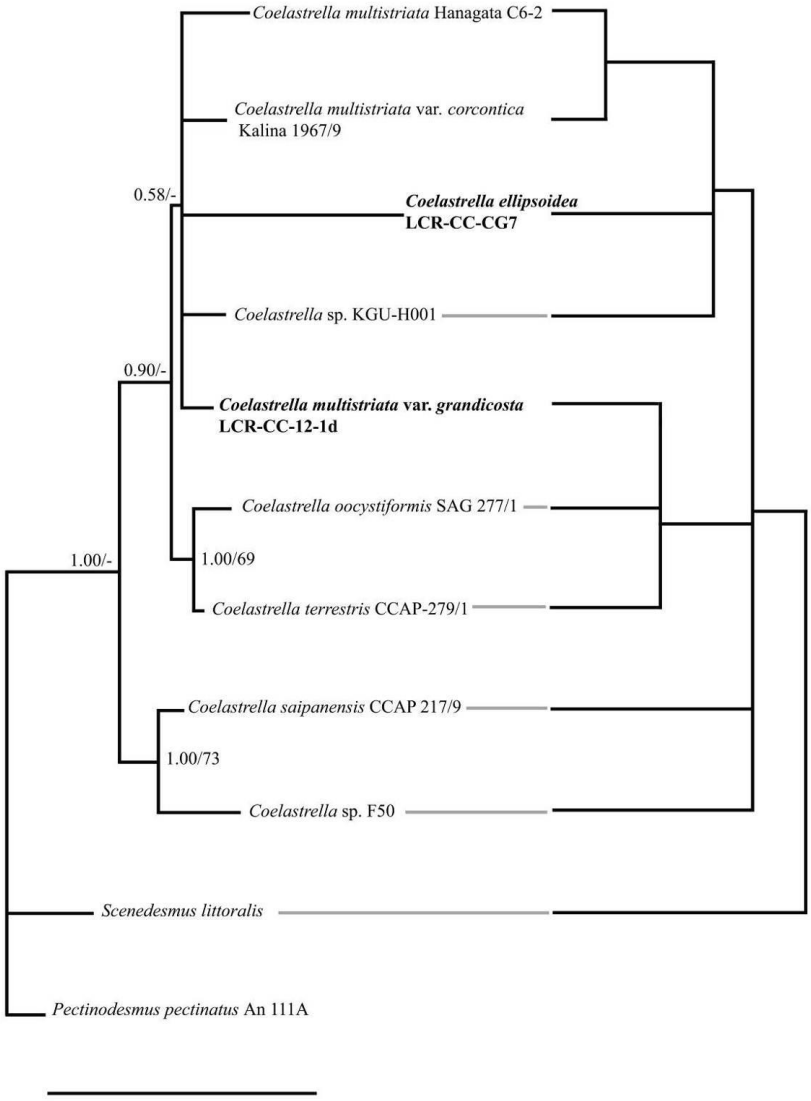

Figure 2.5 Phylogeny of *Coelastrella* spp. Left, Bayesian topology resulting from a partitioned analysis of 18S rDNA exons and introns, compared with (right) one of the four most parsimonious trees resulting from an analysis of binary-coded intron distribution, which most closely matches the Bayesian topology. The bottom four taxa lack introns. Values above branches on the left-hand tree correspond to Bayesian posterior probabilities/Maximum Parsimony bootstrap values. Scale bar = 0.1 substitution per site (apply to left hand topology only).

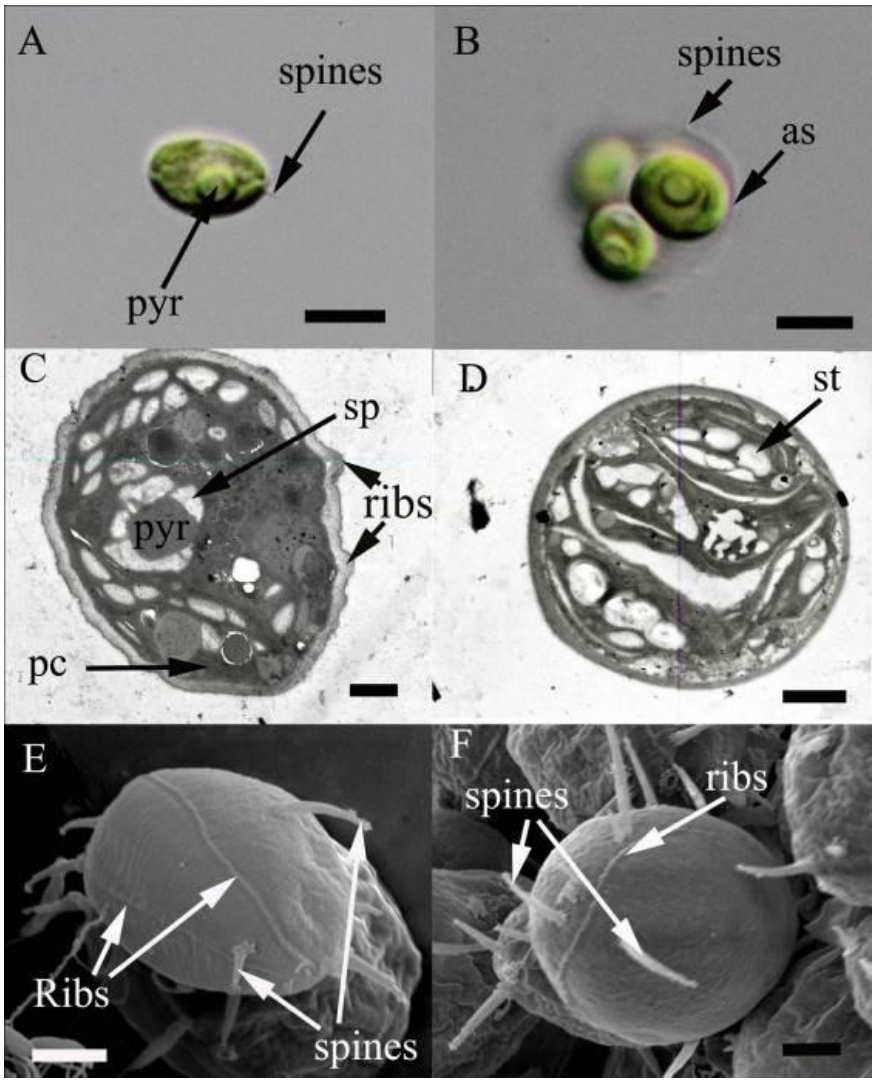

Figure 2.6 *Desmodesmus abundans* (photographed from culture LCR-CC 11-1C-1A). **A, B,** light micrographs, **C, D,** Transmission electron micrographs, **E, F,** Scanning electron micrographs. **A,** Spines are faintly visible by light microscopy, and the pyrenoid is also indicated. **B,** Spines may also occur on the autosporangium wall (as). **C**, Section of the cell showing pyrenoid (pyr) surrounded by starch plates (sp) and ribs or spines on the outer surface. The parietal choloroplast (pc) is also indicated. **D,** Starch (st) is abundant inside the chloroplasts. **E, F,** Ribs and spines are indicated on the cell surfaces. Scales: 10 µm in **A** and **B,** 1 µm in **C, D, E** and **F**.

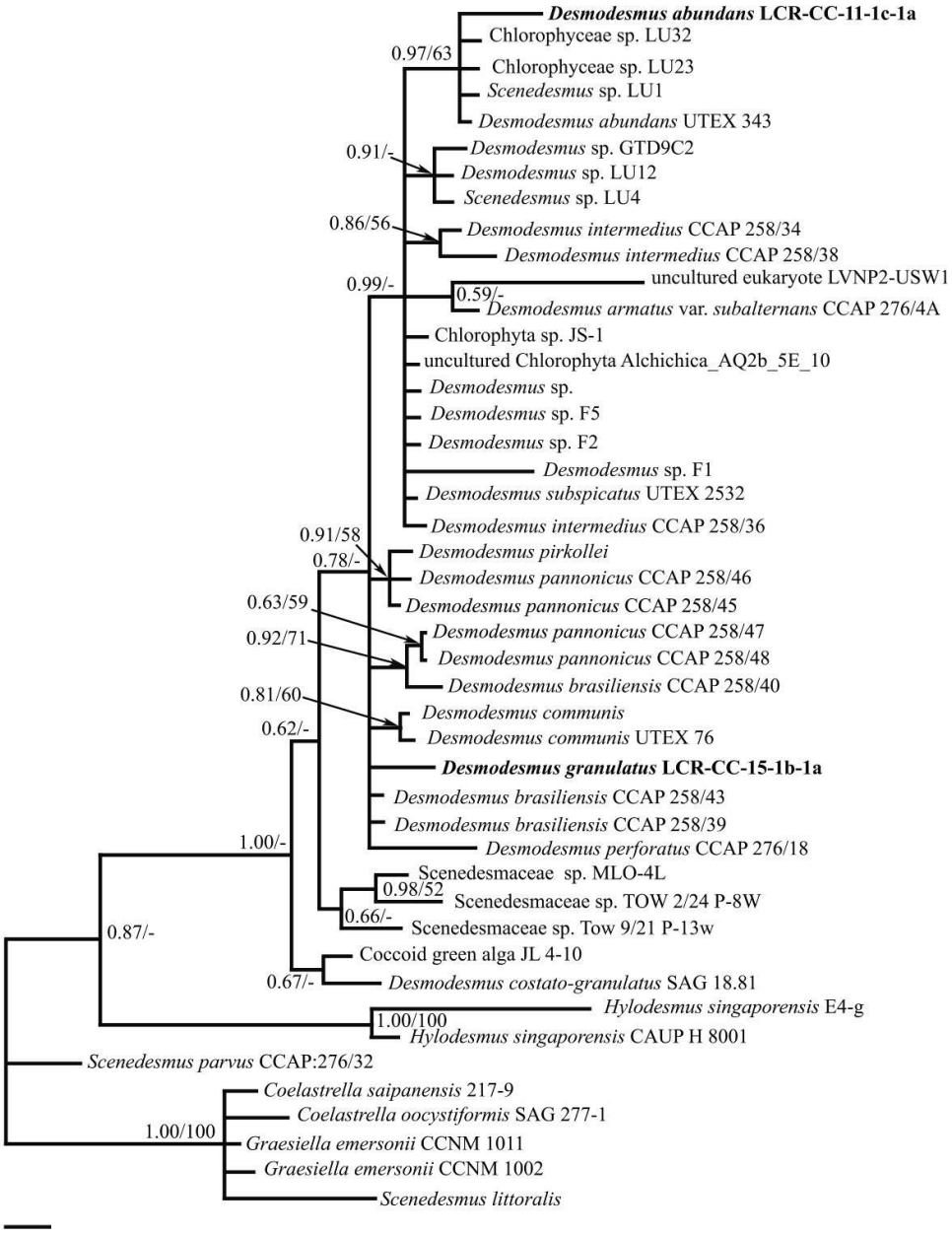

Figure 2.7 Phylogenetic analysis of selected Scenedesmaceae inferred from 18S rDNA sequences. The tree topology is that inferred using MrBayes v3.1.2B4 (2.5 million generations). Values above branches correspond to Bayesian posterior probabilities/Maximum Parsimony bootstrap values. Scale bar represents 0.1 changes/site.

OBSERVATIONS:

The isolate from upper Canyon Creek differed from Chlorophyceae species LU32, LU31 and *Scenedesmus* sp. LU1 by a p-distance of 0.03 over the 18S region sequenced. These strains were isolated from the USA, but descriptive information is not available; they could presumably be referred to *D. abundans*. The topology inferred using MrBayes (Figure 2.7) groups these strains with ours in a robust clade, which was also recovered using the Maximum parsimony bootstrap method with low support (63%).

The cells possess spines of the same length as those described by Tsarenko & John (2002). Most taxa in Scenedesmaceae form coenobia, but they were lacking in our cultures of both this isolate and *D. granulatus* (below). However, coenobium production depends on the habitat and the predators living in that habitat. Coenobia of *D. abundans* as described by Tsarenko & John (2002) are absent in the New Zealand strain under the present cultivation conditions.

CULTURE: LCR-CC-11-1C-1A

***Desmodesmus granulatus* West & G.S.West (Figure 2.8)**

REFERENCE: Tsarenko & John (2002), p. 444.

NEW ZEALAND LOCALITIES: upper Canyon Creek (new record for New Zealand).

GLOBAL DISTRIBUTION: Britain, Portugal and Romania.

DESCRIPTION:

Cells ovoid (8–13 µm long and 6–10 µm wide) to spherical, 6–10 µm diameter. Chloroplast parietal, containing single prominent pyrenoid with starch sheath comprised of few segments and often a single thylakoid membrane traversing the pyrenoid matrix. Warts on cell wall surface, difficult to resolve by LM (Figure 2.8B) but clearly visible under TEM and SEM (Figures 2.8D–G). Warts form on daughter cell walls prior to autospore release (Figure 2.8E). Coenobia not observed. Reproduction by autospore formation (4–8–16 per sporangium).

OBSERVATIONS:

This isolate differed from its nearest relatives by p-distances of 0.06. These relatives are *Desmodesmus brasiliensis* (Bohlin) E.Hegewald CCAP 258/43, 258/40, *D. pannonicus* (Hortobagyi) E.Hegewald 258/47, 258/48, *D. communis* (E.Hegewald) E.Hegewald UTEX 76, AICB 141, and *D. pirkollei* E.Hegewald. The tree topology inferred using MrBayes (Figure 2.7) robustly placed *Desmodesmus granulatus* in a large clade of *Desmodesmus* isolates. However, we were unable to resolve the position of our strain further, likely due to the short sequence we were able to recover (484 bp).

D. brasiliensis, which is closely related according to molecular data, lacks the warty protrusions found in *D. granulatus.* Although some of the closest relatives of our strain show warts on their surfaces, this character does not seem to correspond to a clade of Desmodesmus species. Other species of *Desmodesmus* possess similar structures such as *D. costato-granulatus* (Skuja) E.Hegewald, *D. pannonicus*, *D. communis* and *D. pirkollei* are not close relatives of our *D. granulatus*.

CULTURE: LCR-CC-15-1b-1a

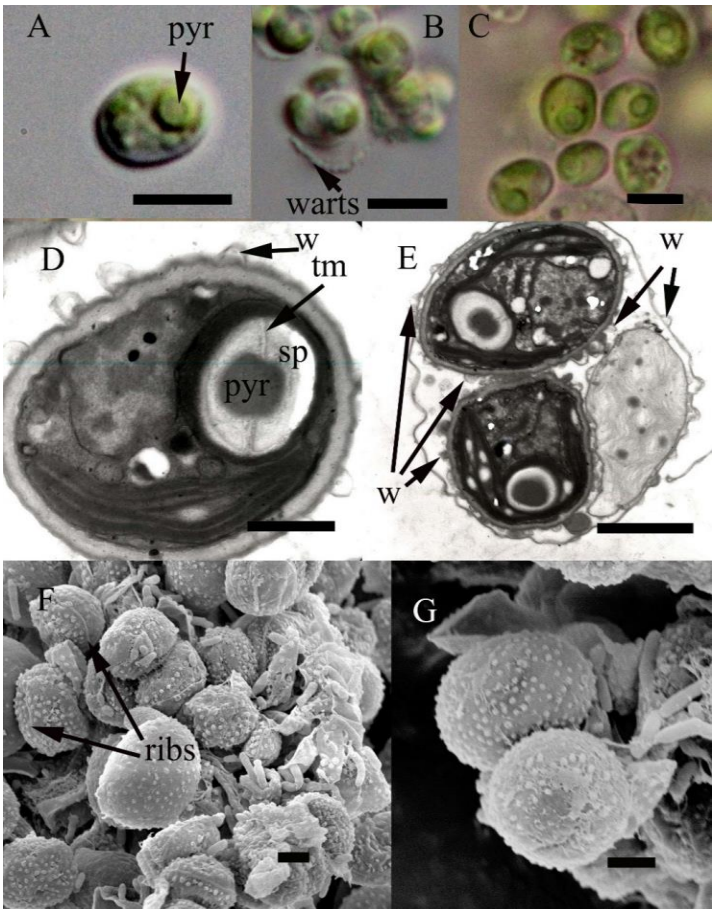

Figure 2.8 *Desmodesmus granulatus* (photographed from culture LCR-CC 15-1b-1a). **A–C,** light micrographs, **D, E,** Transmission electron micrographs, **F**, **G,** Scanning electron micrographs. **A,** Typical mature cell with pyrenoid (pyr) visible. **B,** Warts are rarely visible by light microscopy, shown here on the surface of a detached sporangial cell wall. **C,** Cells of varying size in agarised culture. **D,** Section showing a single prominent pyrenoid (pyr), which has a starch sheath of plates with few segments (sp) and often a single thylakoid membrane (tm) traversing the pyrenoid matrix. Warts (w) are visible on the external surface of the cell wall. **E**, Cells inside a sporangium, as well as the sporangium wall surrounding the daughter cells, possess warts (w). **F, G,** Warts are variably distributed on the cell surfaces, and ribs are also visible on the left-hand cells in **F.** Scales: 10 µm in **A**-**C** 1 µm in **D** and **E.** 1 µm in **F** and **G.**

2.3 DISCUSSION

My study added 1 new variety of a species, 1 new record, and 1 new combination to the list of 26 Scenedesmaceae already described from New Zealand, of which some are still considered provisional (Broady *et al*. 2012). As well as in lowland environments, Scenedesmaceae clearly have significant diversity in New Zealand alpine regions, based on the 2 sites investigated to date. Their presence in alpine New Zealand is not surprising, since Scenedesmaceae on Ross Island, Antarctica are already known (Lesser *et al*. 2002), as well as alpine *Coelastrella* spp. from Europe (Ettl & Gärtner 1995). Lewis & Flechtner (2002) demonstrated that Scenedesmaceae have high diversity in desert soils and also found that they were evolved from aquatic green algae. My strains from alpine regions are also close relatives of aquatic green algae from lowland areas.

A common feature of my alpine strains and Scenedesmaceae isolated from deserts (Lewis & Flechtner 2004) is their lack of coenobia in culture. It is well known that the formation of coenobia can be influenced by the environment. *Scenedesmus subspicatus* cultures that were initially composed of individual cells and formed 8 celled colonies with armoured spines upon the introduction of *Daphnia magna* Straus (Hessen & Van Donk 1993), showed that coenobial colonies can be induced by the biochemical substances produced by grazers. The absence of this morphology in both our strains and those of Lewis & Flechtner (2002) could reflect the lower grazing pressure experienced in the more rigorous habitats from which they were isolated. Nonetheless, this morphology may well remain inducible under the right conditions in our strains.

Many Scenedesmaceae are difficult to recognise using microscopy, because some features are unlikely to be resolved at the light microscope level. Electron microscopy reveals

important details of wall ornamentation, but identification may still be problematic, due to the great morphological plasticity of the members of this family. This is likely to lead to misinterpretation of Scenedesmaceae as members of other groups – the nomenclatural confusion between *Desmodesmus abundans* and *Chlorella fusca* is an example of this – and leads to skepticism of historical records that are accompanied by little supporting information (Broady *et al*. 2012).

Molecular data may assist in avoiding misinterpretations. The identification of *D. abundans* was confirmed by molecular data (although not so *D. granulatus*). The species identification of *D. granulatus* relies on morphological data, and is subject to the uncertainties described above. Usually 18S rDNA sequences are chosen to identify close relatives, due to their wide usage (Hanagata 1998). Internal transcribed spacer (ITS) sequences are gaining favour in Scenedesmaceae (Hegewald *et al.* 2010) as they offer more resolution, but are not yet common enough to supplant 18S rDNA as a diagnostic tool.

Also, it is evident that 18S rDNA sequences for some Scenedesmaceae have been subject to the acquisition and possible movement of introns. In both of our *Coelastrella* strains, introns were identified (Figures 2.2, 2.5). Genbank records show that these introns are commonly present in 18S rDNA sequences of *Coelastrella*. Introns 3 and 4 appear to be homologues, and a search of the RFAM database (Burge *et al*. 2013) using intron 3 matched a known Group I intron (bits score of 90.6 and E-value 5.1e-12). Including the intron sequences in the analysis strengthened some relationships and did not erode others. This suggests a component of vertical inheritance, also implied by the confinement of introns to a single clade of *Coelastrella* (Figure 2.5) and the greater alignability of intron sequences in some strains than others. However, identification as Group I introns implies horizontal transfer, explaining why phylogenies

constructed using sequences and intron distributions are not completely concordant. It is not presently possible to resolve this combination of vertical and horizontal inheritance.

Table 2.2 Names and GenBank accession numbers of strains used in the study. New sequences are indicated in bold letters.

Taxon	Strain	18S accession
Chlorophyceae sp.	LU23	JQ360532
	LU32	JQ360541
Chlorophyta sp.	JS-1	HQ900842
Coccoid green alga	JL 4-10	AY195982
Coelastrella multistriata (Trenkwalder) Kalina & Puncocharova	Hanagata C6-2	AB012846
Coelastrella multistriata corconica T.Kalina & M.Puncochárová) E.Hegewald & N.Hanagata	Kalina 1967/9	AB037082
Coelastrella ellipsoidea (P.M.Novis & G.Visnovksy) K.Gopalakrishnan, P.M.Novis & G.Visnovsky.	LCR-CG7	**KC861672**
Coelastrella multistriata var. *grandicosta* K.Gopalakrishnan, P.M.Novis & G.Visnovsky	LCR-CC-12-1d	**KC861673**
Coelastrella oocystiformis (J.W.G.Lund) E.Hegewald & N.Hanagata	SAG 277-1	AB012848
Coelastrella saipanensis N.Hanagata	CCAP 217-9	AB055800
Coelastrella sp.	F50	JQ867369
	KGU-H001	AB742452
Coelastrella terrestris (Reisigl) Hegewald & N. Hanagata	CCAp-279-1	AB012847
Desmodesmus abundans (Kircher) E.Hegewald	UTEX 343	X73995
	LCR-CC-11-1C-1A	**KC861671**
Desmodesmus armatus var. *subalternans* (G.M. Smith)	CCAP:276/4A	FR865727

E.Hegewald		
Desmodesmus brasiliensis (Bohlin) E.Hegewald	CCAP:258/43	FR865707
	CCAP:258/39	FR865704
	CCAP:258/40	FR865705
Desmodesmus communis (E.Hegewald) E.Hegewald		JQ922412
	UTEX 76	X73994
Desmodesmus costato-granulatus (Skuja) E.Hegewald	SAG 18.81	X91265
Desmodesmus granulatus (West & G.S West) P.Tsarenko	LCR-CC-15-1b-1a	**KC861670**
Desmodesmus intermedius (Chodat) E.Hegewald	CCAP:258/36	FR865701
	CCAP:258/34	FR865699
	CCAP:258/38	FR865703
Desmodesmus pannonicus (Hortobagyi) E.Hegewald	CCAP:258/45	FR865709
	CCAP:258/48	FR865712
	CCAP:258/47	FR865711
	CCAP:258/46	FR865710
Desmodesmus perforates (Lemmermann) E.Hegewald	CCAP:276/18	FR865714
Desmodesmus pirkollei E.Hegewald		AF348496
Desmodesmus sp.	GTD9C2	JQ315186
	LU12	JQ360522
	F1	JF835991.1
	F2	JF835992.1
	F5	JF835993.1
Desmodesmus subspicatus (Chodat) E.Hegewald & A.Schmidt	UTEX 2532	AJ249514.1
Graesiella emersonii Shihira & R.W.Krauss	CCNM 1011	JX051614
	CCNM 1002	JX051613
Hylodesmus singaporensis Eliás, M., Nemcová, Y., Skaloud, P., Neustupa, J., Kaufnerová, V. & Sejnohová., L.	E4-g	FJ715936
	CAUP H 8001	FJ436342

Pectinodesmus pectinatus (Meyen) E.Hegewald, M.Wolf, Al.Keller, Friedl & Krienitz	An 111A	AB037092
Scenedesmaceae sp.	Tow 9/21 p-13w	AY197638
	MLO-4	AY197627
	Tow 2/24 p-8w	AY197634
Scenedesmus littoralis Hanagata		AB055801
Scenedesmus parvus (G.M.Smith) Bourrelly	CCAP:276/32	FR865718
Scenedesmus sp.	LU1	JN707703
	LU4	JQ327826
uncultured Chlorophyta	Alchichica_AQ2b_5E_10	JN825661
uncultured eukaryote	LVNP2-USW124-11-1200R	DQ512601

CHAPTER 3

TAXONOMY OF TREBOUXIOPHYCEAN AND CHLAMYDOMONADALEAN ALPINE ALGAE FROM CANYON CREEK

CHAPTER 3

TAXONOMY OF TREBOUXIOPHYCEAN AND CHLAMYDOMONADALEAN ALPINE ALGAE FROM CANYON CREEK

3.1 INTRODUCTION

Taxonomic studies on alpine algae in New Zealand have been few. These studies are variable in location, extent, and taxa. Mount Philistine, Arthurs Pass National Park (Novis 2001, Novis 2002a, Novis 2002b, Novis *et al*. 2008a, Novis *et al.* 2008b, Novis & Visnovsky 2011b, Novis & Visnovsky 2012) and Mount Cook National Park (Wilson 1976) have received more detailed attention, while other places such as Canyon Lake, Mount Oates, Woolshed Hill and Whakapapa Glacier have been previously studied with one or two samples from each spot (Broady 1996, Novis 2001, Novis *et al*. 2008a, Novis & Visnovsky 2012). Of these sites, Mt. Philistine is the only locality in which culture study and molecular investigation had been combined until a recent study of Scenedesmaceae in upper Canyon Creek (Gopalakrishnan *et al*. 2014). Studies of the alpine algal flora of Mt Philistine had previously revealed five new records for New Zealand (Novis *et al*. 2008a), and nine species new to science (Novis & Visnovsky 2011b, Novis & Visnovsky 2012), showing the power of the combined approach.

Gopalakrishnan *et al*. (2014) documented four strains of Scenedesmaceae from Canyon Creek: of these, *Desmodesmsus granulatus* West & G.S. West was a new record for New

Zealand and *Coelastrella multistriata* var. *gandicosta* K. Gopalakrishnan, P.M. Novis & G. Visnovsky was new to science. Here, we extend this approach to other groups of green algae from the Canyon Creek site, with the aim of comparison with the other site that has received similar treatment (Mt Philistine).

Green algae are extremely diverse, having a wide range of cellular organisation, and also exhibiting different metabolic responses to different environmental conditions (Happey-Wood 1988). The majority of algae present in alpine regions are Cyanobacteria, Chlorophyceae, Trebouxiophyceae and Charophyceae. The last three of these groups are quite frequently identified in snow, and they are the major causes of its green and red coloration. Other algae which are less frequently identified in alpine regions are diatoms, Xanthophyceae, Chryosophyceae, Dinophyceae, and Euglenophyceae (Stein 1963, Kol 1968, Javornický & Hindák 1969). These latter groups are usually only seen with the aid of microscopy (Hoham & Duval 2001). Groups of algae identified from Mt. Philistine previously are Chlorophyta, Cyanophyta, Heterokontophyta and Streptophyta (Novis 2002b, Novis *et al*. 2008a, Novis & Visnovsky 2011b, Novis & Visnovsky 2012).

We report seven strains of green algae. Among these are two proposed as new to science: *Variochloris* sp. and *Ettlia* sp. The species *Lobochlamys segnis* (H.Ettl) T.Pröschold, B.Marin, U.W.Schlösser & M.Melkonian, *Diplosphaera mucosa* Broady and *Chloromonas palmelloides* P. A. Broady, were new records for New Zealand. The species *Pseudococcomyxa simplex* (Mainx) Fott has been identified in New Zealand previously but the genetic distance between some strains is high. *Oocystis minuta* Guillard, H.C.Bold & MacEntee was also previously identified in New Zealand but here we report genomic data for the first time in a New Zealand strain.

3.2 MATERIALS AND METHODS

3.2.1 COLLECTION SITE

Sampling was carried out in upper Canyon Creek, Ahuriri Conservation Park, South Island, New Zealand (Figure 3. 1). Details of the samples from which the taxa described here were isolated are given in Table 3.1. Each sample (approximately 1–2 g) was taken directly into a sterile 9 ml polycarbonate test-tube with a screw-top lid by pushing the uncapped tube through the material to be sampled. Collected samples were refrigerated overnight at the field camp and two days in the laboratory before inoculation of cultures.

3.2.2 CULTURING

Please refer to chapter two.

3.2.3 LIGHT MICROSCOPIC ANALYSIS

Please refer to chapter two.

3.2.4 TRANSMISSION ELECTRON MICROSCOPY

Please refer to chapter two.

3.2.5 DNA ISOLATION AND SEQUENCING

Plates containing unialgal cultures were checked for contamination microscopically. DNA from unialgal cultures was extracted using paramagnetic-particle technology, Automated Maxwell®

16 Instruments (Promega Corporation, Madison, Wisconsin, USA), and the resulting samples processed using Zymo Clean and Concentrate columns, according to the manufacturer's instructions (Zymo Research, Irvine, CA, USA). The extracted DNA was amplified in PCR with primers for the 18S rDNA gene (Hoham *et al*. 2002) and the *rbc*L gene (Nozaki *et al.* 1995) and visualised using agarose gel electrophoresis and ethidium bromide staining. The amplified products were diluted prior to using in Big Dye Terminator 3.1 sequencing reactions, and capillary separation of the products was carried out by Landcare Research, Auckland, New Zealand. Electropherograms were checked using Sequencher 4.8 (Gene Codes Corporation, Michigan, USA).

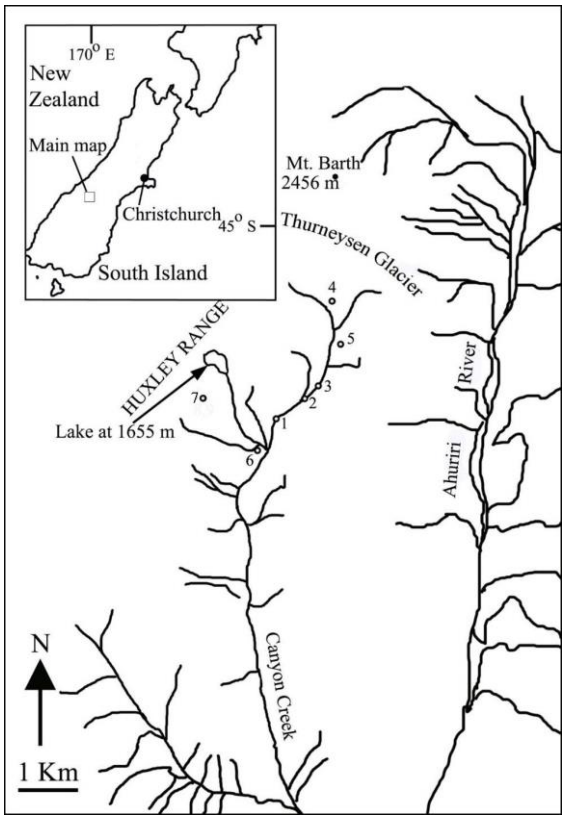

Figure 3.1 Main map shows the collection sites of samples from which strains were isolated (see also Table 1). The inset map shows the location of the main map.

Table 3.1 Origins of samples taken on 16 February 2011, from which the Upper Canyon Creek strains were isolated (see also Figure 3.1).

Sample collection spot (Figure 3.1)	Strain	Description of sample	Altitude (m)	Locality
1	*Oocystis minuta* LCR-CC 3-1a	Mossy boulder	1280	44°11’7.26’’S, 169°35’32.72’’E
2	*Lobochlamys segnis* LCR-CC 5-1a	Moss wash sample	1300	44°11’2.83’’S, 169°35’41.87’’E
3	*Pseudococcomyxa simplex* LCR-CC 6-1b	Bare black soil near camp site	1300	44°10'59.44’’S, 169°35'49.25’’E
4	*Variochloris* sp. LCR-CC 7-1a	Faint coloured snow at the head of Canyon Creek	1400	44°10'24.33’’S, 169°36'2.48’’E
5	*Diplosphaera mucosa* LCR-CC-14-1b	Small stream below tarn	1320	44°10'44.32’’S, 169°36'7.15’’E
6	*Chloromonas palmelloides* LCR-CC-18-1a	Soil on stream bank	1280	44°11'20.49’’S, 169°35'11.38’’E
7	*Ettlia* sp. LCR-CC-26-1f	Green coloured rainwater pool above lake	1700	44°10'58.91’’S, 169°34'39.59’’E

3.2.6 PHYLOGENETIC ANALYSIS

Relationships between the algal strains were investigated by comparing the sequences with datasets of algal sequences compiled from GenBank, aligned using ClustalX 1.8 (Thompson *et al*. 1997), and checked by eye. Analyses were carried out using two methods. The first was the program MrBayes v3.1.2B4 (Ronquist & Huelsenbeck 2003), constructing a Bayesian analysis of phylogeny, using MEGA 6 (Tamura *et al.* 2013) to select the model of DNA substitution (GTR+G+I). Two independent runs of 2.5 million generations were used; each with 4 chains and random starting trees, and a consensus tree was constructed discarding the first 500000 generations as burnin (judged from log-likelihood plots). Means of parameter estimates were compared with their associated variances to assess effective modelling and the efficiency of chain swapping was evaluated using the program output. The second method was a maximum-parsimony full heuristic bootstrap (MPB) analysis implemented in PAUP 4.0b10 (Swofford 2002), employing the following settings: branches collapsed if maximum length equal 0, DELTRAN character state optimization, and assignment of character states not observed in terminal taxa allowed at internal nodes. Nonparametric bootstrap values for nodes were calculated on the basis of 1000 resamplings.

3.3 RESULTS

TAXONOMY

Domain **Eukaryota**

Kingdom **Plantae**

Division **Chlorophyta**

Class **Chlorophyceae**

***Chloromonas palmelloides* Broady (Figure 3.2)**

REFERENCE: Broady 1977

NEW ZEALAND LOCALITIES: upper Canyon Creek (this study).

GLOBAL DISTRIBUTION: Antarctica: Signy Island, South Orkney Islands (Broady 1977)

DESCRIPTION:

Cells wide ellipsoidal or ellipsoidal–oval, 11–20 µm long and 5–15 µm wide, with thick cell wall. Chloroplast perforated and lobed. No pyrenoids were observed in the chloroplast under LM or TEM. Papilla prominent, containing flagellar grooves (Figure 3.2 C). Nucleus central in protoplast. Reproduction by zoosporangia with four or eight zoospores within the parental cell wall (Figure 3.2 A).

OBSERVATIONS:

In the 18S dataset there are 13 strains with identical sequences to our isolate *Chloromonas palmelloides.* These are seven strains identified as *Chloromonas rosae*, four strains of *Chloromonas reticulata*, one strain of *Chloromonas clathrata* and one "*Chloromonas* sp." The 18S rDNA sequences of LCR-CC-18-1a and *Chloromonas palmelloides* SAG 32.86 differ by a p-distance of 0.001; however, these two strains are more similar in morphology than the others. *Chloromonas palmelloides* is the only candidate having an ellipsoidal to oval cell shape with a perforated cup-shaped chloroplast.

CULTURE: LCR-CC-18-1a

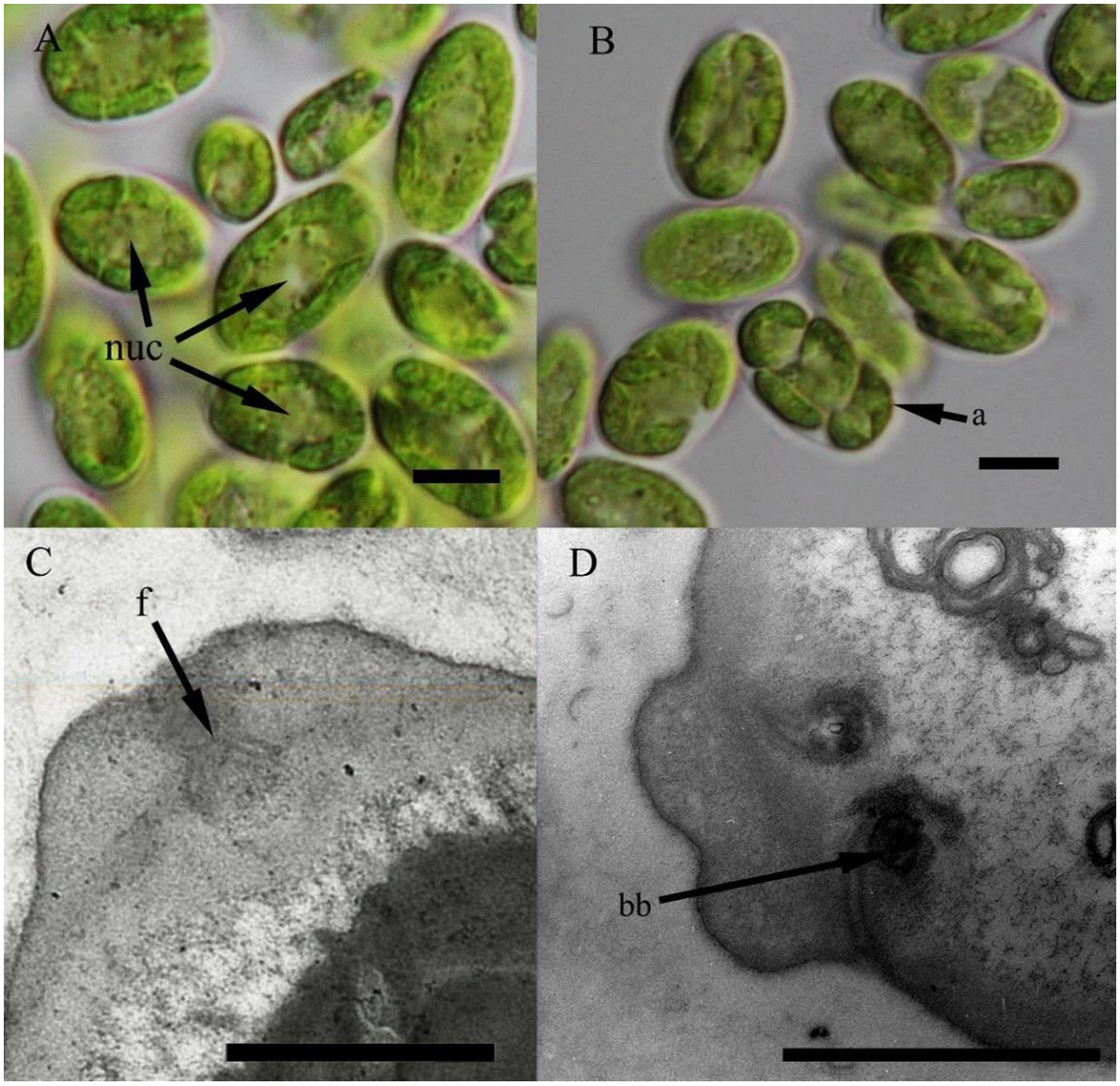

Figure 3.2 *Chloromonas palmelloides* (Photographed from culture LCR- CC-18-1a). **A and B** light micrographs, **C and D** transmission electron micrograph. **A** Mature cells showing nuclei (nuc) **B.** Dividing cells at different stages of autosporangia formation (a). **C** Section of the papilla showing flagellar groove (f) **D** Papilla showing its bimamellate structure and basal bodies (bb) below. Scales: 10 µm in **A** and **B,** 1 µm in **C** and **D.**

***Diplosphaera mucosa* Broady (Figure 3.3)**

REFERENCE: Broady 1983

NEW ZEALAND LOCALITIES: upper Canyon Creek (this study).

GLOBAL DISTRIBUTION: Antarctica (Broady 1983)

DESCRIPTION:

Cells spherical to irregular in shape (6–10 µm long and 5–9 µm wide). Chloroplast cup-shaped, parietal. Mature cells showing single prominent pyrenoid, sometimes surrounded by starch granules. Reproduction by formation of autospores, 2–4 per sporangium (Figure 3.3 B). Cells in colonies adhere to each other with mucilage. Pyrenoid matrix bisected by several parallel thylakoids.

OBSERVATION:

The closest relative of our strain in the phylogenetic tree is *Diplosphaera mucosa* with a p-distance of 0.007. The tree topology inferred using MrBayes and MPB robustly support the *Diplosphaera mucosa* branch with nodal value 0.99 and 71 respectively (Figure 3.10).

The phylogeny demonstrates a sister relationship between my strain and *Diplosphaera mucosa* SAG 48.46 (the original type strain of the species; Figure 3.10). Morphological data are also in close agreement: cell size, shape, and division pattern and mucilage production all correspond closely

CULTURE: LCR-CC-14-1b

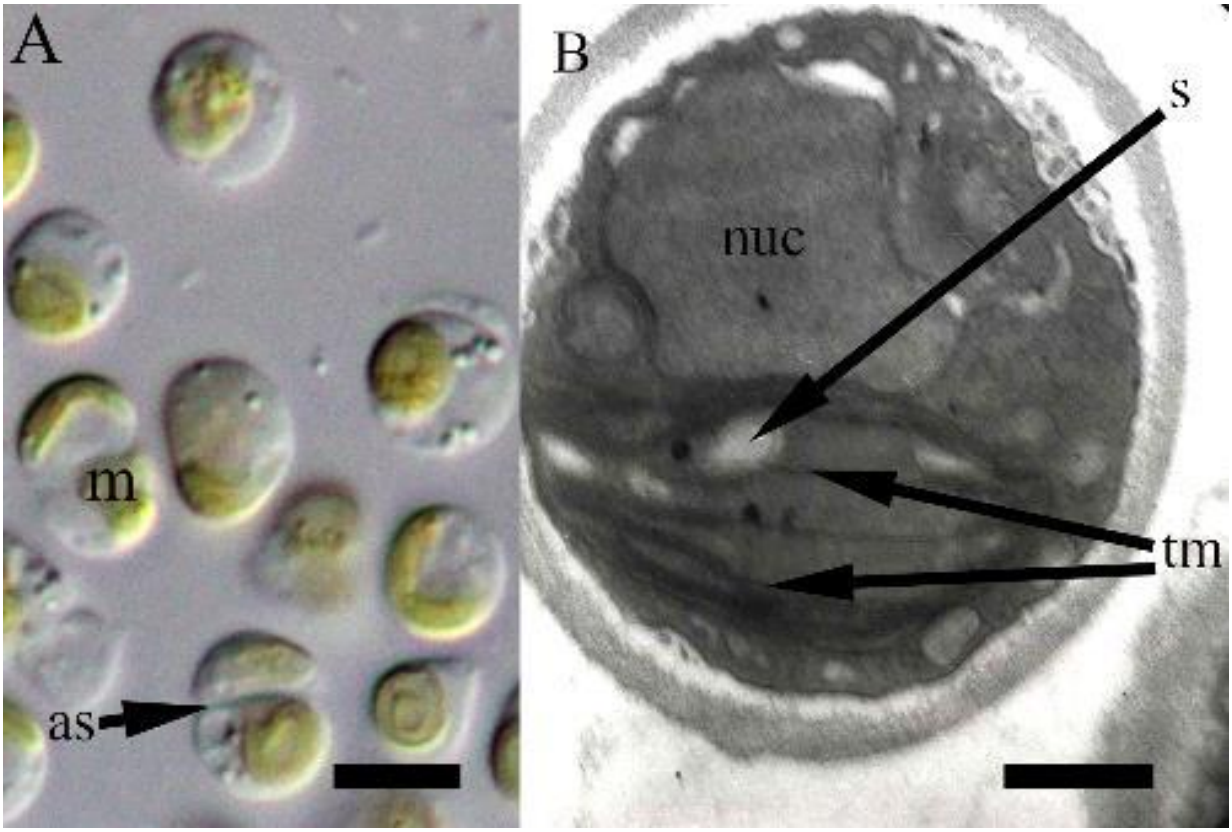

Figure 3.3 *Diplosphaera mucosa* (Photographed from culture LCR- CC-14-1b). **A** light micrographs, **B** transmission electron micrograph. **A** The mature cells showing cup shaped chloroplast (c), and autosporangia (as). **B** Section of the cell showing nucleus (nuc), starch (s) and thylakoid membranes (tm) bisecting the pyrenoid. Scales: 10 µm in **A** and 1 µm in **B.**

***Ettlia* sp. (Figure 3.4)**

NEW ZEALAND LOCALITIES**:** upper Canyon Creek (this study)

GLOBAL DISTRIBUTION: Not found outside New Zealand to date

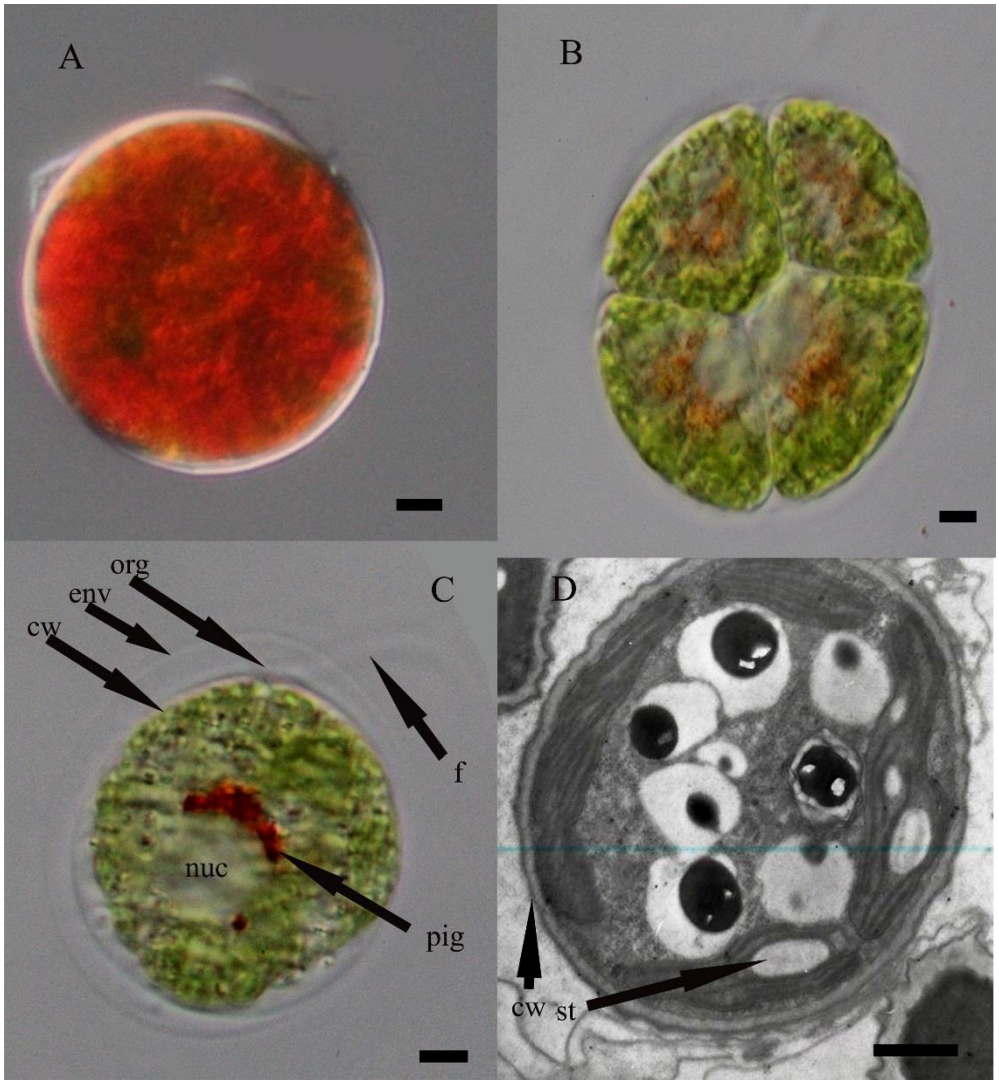

Figure 3.4 *Ettlia* sp. (Photographed from culture LCR-CC-26-1f). **A, B and C** light micrographs, **D** transmission electron micrograph. **A** A cell containing copious red pigment. **B** An autosporangium containing four daughter cells, with red pigment adjacent to each nucleus. **C** The cell showing nucleus (nuc), adjacent pigment (pig), cell wall (cw), envelope (env), flagella (f) are indicated **D.** Section of the cell showing cell wall (cw) and parietal chloroplast containing starch (st); pyrenoids are absent. Scales: 1 µm in **A, B, C and D.**

DESCRIPTION:

Cells large and spherical (Figure 3.4 C) up to 30 (–60) µm in diameter with thin cell walls and an envelope (Figure 3.4 C). Young cells biflagellate, but flagella quickly lost as cell size increases (Figure 3.4 A). Single nucleus at the centre of the cell (Figure 3.4 A, C). Pyrenoids absent. Reproduction by formation of zoospores. 2–4 cells per sporangium (Figure 3.4 B). Abundant red pigment is present in resting cells (3.4A).

OBSERVATION:

This strain is closely related to the genus *Haematococcus* Flotow (Figure 3.9), which is well known for producing copious red pigment (Lorenz & Cysewski 2000). A comparison of 18S rDNA sequences shows a lowest p-distance of 0.004 separating our strain from two isolates of *Hematococcus lacustris* (Girod-Chantrans) Roststafinski, one of *Hematococcus pluvalis* Flotow, one of *Haematococcus capensis* Pocock and one of *Ettlia carotinosa* Komarek. *Ettlia carotinosa* J.Komárek has a paraphyletic relationship with our strain LCR-CC-26-1f (Figure 3.9). Neustupa *et al*. (2011) showed that *Ettlia carotinosa* Komarek strain SAG 213-4 is a close relative of *Haematococcus*, whereas other species of *Ettlia* are not. The genus is thus polyphyletic, with *E. carotinosa* as the type species, justifying my choice of genus name. Thus in Neustupa *et al.* (2011) study it has been concluded that the genomic data of *Ettlia carotinosa* Komarek is far different from all species of *Ettlia*.

Some morphological features, such as size of the cells, division processes and pigment production of *Ettlia* sp. LCR CC-26-1f resemble those of *Haematococcus*. However, it lacks the (diacritical) cytoplasmic strands found in *Haematococcus*. Morphologically, *Ettlia* sp. LCR CC-

26-1f is very similar to *Ettlia carotinosa*, except the former lacks a pyrenoid. Species of *Ettlia* may or may not have pyrenoids according to Ettl & Komárek (1982); however, most of the species to which these authors referred will ultimately need to be placed in other genera.

CULTURE: LCR-CC-26-1f

***Lobochlamys segnis* (H.Ettl) T.Pröschold, B.Marin, U.W.Schlösser & M.Melkonian (Figure3.5)**

REFERENCE: Pröschold *et al.* 2001 p. 289 & 290

NEW ZEALAND LOCALITIES: upper Canyon Creek (this study).

GLOBAL DISTRIBUTION: Czech Republic (Ettl & Gärtner 1995), Alabama (Ettl & Gärtner 1995), Romania (Cărăuş 2012).

DESCRIPTION:

Cells ellipsoidal or near-cylindrical or oviform in shape, 10–15 µm long, 5–15 µm wide (Figure 3.5 A). Flagella not observed. Chloroplast cup-shaped (Figure 3.5 C). Nucleus in central or slightly anterior position (Figure 3.5 C). Reproduction by autospores containing 4–6–8 daughter cells.

OBSERVATION:

18S rDNA Sequences of the strains CCAP 11/71 and NIES-2240 are identical to the strain isolated from upper Canyon Creek, and six more strains are separated from ours by a p-distance of 0.002. The strain 5-1a is in a robust clade with 3 other *Lobochlamys segnis* strains (Figure 3.9).

CULTURE: LCR-CC-5-1a

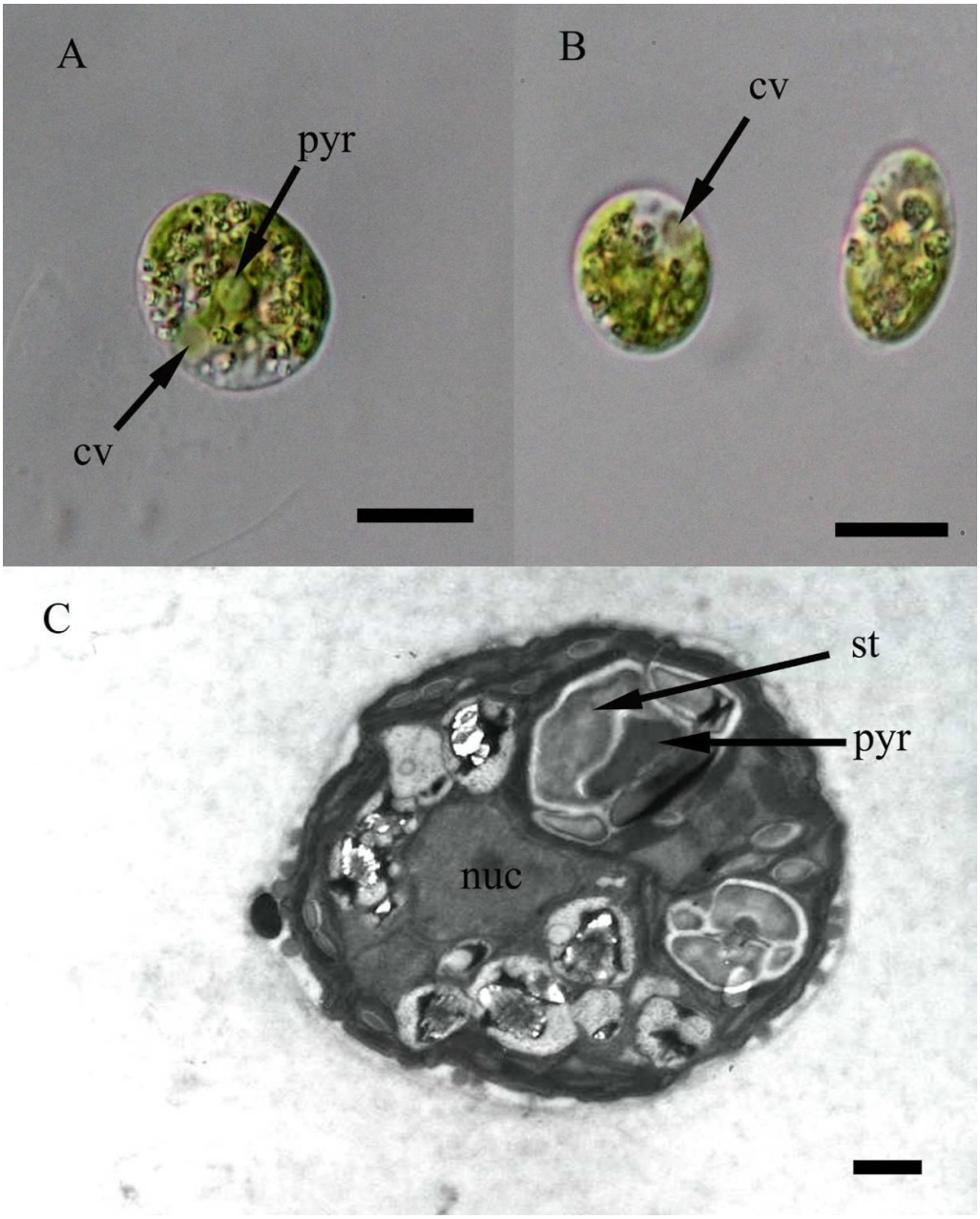

Figure 3.5 *Lobochlamys segnis* (photographed from culture LCR- CC-5-1a). **A, B** light micrographs, **C.** transmission electron micrograph. **A.** The pyrenoid (pyr) and one contractile vacuole (cv) are indicated. **B.** The contractile vacuole (cv) is indicated. **D**. Section of the cell showing nucleus (nuc) and pyreniods (pyr) surrounded by large starch shells (st). Scales: 10 µm in **A** and **B** 1 µm in **C.**

Class **Trebouxiophyceae**

***Oocystis minuta* Guillard, H.C.Bold & MacEntee (Figure 3.6)**

REFERENCE: Komárek & Fott 1983, p. 521.

NEW ZEALAND LOCALITIES: Mt. Philistine and upper Canyon Creek (this study).

GLOBAL DISTRIBUTION: USA, Japan, Iceland (Ettl & Gärtner 1995).

DESCRIPTION:

Cells ovoid, spherical or near-spherical (10–15 μm long and 5–10 μm wide) in shape (Figure 3.6 A). Chloroplast green, containing starch (Figure 3.6 D), parietal, lobed, with 2–4 incisions in healthy cells (Figures. 3.6 A, C). Pyrenoid absent. Reproduction by autospores, 2–4–8 per sporangium, gradually separating through expansion of mucilage matrix (Figure 3.6 B). Cell wall thin and smooth.

OBSERVATION:

The closest *rbc*L sequences to our strain were those of *Pseudococcomyxa simplex* LCR-PSEP (from Mt. Philistine), *Coccomyxa* sp. R2 (China) and *Coccomyxa rayssiae* UTEX 273 (USA). All these 3 strains are separated from our strain by a p-distance value of 0.138. However, the shape, size and other features of our strain resemble *Oocystis minuta*. The p-distance separating strain LCR-CC-3-1a from *Oocystis apiculata* UTEX B 418 is 0.154. *O. apiculata* is in a separate clade that is not sister to *O. minuta* (Figure 3.10): if my identification is accurate this would result in polyphyly in this genus (Figure 3.10). Sequences of *rbc*L for *Oocystis minuta* isolated from elsewhere are not available. *Oocystis minuta* was identified at Mt. Philistine (Novis 2001)

only on the basis of morphological criteria which has relative small differences while comparing with *Oocystis minuta* from Canyon Creek which include the presence of pyrenoid, apical thickness and small difference in the shape and size.

CULTURE: LCR-CC-3-1a

***Pseudococcomyxa simplex* (Mainx) Fott 1981 (Figure 3.7)**

REFERENCE: Ettl & Gärtner 1995, p. 426.

NEW ZEALAND LOCALITIES: Mt. Philistine (Novis & Visnovsky 2012)

GLOBAL DISTRIBUTION: North America (Ettl & Gärtner 1995), Asia: Japan (Ettl & Gärtner 1995), Australia: Victoria, Antarctica: Signy Island, South Georgia, Wilkes land, Victoria Land (Broady 1987)

DESCRIPTION:

Cells pyriform to ellipsoidal and slightly curved in shape, 5–12 µm long and 2–5 µm wide (Figure 3.7 A). While comparing the cell surface curvatures, one side is often broader than the other (Figure 3.7 B). Pyrenoid absent. Nucleus in posterior position (Figure 3.7 B). Reproduction by autospores, which divide through an oblique plane, and are usually covered by a mucilage matrix. This mucilage holds the daughter cells, after sporangia rupture, until they develop into adult cells.

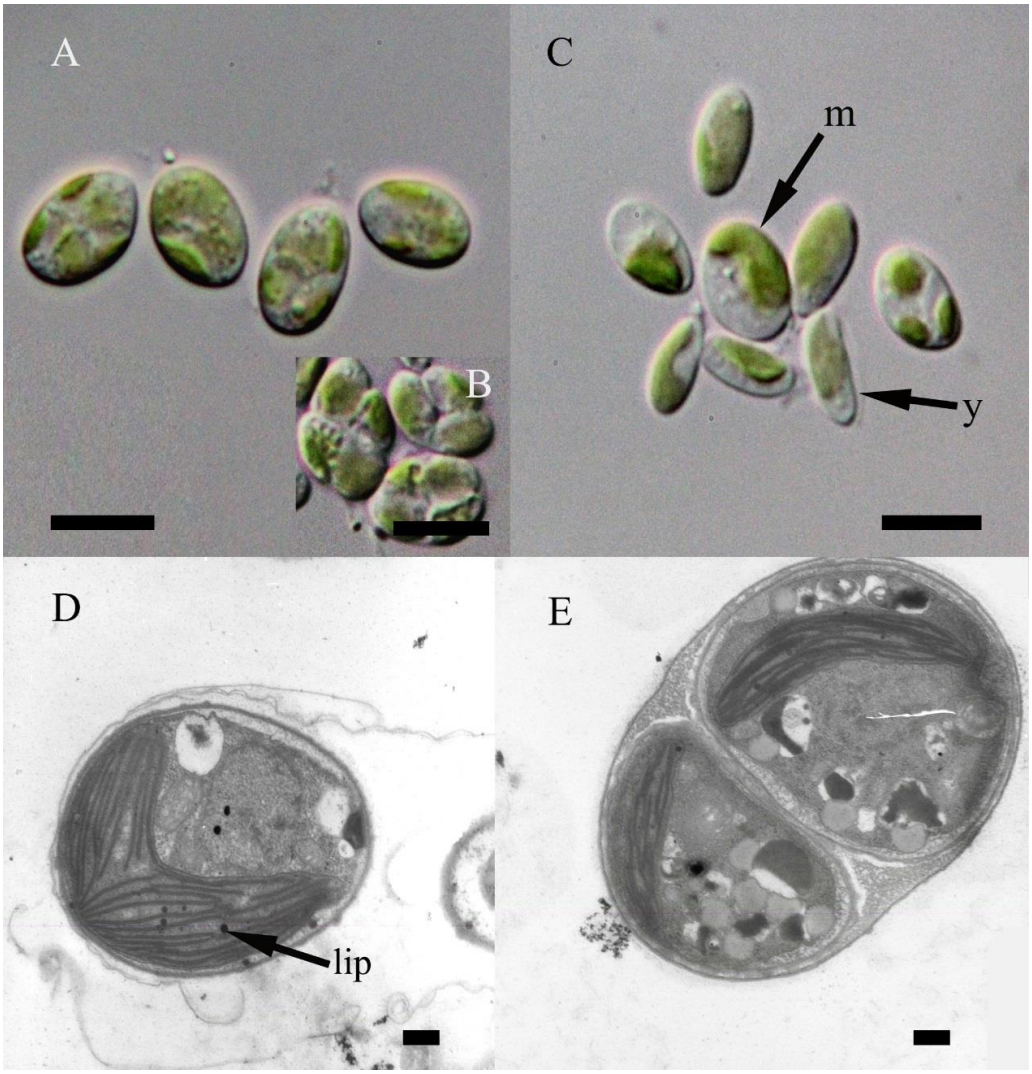

Figure 3.6 *Oocystis minuta* (Photographed from culture LCR-CC-3-1a). **A, B and C** light micrographs, **D, E** transmission electron micrographs. **A.** Typical mature cells. **B.** autosporangia, each containing four daughter cells **C.** Young (y) and mature (m) cells. **D**. Section of a recently divided cell showing remnant envelopes and the chloroplast containing lipid (lip). **E.** Section of an autosporangium. Scales: 10 µm in **A, B** and **C** 1 µm in **D** and **E.**

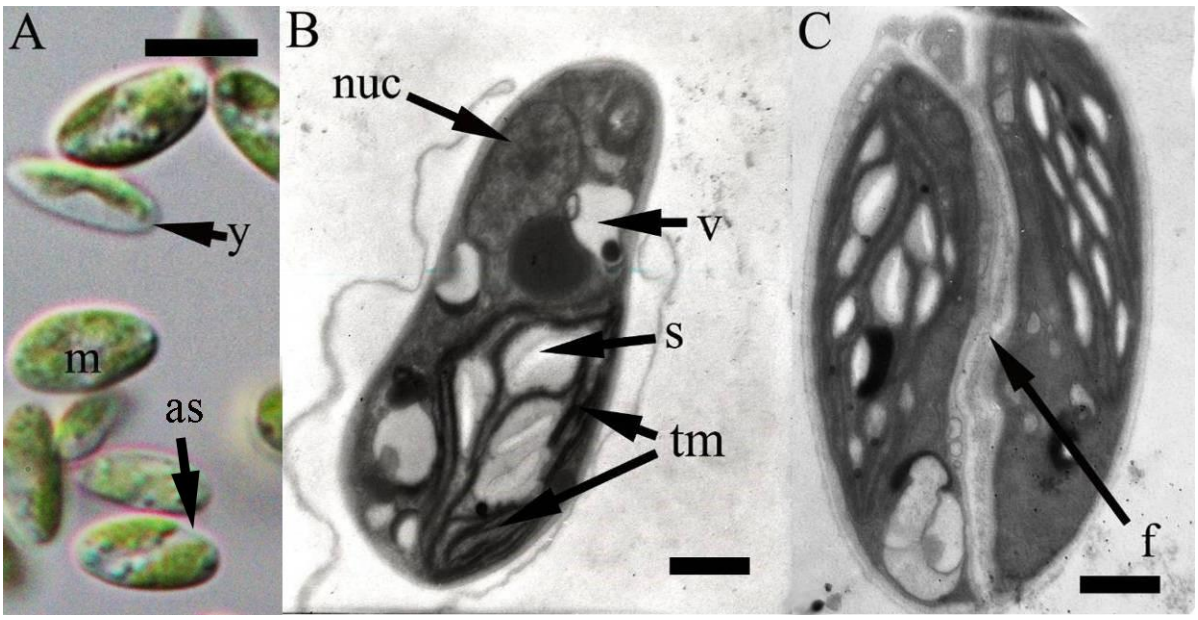

Figure 3.7 *Pseudococomyxa simplex* (Photographed from culture LCR-CC-6-1b). **A** light micrographs, **B & C** transmission electron micrographs. **A.** Elongated young cells (y) and more rounded mature cells (m); the arrow indicates the oblique division plane in an autosporangium (as). **B.** Section of the cell showing nucleus (nuc), vacuole (v), starch (s) and thylakoid membranes (tm). Pyrenoids are absent. **C**. Section of a dividing cell cell showing furrow (f). Scales: 10 µm in **A,** 1 µm in **B** and **C.**

OBSERVATIONS:

A p-distance of 0.007 separates isolates from upper Canyon Creek and Mt. Philistine. The topology inferred using MrBayes and MPB groups these strains together in a robust clade (Figure 3.10). Reproduction by autospores, 2 per sporangium, formed by an oblique division within the parent cell (Figure 3.7 A). The identification is supported by the oblique division plane and genetic proximity to *P. simplex* LCR-MP-CG3.

CULTURE: LCR-CC-6-1b

***Variochloris* sp. (Figure 3.8)**

NEW ZEALAND LOCALITIES: upper Canyon Creek (this study).

GLOBAL DISTRIBUTION: Not found outside New Zealand to date

DESCRIPTION:

Cells spherical to ellipsoidal in shape (5–10 μm long and 4.5–9 μm wide). Chloroplast green and lobed. The pyrenoid contains pyrenoglobuli (Figure 3.8 C, D). Reproduction by autospores with 2–8 daughter cells per sporangia (Figure 3.8 C). Thylakoids inside the pyrenoid is looped and surrounded by pyrenoglobuli.

OBSERVATIONS:

This isolate differed from its nearest relative *Variochloris pyrenoglobularis* Novis & Visnovsky CG2 by a p-distance of 0.024. The two strains were placed in a robust sister relationship using MrBayes and MPB. LCR-CC-7-1a contains pyrenoglobuli similar to those of *Heveochlorella hainangensis* (Zhang *et al.* 2008) and *V. pyrenoglobularis* (Novis & Visnovsky 2012). While comparing the morphology with *pyrenoglobularis* CG2, the shapes of the cells are not identical, they are, spherical to ellipsoidal to pyriform but in LCR-CC-7-1a the cells are specrical in shape. The chloroplast of LCR-CC-7-1a lobed and not cup shaped as *Variochloris pyrenoglobularis* CG2. LCR-CC-7-1a apparently has only a single pyrenoid, and apparently also reproduces with more autospores

CULTURE: LCR-CC-6-1b

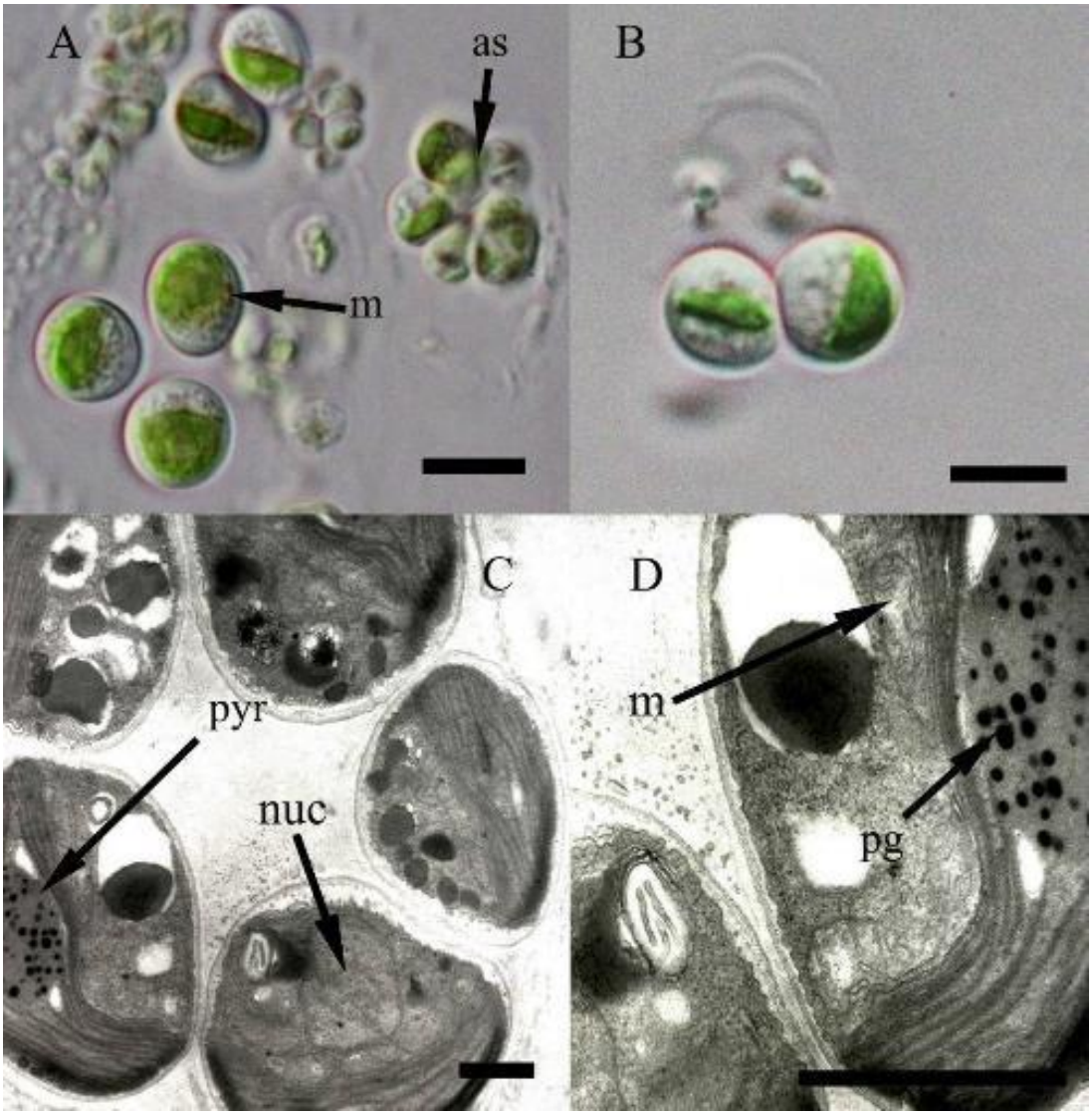

Figure 3.8 *Variochloris* sp. (photographed from culture LCR- CC-7-1a). **A & B** light micrographs**, C & D** transmission electron micrographs. **A.** Mature cells (m) and autosporangia (as) **B.** Daughter cells from the autosporangium. **C**. Section of the cell showing pyrenoid (pyr) with pyrenoglobuli and nucleus (nuc) **D.** Higher magnification view of pyrenoid matrix containing pyrenoglobuli (pg) and mitochondria (m). Scales: 10 µm in **A** and **B,** 1 µm in **C** and **D.**

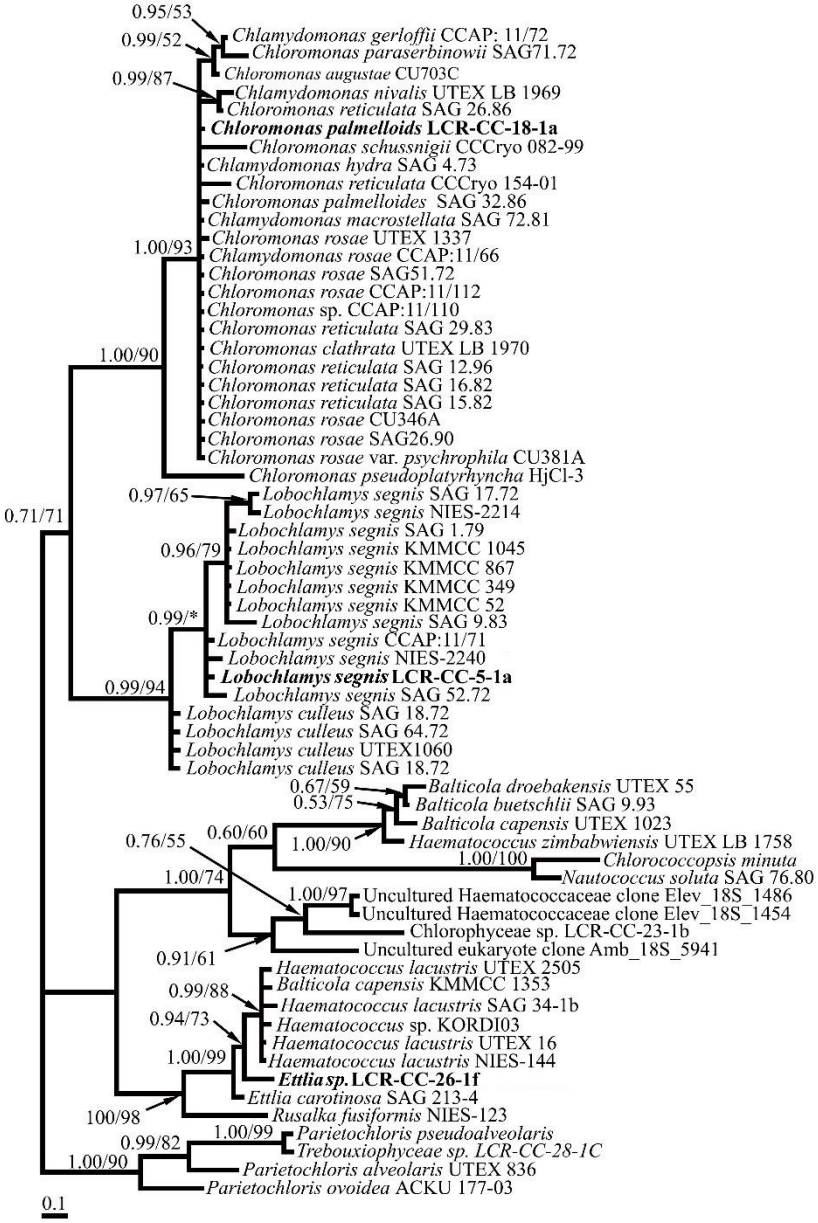

Figure 3.9 Phylogenetic analysis of selected strains inferred from 18S rDNA sequences. The tree topology is that inferred using MrBayes v3.1.2B4. Values above branches correspond to Bayesian posterior probabilities/Maximum Parsimony bootstrap values. Scale bar represents 0.1 changes/site. The trebouxiophycean genus *Parietochloris* is used as an outgroup for the remaining (chlorophycean) strains.

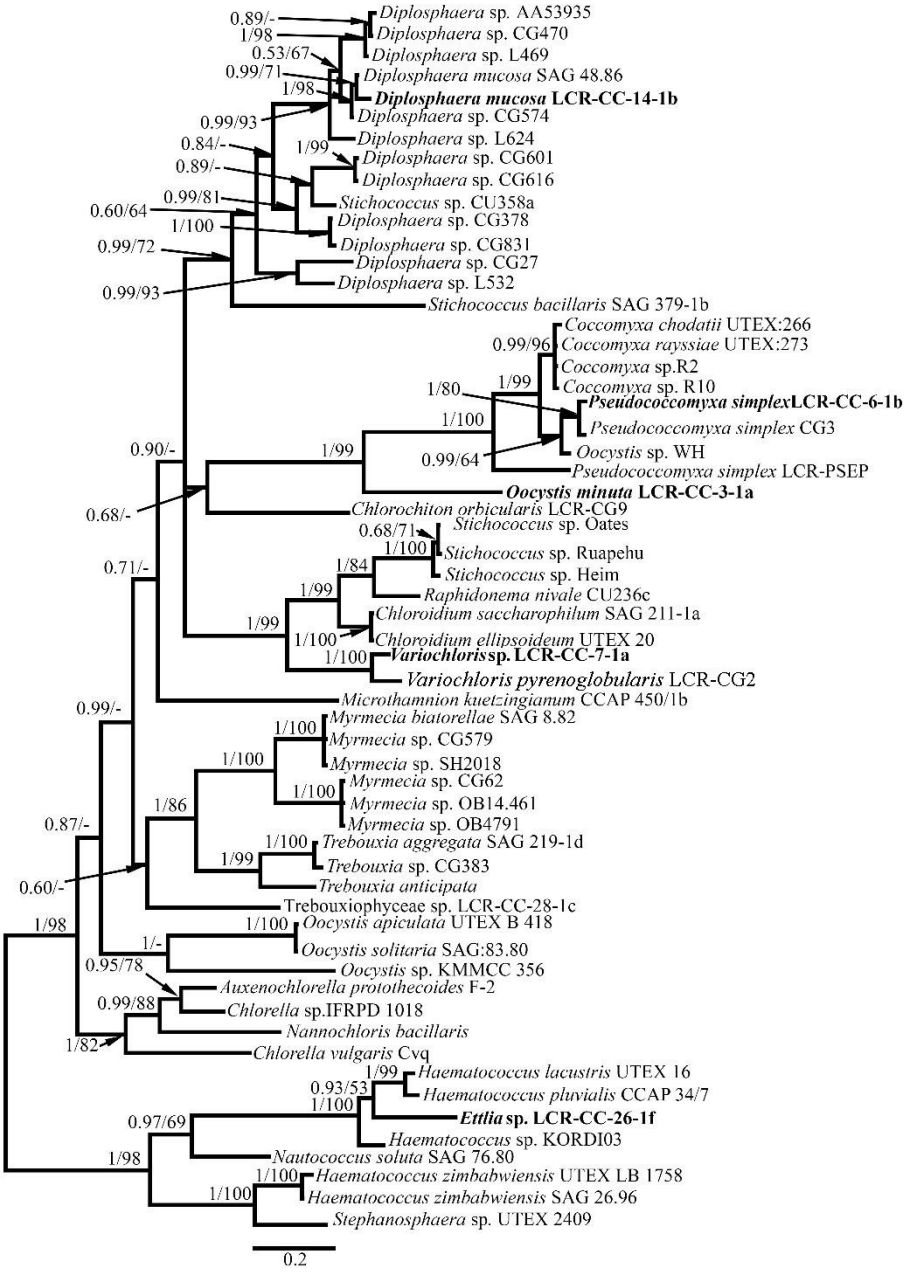

Figure 3.10 Phylogenetic analysis of selected strains inferred from *rbc*L sequences. The tree topology is that inferred using MrBayes v3.1.2B4. Values above branches correspond to Bayesian posterior probabilities/Maximum Parsimony bootstrap values. Scale bar represents 0.1 changes/site.

3.4 DISCUSSION

Two strains of Trebouxiophyceae identified from Canyon Creek had been recorded from New Zealand previously, and five were new to New Zealand of which two were proposed as new to science. The unusual degree of attention that Canyon Creek and Mt. Philistine have received in New Zealand make them interesting biogeographically, since the distribution patterns and dispersal of alpine algae are poorly understood. The combination of culturing, microscopy and genetic analysis can provide more robust identifications than many available historically (Pröschold *et al*. 2001, Rindi *et al.* 2008), allowing firmer conclusions to be drawn about both relationships and distribution patterns of taxa.

The Canyon Creek site is an alpine basin in the Ahuriri Conservation Park and the Mt. Philistine site is a series of linked alpine basins in Arthur's Pass National Park, where algal distribution has been studied quite extensively (references below). Although these two sites are both in the South Island of New Zealand, some exclusive species might be expected due to their differences in latitude and position relative to the Main Divide of the Southern Alps. They are separated by approximately 200 km.

Studies at Mt. Philistine have revealed five new species of Cyanobacteria (Novis & Visnovsky 2011b) and seven new species of Chlorophyta to science (Novis & Visnovsky 2012). The studies have also introduced one species of Chrysophyceae, one species of Xanthophyceae, two species of Klebsormidiophyceae (Novis 2006, Novis *et al*. 2008a, Novis & Visnovsky 2011a) and two additional species of Chlorophyta as new records for New Zealand (Novis 2002b, Novis *et al*. 2008a). These results suggest a large unknown diversity in the alpine zone; however, comparison with another site is needed to determine whether this diversity is smaller and widespread, or larger and range-restricted.

Concluding that a species of microalgae is absent from any zone is strictly non-falsifiable, because it is impractical to inspect the entire zone microscopically or with molecular tools; consequently, microbial taxa may be missed by undersampling (De Wit & Bouvier 2006, Foissner 2006). Since subsequent papers continued to add information on the biota of Mt. Philistine (Novis 2002b, Novis *et al*. 2008a, Novis *et al*. 2008b, Novis & Visnovsky 2011b, Novis & Visnovsky 2011a, Novis & Visnovsky 2012) it is very likely that chlorophycean species have been overlooked from Canyon Creek. Conclusions are further complicated by the fact that cultured strains may not include the dominant organisms in the field, which might not grow in the laboratory. Nonetheless, evidence can gradually accumulate, lending confidence to the conclusion that the dominant taxa at least have been discovered (Novis *et al.* 2008a). With this in mind, a comparison between the known floras of Mt. Philistine and Canyon Creek may be informative.

Pseudococomyxa simplex is one of the species found in both Mt. Philistine and Canyon Creek samples. This is perhaps unsurprising, since the species is widespread in Antarctica and elsewhere, and is clearly easily dispersed and robust (Broady 1987). However, molecular data suggest a level of cryptic diversity in this species; the strains known from New Zealand vary substantially, and do not all correspond to the same species (or most likely even the same genus). The Mt. Philistine (Novis & Visnovsky 2012) and Canyon Creek isolates, however, are almost identical. All strains were recovered most commonly from mineral soil (from which this species has also been cultured in Antarctica (Broady 1987)).

A variety of cyanobacteria have been described from Mt. Philistine. Those for which molecular data are available for includes *Scytonematopsis maxima* Novis & Visnovsky, sp. nov, *Tolypothrix pseudorexia* Novis & Visnovsky, sp. nov, *Hormoscilla irregularis* Novis &

Visnovsky, sp. nov, *Phormidium arthurensis* Novis & Visnovsky, sp. nov and *Godleya alpine* Novis & Visnovsky, gen. et sp. nov. None of these have so far been found at the Canyon Creek site. *Chloromonas rubroleosa* H.U.Ling & R.D.Seppelt has been identified in surface snow from tarns on Mt. Philistine (Novis 2002b) and the lake in Canyon Creek (P.M. Novis, unpublished observations). However, genomic data for this species are not yet available. Other Mt. Philistine chlamydomonads that lack molecular data are *Chlamydomonas* cf. *noctigama*, *Chla.* cf. *moewusii*, *Lobochlamys* cf. *culleus*, *Chloromonas* cf. *rosae* var. *polychloris*, other *Chloromonas* spp. of unknown species affinity (all from Novis 2001), and many snow algal cysts that are presumed to derive from chlamydomonad vegetative cells. Of all these species, *L.* cf. *culleus* and *Chlo*. cf. *rosae* var *polychloris* could represent the same taxonomic entities as Canyon Creek strains (*Lobochlamys segnis* and *Chloromonas palmelloides* Broady respectively); although molecular data are lacking, these strains seem at the least to be very close relatives, and were derived from very similar habitats (moss and soil samples).

The proposed new species *Ettlia* sp. LCR-CC-26-1f is apparently absent from Mt. Philistine. Laboratory experiments in liquid culture suggest that the optimum growth of this species is below 10°C (unpublished observations), raising the possibility that it is a snow alga, cultured from a melt pool from which snow had recently disappeared. If so, it could be a species contributing to the widely distributed "large, red, spherical cysts" found in snow, including from Mt. Philistine and Canyon Creek, which are impossible to identify using morphology. *Ettlia* sp. LCR-CC-26-1f can produce profuse red pigment (although this is well known in its near relative *Haematococcus*, which is not a snow alga). Molecular cloning studies of red snow samples would be informative in this regard, but no such studies have been carried out in New Zealand to date.

Among Scenedesmaceae, *Coelastrella multistriata* var. *grandicosta* Gopalakrishnan *et al.* (2014) from Canyon Creek is the only form with a near relative–*Coelastrella ellipsoidea* (P.M.Novis & G. Visnovsky) Gopalakrishnan *et al*. (2014)–known from Mt. Philistine. The other two species from Canyon Creek are characteristic of plankton and were recovered from ponds that are frequently replenished by a meltwater stream; such streams are far smaller and more ephemeral on Mt. Philistine, and ponds much sparser and shorter lived. Consequently, typical *Scenedesmus*/*Desmodesmus* forms appear to be absent.

A strain identified as cf. *Oocystis minuta* was described from Mt. Philistine by Novis (2001). All features agree well with the Canyon Creek strain, except that the Mt. Philistine cells usually contained a pyrenoid; in the absence of molecular data from the latter strain the taxonomic significance of this is uncertain, but it seems unlikely that the two strains should be regarded as the same species. The Mt. Philistine strain was recovered most often from soil and moss samples, as was that from Canyon Creek.

In summary, the very incomplete biogeographical picture that emerges is tantalising. Among species for which molecular data are available from both sites, only *P. simplex* has definitively been found in both. However, the species of *Variochloris* and *Coelastrella* found at both sites are closely related, and this seems a common pattern when Mt Philistine strains lacking molecular data are taken into account. It is certain that some chlamydomonads found in New Zealand can disperse great distances (Novis *et al*. 2008a), yet this may be infrequent and species-specific, allowing for some local divergence when species are not capable of surviving long-distance dispersal or successfully establish or compete in new sites.

Although Mt. Philistine and Canyon Creek are both alpine sites, the dynamics of water availability in each varies. The Main Divide of the Southern Alps runs in parallel to the

prevailing westerly winds, creating a strong rainfall gradient: Mt. Philistine is slightly west on this gradient, whereas Canyon Creek is approximately 10 km to the east. A weather station located on Mt Philistine has recorded an annual rainfall of 5426.3 mm per year between 1995 and 2011. No such station is located near Canyon Creek, but modelled environmental data obtained from LENZ (Table 4; Leathwick 2002) shows that Canyon Creek receives less precipitation. It does, however, possess a more consistent stream and associated ponds, and the large lake at the top of the site presumably affects the local environment (Changnon & Jones 1972). Habitats relying on precipitation for moisture in Canyon Creek are likely to be drier; interestingly, it is in such habitats (moss and soil) that the most similar species seem to be found. Species occupying these habitats may be more tolerant of water loss and therefore more likely to survive dispersal. However, the complexity of the environment is high and it is very difficult to draw conclusions from the limited data currently available.

Table 3.2 LENZ data (Table 4; Leathwick 2002) and CliFlo station data (CliFlo 2014) of Canyon Creek and Mt. Philistine.

Parameter		Mt. Philistine	Canyon Creek
Mean annual temperature (°C)	LENZ: bottom of site	5.5	4.7
	LENZ: top of site	3.6	3.1
	Cliflo	3.5	-
Mean annual solar radiation (MJ m^{-2} d^{-1})	LENZ, bottom of site	13.7	12.9
	LENZ, top of site	13.5	12.8
	Cliflo	11.3	-
Monthly water balance ratio	LENZ, top of site	73	192
	LENZ, bottom of site	98	217
	Cliflo	-	-

Table 3.3 Names and GenBank accession numbers of strains used in the study for 18S rRNA analysis.

Taxon	Strain	18S rRNA accession
Balticola buetschlii (Blochmann) Droop	SAG 9.93	KC196720
Balticola capensis (M.A.Pocock) Droop	UTEX 1023	KC196719
Balticola capensis (M.A.Pocock) Droop	KMMCC 1353	JQ315535
Balticola droebakensis (Wollenweber) Droop	UTEX 55	KC196721
Chlamydomonas gerloffii H.Ettl	CCAP: 11/72	FR865610
Chlamydomonas hydra H.Ettl	SAG 4.73	JN903988
Chlamydomonas macrostellata J.W.G.Lund	SAG 72.81	U70785
Chlamydomonas nivalis (F.A.Bauer) Wille	UTEX LB 1969	U57696
Chlamydomonas rosae H.Ettl & O.Ettl	CCAP:11/66	FR865603
Chlorococcopsis minuta (G.Arce & H.C.Bold) S.Watanabe & G.L.Floyd		M62996

Chloromonas augustae (Skuja) T.Pröschold, B.Marin, U.W.Schlösser & M.Melkonian	CU703C	AF517095
Chloromonas clathrata (Pascher) Korshikov ex H.Ettl	UTEX LB 1970	U70791
Chloromonas palmelloides P.A.Broady	SAG 32.86	JN904006
Chloromonas paraserbinowii (Skuja) Gerloff & H.Ettl	SAG71.72	AF517089
Chloromonas pseudoplatyrhyncha (Pascher) P.C.Silva	HjCl-3	AB548689
Chloromonas reticulata (Goroschankin) Gobi	SAG 26.86	AJ410447
Chloromonas reticulata (Goroschankin) Gobi	CCCryo 154-01	GU117583
Chloromonas reticulata (Goroschankin) Gobi	SAG 29.83	AJ410448
Chloromonas reticulata (Goroschankin) Gobi	SAG 12.96	AJ410451
Chloromonas reticulata (Goroschankin) Gobi	SAG 16.82	AJ410450
Chloromonas reticulata (Goroschankin) Gobi	SAG 15.82	AJ410449
Chloromonas rosae H.Ettl	UTEX 1337	U70796
Chloromonas rosae H.Ettl	SAG51.72	AB624565
Chloromonas rosae H.Ettl	CCAP:11/112	FR865528

Chloromonas rosae H.Ettl	CU346A	AF517094
Chloromonas rosae H.Ettl	SAG26.90	AF517090
Chloromonas rosae var. *psychrophila* R.W.Hoham, T.A.Bonome, C.W.Martin, & J.H.Leebens-Mack	CU381A	AF517093
Chloromonas schussnigii H.Ettl	CCCryo 082-99	GU117584
Chloromonas sp.	CCAP:11/110	FR865527
Ettlia carotinosa J.Komárek	SAG 213-4	GU292342
Haematococcus lacustris (Girod-Chantrans) Roststafinski	SAG 34-1b	AF159369
Haematococcus lacustris (Girod-Chantrans) Roststafinski	UTEX 2505	U70590
Haematococcus lacustris (Girod-Chantrans) Roststafinski	UTEX 16	DQ009774
Haematococcus lacustris (Girod-Chantrans) Roststafinski	NIES-144	AB360747
Haematococcus sp.	KORDI03	FJ877140
Haematococcus zimbabwiensis Pockock	UTEX LB 1758	U70797
Lobochlamys culleus (H.Ettl) T.Pröschold, B.Marin, U.W.Schlösser & M.Melkonian	SAG 18.72	AJ410462

Lobochlamys culleus (H.Ettl) T.Pröschold, B.Marin, U.W.Schlösser & M.Melkonian	SAG 64.72	AJ410463
Lobochlamys culleus (H.Ettl) T.Pröschold, B.Marin, U.W.Schlösser & M.Melkonian	UTEX1060	FJ211064
Lobochlamys culleus (H.Ettl) T.Pröschold, B.Marin, U.W.Schlösser & M.Melkonian	SAG 18.72	U70594
Lobochlamys segnis (H.Ettl) T.Pröschold, B.Marin, U.W.Schlösser & M.Melkonian	SAG 17.72	AJ410464
Lobochlamys segnis (H.Ettl) T.Pröschold, B.Marin, U.W.Schlösser & M.Melkonian	NIES-2214	AB701525
Lobochlamys segnis (H.Ettl) T.Pröschold, B.Marin, U.W.Schlösser & M.Melkonian	SAG 1.79	AJ410457
Lobochlamys segnis (H.Ettl) T.Pröschold, B.Marin, U.W.Schlösser & M.Melkonian	KMMCC 1045	JQ315506
Lobochlamys segnis (H.Ettl) T.Pröschold, B.Marin, U.W.Schlösser & M.Melkonian	KMMCC 867	JQ315507
Lobochlamys segnis (H.Ettl) T.Pröschold, B.Marin, U.W.Schlösser & M.Melkonian	KMMCC 349	JQ315508
Lobochlamys segnis (H.Ettl) T.Pröschold, B.Marin, U.W.Schlösser & M.Melkonian	KMMCC 52	JQ315765

Lobochlamys segnis (H.Ettl) T.Pröschold, B.Marin, U.W.Schlösser & M.Melkonian	SAG 9.83	U70593
Lobochlamys segnis (H.Ettl) T.Pröschold, B.Marin, U.W.Schlösser & M.Melkonian	CCAP:11/71	FR865609
Lobochlamys segnis (H.Ettl) T.Pröschold, B.Marin, U.W.Schlösser & M.Melkonian	NIES-2240	AB701524
Lobochlamys segnis (H.Ettl) T.Pröschold, B.Marin, U.W.Schlösser & M.Melkonian	SAG 52.72	AJ410456
Nautococcus soluta Archibald	SAG 76.80	AB360749
Parietochloris alveolaris (H.C.Bold) S.Watanabe & G.L.Floyd in Deason, Silva, Watanabe & Floyd	UTEX 836	EU878373
Parietochloris ovoidea T.I.Mikhailyuk & E.M.Demchenko	ACKU 177-03	EU878374
Parietochloris pseudoalveolaris (T.R.Deason & H.C.Bold) S.Watanabe & G.L.Floyd		M63002
Rusalka fusiformis (Matvienko) T.Nakada	NIES-123	AB360750
Uncultured eukaryote clone	Amb_18S_5941	EF024078
Uncultured Haematococcaceae clone	Elev_18S_1486	EF024944
Uncultured Haematococcaceae clone	Elev_18S_1454	EF024917

Table 3.4 Names and GenBank accession numbers of strains used in the study used for *Rbc*L analysis.

Taxon	Strain	*rbc*L accession
Auxenochlorella protothecoides (Krüger) Kalina & Puncochárová	F-2	EU038285
Chlorella sp.	IFRPD 1018	AB260911
Chlorella vulgaris Beyerinck	Cvq	EU038286
Chloroidium ellipsoideum (Gerneck) Darienko, Gustavs, Mudimu, Menendez, Schumann, Karsten, Friedl & Proschold	UTEX 20	EF113427
Chloroidium ellipsoideum (Gerneck) Darienko, Gustavs, Mudimu, Menendez, Schumann, Karsten, Friedl & Proschold	UTEX 20	EF113427
Chloroidium saccharophilum (W.Krüger) Darienko, Gustavs, Mudimu, Menendez, Schumann, Karsten, Friedl & Proschold	SAG 211-1a	AM260446
Coccomyxa chodatii Jaag	UTEX:266	FJ217383
Coccomyxa rayssiae Chodat & Jaag	UTEX:273	FJ217384
Coccomyxa sp.	R2	HQ335208
Coccomyxa sp.	R10	HQ335209
Diplosphaera sp.	L624	JN573860
Diplosphaera sp.	CG470	JN573833

Diplosphaera sp.	AA53935	JN573824
Diplosphaera sp.	CG378	JN573822
Diplosphaera sp.	CG831	JN573835
Diplosphaera sp.	CG616	JN573826
Diplosphaera sp.	CG601	JN573825
Diplosphaera sp.	L532	JN573852
Diplosphaera sp.	CG27	JN573830
Diplosphaera sp.	CG27	JN573830
Diplosphaera sp.	CG378	JN573822
Diplosphaera sp.	CG831	JN573835
Diplosphaera sp.	CG616	JN573826
Diplosphaera sp.	CG601	JN573825
Diplosphaera sp.	CG574	JN573831
Diplosphaera sp.	L624	JN573860
Diplosphaera sp.	L469	JN573847

Diplosphaera sp.	L532	JN573852
Diplosphaera sp.	CG831	JN573835
Diplosphaera sp.	CG27	JN573830
Diplosphaera mucosa	SAG 48.86	AM260444
Haematococcu lacustris (Girod-Chantrans) Roststafinski	UTEX 16	EF113446
Haematococcus pluvialis Flotow	CCAP 34/7	FJ438476
Haematococcus sp.	KORDI03	GU395291
Haematococcus zimbabwiensis Pockock	UTEX LB 1758	EF113447
Haematococcus zimbabwiensis Pockock	SAG 26.96	AB360757
Microthamnion kuetzingianum Nägeli ex Kützing	CCAP 450/1b	EF589152
Myrmecia biatorellae J.B.Petersen	SAG 8.82	AF499685
Myrmecia sp.	OB4791	JN573812
Myrmecia sp.	OB14.461	JN573811
Myrmecia sp.	CG62	JN573810
Myrmecia sp.	SH2018	JN573809
Myrmecia sp.	CG579	JN573808

Myrmecia sp.	CG579	JN573808
Nannochloris bacillaris Naumann		AB383150
Nautococcus soluta Archibald	SAG 76.80	AB360758
Oocystis apiculata West	UTEX B 418	EF113459
Oocystis solitaria	SAG:83.80	FJ968739
Oocystis sp	KMMCC 356	JQ315493
Oocystis sp.	WH	EF012701
Pseudococcomyxa simplex (Mainx) Fott	CG3	HM754405
Pseudococcomyxa simplex (Mainx) Fott	LCR-PSEP	EF589155
Raphidonema nivale Lagerheim	CU236c	EF589151
Stephanosphaera sp.	UTEX 2409	AB360759
Stichococcus bacillaris Nägeli	SAG 379-1b	AM260442
Stichococcus sp.	CU358a	EF589147
Stichococcus sp.	Heim	EF589150
Stichococcus sp.	Ruapehu	EF589149
Stichococcus sp.	Oates	EF589148

Trebouxia aggregata (Archibald) Gärtner	SAG 219-1d	EU123967
Trebouxia anticipata Ahmadjian ex Archibald		AF189069
Trebouxia sp.	CG383	JN573828
Chlorochiton orbicularis	LCR-CG9	HM754409
Variochloris pyrenoglobularis	CG2	HM754404

CHAPTER 4

STRAIN SELECTION

CHAPTER 4

STRAIN SELECTION

4.1 INTRODUCTION

4.1.1 IMPORTANCE OF STRAIN SELECTION

Strain selection is a prerequisite to achieve the optimum yield of secondary metabolites, since these are not produced in equal amount by all strains (Lang *et al.* 2011). The biosynthesis of secondary metabolites is genetically controlled by the organism, and the productivity of the culture can be improved by selecting a high yielding strain (Ramawat & Merillon 1999).

4.1.2 PARAMETERS USED FOR STRAIN SELECTION

Selection of algal strains for secondary metabolite production is of critical importance since it determines the overall efficiently of the production process (Duong *et al*. 2012). Algal strains can be selected by optimising growth characteristics and physiological properties, including:

- The specific growth rate (μ) of the selected strain;
- Quantity of the compound of interest produced;
- Foam formation (in submerged processes foam formation risks contamination and the loss of broth; Ghildyal *et al.* 1988);
- Extracellular compounds which could disturb cell growth and/or the rate of production of the desired product;

- Sensitivity to slight changes in the growth parameters such as temperature, pH and light intensity.

In the present research project, I was looking to optimise production of fatty acids (FAs) from the selected strain. Before analyzing the FA content of a large number of strains, it is important to reduce the number of strains for testing using a strategy, such as close phylogenetic relationship with known high-producing strains, or suggestive morphological features. For instance, strains showing oil globules in the cytoplasm might be chosen for FA analysis (Přibyl *et al.* 2012). Similarly for pigment analysis, pigmented colonies and those showing evidence of surviving under the exposure of ultraviolet light are some of the criteria for selecting strains; such pigments may be alloxanthin, antheraxanthin, astaxanthin, beta-carotene or zeaxanthin or a combination of these. Choosing strains for analysis on the basis of colony colour is an effective method to discover strains which are rich in carotenoids (Sandesh Kamath *et al.* 2008).

In relation to FAs, and while it is possible to observe oil bodies in the cytoplasm of the cell using microscopy (Tzen *et al.* 1993), further investigation needs to be conducted to detect the exact composition of these oil bodies in every strain. When commercial fatty acid production is the goal, determining fatty acid composition in all candidate strains is very important. When selecting a strain for polyunsaturated acid (PUFA) production, it is recommended to grow each algal strain as multi-subcultures to increase the biomass for both qualitative and quantitative analyses (Ramawat & Merillon 1999). This method enables choosing a strain with the best production of PUFAs and the best specific growth rate.

4.1.3 WHY COULD INTERESTING FATTY ACIDS BE FOUND IN ALPINE STRAINS?

Fatty acid production is one among several adaptive features, such as biosynthesis of pigments, mucilage production, and spore formation, employed by algae to survive adverse conditions (Whitelam & Codd 1986). Algae in alpine regions are frequently exposed to conditions such as high light intensity, UV radiation, and low temperatures, leading to the expectation that they may produce rare FAs in good quantity, although studies to date have been limited (Bigogno *et al*. 2002). The general components of membrane lipids are PUFAs. PUFAs production is strictly regulated. However in certain algae, which are isolated from the cold environment where they face unstable conditions including light intensity, temperature and ultraviolet radiation, can produce high proportion of PUFAs by inducing. It is difficult for algae to produce PUFAs immediately following rapid change of temperature (Khozin *et al*. 1997). So, to overcome this difficulty, PUFAs are stored as triacylglycerol (TAG). Usually the high content of TAG is present in ice algae (Falk-Peterson *et al*. 1998). During sudden reduction in temperature, TAG can disassociate to PUFAs which are essential for the organism to adapt and survive in those extreme environments (Whitelam & Codd 1986). Thus, algae from cold environments are rich of PUFAs for their survival, and these are stored in other forms.

4.1.4 FATTY ACID PROFILE AND QUANTITY

Different strains contain different profiles of FAs in different quantities (Volkman *et al.* 1989). In this I report the FA profile of ten different strains isolated from the alpine zone, Canyon Creek, Canterbury, New Zealand (Table 4.1 & 4.2).

Several studies have shown that the different phases of growth produce different quantities of FAs (Fidalgo *et al.* 1998, Bigogno *et al*. 2002). Thus, if the presence of any rare FA is identified, the accumulation of that specific FA could be increased by finding the optimal conditions. For example, Li *et al.* (2008) found an increase in lipid accumulation due to the effect of reduction of nitrogen in the culture medium and Solovchenko *et al.* (2008) demonstrated increased Arachidonic acid (AA) accumulation in *Parietochloris incisa* as an effect of light intensity and nitrogen starvation.

4.1.5 USES OF FATTY ACID PROFILE

Mostly, algal FA profiles are determined for the production of biodiesel (Ratledge 2004, Liu *et al.* 2011) and for feeding fish and oyster larval cultures (Brown *et al.* 1997, Martínez-Fernández *et al.* 2006). Fatty acid profiles are also used as trophic markers in feeding experiments for herbivorous copepods (Graeve *et al.* 1994). Furthermore, FA profiles are also used for the classification of algae (Volkman *et al.* 1998, Sahu *et al.* 2013,). Generally, genomic approaches have been used for the classification of micro-organisms. Classification by phospholipid profiles has also been successfully used to estimate the diversity of microbial communities (Findlay *et al.* 1990, Boschker & Middelburg 2002), a process known as chemotaxonomic analysis. This is based on the observation that while some FAs are found to be common in microorganisms, others are more specific and abundant in particular groups (Boschker & Middelburg 2002, Kaur *et al.* 2005). Community analysis based on difference or similarity relative matrices of FAs correlates well with classification patterns observed using DNA (Polymenakou *et al.* 2005a, Kunihiro *et al.* 2011). However, phylogenetic resolution of the FA methods is lower than that achieved with DNA; combining the two is often a useful compromise (Urakawa *et al.* 2001,

Polymenakou *et al.* 2005b, Kunihiro *et al*. 2011) because determining close relatives of high producing strains helps to reduce the number of strains that need to be screened.

4.1.6 SPECIFIC CELL GROWTH RATE

The specific cell growth rate (μ) is an important parameter to consider for strain selection for PUFA production, because it will determine the time needed to produce a certain amount of biomass cultivated in a determined environment, for example a bioreactor. Superficially, maximising the biomass produced would seem to have the important effect of maximising secondary metabolite production; however, optimum parameter settings for maximising biomass production and secondary metabolite production are not always the same. In such a case, maximum biomass is attained initially, then the optimum conditions for the production of secondary metabolites are imposed to make their production as high as possible (Lorenz 2000). During the study, it is essential to analyse μ and PUFA during the incubation period in order to optimise parameters such as light intensity, temperature and CO_2 concentration. Cultivation of algae in batch culture always produces a sigmoidal growth curve representing four defined phases:

a) Lag phase: at this stage cell growth is almost nil; the cells adjust to the nutrient content in the new medium and to other parameters.
b) Exponential phase: here the cells start to divide, with associated consumption of nutrients. The μ is maximum during this phase, and primary metabolites are produced.
c) Stationary phase: μ is zero. At this stage primary metabolism comes to a halt.

d) Decline phase: the cell count starts to decrease as the result of cell death due to the unavailability of nutrients in the medium, catabolises production, and other factors. Here, μ has a negative value

The lowest rate of secondary metabolite production occurs during the lag phase and the initial stages of the exponential phase, whereas it increases at the end of the exponential phase (Weinberg 1970). Also, primary metabolites produced at this stage start to be converted into secondary metabolites. During the stationary phase, cells stop their multiplication and some of the primary metabolites are converted into secondary metabolites. These secondary metabolites accumulate in stationary cells. However, if the cells are not harvested at this stage the metabolites start to degrade (Cresswell *et al.* 1989).

4.1.7 AIM OF THE STUDY

The specific objectives of the present study were:

1. To study the FA profiles of strains chosen based on their morphological and growth characteristics.
2. To select a single strain which produces an industrially important FA in good quantity.
3. To do relationship analysis between strains as measured using chemotaxonomic and phylogenetic methods.

4.2 MATERIALS AND METHODS

4.2.1 STRAIN SELECTION FOR FATTY ACID ANALYSIS

Relative growth rates were determined for all 13 strains of microalgae isolated. Equal volume (two loops) of culture from the stock plates were used for the analysis. The culturing procedure followed section 2.2.3, with platesincubated for three weeks. Among the thirteen strains cultured, ten were selected for the FA analysis on the basis of their relative growth rates, estimated by measuring the surface area covered by colonies and how quickly the plates developed.

4.2.2 FATTY ACID ANALYSIS

The colonies from the full grown plates were separated and collected aseptically in a laminar flow hood using sterile surgical blades into 15 ml falcon tubes and freeze dried. A sample (~10 mg) of freeze dried biomass samples was placed in a weighed vial for the derivatisation of fatty acid methyl esters (FAME) for gas chromatography analysis. Ten µl of a 1 µg μl^{-1} solution of arachidonic acid (used as an internal standard for methylation and concentration) and 0.5 ml of 1% sodium base reagent were added, and incubated at 80 °C for 30 min. After cooling to room temperature 0.5 ml of 5% methanolic HCl was added to the vial, repeating the incubating cycle. The FAME were then extracted into 1 ml of hexane. Hexane was evaporated under argon gas and the FAME residue re-dissolved into 50 µl chloroform, obtaining a sample ready for gas-liquid chromatography (GLC) analysis (Svetashev *et al.* 1995). Gas-liquid chromatography analysis was performed on an Agilent Technologies 6890N Network GLC system equipped with a flame ionisation detector. The gas-chromatography capillary column was Bp-20 (WAX) (30 m

length, with an internal diameter of 0.32 mm, and 0.25 µm film phase) with a polar liquid phase of polyethylene glycol (SGE International Pty Ltd., Australia). Sample 1 µl was injected into the GLC using an Agilent 7683 series auto sampler (or manually with a 10 µl SGE micro-syringe). The injector and the flame ionisation detector temperature were both at 250 °C, and the column temperature was held at 19 °C for 45 min. The carrier gas (Hydrogen) pressure was 0.38 MPa with the flow rate of 46.6 ml min^{-1}. The split ratio was 30:1. The hydrogen flow rate was 40 ml min^{-1}, the air flow rate was 450 ml min^{-1}, and the make-up flow rate (Nitrogen) was 20 ml min^{-1}. The chromatograph was integrated using Agilent Technologies Enhanced ChemStation software. Individual peaks of FAME were identified by comparison with standards of FAME and by equivalent chain length (ECL) values (Stránsky *et al.* 1997). The 23:0 standard was used to determine total lipid mass and the relative concentrations of each FA was determined by comparing peak areas. The FA analysis was carried out by Dr J. Ryan at Callaghan Innovation, Wellington, New Zealand.

4.2.3 TEMPERATURE SENSITIVITY

The ten strains analyzed for fatty acids were sub-cultured by following the same culturing procedure as explained in section 2.2.3 and incubated at different temperatures up to 20 °C. Relative growth rates of the algal strains were estimated as described in Section 4.2.1.

4.2.4 CHEMOTAXONOMIC AND PHYLOGENETIC METHODS

Evolutionary relationships between the algal strains were investigated by comparing the cladogram of 18S sequences constructed using the maximum composite likelihood distances

method with a dendrogram constructed using Euclidean distances based on FA profiles. Datasets of genomic sequences were aligned using ClustalX 1.8 (Thompson *et al*. 1997), and checked manually. Analyses were carried out by the neighbor-joining method in MEGA 6 (Tamura 2013), based on a maximum composite likelihood model of nucleotide substitution, pairwise deletion of missing data, and 1000 bootstrap replications. The dendrogram of FA results based on profile similarities by Euclidean distance was calculated for all ten strains using statistical computing package R (R Development Core Team 2014). Among the ten strains 18S rDNA gene were sequenced for only six strains. These six strains were used to analyse the relationship between PUFA profiles and the rDNA dendrogram.

4.3 RESULTS

4.3.1 PUFA CONTENT

The strains *Ettlia sp.* LCR-CC-26-1f, *Chloromonas palmelloides* LCR-CC-18-1a, *Pseudococcomyxa simplex* LCR-CC-6-1b, *Lobochlamys segnis* LCR-CC-5-1a, LCR-CC-13-1c (uncharacterised strain), LCR-CC-11-1d (uncharacterised strain), *Desmodesmus abundans* LCR-CC-11-1c-1a, *Desmodesmus granulatus* LCR-CC-15-1b-1a, LCR-CC-28-1a-1a (uncharacterised strain) and *Coelastrella multistriata* var. *grandicosta* LCR-CC-12-1d were chosen for the FA analysis on the basis of the close phylogenetic relationships with known high-producing strains (only for the strains whose close relatives are explored for the fatty acid profile) and the surface area covered by colonies and how quickly the plates developed. The uncharacterised strains were selected only on the basis of the relative growth rate. In the analysis, each strain showed a distinct FA profile (Tables 4.1, 4.2).

Over all ten strains, the average percentage of monounsaturated fatty acids (MUFAs) among the total FA profile was 31.0%, whereas the PUFAs was 41.0%, with the remainder being saturated FAs. Figure 4.2 shows the comparative analysis of PUFAs among all ten strains.

Except for two strains, *Chloromonas palmelloides* (LCR-CC-18-1a) and *Coelastrella ellipsoidea* (LCR-CC-15-1b-1a), all the strains have PUFAs at higher percentages than MUFAs and saturated FAs. Among the ten strains *Lobochlamys segnis* (LCR-CC-5-1a) contained the highest observed PUFA content, at 67%, followed by strain LCR-CC-13-1c at 54%. The lowest PUFA content was detected in the strain *Chloromonas palmelloides* (LCR-CC-18-1a) (Figure 4.1), with 16% of PUFAs among the total FAs.

Overall, the maximum percentage of PUFAs corresponded to Alpha linolenic acid (ALA) (31%), followed by Linoleic acid (LA) (18%) (Table 4.1). The PUFA present in the highest proportion in *Lobochlamys segnis* is ALA, which accounted for 31% of the total PUFAs.

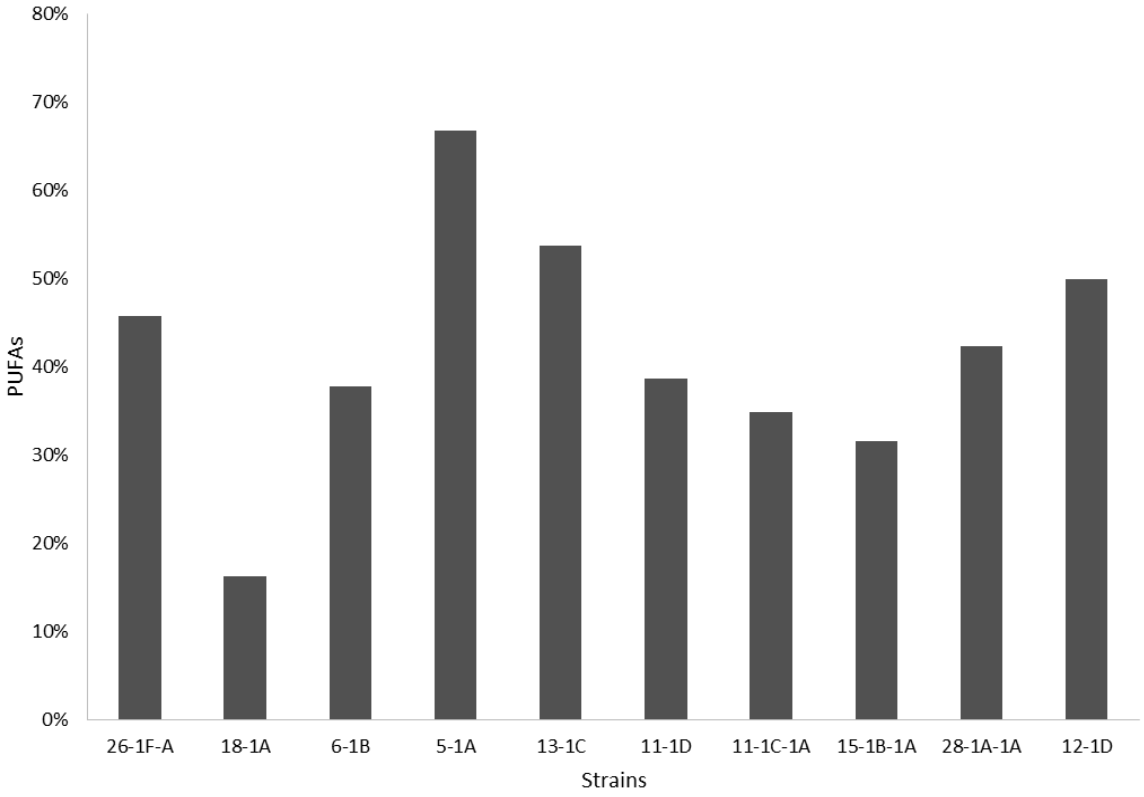

Figure 4.1 Percentage of PUFAs in the selected ten alpine strains

Strain LCR-CC-13-1c contained the second highest percentage PUFA content among the ten strains. The PUFA content of this strain also mostly comprised LA and ALA, at 28.3% and 22.9% respectively. Along with these PUFAs, the strain LCR-CC-13-1c contained 1.5% of eicosadienoic acid. The amount of PUFAs accumulated in *Coelastrella multistriata* var. *grandicosta* (LCR-CC-12-1d), which is a new variety (Gopalakrishnan *et al*. 2014), was 50% of the total FA.

Table 4.1. Polyunsaturated fatty acids profile of all ten strains

Name	FA	*Ettlia sp.* LCR-CC-26-1F	*Chloromonas palmelloides* LCR-CC-18-1A	*Pseudococcomyxa simplex* LCR-CC-6-1B	*Lobochlamys segnis* LCR-CC-5-1A	LCR-CC-13-1C*	LCR-CC-11-1D*	*Desmodesmus abundans* LCR-CC-11-1C-1A	*Desmodesmus granulatus* LCR-CC-15-1B-1A	LCR-CC-28-1A-1A*	*Coelastrella multistriata* var. *grandicosta* LCR-CC-12-1D
Linoleic acid	18:2 (n-6)	31.3%	1.6%	12.4%	18.2%	28.3%	18.4%	9.8%	16.2%	11.5%	29.5%
Alpha linolinic acid	18:3 (n-3)	7.7%	12.9%	21.8%	31.2%	22.9%	11.0%	20.7%	11.4%	27.2%	17.6%
Stearidonic acid	18:4 (n-3)	1.1%	0.1%	-	1.4%	-	5.1%	0.9%	-	-	-
Eicosadienoic acid	20:2 (n-6)	-	-	-	-	1.5%	-	-	1.3%	-	-
Eicosatrienoic acid	20:3 (n-3)	1.0%	0.2%	0.9%	-	-	-	-	2.1%	0.6%	0.6%
Arachidonic acid	20:4 (n-6)	-	0.2%	0.7%	-	-	-	-	-	-	-
Other fatty acid	22:3	2.0%	0.3%	1.9%	16.1%	-	2.3%	1.5%	-	1.0%	1.0%
Clupanodonic acid	21:5 (n-3)	0.8%	-	-	-	1.1%	1.7%	-	-	2.0%	-
Docosapentaenoic acid	22:5 (n-6)	1.9%	1.1%	-	-	-	-	1.9%	0.6%	-	1.2%
Total		46%	16%	38%	67%	54%	39%	35%	32%	42%	50%

* Uncharacterised species

Table 4.2 Saturated fatty acid profile of all ten strains

FA	*Ettlia sp.* LCR-CC-26-1F	*Chloromonas palmelloides* LCR-CC-18-1A	*Pseudococcomyxa simplex* LCR-CC-6-1B	*Lobochlamys segnis* LCR-CC-5-1A	LCR-CC-13-1C*	LCR-CC-11-1D*	*Desmodesmus abundans* LCR-CC-11-1C-1A	*Desmodesmus granulatus* LCR-CC-15-1B-1A	LCR-CC-28-1A-1A*	*Coelastrella multistriata* var. *grandicosta* LCR-CC-12-1D
14:0	-	-	1.3%	-	-	-	-	-	-	-
16:0	14.9%	8.0%	20.6%	2.1%	13.0%	22.4%	21.8%	13.6%	14.3%	10.4%
17:0	0.7%	-	0.2%	-	-	1.4%	1.0%	0.7%	1.3%	0.7%
18:0	5.3%	2.0%	4.5%	15.2%	4.9%	5.3%	2.3%	2.0%	2.5%	3.0%
19:0	1.0%	-	-	1.2%	-	-	-	0.5%	-	-
20:0	-	0.2%	0.7%	-	0.3%	-	-	5.0%	0.3%	0.4%
22:0	0.9%	0.4%	1.8%	5.7%	-	-	-	-	-	-
24:0	4.3%	0.9%	2.7%	6.3%	4.7%	1.9%	1.6%	1.8%	3.1%	5.2%
Total	27%	12%	32%	31%	23%	31%	27%	24%	22%	20%

* Uncharacterised species

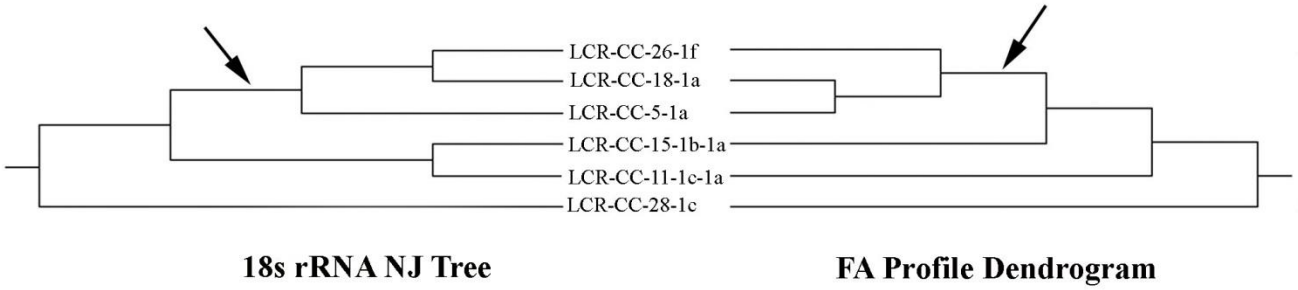

Figure 4.2 Dendrogram (right) based on fatty acid profile similarities between six species for which 18S rDNA sequences were available, compared to a Neighbour Joining (NJ) cladogram (left) constructed from maximum composite likelihood distances based on 18S rDNA gene sequences. Arrow marks show successful seperate the taxa into volvocales and the outgroup.

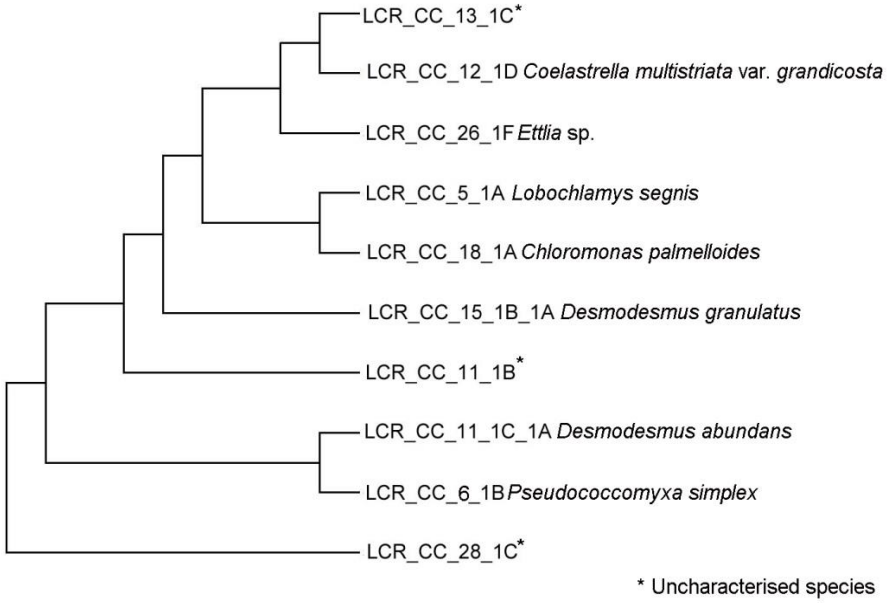

Figure 4.3 A dendrogram based on fatty acid profile of all ten strains

4.3.2. RELATIONSHIP BETWEEN STRAINS BASED ON PUFAS PROFILES AND rDNA

Ten strains were considered for PUFA analysis. Among these strains, seven were characterised and three were uncharacterised strains. The three uncharacterised strains were considered for the PUFA analysis because they were among the ten strains which showed good relative growth rate. A comparative dendrogram was made for this study between the 18S rDNA sequenced six strains. Figure 4.2 shows the comparison between the dendrogram based on the FA profile dissimilarities and the Neighbor Joining tree constructed from the 18S gene sequences. The two methods agree with each other at high taxonomic resolution, as they both successful split the taxa into volvocales (26-1f, 5-1a, and 18-1a) and the remainder (Figure 4.2). Beyond the higher taxonomic classification, the 18S phylogeny performed better than the FA profile analysis. For instance, Scenedesmacean taxa (11-1c-1a and 15-1b-1a) are grouped by 18S reconstruction whereas FA analysis presents these as a grade.

4.3.3. RELATIVE GROWTH RATES OF STRAINS

Among all strains, *Lobochlamys segnis* LCR-CC-5-1a showed the maximum estimated specific cell growth rate. It covered a complete 5.5 cm diameter plate in one week, while the other strains took more than 3 weeks to achieve the same. When the algae were transferred to a 20 ^{o}C incubator with 3.0% CO_2, most of the strains did not survive. However, *Lobochlamys segnis* LCR-CC-5-1a and *Coelastrella multistriata* var. *grandicosta* LCR-CC-12-1d did survive but the growth of the former was much greater than that of the later.

4.4 DISCUSSION

The main criterion for a strain to be chosen for FA production is that it should yield a FA which has a high market value (Borowitzka 1992, Rodolfi *et al.* 2009). In nature, FAs in algae are produced for specific functions. For instance, PUFA production helps organisms to survive and adapt in extreme low temperature environments (Murata *et al.* 1975, Sato & Murata 1980, Lynch & Thompson 1982, Renaud *et al.* 2002). Thus the strains isolated from the alpine region were analysed for choosing algae for PUFAs production.

Lang *et al.* (2011) stated that green algae usually contain a lower proportion of PUFAs than MUFAs and saturated fatty acids. In the present study eight among the ten species isolated from an alpine region have PUFAs in proportions higher than MUFAs and saturated FAs. This observation provides evidence that the alpine environment selects for strains with high PUFA content, as hypothesised. Furthermore, the PUFA composition of strains isolated from tropic regions (which is also typically lower than that of MUFAs and saturated FAs) can be increased by lowering the cultivation temperature (Renaud *et al.* 1995). In another study done with six algae, including *Cryptomonas*, *Isochrysis, Prymnesiophyte* and *Rhodomonas* the percentage of PUFAs also increased when they were grown at lower temperatures (Renaud *et al*. 2002). Strains of Scenedesmaceae isolated from a hot environment (Sahara Desert) had very low concentrations of unsaturated fatty acids (Grama *et al.* 2014), but Scenedesmaceans, in this study, display a high degree of unsaturation. Additionally, all three species contain DPA, which was absent from the Saharan strains.

On the other hand, some strains have shown decreases in PUFA composition when the temperature is decreased, such as the marine diatom *Chaetoceros* sp. (Renaud *et al.* 2002).

Therefore, although the temperature has an effect on FA production, this effect would depend on the species and habitat of isolation.

The effective cultivation of algae requires consideration on cell growth kinetics, tolerance to temperature, pH, salinity, CO_2 concentration, level of oxygen, nutrient composition and resistance to shearing force (Brennan & Owende 2010). In my initial studies I generated biomass on agar plates (solid phase static cultures) and it was not possible to check cell sensitivity to shear stress. *Lobochlamys segnis* displayed the highest specific cell growth rate at the full range of temperatures tested (10–20 ^{o}C). Strains able to grow at low temperature are desirable, due to the relationship between FA and temperature described above. However, from an industrial perspective, growth of algae in large scale reactors at low temperature is not always economically feasible. Conversely, these algae may also produce FAs at higher temperature, or production can be induced by reducing the temperature when they reach the stationary phase without dramatically affecting the strain's viability. Most algae in polar regions are psychotrophs, not psychrophiles, being able to grow at moderate temperature, normally up to 20^{o}C (Tang *et al.* 1997). Thus tolerance of a wide temperature range is an important criterion in strain selection.

Whitelam & Codd (1986) noted that alpine algae live under extreme environmental conditions, especially in terms of temperature, light intensity and radiation, and that PUFAs have an important protective role to mitigate these conditions. In this instance, it is important to consider that the fatty acid profile of a same species grown in different culturing conditions show different fatty acid profile (Renaud *et al*. 2002). Since differences in culturing conditions influence FA profiles, there should be an even greater influence from the environment from which the strains are isolated, because environmental parameters such as light intensity,

temperature, ultraviolet radiation, nutrient composition and rainfall level are quite spatially varied. For instance, a strain of *Lobochlamys segnis* isolated from a tropical region produced 41% of MUFAs and 39.8% of PUFAs when growing at 25-28^{o}C with Photon Flux Density (PFD) 400 µmol m^{-2} s^{-1} and supplemented with 3.0% CO_2 (Bogen *et al.* 2013). In comparison, the PUFA content of *Lobochlamys segnis* LCR-CC-5-1a grown at 20^{o}C with PFD 178 µmol m^{-2} s^{-1} and 3.0% CO_2 was 67.09% PUFAs, relatively more than the tropical strain. This seems to confirm that the habitat from which the strain was isolated has an effect on PUFA production.

It is possible to estimate the level of PUFAs in algal strains by correlating them with the secondary metabolites of close relatives in the phylogenetic tree. In certain cases, it is very fortunate that such relatives of the Canyon Creek strains have been subjected to FA analysis For example, *Ettlia* sp. is a close relative of *Ettlia carotinosa*, *Hematococcus lacustris*, *Hematococcus pluvalis* and *Haematococcus capensis*. *H. pluvalis* (Figure 3.9) is the main commercial algal source of astaxanthin, which is a Food and Drug Administration (FDA) approved food coloring agent. In the absence of other data, it would be expected that *Ettlia* sp. may also produce astaxanthin. *Ettlia* sp. cells produce abundant red pigment, which may be the same compound (Figure 3.8 A).

The FA profile dendrogram and the 18S rDNA phylogeny do not completely agree. In the phylogenetic analysis, p-distances must be corrected for multiple substitutions for accurate tree reconstruction (Felsenstein 2004). Numerous evolutionary models are available that attempt to correct distances in this way; the simplest is Jukes-Cantor or variations thereof (Jukes & Cantor 1969). Some of these are quite sophisticated, modelling independent frequencies of change for every possible base combination. The use of Euclidean distances to reconstruct relationships is similar to the use of p-distances; therefore it would not be surprising if such methods needed

advancement. It is known that DNA tends to be more accurate than chemotaxonomy (Urakawa *et al.* 2001, Polymenakou *et al.* 2005b, Kunihiro *et al*. 2011), perhaps partly for that reason.

4.5 CONCLUSION

This study aimed to select a strain with an optimum yield of economically important PUFAs. To do this, five criteria (section 4.1.2) were considered, but only a subset were effective due to the limitations of growing candidate strains on agarised media; these were growth rate and quantity of the compound of interest. Strains showing the best growth were selected for FA analysis, and the profiles were compared to select the best candidate. Strain *Lobochlamys segnis* LCR-CC-5-1a was chosen on the grounds that:

- It grew the fastest of all candidates (by a considerable margin) at the full range of temperatures considered; since previous research indicates a relationship between PUFA content and growth temperature, its physiology suggests that its capacity to produce PUFAs is likely superior to the other strains.
- It demonstrated a high content of ALA, an industrially important FA (31% of all FAs).

Phylogenetic studies were not informative concerning the potential of this strain to produce PUFAs, because although other strains of this species have been examined in the past, PUFA profiles are lacking.

CHAPTER 5

INFLUENCE OF CARBON DIOXIDE CONCENTRATION ON GROWTH OF *LOBOCHLAMYS SEGNIS* LCR-CC-5-1A IN AIRLIFT PHOTOBIOREACTORS

CHAPTER 5

INFLUENCE OF CARBON DIOXIDE CONCENTRATION ON GROWTH OF *LOBOCHLAMYS SEGNIS* LCR-CC-5-1A IN AIRLIFT PHOTOBIOREACTORS

5.1 INTRODUCTION

Algae are widely used for the commercial production of pigments and fertilizers (Borowitzka 1999) and for animal nutrition (Becker 2007). The cultivation of algae is carried out using different systems, such as tanks, raceway ponds, large bags, fermenters and reactors (Borowitzka 1999). Each type of cultivation has its own advantages and disadvantages (Borowitzka 1999) (explained in detail in Chapter 1). It is therefore essential to carefully select the process and particularly the reactor which offer the best fit to the strain and the product that is expected from it. The cultivation of algae in open systems usually performs poorly for several reasons, such as contamination (Carvalho *et al.* 2006), deficient mixing, and cell disruption when proper mixing is attempted. Over the last two decades research to overcome these disadvantages has accelerated. Important progress has been made in the understanding of algal biology, including the effect of sheer stress on the production of secondary metabolites (Mantzouridou *et al.* 2002), the role of nitrogen on algal growth and lipid accumulation (Li *et al.* 2008), and the responses of algae to different growth conditions. These improvements, together with more sophisticated reactor design, have resulted in substantial progress in large-scale algal culture systems.

In the present study, *Lobochlamys segnis* LCR-CC-5-1a was grown in concentric ALRs to determine the optimum parameter values required for maximum biomass and PUFAs (considering ALA in particular). The AL-PBR was selected for cultivation, because it enables proper mixing while minimising shear stress on the cells (see section 1.6.2). Because of the fluidynamic patterns produced as a result of the design, the mixing inside the reactor ensures that all cells receive the same level of PFD (usually supplied from an external and artificial source at lab level). A consequence of this fact is that all cells replicate at the same specific growth velocity, a key parameter needed to calculate algal growth kinetics accurately, which is a basic requirement when working with the algae-reactor system from an engineering perspective.

AL-PBRs are very efficient. For example, in a study by Merchuk et al (1998) the cultivation of *Porphyridium* sp. was carried out in two different tubular reactors: a bubble column and an airlift reactor (ALR). When both the reactors were supplied with low PFD and high gas flow rate, the growth rate of *Porphyridium* sp. was the same. But when high PFD and low gas flow rate were supplied the ALR showed superior performance over the bubble column. The major reasons for the efficiency of an ALR are that the cells are exposed to equal PFD in a uniform pattern, and the gas flow rate required for efficient mixing is achieved under less gas flow than in other reactors. The mixing or circulation of liquid in an ALR is enabled by the pressure difference between the riser and the downcomer of the reactor:

$$\Delta P = g \,.\, h \,.\, (\rho_2 - \rho_1) \qquad \text{(Eq. 1)}$$

where ΔP is the pressure difference, g is the gravitational constant, h is the density of the media in the reactor and ρ_2 and ρ_1 are gas holdup of the riser and the downcomer.

5.1.1 AIRLIFT REACTORS

Although conventional fermenters satisfy the major requirements for culturing microorganisms – the gas-medium interface for the supply of oxygen and the removal of waste gases, means of agitation to ensure proper nutrient distribution and to minimize damage resulting from the addition of concentrated acid or base (for pH control), means for heat transfer (for temperature control), and a contamination-free environment – ALRs are considered to be superior to traditional stirred-tank fermenters for the growth of microorganisms. The more successful growth reported in ALRs arises from the difference in fluid dynamic mixing patterns between ALRs and more conventional fermenters (Tanaka 1987, Kessler *et al.* 1993).

Hydrostatic pressure differences resulting from gas being injected into a baffled chamber containing liquid are used for the concept of airlift. The "Pachuca Tank", used in the metalurgy industry to leach ores of gold, uranium and other metals, is probably the first example of industrial use of the principle for reactor applications (Lamont 1958). The attractive property of the system was its capability to produce efficient mixing without moving parts. The first clearly defined "airlift" reactor was that patented by Lefrancois (1955). Primarily, the ALR was mainly used for large-scale microbiological processes, such as single-cell protein production. However, from the 1980s, ALRs received wide interest in research, which produced the development of technical literature for its many different applications. For instance, the external-loop airlift reactor was developed on the basis of momentum balance using the drift-flux model for gas holdup prediction (Camarasa *et al*. 2001). Also, the model for the prediction of liquid velocity and gas holdup in rectangular reactors was presented by Couvert *et al.* (2001).

The term ALR covers a wide range of gas-liquid or gas-liquid-solid pneumatic contacting devices that are characterized by fluid circulation in a defined cyclic pattern through channels

built specifically for this purpose. The content of ALRs is pneumatically agitated by a stream of air or sometimes other gases. In those cases, the name *gas lift reactors* has been used. In addition to agitation, the gas stream has the important function of facilitating exchange of material between the gas and the liquid phases; oxygen is usually transferred to the liquid, and in some cases reaction products are removed through exchange with the gas phase (Merchuk & Siegel 1988).

All ALRs, regardless of their basic configuration (external-loop or baffled vessel), comprise four distinct sections with different flow characteristics (Merchuk & Gluz 1999), as Figure 5.1 shows:

Riser: The gas is injected at the bottom of this section, and the flow of gas and liquid is predominantly upward through the draft tube.

Downcomer: This section is parallel to the riser and is connected to it at the bottom and at the top. The flow of gas and liquid is predominantly downward. The driving force for recirculation is the difference in mean density between the downcomer and riser; this difference generates the pressure gradient necessary for liquid circulation.

Base: In the vast majority of airlift designs, the bottom connection zone between the downcomer and riser is very simple. According to Merchuk *et al.* (1994) the base does not significantly affect the overall behavior of the reactor, but the design of this section can influence gas holdup, liquid velocity, and solid phase flow.

Gas separator: This section at the top of the reactor connects the riser to the downcomer, facilitating liquid recirculation and gas disengagement. Designs that allow for a gas residence

time in the separator that is substantially longer than the time required for the bubbles to disengage will minimize the fraction of gas recirculating through the downcomer.

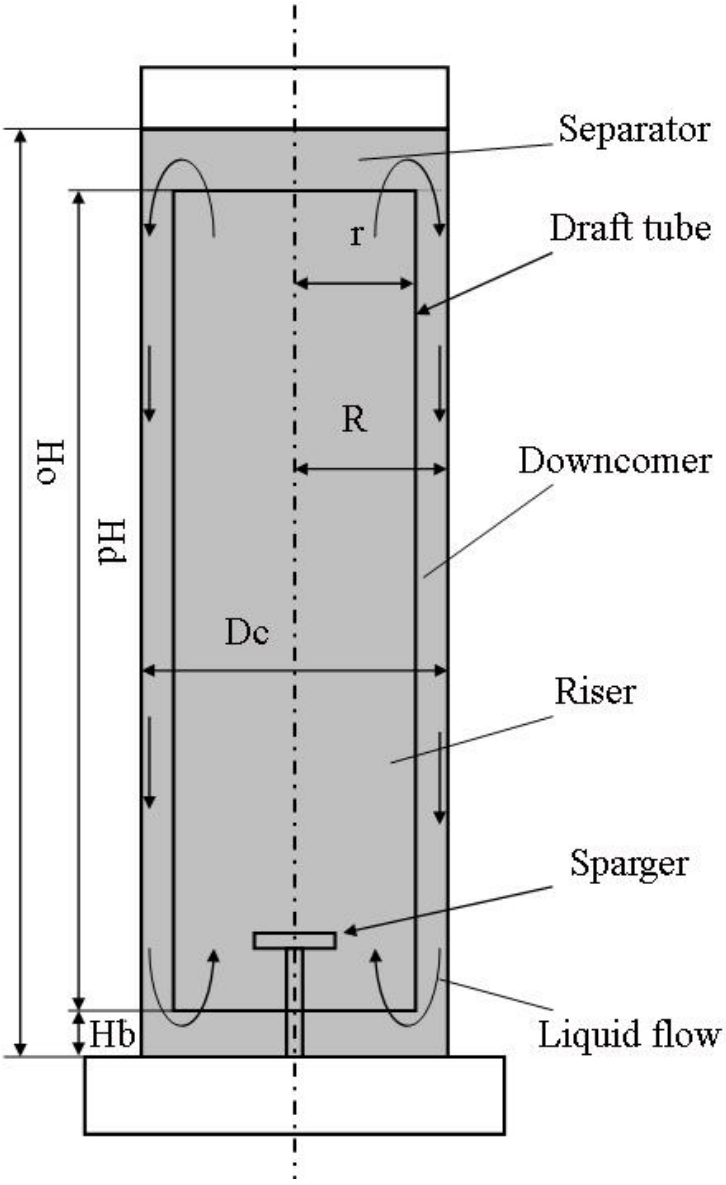

Figure 5.1 Schematic representation of a concentric AL-PBR. Ho and Hd are the height of the liquid column in the reactor and downcomer, respectively, Hb is the bottom clearance, R the distance from the center of reactor to the outer tube, r the riser radius, and Dc the downcomer diameter.

Bubble columns have been advanced as effective photobioreactors like ALRs for large-scale cultivation of microalgae (Sánchez Mirón *et al.* 1999, Sánchez Mirón *et al.* 2000). The main difference between ALRs and bubble columns (which are also pneumatically agitated) lies in the type of fluid flow, which depends on the geometry of the system. The bubble column is a simple vessel into which gas is injected, usually at the bottom, and random mixing is produced by the ascending bubbles. In ALRs, the major pattern of fluid circulation is determined by the design of the reactor, which has a channel for gas–liquid upflow (the riser) and a separate channel for the downflow (the downcomer) (Merchuk & Siegel 1988) (Figure 5.1). The two channels are linked at the bottom and at the top to form a closed loop. The gas is usually injected near the bottom of the riser (Merchuk & Gluz 1999). The extent to which the gas disengages at the top, in the section termed the gas separator, is determined by the design of this section and the operating conditions. The fraction of the gas that does not disengage, but is entrapped by the descending liquid and taken into the downcomer, has a significant influence on the fluid dynamics in the reactor and hence on the overall reactor performance (Merchuk & Gluz 1999). Airlift reactors can be divided into two main types on the basis of their structure: external-loop vessels (Figure 5.2), in which circulation takes place through separate and distinct channels, and baffled (or internal-loop) vessels, in which baffles placed strategically in a single vessel create the channels required for the circulation (Chisti & Moo-Young 1987).

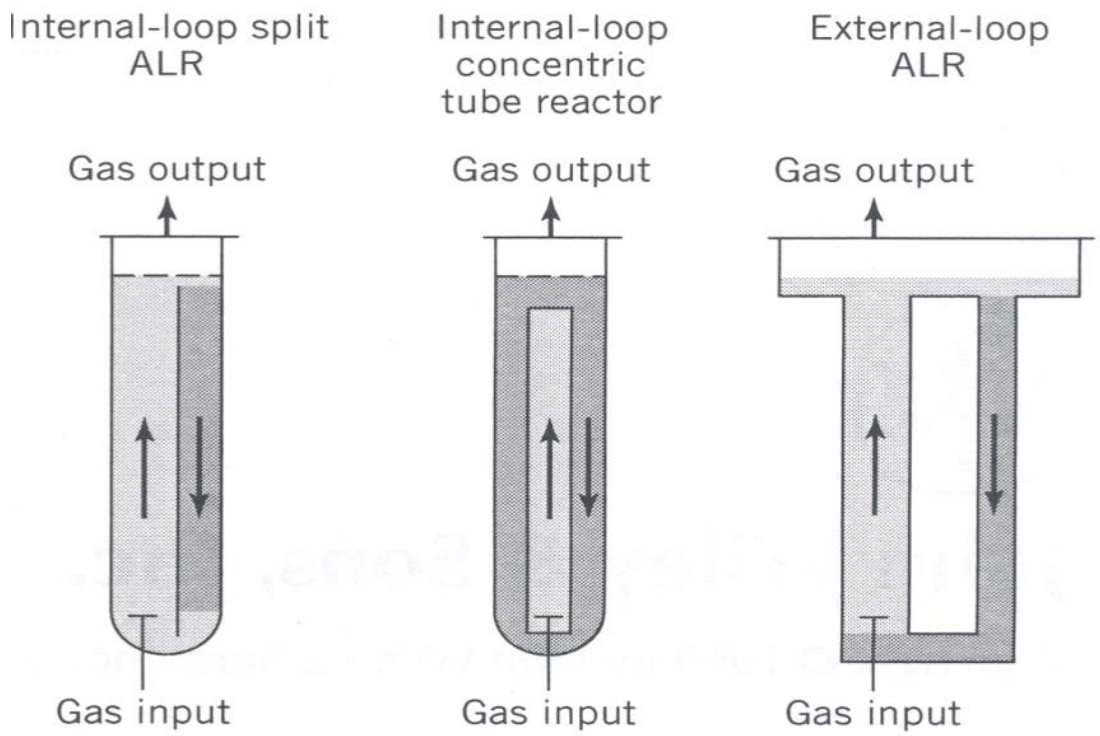

Figure 5.2 Different types of airlift reactor

(Adapted from Merchuk and Gluz (1999))

5.1.2 ADVANTAGES OF AIRLIFT REACTORS

The movement of fluids in a reactor is caused by the energy supplied at a particular point in the reactor by the agitator or sparger. Therefore, the level of energy is high near this point and decreases with distance from it (Chillakuru *et al.* 1991). The momentum transferred from the energy release point into the near surroundings supplies energy to the slower-moving, more distant elements of the fluid (Merchuk & Siegel 1988). This results in a variable shear force at different distances from the energy release point. This shear force difference inside the reactor is maximal for a stirred tank with a flat-blade turbine, which has been reported to be approximately

14 times the mean shear gradient (Chillakuru et al. 1991). Cultures grown in reactors with this kind of uneven shear stress face many difficulties. Cells near the low shear stress region may generate potentially undesirable gradients in temperature and in substrate, metabolite, and electrolyte concentrations. On the other hand, if the cells are near the turbulent zone, the heat and mass transfer are good but very high shear gradients may risk cell integrity or exert some effects on cell morphology and metabolism (Merchuk 1991a). In a culture medium exposed to high shear forces, changes in the morphology of microorganisms are often detected (Da John & Patel 1985). The nature of the relationship between such morphological changes and rates of growth and metabolite production is quite complicated, although it may be of great importance in the design and scale-up of these bioreactors (Merchuk & Gluz 1999).

Shear forces inside an ALR are much more consistent than in other types of reactors because the movement of fluid inside the reactor is due only to the difference in fluid density. The shear force required in the ALR can be selected based on the strain chosen for cultivation; this is important, since the capability of different strains to survive shear stress varies. Cells which are very shear sensitive are cultivated with low shear force in the ALR by controlled design and operation. The method of assessing shear force inside the ALR has been described by Merchuk & Berzin (1995). It has been shown experimentally that velocity fluctuations related to turbulent shear are relatively homogeneously distributed in both the riser and the downcomer (Tan *et al.* 1995). The possibility of supplying constant shear force inside the reactor is the main advantage of an ALR (Kessler et al. 1993, Merchuk & Gluz 1999).

Legrys (1978) emphasised the superiority of ALRs over reactors with mechanical agitators with respect to the mass transfer rate. Also, oxygen transfer efficiency comparison shows that ALRs are among the most efficient agitated systems (Siegel & Merchuk 1988). At

low and homogeneous shear force, ALRs are efficient enough to provide adequate oxygen transfer rates, unlike stirred reactors or simple bubble columns (Merchuk 1990, Merchuk 1991b).

The ratio of downcomer to riser cross-sectional areas is critical to mixing and oxygen transfer in ALRs, and as this ratio is increased the volumetric mass transfer (k_La) and the superficial velocity of the air decrease. In addition, the design and construction of ALRs are much simpler than stirred tank reactors, because ALRs have no moving parts; this is also the reason why the contamination risk is lower in ALRs. Additionally, the maintenance expenses are lower than for other types of reactors because shaft bearing seals and mechanical agitators are absent (Rhodes 1991).

5.1.3 DISADVANTAGES OF AIRLIFT REACTORS

One of the main disadvantages of ALRs is that the volume of liquid cannot go beyond the limit required for proper mixing. Liquid height must always be sufficient to allow liquid recirculation in the reactor and must therefore be above the separation between riser and downcomer. In an ALR it is not possible to change the inlet gas flow without changing fluid dynamics, because mixing is always coupled to the inlet gas flow. The bubbles can cause foam formation. This is a disadvantage in both ALRs and bubble column reactors, because foam is able to trap up to 30% of whole cells in suspension culture (Wu 1995), and is a source of contamination and cell loss (Aunins *et al.* 1986, Ghildyal *et al.* 1988). The efficiency of breaking the bubbles of foam when foaming occurs is very low. However, both bubble bursting and foam formation may be almost completely avoided by the use of cellular protector Pluronic F-68 (Wu 1995) and silicone antifoam (Van Der Pol *et al.* 1993), and by fixing a minimum inlet gas flow rate that meets both the CO_2 requirement of the algae and the need for mixing in the bioreactor.

Numerous studies have shown the benefits of using ALRs for cultivating cells in free suspension, demonstrating that their advantages outweigh their disadvantages.

5.1.4 CARBON DIOXIDE

Algae have the capacity to synthesize carbohydrate directly from CO_2 and water by the process of photosynthesis, which is carried out using light energy (see section 6.1.1). This process has been exploited to reduce CO_2 emission from industries using algae (Keffer & Kleinheinz 2002). CO_2 is one of the major pollutants in industries, such as the petroleum industry (Kadam 2002); thus the potential of algae to reduce these emissions is high.

A reduction of CO_2 is often not the primary goal of algal culturing. The aim is often based on industrially important products produced by the algae, such as human food (Ortega-Calvo *et al.* 1993), animal feed (Becker 2007), health products (Schwimmer & Schwimmer 1955), cosmetics (Becker 2007) and bio plastics (Asada *et al.* 1998). Nonetheless, since CO_2 is required for this production, the use of contaminant CO_2 from industry to generate valuable products combines both objectives. The products concerned may be intracellular, extracellular, or involve the whole cells (for instance, *Spirulina*; Henrikson 1989). To increase the level of production it is necessary to increase the level of biomass, so knowledge of the optimum CO_2 concentration for growth is desirable.

Though dependent upon the light intensity supplied (Palmqvist *et al.* 1994), there is a saturation point for CO_2. Increasing the CO_2 supply above that level will not increase the level of photosynthesis, and could lead to a decrease in biomass accumulation (Delucia *et al.* 1985). An increase in the concentration of CO_2 from 1 to 5% decreases the affinity of inorganic carbon in photosynthesis by microalgae (Aizawa & Miyachi 1986, Tsuzuki & Miyachi 1989). This is

usually due to reduction in activity of carbonic anhydrase and to accumulation of inorganic carbon in cells at high CO_2. Conversely, at low CO_2 concentration it has been reported that pyrenoids develop in some green algae (Miyachi *et al.* 1986, Tsuzuki *et al.* 1986) and carboxysomes in cyanobacteria (Turpin *et al.* 1984); both of these structures are implicated in carbon concentration (Graham & Wilcox 2000). Electron microscopy has revealed an increase in the density of the chloroplast envelope in cells grown at lower CO_2 concentrations. Furthermore, the density of the plasma membrane in *Dunaliella tertiolecta* increases at high CO_2 concentration (Tsuzuki et al. 1986). Although protein composition and starch components have been studied, CO_2-dependent changes in lipid composition have been little investigated to date.

In the present study, cell production rate and μmax were studied at three different CO_2 concentrations (1.5, 3.0, and 4.5% CO_2 in atmospheric air). The aim was to determine an optimum concentration for the subsequent experiments on optimization of light intensity and temperature.

5.2 MATERIALS AND METHODS

5.2.1 AIRLIFT PHOTOBIOREACTOR DESIGN AND CONSTRUCTION

Two AL-PBRs with built-in temperature control jackets were made from glass tubes. The dimensions of the AL-PBR are shown in Figure 5.3. The draft tubes inside the reactors were set by attaching two glass arms from the internal surface of the reactor. The cooling jacket was designed in such a way that the whole reactor could be completely covered by the cooling water, thus ensuring that the culture was kept at a constant temperature. The shape of the bottom was round, to facilitate fluid recirculation and avoid "death zones' where cells can accumulate. It was also designed with a small elevation to promote recirculation of the culture medium between the

downcomer and the riser. The mouth of the reactor was closed with a rubber cork containing ports for the sparger, sample collection, vent and inoculum. The temperatures of the reactors were maintained throughout the experiments using water which was recirculated from a controlled-temperature water-bath through the external jackets of the reactors. The temperature in the water bath was maintained using a high precision refrigerated recirculating bath (TX150 - R4, Grant Instruments (Cambridge) Ltd, UK). The rate of CO_2 flow was adjusted to the correct proportion using two mass flow controllers (MC series, Digital mass flow controller, Alicat Scientific, Tucson, USA) to provide an inlet flow rate of 1 L min^{-1}, which was found to produce the best mixing in preliminary trials.

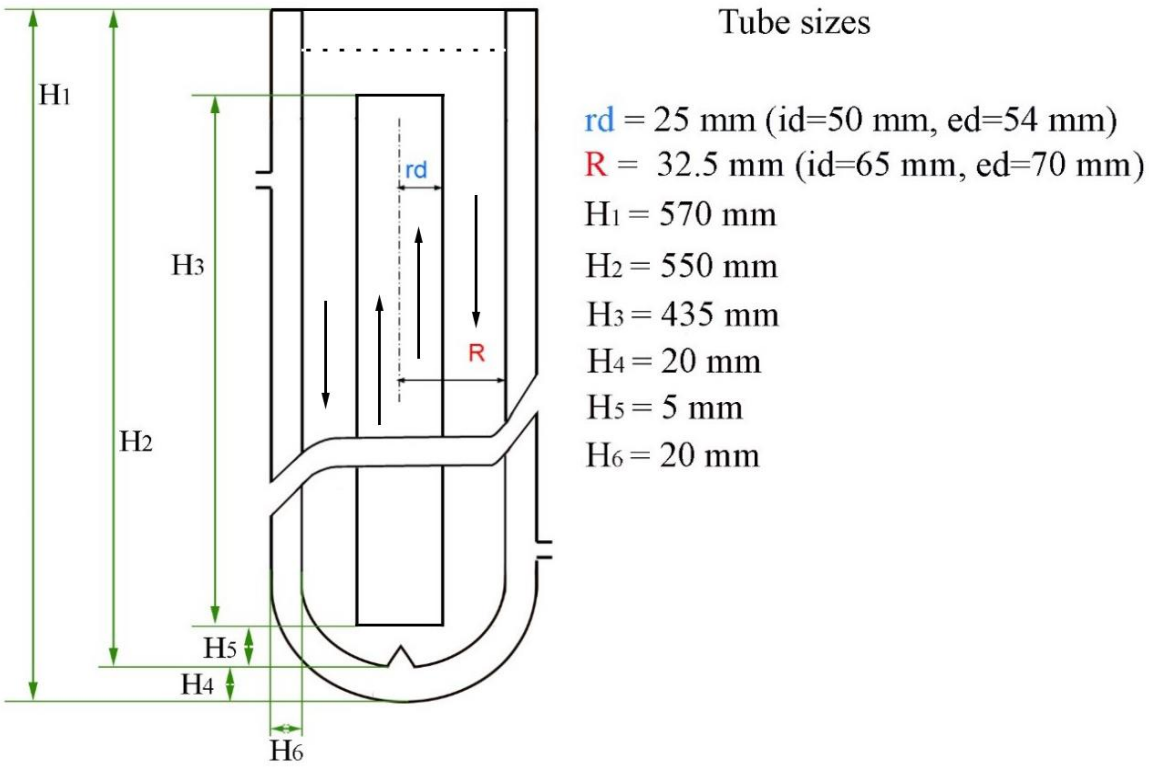

Figure 5.3 Dimensions of the airlift photobioreactors used in experiments to determine optimal CO_2 concentration, photon flux density and temperature.

5.2.2 CARBON DIOXIDE OPTIMIZATION

Two replicate AL-PBRs were used for this study. The total volume of each reactor was 1.5 L. MLA medium (Bolch & Blackburn 1996) was used in the AL-PBRs. The composition of the MLA medium used is shown in Table 5.1. The seed inoculum was prepared in the reactor before starting the experiment. Parameters maintained for the inoculum preparation were 20^{o}C, 3.0 % CO_2 at l L min^{-1} supplied through a sparger, and a PFD of 178 µmol m^{-2} s^{-1}. Seed inoculum was taken from log-phase cultures at approximately 96 hours (Figure 5.4) and used for inoculating the reactors. The reactors were supplied with 3% CO_2 at the rate of l L min^{-1} to each individual reactor. 3% CO_2 was obtained by mixing pure carbon dioxide from a cylinder with atmospheric air from a compressed air supply using two mass flow controllers (MC series, Digital mass flow controller, Alicat scientific, Tucson, USA). Before passing the 3% CO_2 to the sparger it was humidified by bubbling in a 1.5 L flask containing water. Illumination was provided using five fluorescent tube lights with a photosynthetically active radiation spectrum (F85W/GRO-LUX, Sylvania). Photosynthetically active radiation is generally measured as µmol photons m^{-2} s^{-1}. In this experiment, three different concentrations of CO_2 (1.5, 3.0 and 4.5%) were used for the cultivation of algae. The temperature of the reactors was maintained at 20^{o}C throughout the experiments.

Table 5.1. MLA medium composition (Bolch & Blackburn 1996)

Components	Final Concentration ($mg.L^{-1}$)
Salts/nutrients	
$MgSO_4 .7H_20$	49.10
$NaNO_3$	170.00
K_2HPO_4	34.80
$H3BO_3$	2.40
Trace metal mix	
Na_2EDTA	4.56
$FeCI_3.6H20$	1.58
$NaHCO_3$	1.20
$MnCI_2 .4H_20$	0.36
$CuSO_4 .5H_20$	0.01
$ZnSO_4 .7H_20$	0.022
$CoC1_2 .6H_20$	0.01
$Na_2MoO_4 .2H_20$	0.006
Additional nutrients/trace metals	
H_2SeO_3	0.0012
$CaC1_2.2H_20$	29.40
$NaHCO_3$	16.80
Na_2SO_3	12.60
Vitamins	
Thiamine HCI	0.10
Biotin	5×10^{-4}
Cyanocobalamin (B12)	5×10^{-4}

5.2.3 CELL COUNTING

Samples from both reactors were collected in sterile 10 mL vials using a sterile syringe at 24 hour intervals after inoculation, and the samples were used for cell counting. The cell counting was done using a hemocytometer. The hemocytometer and coverslip were cleaned with lens tissue before starting. A well-homogenized suspension of cells in the culture medium was introduced into the V-shaped well with a micropipette. Pipetting was terminated when the mirrored surface was covered. The counting grid was examined at 100x magnification under a light microscope (Olympus BX60, New Zealand) and the sample diluted if necessary to enable counting of individual cells.

Cell count calculation:

$$\text{Cell count} = \text{Average number cells per square} \times \text{dilution factor} \times 10^4$$

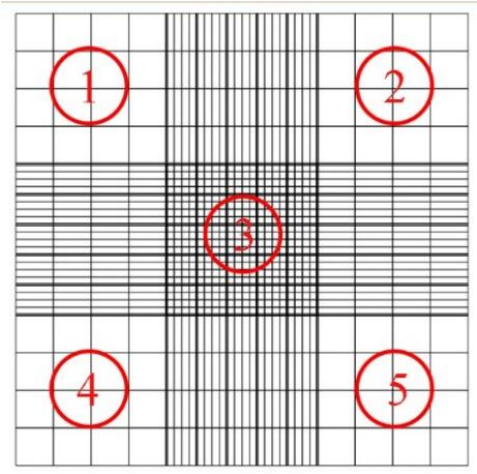

$$\text{Avg. no. of cells} = \frac{\text{sum of cells from the squares 1,2,3,4 and 5}}{5}$$

$$\text{Dilution factor} = \frac{\text{total volume (sample + diluting liquid)}}{\text{Volume of the sample}}$$

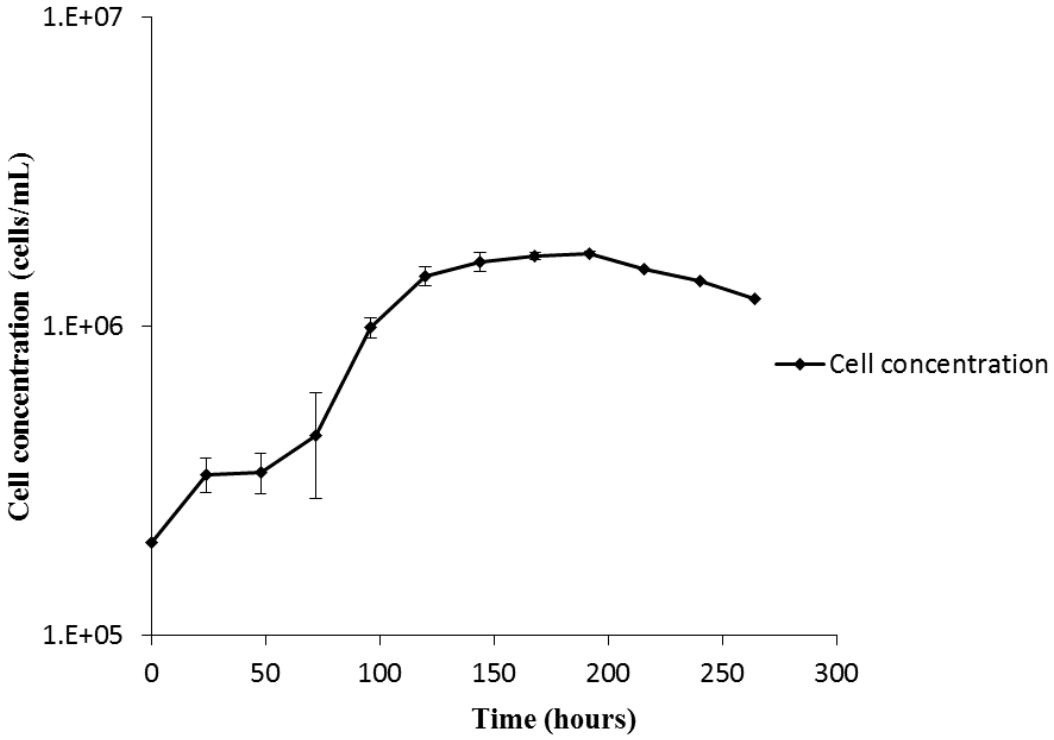

Figure 5.4 Growth curve of *Lobochlamys segnis* at 20°C and photon flux density 178 µmol m^{-2} s^{-1} with 3% CO_2. Points represent means ± S.D

5.2.4 MAXIMUM SPECIFIC GROWTH VELOCITY (µMAX)

Mean cell concentrations spanning the period of exponential cell growth were used to calculate µmax for each condition tested. These times were between 24 to 144 hours for the 1.5% CO_2 experiment, 24 to 72 hours for the 3.0% CO_2 experiment and 24 to 120 hours for the 4.5% CO_2 experiment.

The μmax was calculated using the following formula

$$\mu max = \frac{\mathrm{Ln}\left({}^{N_2}/_{N_1}\right)}{(t_2 - t_1)} \qquad \text{(Eq. 2)}$$

Where N_2 and N_1 are the cell concentrations at times t_2 and t_1 respectively.

5.2.5 STATISTICAL ANALYSIS

Means of the cell concentrations were analyzed for significant differences using two-way analysis of variance (ANOVA; time x CO_2 concentration) on the statistical computing package R (R Development Core Team 2014). Homogeneity of variance was assessed by fitting the ANOVA models and then plotting fitted values against residuals and visually inspecting the graphs. Wherever necessary, data were square root-transformed to achieve homogeneous variance. Where significance was present between the effects of CO_2 concentration, time, and their interaction, differences between individual means were determined using Tukey tests.

Comparisons of cell growth parameters under different CO_2 concentrations were made using logistic model fitting. The nonlinear least square (nls) model fitting function in R was used with the following equation:

$$y = \frac{\Phi 1}{\{1 + e^{[-(\Phi 2 + \Phi 3 x)]}\}} \qquad \text{(Eq. 3)}$$

Where y is the cell count, x is the time after the start of the experiment, Φ_1 is the maximum estimated population size, Φ_2 is the intercept and Φ_3 is the growth parameter. Starting values for Φ_1 were estimated from the maximum cell counts, and starting values for Φ_2 and Φ_3

were determined by substituting the starting value for Φ_1 into an equation for a logistic growth curve in the package "car" (Fox & Weisberg 2011).

Growth rates for each fitted model were calculated using the equation

$$\frac{\Delta y}{\Delta x} = \Phi_3 y\,(1 - y/\,\Phi_1) \qquad \text{(Eq. 4)}$$

where $\Delta y/\Delta x$ is the growth per hour, and the other parameters are as above.

Cell production rate was calculated by rearranging the second equation.

Cell production rate from the experimental μmax was estimated by using this division rate to calculate the number of cells added over the hour encompassing the maximum growth rate. This was done using equations 5–7.

$$\text{Cell production rate} = \mu\text{max} \times C_{T(1/2)} \qquad \text{(Eq. 5)}$$

Where $C_{T(1/2)}$ is the cell count at 30 minutes to $T_{1/2}$ (the time at which the cell count is half the maximum), and is calculated by

$$C_{T(1/2)} = \frac{\Phi 1}{1+e^{(-1\times(\Phi 2+\Phi 3\times(T-0.5))}} \qquad \text{(Eq. 6)}$$

$T_{1/2}$ was calculated using equation 7.

$$T = \Phi 1 \times C_T\,(1 - (\frac{C_T}{\Phi 1}) \qquad \text{(Eq. 7)}$$

C_T is cell count at $T_{1/2}$, and is calculated by

$$C_T = \frac{\left(Ln\left(\left(\frac{\Phi 1}{\Phi 1/_2}\right)-1\right)+\Phi 2\right)}{(\Phi 3\times(-1))} \qquad \text{(Eq. 8)}$$

$\Phi_{1\text{-}3}$ are as defined for equation 3.

5.3 RESULTS

5.3.1 PERFORMANCE OF AIRLIFT PHOTOBIOREACTOR

The reactor worked successfully during the course of the experiments. Figure 5.5 shows a photograph of one of the two identical reactors used, as well as a schematic representation.

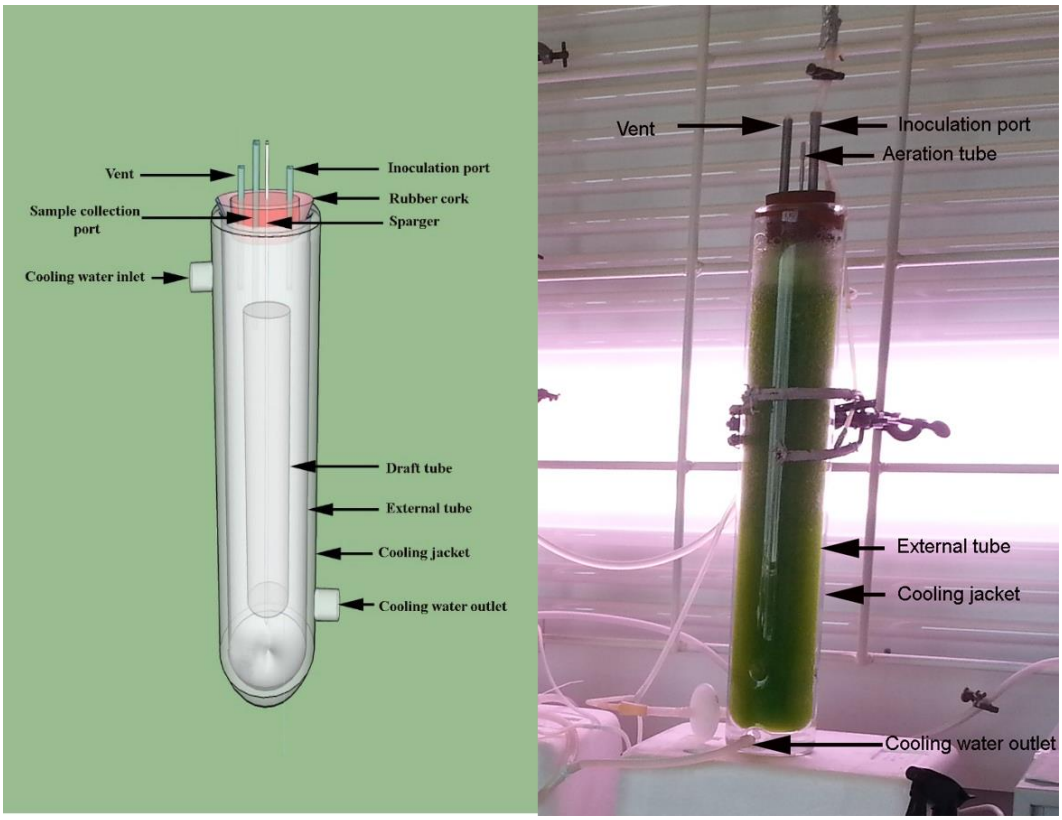

Fig. 5.5. Schematic representation and actual airlift reactor used in this study.

5.3.2 EFFECT OF CO_2 CONCENTRATION ON ALGAL GROWTH

The crude growth curves obtained during experiments with the three different CO_2 concentrations are shown in Figure 5.6. These differed in growth kinetic patterns. The μ at exponential phase increased from 1.5 to 3.0% CO_2 and decreased when CO_2 was increased to 4.5%. The μmax obtained with 3.0% CO_2 was $6.54x10^{-02}$ h^{-1}. On the basis of μmax, 3.0% CO_2 concentration was selected as optimal for the cultivation of this strain.

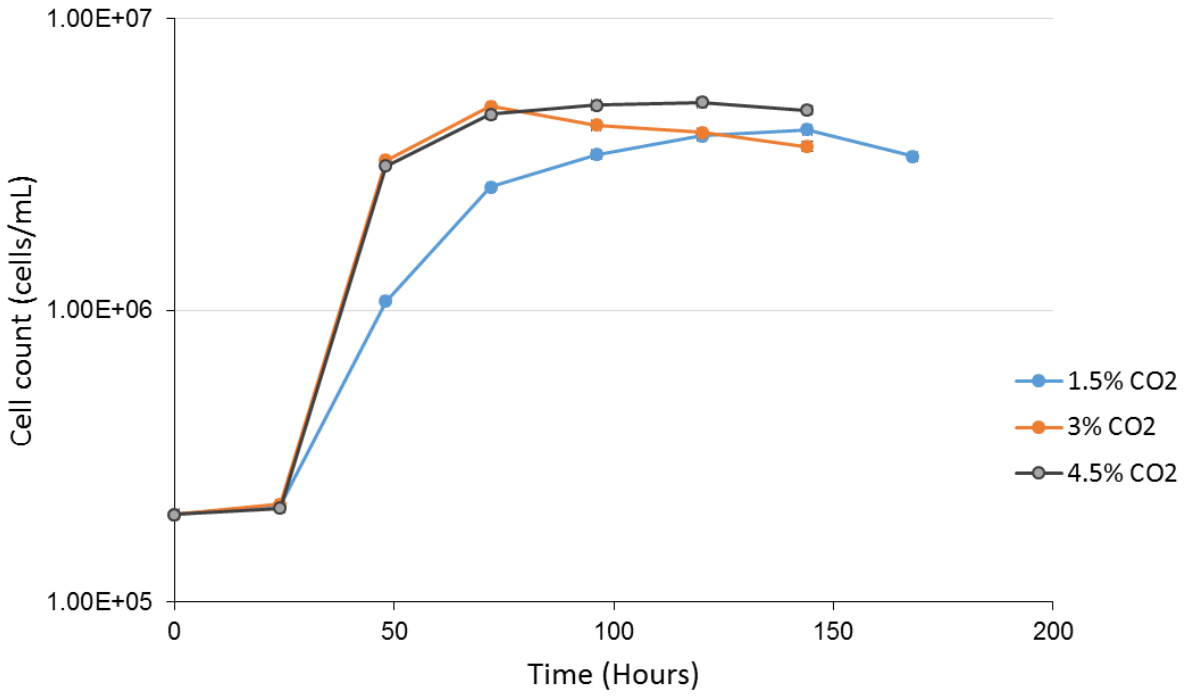

Figure 5.6. Growth curve of *Lobochlamys segnis* LCR-CC-5-1a at three different concentration of CO_2.

Means of cell count replicates differ from each other as functions of both time and CO_2 concentration, and in their interaction, according to ANOVA results (Table 5.2). The logistic models fitted to the experimental data are shown in Figure 5.7. According to the logistic models fitted, the cell production rate (Fig. 5.8) increases with the increase in CO_2 concentration up to 3.0%. The estimated cell production rate occurring at 3.0% CO_2 was 2.00×10^5 cells mL^{-1} h^{-1} but the uncertainties are large. The highest maximum estimated population size (Φ_1, 4.97×10^6 cells mL^{-1}) occurred at 4.5% CO_2, (Fig. 5.9). There appeared to be a slight upward trend over the CO_2 concentrations tested.

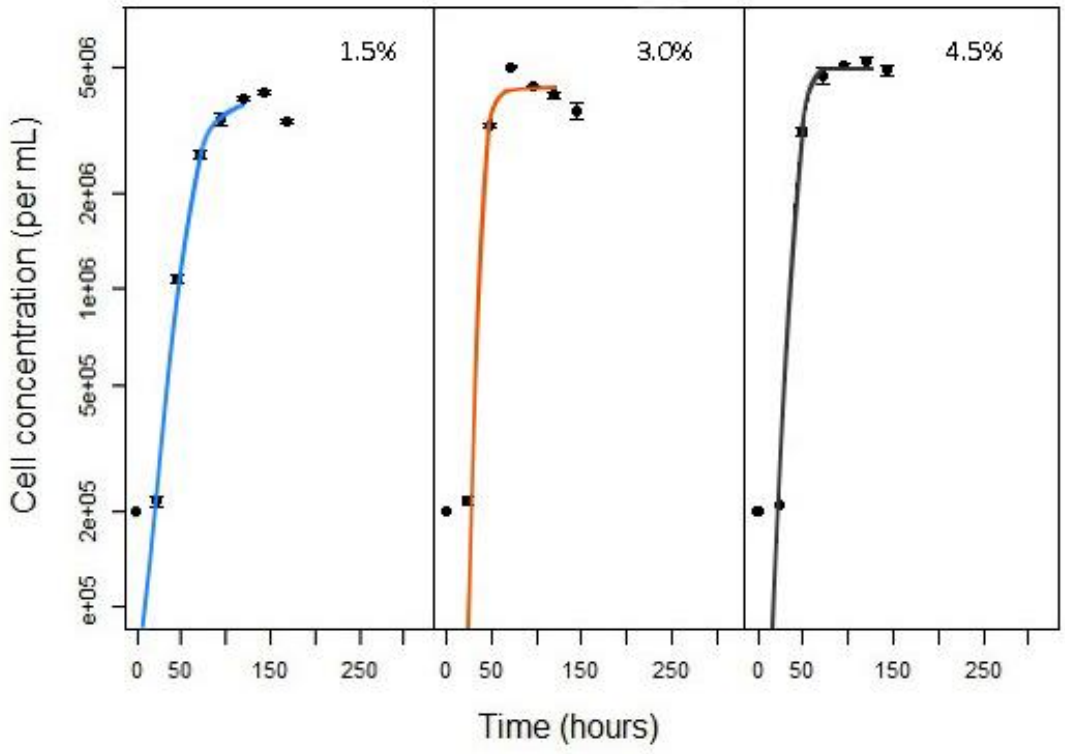

Figure 5.7 Logistic growth curves fitted to experimental data (symbols: means ± SE) of *Lobochlamys segnis* cell concentrations over time, when cultivated under different CO_2 concentrations. Curves were fitted using the nonlinear least squares (nls) function in R (R Devolopment Core Team 2014).

The Tukey tests demonstarted, there were numerous combinations of time and CO_2 concentration that were significantly different from each other; however, many were trivial (e.g. beginning and end of same or different experiments). Notable differences occurred where the maximum estimated population size at different CO_2 concentrations are compared. At 1.5% CO2 the maximum estimated population size was reached at 144 hours and this was significantly with 3.0% CO_2 at 72 hours was significantly with 4.5% CO_2 at 72 hours.

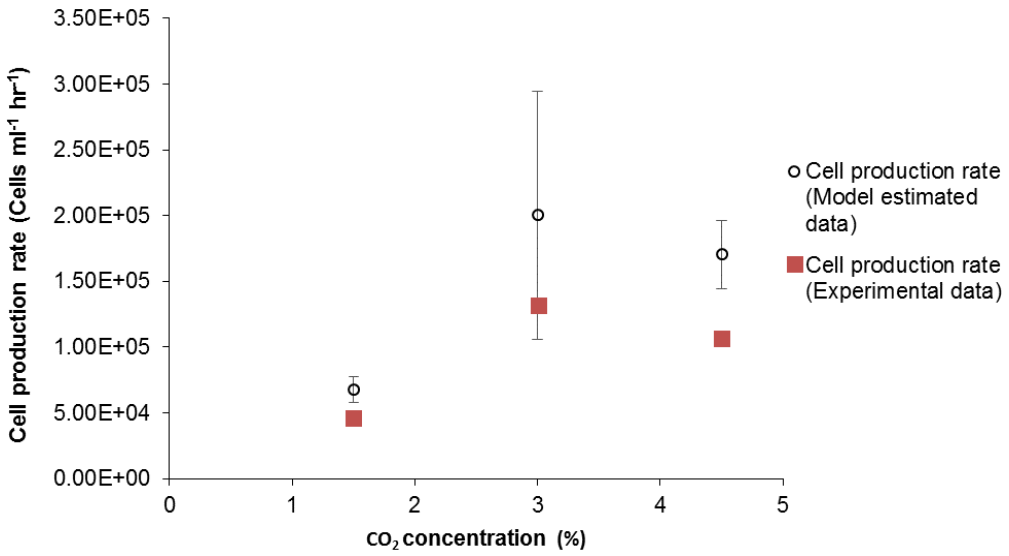

Figure 5.8 Maximum cell production rate (Φ_3) estimated from logistic growth models and from converted μmax values from crude curves fitted to different CO_2 concentrations tested. Error bars indicate standard error from the mean.

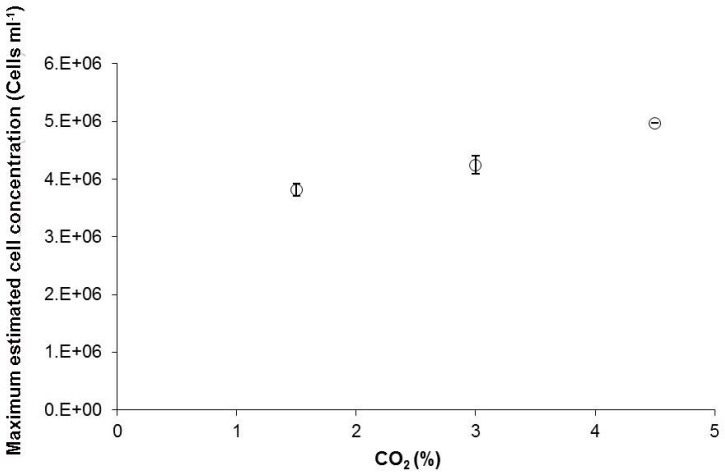

Figure 5.9 Maximum estimated population sizes (Φ_1) from logistic growth models fitted to cell concentration data over time, related to different CO_2 concentrations under which the populations were grown. Error bars indicate standard error from the mean**.**

Table 5.2 Results of two way ANOVA in which cell concentration data were modelled as a function of CO_2 concentration and time

	Df	Sum square	Mean square	F value	Pr(>F)
CO_2	2	6.892e+12	3.446e+12	261.19	4.70e-16***
Hours	7	1.336e+14	1.908e+13	1446.57	< 2e-16 ***
CO_2:Hours	12	9.890e+12	8.242e+11	62.47	3.87e-14***
Residuals	22	2.902e+11	1.319e+10		

Signif. codes: 0 '***' 0.001 '**' 0.01 '*' 0.05 '.' 0.1 ' ' 1

5.4 DISCUSSION AND CONCLUSION

Growth parameters of *Lobochlamys segnis* LCR-CC-5-1a were affected by CO_2 concentration. The μmax achieved by *Lobochlamys segnis* LCR-CC-5-1a increases from 1.5% to 3% CO_2 and decreased on further increasing the CO_2 concentration. The parameter estimates from the modelling results agree, but their associated standard errors suggests that the difference between 3.0 and 4.5% is not significant (Figure 5.8). Further investigations with higher than 4.5% CO_2 concentration were not pursued, since saturation is determined from growth rates and there was no improvement beyond 3.0% CO_2. Further increasing the CO_2 concentration may either maintain the same μmax or reduce the μmax.

Therefore, my results suggest that 3.0% is the optimum concentration for growth of *Lobochlamys segnis* LCR-CC-5-1a. This optimum falls in the range of 1.0 to 5.0%, regarded by others as the optimal CO_2 concentration for cultivating the majority of photosynthetic microorganisms in the laboratory (Semenenko *et al.* 1966). Certain algae can survive and grow at high concentrations of CO_2. Examples include *Euglena gracilis*, which can tolerate up to 45% CO_2 (Nakano *et al.* 1996), and *Scenedesmus* sp., which can survive 80%, with a μmax at 10–20% (Hanagata 1992). However, algae grown at high concentrations of CO_2 are rare (Sergeenko *et al.* 2000, Kodama *et al.* 1993). Increasing the CO_2 concentration to 10–100% inhibits the growth of most algal cultures. From an industrial point of view, increasing CO_2 input without increase in the yield (as occurs in my strain between 3.0 and 4.5% CO_2) is not recommended as it wastes resources. However, this could be reasonable if part of the objective is to scrub CO_2 as a

pollutant. Thus according to the present study, 3.0% CO_2 is recommended as the optimum concentration for the maximum growth rate of *Lobochlamys segnis* LCR-CC-5-1a.

CHAPTER 6

INFLUENCE OF PHOTON FLUX DENSITY ON *LOBOCHLAMYS SEGNIS* LCR-CC-5-1A GROWTH AND POLY UNSATURATED FATTY ACID PRODUCTION

CHAPTER 6

INFLUENCE OF PHOTON FLUX DENSITY ON *LOBOCHLAMYS SEGNIS* LCR-CC-5-1A GROWTH AND POLY UNSATURATED FATTY ACID PRODUCTION

6.1 INTRODUCTION

Light is a form of radiant energy ranging from 400 to 700 nanometers within the broad spectrum (Figure 6.1). Photosynthetically active radiation (PAR; mostly red and blue regions) covers 43% of the total solar radiation (Thimijan & Heins 1983) and is converted into chemical energy by photosynthesis (Murata *et al*. 2007). This converted chemical energy is stored in the bonds of sugar molecules. Photosynthesis is the only biological process which can harvest energy from the sun, and is carried out by most plants and algae; such organisms are called photoautotrophs. Most of the energy and oxygen required for life on Earth are produced by photosynthesis (Bryant & Frigaard 2006). The following is the chemical equation of photosynthesis:

$$6CO_2 + 6H_2O + \text{Sunlight} \longrightarrow C_6H_{12}O_6 + 6O_2$$

Among the photoautotrophs, microalgae are cultivated for several uses, including food, fertilizer, feed and fuel. The cell composition of each algal species can vary widely, depending on the culture conditions under which it is grown (Richmond 2008). Certain variables have to be

optimised for culturing the algae for maximum biomass and product, comprising irradiance, mixing, nutrients – including CO_2 among them – and temperature. Among all the environmental factors, one of the most significant is light energy, because it has a vital role in photosynthesis and yield and, as a consequence, an important influence as well on the commercial efficiency of the algal cultivation process (Cuaresma *et al.* 2009). Irradiance is directly linked to photon flux density (PFD), which is defined as the number of photons per second per unit area. Organic materials that are produced from light energy usually increase their concentrations up to a certain point of PFD, which is called the saturation point. If the PFD is increased above the saturation point, the photosynthesis or the organic material production starts to decrease due to the oxidative damage to pigments, proteins and lipids in the thylakoid membrane, thereby impairing overall photosynthetic efficiency. This damage is known as photo oxidation. If the PFD is increased above the saturation point, the photosystem ultimately starts to become impaired and this impairment is called photoinhibition (Szabó *et al.* 2005).

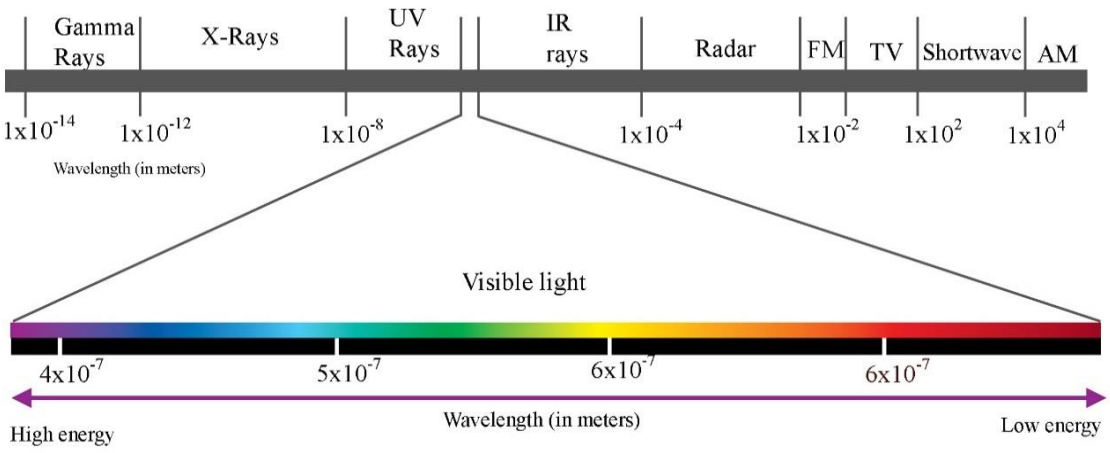

Figure 6.1 Light (Electromagnetic) spectrum

There is a wide variation in the spectrum of light harvesting between embryophytes and algae, because algae not only use chlorophyll like embryophytes for harvesting light but also different antenna pigments for doing it. Different colored pigments absorb different wavelengths of light (Lüder *et al.* 2002). Chlorophylls absorb primarily blue and red light. Also, they do not absorb the green part of the spectrum so chlorophyll-containing tissues appear green in color (Delepine 1951). On the other hand, carotenoids absorb primarily blue and green light, protecting chlorophyll from photo oxidation as well (Armstrong & Hearst 1996). Phycobiliproteins present in cyanobacteria and certain eukaryotic algae (rhodophytes, cryptomonads, glaucocystophytes) absorb primarily blue or red light and they can absorb photons from very low PFD (Moore *et al.* 1995, Moore & Chisholm 1999, Partensky *et al.* 1999). Since the amount of light absorbed depends upon the pigment composition and concentration found in the alga, light absorption by different algae may vary across the spectrum.

6.1.1 BIOCHEMISTRY OF PHOTOSYNTHESIS

Photosynthesis comprises two processes: the light-dependent reactions (photosystems I and II) and the Calvin cycle ("dark reactions"). The following is the equation of the light-dependent reaction (Raven *et al.* 2005):

$$6\ H_2O + 6\ NADP^+ + 9\ ADP + 9\ P_i + \text{light} \rightarrow 6\ NADPH + 6\ H^+ + 9\ ATP + 3\ O_2$$

The light dependent reactions occur on the thylakoid membranes, where the initiation of the process for converting energy from light to chemical energy happens. Thylakoids are the membranes present inside the chloroplasts (Kieselbach *et al.* 1998). Photons of light are absorbed by an antenna complex of pigment molecules. These molecules are a cluster of protein

or chlorophyll molecules fixed in the thylakoid membrane. The pigment molecules are excited from the ground energy state to a higher energy level by the absorption of photons. Once the photons strike photosystem II, the electron transport chain receives the energized electrons and the electrons lost by photosystem II are substituted by a process called photolysis, which involves the oxidation of a water molecule, producing free electrons and oxygen gas. From the perspective of the light dependent reactions, oxygen is a waste product, but numerous species benefit from its production (Pushkar *et al.* 2008).

The energy from the free electron produced by photosystem II is used to pump hydrogen ions from the stroma to the thylakoid, creating a concentration gradient, and this gradient powers a protein called ATP synthase, which phosphorylates ADP to ATP. The electrons leaving photosystem II, which are low in energy, are driven back to photosystem I. The low energy electrons entering photosystem I are re-energized from light received in photosystem I and passed through a second electron transport chain where they are used to reduce the electron carrier $NADP^+$ to NADPH. When the chloroplast is receiving a constant PFD, NADPH and ATP molecules are transported to the Calvin cycle in the stroma.

The Calvin cycle of photosynthesis is the process of producing glucose from CO_2 that takes place in the stroma, which is a fluid surrounding the thylakoids. The following is the equation that represents the Calvin cycle (Raven *et al*. 2005).

$$3\ CO_2 + 9\ ATP + 6\ NADPH + 6\ H^+ \rightarrow C_3H_6O_3\text{-phosphate} + 9\ ADP + 8\ P_i + 6\ NADP^+ + 3\ H_2O$$

The energy produced by photosystems I and II is used by the enzyme ribulose 1, 5-bisphosphate carboxylase/oxygenase, commonly known as Rubisco, in the stroma for the production of sugars in the dark reactions (Feller *et al.* 2008). The Calvin cycle is powered by

ATP and NADPH produced during the light-dependent reactions in the stroma. Glucose phosphate, which is the starting molecule for the synthesis of starch and cellulose, is produced through the Calvin cycle. Autotrophs produce sugars to use as storage molecules and structural components. By utilizing the energy from light, along with the inputs of water and CO_2; photoautotrophs act as glucose factories.

6.1.2 PHOTON FLUX DENSITY OPTIMIZATION

There are two main reasons to optimize the PFD when growing algae in an industrial process:

1. To increase the μ to achieve maximum biomass (Qiang & Richmond 1996)
2. To stimulate the organisms to produce the maximum concentration of a desired product (e.g., FAs, lipid or carotenoids) (Carvalho & Malcata 2005, Solovchenko *et al*. 2008).

The optimal PFD depends on the species, temperature and nutritional condition of the algae (Nyholm & Källqvist 1989). For instance the μ of *Chlorella pyrenoidosa* strain 7-11-05 was studied at two different temperatures, 25 and 39^{o}C. When the culturing temperature was 25^{o}C, the culture reached photo inhibition above 1000 lm/ft^2. On the other hand, the same culture reached photo inhibition at 600 lm/ft^2 when culturing temperature was maintained at 39^{o}C (Sorokin & Krauss 1958).

6.1.3 EFFECT OF PHOTON FLUX DENSITY ON SECONDARY METABOLITES

Photon flux density not only has a direct role in the photosynthetic activity of algae, but it has also been reported to cause variations in secondary metabolite composition (Richardson *et al.* 1983). Examples of these changes for various algal species are described in Table 6.1. Oxidative destruction of PUFAs has been recorded under high PFD (Harwood 1998). In contrast, high PFD

is recommended for the accumulation of certain FAs, such as palmitoleic acid (C16:1). Normally, the production and accumulation of polar lipids, especially chloroplast-associated lipids, are high at low PFD, whereas total polar lipid content declines at high PFD along with an increase in the amount of neutral storage lipids (Orcutt & Patterson 1974, Napolitano 1994, Brown *et al.* 1996, Khotimchenko & Yakovleva 2005). The total phospholipid content declines and the nonpolar lipid accumulation increases in the green alga *Cladophora* sp. when exposed to a PFD of 300 $\mu mol\ m^{-2}\ s^{-1}$ (Napolitano 1994). The lipid content of *Pavlova lutheri* increased significantly when PFD was increased to 120 $\mu mol\ m^{-2}\ s^{-1}$, as reported by Carvalho and Malcata (2005). Generally, at high PFD, there is a rise in the production of triacylglycerol (TAG) because it acts as a protective mechanism to avoid damage to the photosynthetic apparatus. Also, FAs synthesized above the amount required by the cell are stored as TAG, which can be catabolized to deliver metabolic energy (Sharma *et al.* 2012)

The abundance and type of carotenoids are also influenced by PFD. For example, at low intensity PAR, 35 $\mu mol\ m^{-2}\ s^{-1}$, the μ of the green microalga *Parietochloris incisa* is not only slow but the ratio between carotenoid and chlorophyll eventually also decreases. In contrast the μ and the carotenoids β-carotene and lutein increase with increase in PFD (Solovchenko *et al.* 2008).

Table 6.1 Changes in lipid and fatty acid composition in different algal species reported due to change in photon flux density.

Microalgae	Change in light regime	Lipid profile change after induction	Reference
Chaetoceros muelleri	UV-A	Increased monounsaturated FA	Liang *et al*. (2006)
Coccomyxa simplex	High UV-B	Increase in lipid production	Jiang & Chen (1999)
Isochrysis galbana	Shorter light period	Increase of PUFA	Bandarra *et al.* (2003)
Nannochloropsis oculata	UV-A	Increase of PUFA, structural lipids	Srinivas & Ochs (2012)
Nannochloropsis sp.	UV-A	Increase in saturated FA to PUFA ratio	Forján *et al.* (2011)
Pavlova lutheri	High PFD	Increase in lipid production	Carvalho & Malcata (2005)
Phaeodactylum tricornutum	UV radiation	Increased EPA and PUFA	Liang *et al.* (2006)

Pleurosigma Antarctica	Low UV-B	Increase in PUFA, structural lipids	Jiang & Chen (1999)
Prorocentrum minimum	Dark treatment	Marginal increase in phospholipids	Mock & Kroon (2002)
Selenastrum Capricornutum	Dark treatment	Increase in linoleate FA	Mock & Kroon (2002)
Tetraselmis sp.	UV-B radiation	Increase in saturated and monounsaturated FA	Goes *et al.* (1995)
Thalassiosira pseudonana	Continuous or light/dark cycled strong light at stationary phase	Increased TAG	Brown *et al*. (1996)
Thalassiosira pseudonana	Cycled strong light at exponential growth	Increased PUFA	Brown *et al*. (1996)

PFD interacts with the different phases of algal growth to have a strong influence on FA composition. For instance, Brown *et al* (1996) studied the μ and FA accumulation in *Thalassiosira pseudonana* at various stages of growth. A strain cultivated at 50 μmol m^{-2} s^{-1} PFD contained less TAG with saturated FAs and MUFAs than cultures at high PFD. By contrast, maximum PUFA production occurred during the exponential growth phase at higher PFD, 100 μmol m^{-2} s^{-1} (Brown *et al*. 1996). Mock & Kroon (2002) cultured three different strains of marine ice diatoms at 2 and 15 μmol photons m^{-2} s^{-1} and found double the quantity of Monogalactosyldiacylglycerol (MGDG), containing EPA, in the former. Gandarra *et al* (2003) found that *Isochrysis galbana* produces maximum PUFAs when exposed to high PFD for a short duration.

6.1.4 TYPES OF LIGHT SOURCES

In nature, algae use sunlight as the source of light for photosynthesis. Usually sunlight is used for culturing algae in raceway ponds (Jonker & Faaij 2013). But sunlight cannot be used to carry out an experiment with specific irradiance. Therefore it is necessary to use an artifical light source in the laboratory to allow PFD to be accurately controlled, in order to determine optimal conditions for production of particular compounds by different species

Different light sources suitable for algal experiments in the laboratory are:

1. Incandescent lamps (tungsten or halogen lamps)
2. Discharge lamps (mercury, xenon, fluorescent lamps)
3. Light-emitting diodes (LEDs)
4. Lasers

6.1.5 INFLUENCE OF MIXING AND REACTOR DESIGN ON PFD RECEIVED BY CELLS

Photobioreactors allowing the cultivation of a single species of microalgae for prolonged durations are used to cultivate algae at laboratory and pilot scales. The reactors are usually made of straight transparent tubes, mainly of plastic or glass. Generally concentric AL-PBRs are provided with continuous external illumination. The medium containing the cells is mixed in a circular motion because the content moves though the downcomer and the riser in opposite directions. Due to this type of mixing the cells are not exposed to uniform PFD because the downcomer is closer to the light source than the riser (and the riser is increasingly shaded by cells in the downcomer as the culture becomes more dense). This effect results in variable PFD experienced by the cells (Silvera & Cortina 2013), which may reduce photoinhibition and the possibility of biomass loss (Ogbonna & Tanaka 2000).

6.1.6 AIMS OF THE STUDY

The specific objectives of the present study were to determine the PFD required by *Lobochlamys segnis* LCR-CC-5-1a cultivated in AL-PBRs to achieve the following:

1. its maximum specific growth velocity.
2. its maximum estimated population size.
3. its maximum production of PUFAs, and particularly omega-3 FAs and ALA.

6.2 MATERIALS AND METHODS

6.2.1 GROWTH RATE STUDIES IN AIRLIFT PHOTOBIOREACTOR

Two replicate AL-PBRs were used (Figure 6.2). The total volume of each was 1.5 L. The complete reactor design is described in detail in Chapter 5. The medium used was MLA medium (Bolch & Blackburn 1996) (Table 5.1).

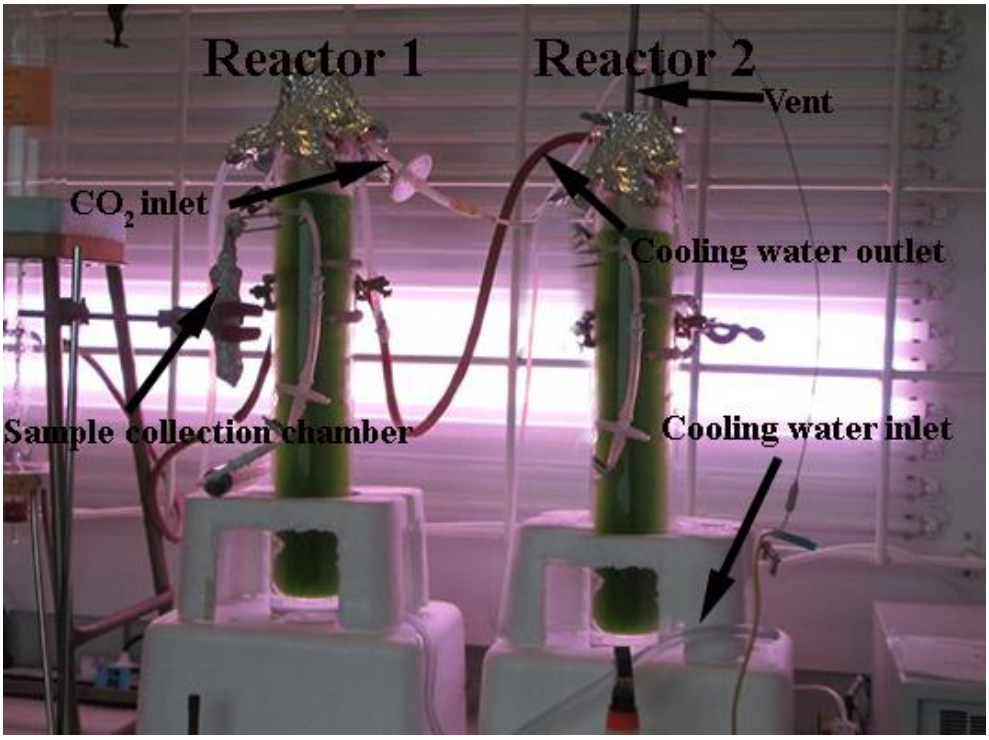

Figure 6.2 *Lobochlamys segnis* LCR-CC-5-1a cultivation in two replicate airlift photobioreactors.

Development of the seed inoculum, inoculation of the two replicate AL-PBRs in experiments, and culture conditions excepting PFD were as described in section 5.2.2. In these experiments, seven different PFDs were tested by turning on different numbers of fluorescent

tube lights. Table 6.2 shows the resulting irradiance levels inside the reactor for the different condition tested. The temperature of the reactors was maintained at 20^{o}C throughout the experiments. Sample collection was as described in section 5.2.3, except that in this case the samples were used for both cell counting and FA analysis.

Table 6.2. Range of photon flux density used for the study

Number of tube lights	Irradiance inside the reactor (μmol m^{-2} s^{-1})
1	38
2	77
3	115
5	178
7	210
10	236
18	253

Samples for FA analysis were frozen at -20^{o}C prior to freeze drying. FA analysis for both reactors was carried out at Callaghan Innovation (Wellington, New Zealand) for both the exponential growth and stationary phases. The FA analysis methodology used for this assessment is described below.

6.2.2 CELL COUNTING

Cell counting was performed as explained in Chapter five, section 5.2.3.

6.2.3 MAXIMUM SPECIFIC GROWTH VELOCITY

Calculation of μmax was carried out using the method described in section 5.2.4. The time intervals used for each level of PFD were as follows: between 24 and 96 hours for the 38 μmol m^{-2} s^{-1} PFD experiment, between 24 and 72 hours for the 77, 115 and 253 μmol m^{-2} s^{-1} PFD experiments and between 24 and 48 hours for the 178, 210 and 236 μmol m^{-2} s^{-1} PFD experiments.

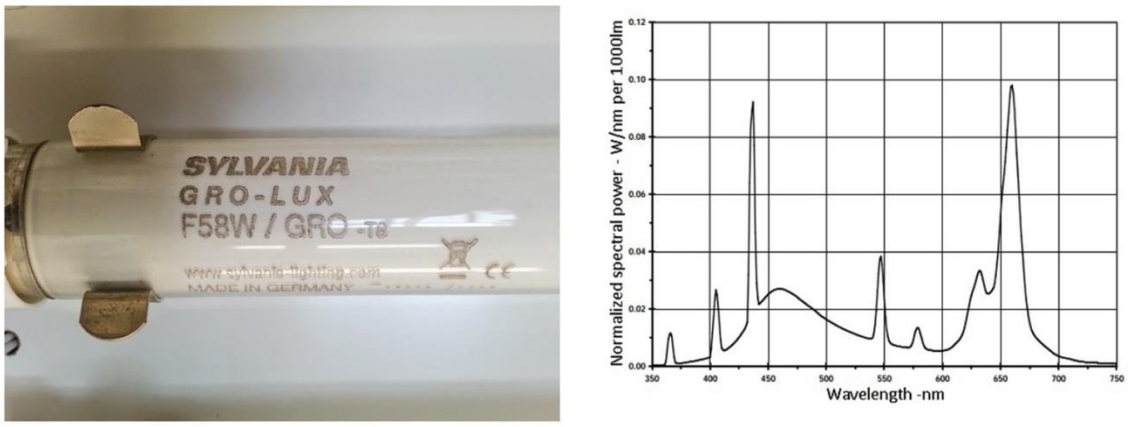

Figure 6.3 Special fluorescent tube lights used for the experiments and their spectral power distribution (from Sylvania catalog, technical information bulletin).

6.2.4 FREEZE DRYING

The algae collected as samples were centrifuged at 1800 x g for 20 min to separate the biomass from the broth. The separated biomass was stored in the freezer (2 -5°C). The frozen samples with perforated caps were loaded in the vacuum chamber of the freeze dryer (Labconco, Kansas City, Missouri, USA) and dried under refrigeration and vacuum for 24–36 hours. The resulting samples were used for FA analysis.

6.2.5 FATTY ACID ANALYSIS

FA analysis was performed as explained in section 4.2.2.

6.2.6 STATISTICAL ANALYSIS

Statistical analysis was performed as explained in section 5.2.6.

6.3. RESULTS

6.3.1 EFFECT OF PHOTON FLUX DENSITY ON ALGAL GROWTH

Figure 6.4 shows growth curves for the different PFDs tested. Table 6.3 below shows the values of μmax, calculated from crude curves fitted to the experimental data, corresponding to each PFD. Three different sets of μmax were observed: in order of lowest to highest μmax, the first occurred under PFD 38 μmol m^{-2} s^{-1}, the second set under PFDs 77, 115 and 253 μmol m^{-2} s^{-1}, and the third set under PFDs 178, 210, and 236 μmol m^{-2} s^{-1} . As shown in Figure 6.4, the μmax increases between PFD values of 38 and 178 μmol m^{-2} s^{-1} gradually, and reaches its μmax of $9.20x10^{-2}$ h^{-1} at the latter PFD value. On further increasing the PFD, the μmax declined.

Table 6.3 Maximum growth rate (μmax) corresponding to cell concentrations spanning the period of exponential cell growth for each photon flux density

PFD (μmol m^{-2} s^{-1})	μmax (h^{-1})
38	$3.92x10^{-2}$
77	$5.88x10^{-2}$
115	$5.98x10^{-2}$
178	$9.20x10^{-2}$
210	$8.52x10^{-2}$
236	$8.42x10^{-2}$
253	$5.70x10^{-2}$

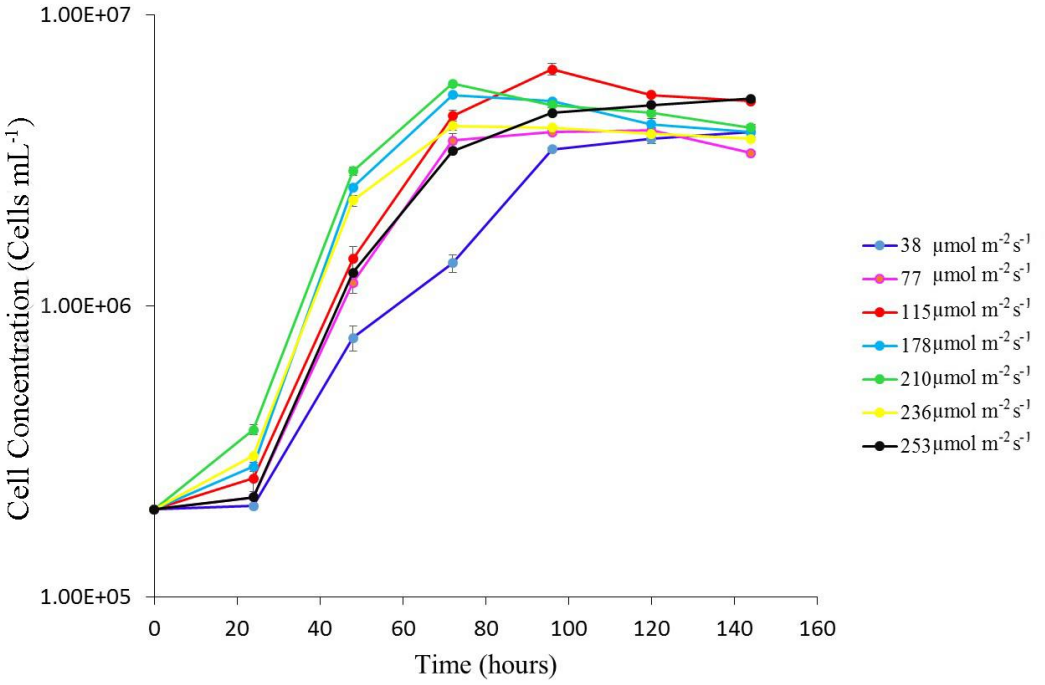

Figure 6.4 Growth curve of *Lobochalamys segnis* LCR-CC-5-1a at different photon flux densities. Error bars indicate standard deviation from the mean.

Means of cell concentration replicates differ from each other as functions of both time and PFD, and in their interaction, according to ANOVA results (Table 6.4). Tukey tests identified numerous significant differences, many of which are trivial (e.g. differences between cell concentrations at the start and end of the same and different experiments). Significant differences of interest are

- cell concentrations under 115 µmol m^{-2} s^{-1} at 96 hours with 178 µmol m^{-2} s^{-1} at 72 hours, and with 236 µmol m^{-2} s^{-1} at 96 hours;

- cell concentrations under 236 µmol m^{-2} s^{-1} at 96 hours and 210 µmol m^{-2} s^{-1} at 72 hours;

- cell concentrations under 77 µmol m^{-2} s^{-1} at 96 hours and both 178 and 210 µmol m^{-2} s^{-1} and 210 µmol m^{-2} s^{-1} at 72 hours.

- cell concentrations under 32 µmol m^{-2} s^{-1} at 114 hours with both 178 and 210 µmol m^{-2} s^{-1} at 72 hours, 115 µmol m^{-2} s^{-1} at 96 hours and 253 at 144 hours.

The logistic models of cell concentrations over time at different PFDs are shown in Figure 6.5. According to the logistic models fitted, the cell production rate (Φ_3; see Eqn 3, Chapter 5) of *L. segnis* LCR-CC-5-1a increased with increase in PFD from 38 µmol m^{-2} s^{-1} to 210 µmol m^{-2} s^{-1} (Figure 6.6). Increasing the PFD above 210 µmol m^{-2} s^{-1} resulted in a decline in the cell growth rate (Figure 6.6). The maximum cell production rate is recorded at a PFD of 210 µmol m^{-2} s^{-1}, but the growth parameter estimate from this experiment is considered to be an outlier because model fitting performed poorly. A data point at the end of the exponential growth period in this experiment had to be omitted for model fitting to succeed; consequently, the growth parameter estimate was artificially inflated. If this experiment is omitted, the cell production rate of 1.4 x 10^5 cells mL^{-1} h^{-1} was recorded in the cultures exposed to 115 and 178 µmol m^{-2} s^{-1} PFD.

In general, the results of the µ calculations from the experimental data support the modelled data (Figure 6.6). The cell production rate calculated from experimental data falls within the standard error of the modelled estimates at the PFD values 38, 77, 115 and 178 µmol m^{-2} s^{-1}. However, this is not the case at the PFD values of 210, 236 and 253 µmol m^{-2} s^{-1}, although the decreasing trend is the same.

The maximum estimated population size (Φ_1; see Eqn 1, Chapter 5) was approximately consistent across experiments (4–5 x 10^6 cells mL^{-1}), except for the experiment at PFD 115 µmol m^{-2} s^{-1} (approximately 6 x 10^6; Figure 6.7). This estimate also had the highest uncertainty. The

relationship between PFD and maximum estimated population size did not follow the unimodal distribution observed for the maximum growth rate (Φ_3; Figure 6.6).

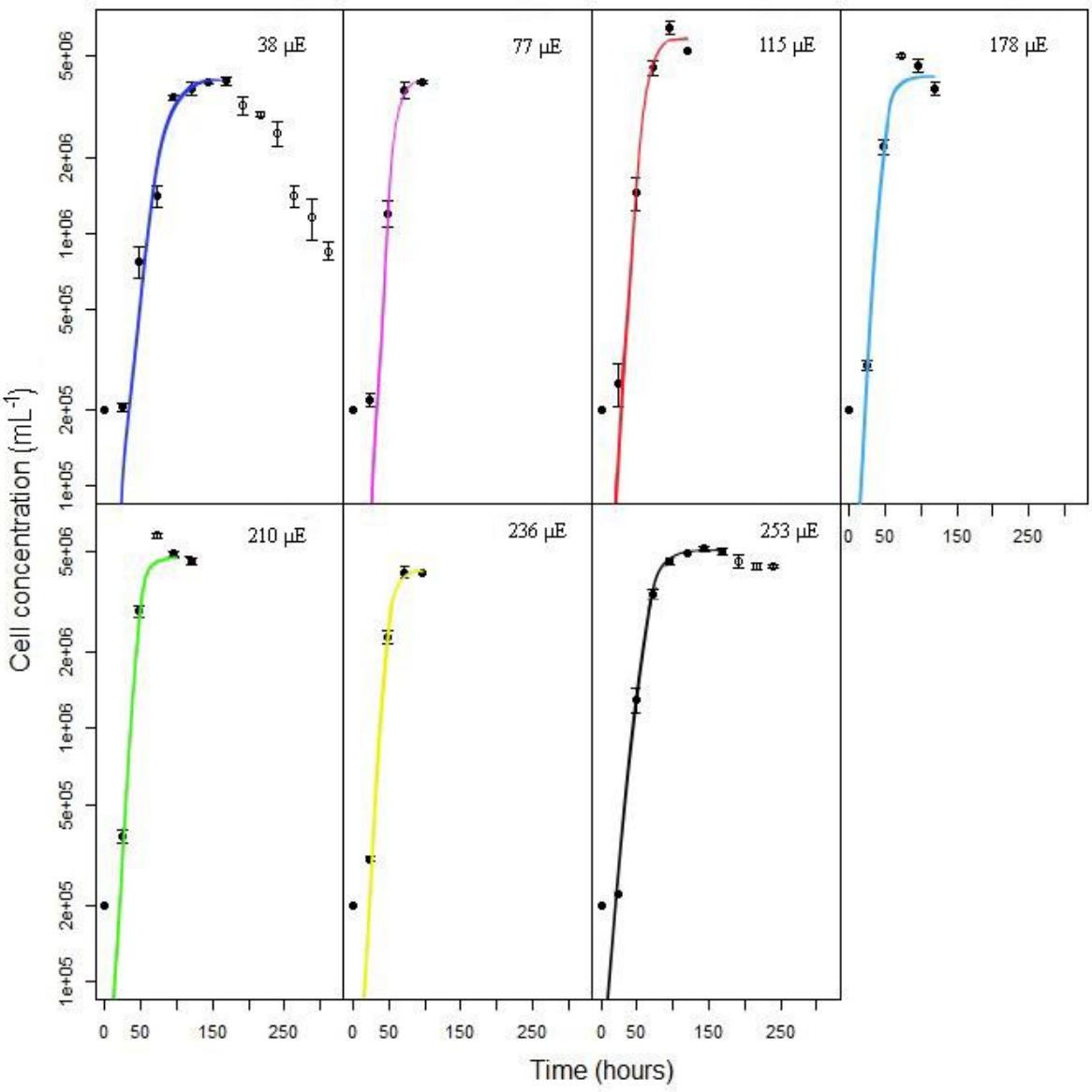

Figure 6.5 Logistic growth curves fitted to experimental data (symbols; means ± SE) of *Lobochalamys segnis* cell concentrations over time, under exposure to different levels of photon flux density. Curves were fitted using the nonlinear least squares (nls) function in R. Points omitted from model fitting are unfilled.

Table 6.4 Results of two way ANOVA in which cell count data were modelled as a function of PFD and time

	Df	Sum square	Mean square	F value	Pr (>F)
PFD	6	3208427	534738	278.06	< 2e-16 ***
Hours	13	47254813	3634986	1890.18	< 2e-16 ***
PFD:Hours	33	2096588	63533	33.04	< 2e-16 ***
Residuals	53	101923	1923		

Signif. codes: 0 '***' 0.001 '**' 0.01 '*' 0.05 '.' 0.1 ' ' 1

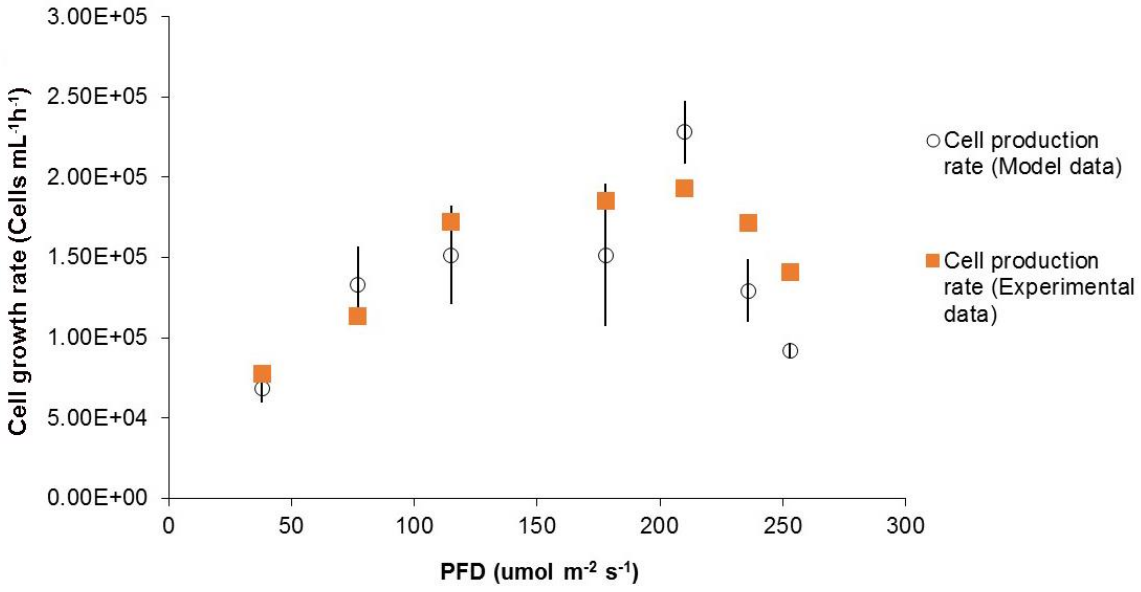

Figure 6.6 Cell production rates (Φ_3) estimated from logistic growth models of cell concentration data and experimental data at different PFDs tested. Error bars indicate standard error from the mean.

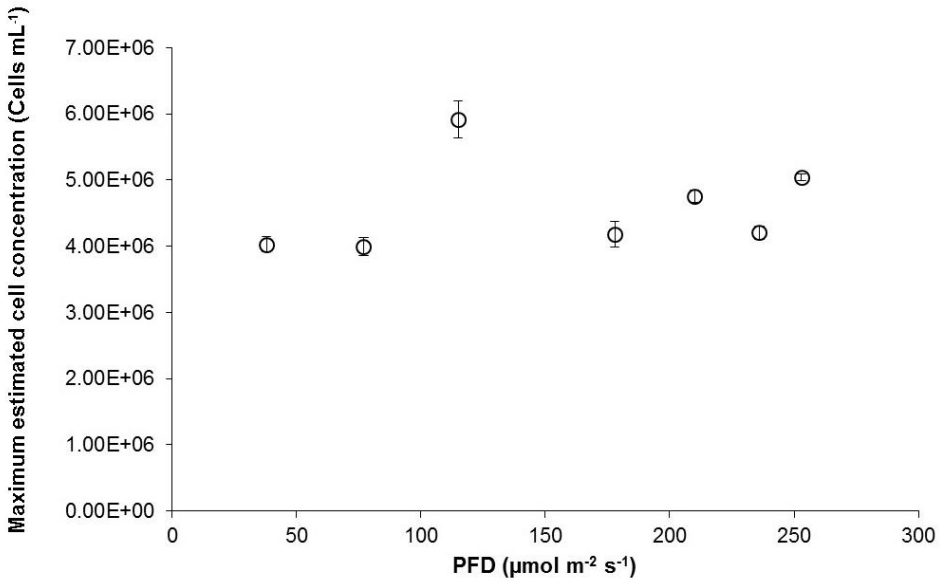

Figure 6.7 Maximum estimated population sizes (Φ_1) estimated from logistic growth models of cell count data, at the different photon flux densities tested. Error bars indicate standard error from the mean.

6.3.2 INFLUENCE OF PHOTON FLUX DENSITY ON POLY UNSATURATED FATTY ACID PRODUCTION

6.3.2.1 PUFA concentration in *Lobochlamys segnis* LCR-CC-5-1a at different growth phases.

The means of the PUFA concentration in *Lobochlamys segnis* LCR-CC-5-1a at different PFDs during the exponential and stationary phases are shown in Figure 6.8. Means of PUFA concentration replicates differ from each other as functions of both time and PFD, according to ANOVA results and Tukey tests (Table 6.5; Figure 6.9). However, the interaction effect between different PFDs and growth phases was not significant (Table. 6.5); thus, the effect of PFD does

not depend on growth phase. Tukey tests showed that the combinations responsible for the significant differences were the samples collected from the 236 µmol m^{-2} s^{-1} PFD experiment at exponential phase, compared with the stationary phase samples from the experiments carried out at 38 and 210 µmol m^{-2} s^{-1} at stationary phase (Figure 6.9).

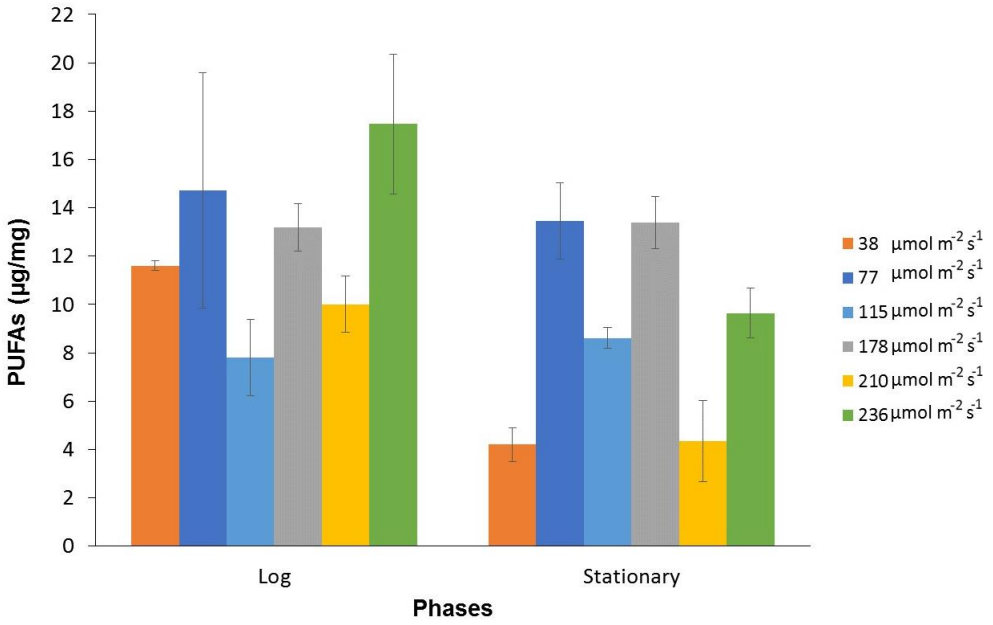

Figure 6.8 Relationship between polyunsaturated fatty acids concentration at different intensities of light at exponential and stationary phase. Bars represent means ± standard errors.

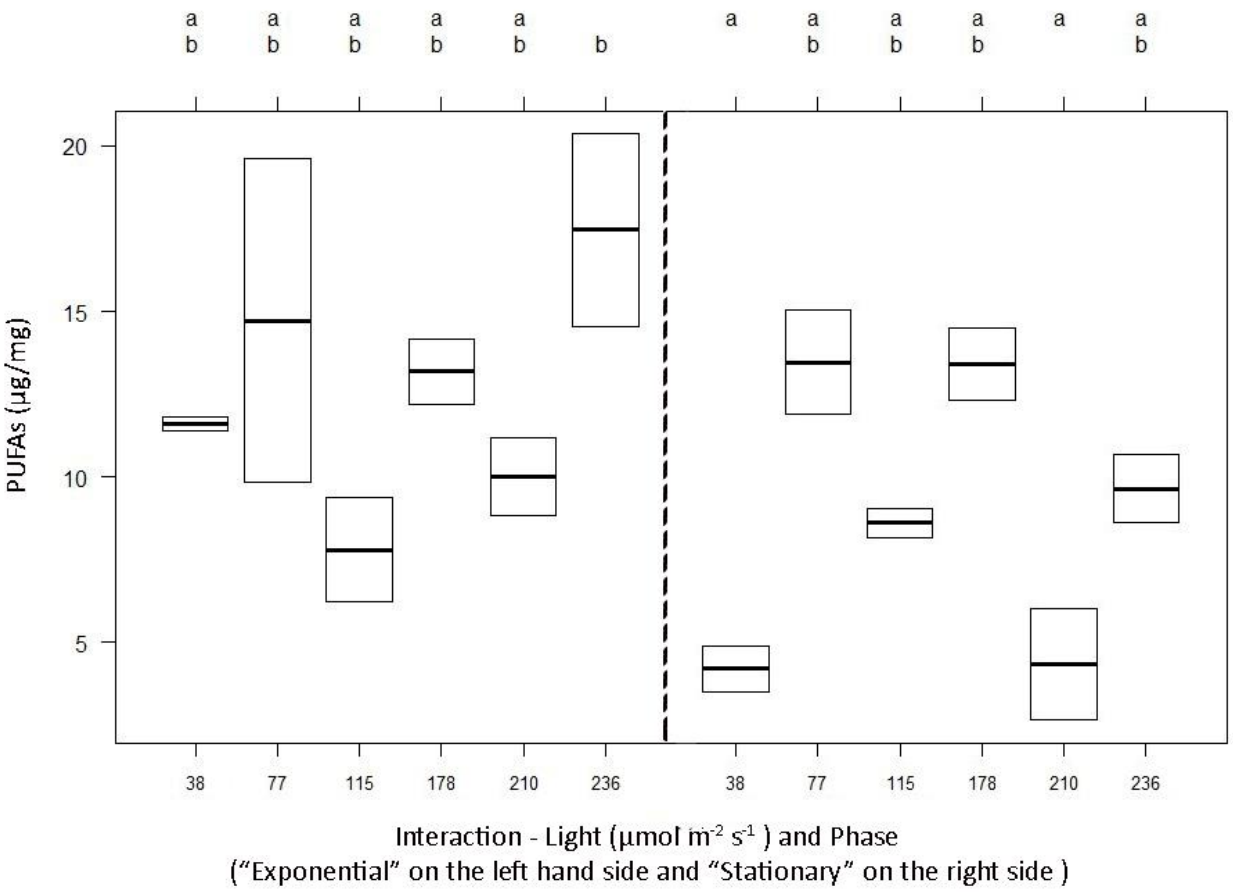

Figure 6.9 Results of Tukey tests on the ANOVA model from Table 6.5. The values on the X axis are different PFDs under which experiments were carried out (exponential phase on the left hand side and the stationary phase on the right hand side). The numbers on the Y axis represent µg of PUFAs per mg of algae biomass. The line in the box plots represent the means of the PUFAs concentration and the boxes represent the quartiles. The letters above the plot indicate significant differences between means according to Tukey test results; treatments sharing the same letters are not significantly different.

Table 6.5 Results of two way ANOVA in which polyunsaturated fatty acids concentrations were modelled as a function of Photon flux density and phase

	Df	Sum square	Mean square	F value	Pr(>F)	
PFD	5	2.11E+02	4.22E+01	5.612	0.00679	**
Phase	1	7.42E+01	7.42E+01	9.862	0.00853	**
PFD:Phase	5	7.59E+01	1.52E+01	2.016	0.1483	
Residuals	12	9.03E+01	7.52E+00			

Signif. codes: <0.001 '***' 0.001 '**' 0.01 '*' 0.05 '.' 0.1 ' ' 1

6.3.2.2 Omega-3 fatty acid accumulation in *Lobochlamys segnis* LCR-CC-5-1a at various intensities of light at different growth phases.

Figure 6.10 shows the means of omega-3 FA concentrations in *Lobochlamys segnis* LCR-CC-5-1a at different PFDs during the exponential and stationary phases of growth. The means differ from each other as functions of both time and PFD, according to ANOVA results and Tukey tests (Table 6.6; Figure 6.11). However, the interaction effect between PFD and growth phases was not significant (Table. 6.10); thus, it is not possible to conclude that the effect of PFD varies by growth phase. The 11 combinations contributing to the significant differences are shown in Figure 6.11. These were:

- 38 µmol m^{-2} s^{-1} PFD at exponential phase with 236 µmol m^{-2} s^{-1} at exponential phase;

- 77 µmol m^{-2} s^{-1} PFD at exponential phase with 38 and 210 µmol m^{-2} s^{-1} at stationary phase;

- 115 µmol m^{-2} s^{-1} PFD at exponential and stationary phases with 236 µmol m^{-2} s^{-1} at exponential phase;

- 38 µmol m^{-2} s^{-1} at stationary phase with 178 and 236 µmol m^{-2} s^{-1} PFD at exponential phase and with 77 and 178 µmol m^{-2} s^{-1} at stationary phase;

- 210 µmol m^{-2} s^{-1} PFD at stationary phase with 236 µmol m^{-2} s^{-1} at stationary phase.

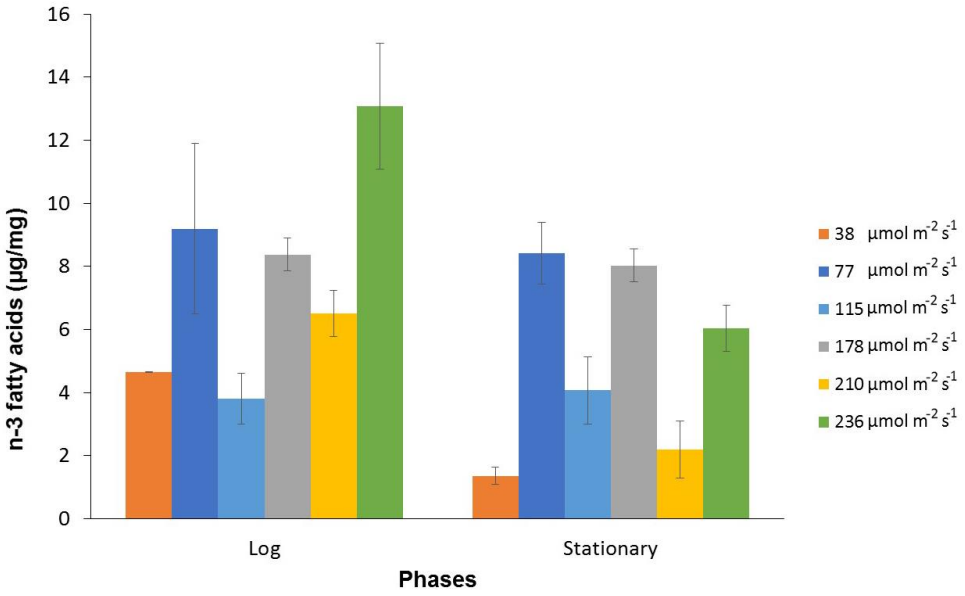

Figure 6.10. Relationship between Omega 3 fatty acid concentration at different intensities of light at exponential and stationary phases. Bars represent means; error bars indicate standard error from the mean.

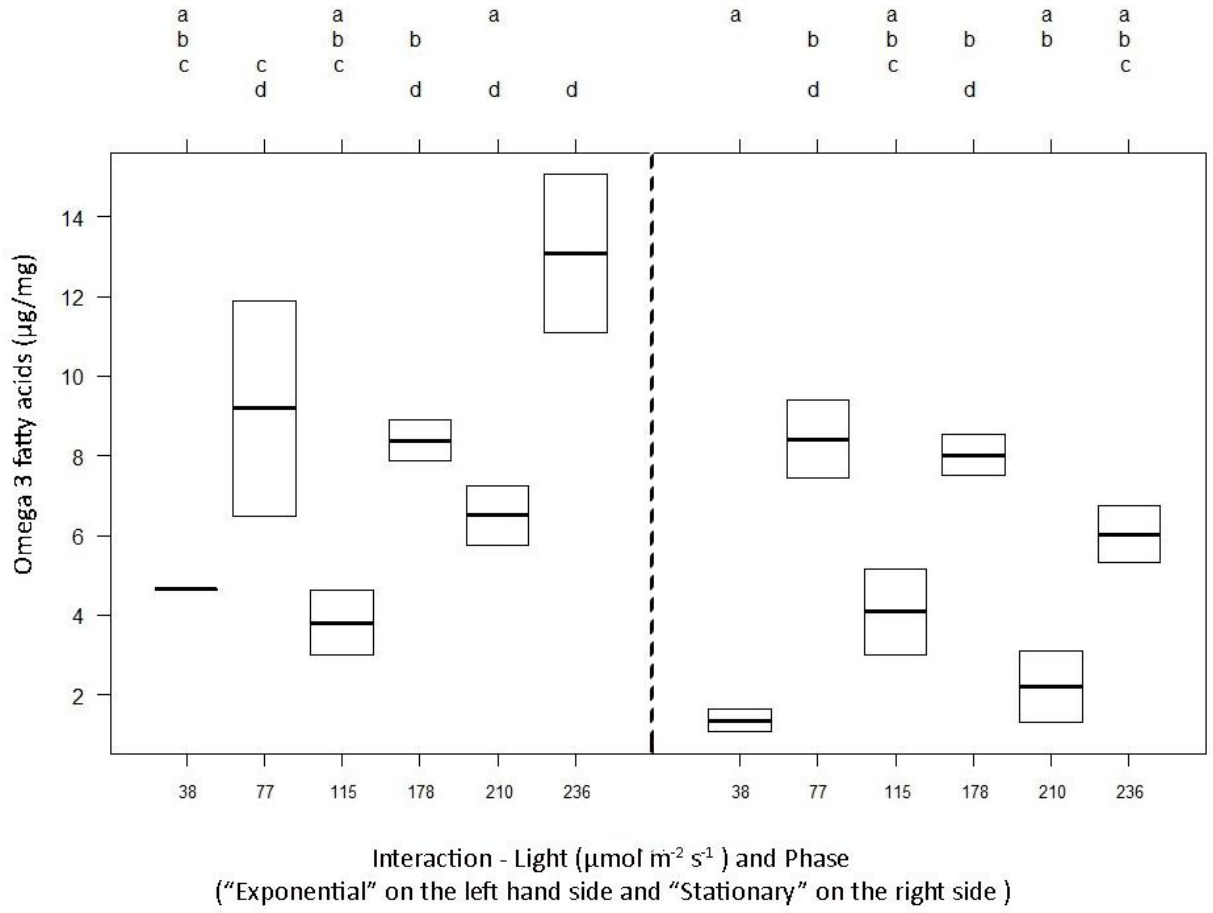

Figure 6.11. Results of Tukey tests on the ANOVA model from Table 6.6. The values on the X axis represent the values of the different PFDs under which experiments were carried out (exponential and stationary phases of growth on the left and right hand sides respectively). The values on the Y axis are µg of omega 3 fatty acids per mg of algal biomass. Lines in the boxes represent means and boxes represent quartiles. The letters above the plot indicate significant differences between means according to Tukey test results; treatments sharing the same letters are not significantly different.

Table 6.6 Results of two way ANOVA in which omega3 fatty acids concentrations were modelled as a function of PFD and phase.

	Df	Sum square	Mean square	F value	Pr(>F)	
PFD	5	2.11E+02	4.22E+01	5.612	0.00679	**
Phase	1	7.42E+01	7.42E+01	9.862	0.00853	**
PFD:Phase	5	7.59E+01	1.52E+01	2.016	0.1483	
Residuals	12	9.03E+01	7.52E+00			

Signif. codes: <0.001 '***' 0.001 '**' 0.01 '*' 0.05 '.' 0.1 ' ' 1

6.3.2.3 Alpha-linolenic acid accumulation in *Lobochlamys segnis* LCR-CC-5-1a at various PFD at different growth phases.

Figure 6.12 shows the ALA concentration in *Lobochlamys segnis* LCR-CC-5-1a under different PFDs during the exponential and stationary growth phases. Means of ALA concentration replicates differed significantly from each other as functions of both growth phase and PFD, according to ANOVA results and Tukey tests (Table 6.7; Figure 6.13). However, the interaction effect between different PFDs and growth phases was not significant (Table. 6.7); thus, it cannot be concluded that the effect of PFD on ALA concentrations depends on growth phase. The difference resulting in the significant differences between means, as shown by Tukey

tests (Figure 6.13) was the combination 236 µmol m^{-2} s^{-1} PFD at exponential phase with 38 µmol m^{-2} s^{-1} at stationary phase.

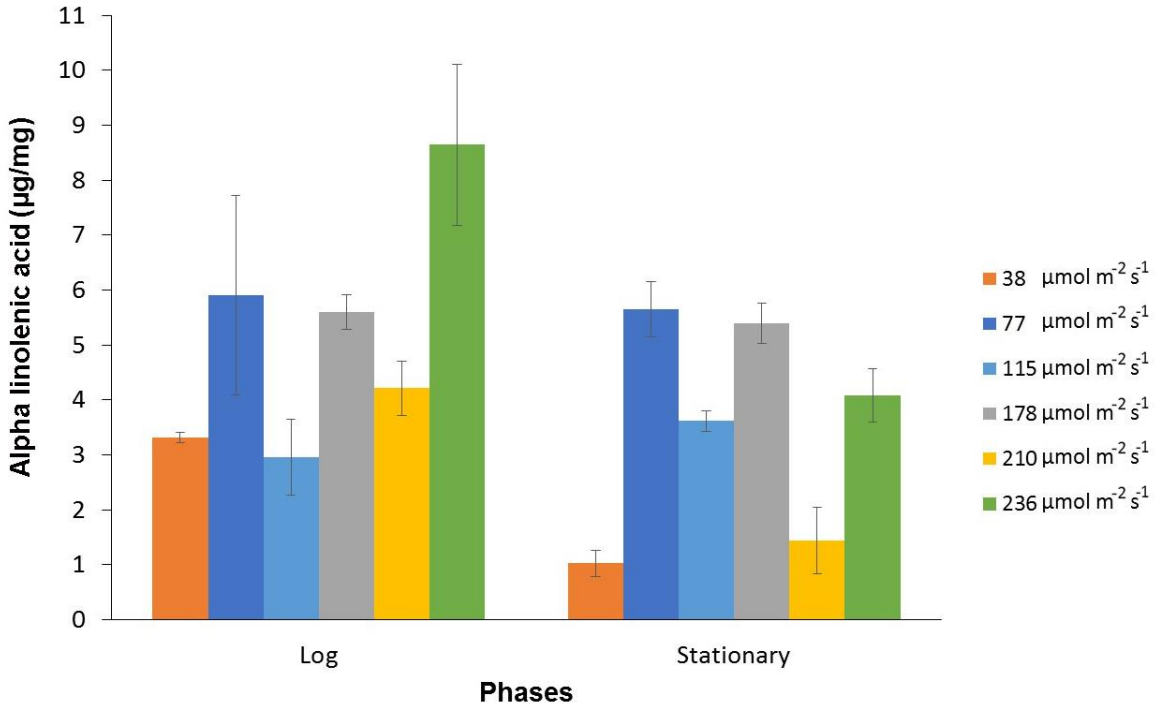

Figure 6.12 Relationship between alpha linolenic acid concentration at different intensities of light at exponential and stationary phases. Bars represent means; error bars indicate standard error from the mean.

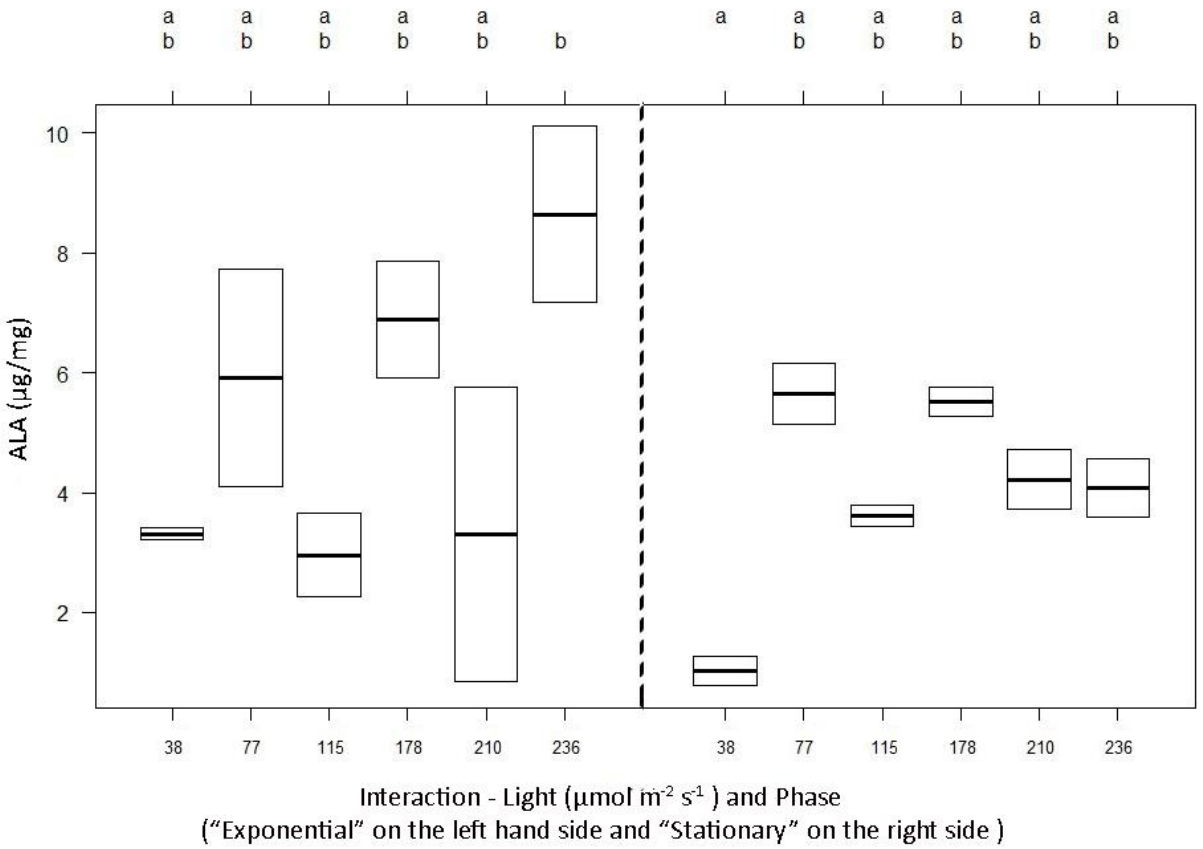

Figure 6.13 Result of Tukey tests on the ANOVA model in Table 6.7. The values on the X axis are the different PDFs under which experiments were conducted (exponential phase on the left hand side and the stationary phase on the right hand side). Values on the Y axis represent µg of ALA per mg of algae biomass. Lines in the boxes represent means, and the boxes represent the quartiles. Letters above the plot indicate significant differences between means according to Tukey test results; treatments sharing the same letters are not significantly different.

Table 6.7 Results of two way ANOVA in which alpha linolenic acid concentrations were modelled as a function of PFD and time

	Df	Sum square	Mean square	F value	Pr(>F)	
PFD	5	9.587	1.9173	6.988	0.00471	***
Phase	1	1.401	1.4007	5.105	0.04742	*
PFD:Phase	4	2.295	0.5737	2.091	0.15693	
Residuals	10	2.744	0.2744			

Signif. codes: <0.001 '***' 0.001 '**' 0.01 '*' 0.05 '.' 0.1 ' ' 1

6.4 DISCUSSION

6.4.1. RESPONSES OF *LOBOCHLAMYS SEGNIS* LCR-CC-5-1A TO CHANGE IN PFD, AND PERFORMANCE OF MODELLING THESE RESPONSES

The alpine strain *Lobochlamys segnis* LCR-CC-5-1a showed different growth responses in experiments conducted under different PFDs. This was evident in different measures of growth rate from the experimental data (Figures 6.4 & 6.5) and cell production rate from the modelled estimates and the experimental data (Figure 6.6). In addition, ANOVA and Tukey tests indicated significant differences between means of cell counts at comparable times between experiments, reinforcing the different responses under different PFD. By contrast, the maximum cell concentration estimates did not suggest a strong relationship with PFD (Figure 6.7).

According to the modelled estimates, the saturation point is a peak on quite a broad curve, and production is high across the interval 115–210 µmol m^{-2} s^{-1}. In fact, the highest growth rate occurred at both 115 and 178 µmol m^{-2} s^{-1} but only if the 210 µmol m^{-2} s^{-1} result is ignored (in the case of the logistic models). The requirement to omit a data point for successful model fitting means that the estimate here is very dubious, and resulted from coincidental placement of data points with respect to the beginning and end of the exponential growth phase. Undoubtedly, model fitting would have performed better if the population had been sampled more frequently. In the meantime, it is not possible to completely exclude the possibility of an optimum at 210 µmol m^{-2} s^{-1}. However, such an optimum would be unlikely to be significantly more productive than 178 µmol m^{-2} s^{-1}, as noted above.

The flatness of the curve around the optimum is one reason why this is difficult to identify (Figure 6.6). As noted earlier (section 4.1.2.), minimal change in growth rates when conditions vary from their ideal, as demonstrated here, is very desirable for an industrial process.

Cell production rates as calculated from crude curves fitted to the experimental data strongly agree with the fitted models (Figure 6.6). Both methods suggest a broad optimum between PFD values of 115 and 210 µmol m^{-2} s^{-1}. However, there are differences between the cell production rates calculated from the crude curves and the modelled estimates at the PFDs of 210, 236 and 253 µmol m^{-2} s^{-1}. It is worth noting that the method used to do this calculation from the crude curves does not allow estimation of errors; if this was done, the errors inherent in these estimates could well overlap.

The optimum PFD value, at which the highest µmax occurs across the experiments at different PFD, differs between Table 6.3 and when µmax is converted to cell production rates for comparison with logistic models (Figure 6.6). In fact, this is not a contradiction: the different

optimum PFD after conversion results from using the logistic models to determine the point at which $T_{1/2}$ (the time at which growth rate is maximum) occurs. But this logistic model is very likely erroneous, as pointed out above.

Anecdotally, it seems likely that experimental errors were greater at higher PFDs, although these are difficult to estimate in retrospect. Biomass production at these PFDs was accompanied by the production of substantial exopolysaccharides (EPS), which made the culture more viscous in nature, reducing photon penetration into the reactor and potentially interfering with mixing. Others have documented a reduction in growth rate due to EPS (You & Barnett 2004). Moreno *et al.* (1998) found that changes to nutritional, environmental or physical properties to increase the production of EPS have a negative effect on biomass growth. These results suggest that the production of EPS in my study could be a reason for the decline in growth at higher PFDs.

6.4.2. RESPONSE OF PUFA PRODUCTION TO CHANGES IN PFD

Omitting the experiment undertaken at PFD 210 µmol m^{-2} s^{-1}, the maximum cell production of $1.52x10^5$ cells mL^{-1} h^{-1} was achieved in both the PFDs 115 and 178 µmol m^{-2} s^{-1}, as noted above. A recommended level of PFD from these experiments depends on the responses of both growth rate and PUFA production to PFD. At 178 µmol m^{-2} s^{-1} the mean level of PUFA production was almost double that at 115 µmol m^{-2} s^{-1} during both exponential and stationary phases - although due to experimental variation this difference was not significant.

It must be noted that the general lack of relationship between PUFA production and PFD is not always in agreement with results in the literature (e.g., Volkman *et al.* 1991, Tonon *et al.* 2002, Mansour *et al.* 2005). Usually the FA composition of algae increases or decreases steadily with the increase in PFD (Khotimchenko *et al.* 2005, Napolitano 1994) but in this study, the FAs production with respect to gradual change in the PFD is irregular (Figures 6.8, 6.10 and 6.12). This apparent effect is due to high variation between replicates; most of the means are not significantly different from each other (Figures 6.8, 6.10 and 6.12). The reasons behind this are unknown, but the most likely possibility is due to the associated production of unbalanced EPS, which may have interfered with FA production, with the irregular result observed. In addition, the increase in the density of the broth with the increase in EPS reduced the PFD received by the culture. This suggestion is supported by the finding that there is a strong relationship between the production of EPS and FAs (Mensens *et al.* 2014).

In the present study, *L. segnis* LCR-CC-5-1a showed changes in μ (Figure 6.4) and FA profile at different PFDs (Figure 6.8). Changes in concentrations of total omega 3 FAs and ALA specifically in response to PFD change were similar (Figures 6.10 and 6.12). The quantity of PUFAs in the exponential phase was always equivalent to or greater than that in the stationary phase. Some studies have demonstrated a reduction in FA concentration from the exponential to the stationary phase (Volkman *et al.* 1991, Tonon *et al.* 2002). But in my case at the optimum PFD for μmax, maximum concentration of PUFAs, omega 3 fatty acids and ALA are the same in both the exponential and stationary phases, and sometimes greater in the exponential phase.

6.5 CONCLUSION

The maximum specific cell production rate of $1.52x10^5$ cells mL^{-1} h^{-1} was observed to occur at a PFD of both 115 and 178 µmol m^{-2} s^{-1}. To maximize the production of biomass, a PFD value within this range is therefore recommended for growing the strain LCR-CC-5-1a. The concentrations of PUFAs, omega 3 FAs, and ALA at different values of PFD tested were somewhat irregular, with no defined pattern (except that the level measured at the maximum PFD during the exponential phase tended to be significantly higher than at the lowest PFD. during stationary phase). Mean PUFA production was higher at 178 than at 115 µmol m^{-2} s^{-1}; although these means were not significantly different, the conservative approach is to regard the former as the optimum PFD. Furthermore, no significant differences of PUFAs, omega 3 FAs, or ALA composition were observed between the exponential and stationary phase at this optimum PFD, which is a desirable result from an industrial perspective. In conclusion, a PFD of 178 µmol m^{-2} s^{-1} is appropriate for mass growth and PUFA production from *L. segnis.*

CHAPTER 7

INFLUENCE OF TEMPERATURE ON GROWTH AND POLY UNSATURATED FATTY ACIDS PRODUCTION OF *LOBOCHLAMYS SEGNIS* LCR-CC-5-1a

CHAPTER 7

INFLUENCE OF TEMPERATURE ON GROWTH AND POLY UNSATURATED FATTY ACIDS PRODUCTION OF *LOBOCHLAMYS SEGNIS* LCR-CC-5-1A

7.1 INTRODUCTION

A broad range of temperature occurs within the biosphere, ranging from about 100^{o}C in hot springs (and hotter in some deep sea vents) to -89.2^{o}C at Vostok station in Antarctica (Lyons 1997). Within many of these extreme environments, such as hot springs (Castenholz 1977), alpine zones (Novis 2002b) and Antarctic regions (Broady 1996), algae have been identified and studied. Although the range of temperature supporting the growth of algae is wide, the conditions under which different species or strains can grow may not overlap. Algae are classified into three ecological groups based on their preferred temperatures for growth and development (Chen & Berns 1980):

1. Thermophiles optimum growth temperature is above 45^{o}C
2. Mesophiles grow at 10 to 45^{o}C, although growth rates are greatly reduced at the bottom of this range, and
3. Psychrophiles grow in environments at or below 10^{o}C

7.1.1. EFFECT OF TEMPERATURE

Temperature has an important effect on the growth and survival of microalgae. Cellular chemical composition (Renaud *et al*. 2002), the uptake of nutrients (Fujimoto *et al.* 1997, Reay *et al.* 1999), photosynthesis (Davison 1991), and growth rates (Goldman & Carpenter 1974, Renaud *et al*. 2002) are strongly influenced by temperature. Kinetic properties and the speed of reactions catalysed by enzymes depend on temperature (Jordan & Ogren 1984). Thus it is expected that growth will be promoted by optimizing the speed at which these reactions occur. In addition to temperature, various other factors such as photon flux density (PFD) and nutrient composition also effects growth rates. The reduction in the temperature below the optimum will (by definition) affect growth rate (μ), but not necessarily survival. Metabolic activities may remain functional at temperatures as low as 0°C (Arrigo & Sullivan 1992).

Table 7.1 Optimum temperature for growth of snow algae (Hoham 1975).

Species	Optimum temp. (°C)	Collected from
Chlainomonas kolii	≤ 4	Washington State, U.S.A
Chlainomonas rubra	≤ 4	Washington State, U.S.A
Chlamydomonas yellowstonensis	16	Mt. Bachelor, Oregon
Chodatia tetralantoidea	23	Japan
Raphidonema nivale	10	Mt. Bachelor, Oregon
Stichococcus bacillaris	4	Washington State, U.S.A

7.1.2. OPTIMUM GROWTH TEMPERATURES

Optimal growth temperatures for microalgae are diverse (0-45°C) amongst different species (e.g. Hoham 1975, Admiraal 1976, Seaburg *et al.* 1981). Optima for different algae isolated from the same habitat may differ. Algae collected from snow (Table 7.1) are examples of this with a variation in optimal temperatures of nearly 20°C.

7.1.3 EXTREME TEMPERATURE CONDITIONS

In alpine and polar regions algae are commonly found in ice sheets at temperatures well below 0°C (Ling & Seppelt 1990, Yoshimura *et al.* 1997). However, certain algae from alpine and polar regions are not restricted to low temperature habitats. The diatom *Nitzschia stellata* collected from very cold environments in Antarctica (Arrigo and Sullivan 1992) is an example of this. This species was isolated from a sea ice habitat at -2°C and demonstrated a positive growth response with increase in temperature. When tested at -6°C, -2°C and 6°C the highest photosynthetic efficiency occurred at 6°C. Thus this alga was not growing in optimal conditions in the field, but was simply resistant to the colder temperatures.

Phormidium bijahensis from hot springs of Yellowstone National Park at 80°C, has been used for studies of growth and photosynthetic ability (Mann and Schlichting 1967). Since this species can withstand long periods at temperatures up to 80°C, it is expected that it and other thermophiles might be able to survive for short periods of time at temperatures as high as 100°C (Schlichting 1974).

7.1.4 EFFECT OF TEMPERATURE ON SECONDARY METABOLITES

Both μ and PUFA accumulation depend strongly on the temperature at which algae grow (Table 7.2; Guschina & Harwood 2006, Morgan-Kiss *et al.* 2006). Commonly, a temperature increase results in a greater concentration of saturated FAs, while lowering the growth temperature increases the concentration of unsaturated FAs (Murata *et al*. 1975, Sato & Murata 1980, Lynch & Thompson 1982, Renaud *et al*. 2002). The temperature change alters the physical nature of the internal membranes of cells. The increase in unsaturated FAs at low temperature is to maintain membrane fluidity. Otherwise, low temperatures may result in loss of fluidity and cessation of metabolic activity. These changes in FAs help cell survival during shifts in temperature (Somerville 1995).

In *Dunaliella salina*, lipids containing unsaturated FAs increased by 20% with a decrease of temperature from 30°C to 12°C (Thompson Jr 1996). The concentration of unsaturated FAs in *Chlorella vulgaris* and *Botryococcus braunii* decreased as a response to temperature increase (Sushchik *et al.* 2003). Increase in temperature of cultures of *Nannochloropsis salina* raised μ moderately, and also the total lipid concentration (Boussiba *et al.* 1987). Other species shown to increase their lipid content as temperature increases include *Isochrysis* sp. and *Nannochloropsis oculata*. In contrast, some species decrease lipids at higher temperatures, for instance *Chaetoceros* sp, *Rhodomonas* sp. and *Cryptomonas* sp. (Renaud *et al*. 2002). When *Chaetoceros* sp, *Rhodomonas* sp, and *Selenastrum capricornutum* were grown in culture at sub-optimal temperatures there was an increase in the relative concentration of the monounsaturated omega-9 FA oleate, but a reduction in the percentage of linoleate (C18:2n-6) and stearidonic acid (C18:4n-3) (McLarnon-Riches *et al.* 1998). When the culture temperature of *Isochrysis galbana* was raised to 30°C, the rate of accumulation of total lipids increased but the concentration of

non-polar lipids declined (Zhu *et al.* 1997). When grown at 15°C, this strain showed an increased amount of PUFAs such as ALA and DHA, but decreased amounts of saturated and monosaturated FAs (Zhu *et al*. 1997).

The production of EPA also differs with temperature, with the optimum temperature for production being dependent on the species. For instance, an increase in temperature from 15 to 25°C increases the production of EPA in *Pavlova lutheri*, but *Phaeodactylum tricornutum* shows a decrease in EPA production when temperature is increased over the same range. Table 7.2 shows examples of changes in the profiles of algal lipids as a function of the growth temperature.

Table 7.2. Changes in lipid and fatty acid composition with temperature change in diverse microalgae.

Microalga	Change in temperature (°C)	Lipid profile changes	Reference
Cryptomonas sp.	33 to 27	Increase in total lipid by 9.19%	Renaud *et al*. (2002)
Chaetoceros sp.	35 to 25	Increase in total lipid by 38.84%	Renaud *et al*. (2002)
Chlorella vulgaris	30 to 25	Lipid production increased by 149.33%	Converti *et al*. (2009)
Dunaliella salina	30 to 12	Increase in unsaturated lipids	Thompson (1996)
Isochrysis galbana	15 to 30	Increase in neutral lipids	Zhu *et al*. (1997)
Isochrysis galbana	15 to 30	Increase in total lipids	Zhu *et al*. (1997)
Isochrysis sp.	25 to 27	Lipid production increased by 4.84%	Renaud *et al*. (2002)

Nannochloropsis oculata	20 to 25	Lipid production increased by 75.83%	Converti *et al.* (2009)
Nannochloropsis salina	Increased the temperature (winter[a] to summer[b])	Increase in total lipids	Boussiba *et al*. (1987)
Ochromonas danica	15 to 30	Increase in total lipids	Aaronson (1973)
Pavlova lutheri	15 to 25	Increased relative amount of EPA	Tatsuzawa & Takizawa (1995)
Phaeodactylum tricornutum	25 to 10 for 12 hours	Highest yields of PUFA and EPA	Jiang & Gao (2004)
Rhodomonas sp.	33 to 27°	Lipid production increased by 58.75%	Renaud *et al*. (2002)
Selenastrum capricornutum	25 to 10	Increase in oleate fatty acid	McLarnon-Riches *et al*. (1998)
Spirulina platensis,	30 to 40	Saturated FAs increased	Sushchik *et al*. (2003)

[a] Maximum temperature 30–35°C, minimum 17–23°C.

[b] Maximum temperature 15–20°C, minimum 5–12°C.

7.1.5 AIMS OF THE STUDY

The objective of the present study was to determine the temperature required by *Lobochlamys segnis* LCR-CC-5-1a cultivated in airlift photobioreactors (AL-PBRs) to achieve the following.

1 Maximum specific growth rate.

2 Maximum cell concentration.

3 Maximum production of PUFAs, and particularly omega-3 FAs and ALA.

7.2 MATERIALS AND METHODS

7.2.1. GROWTH RATE STUDIES IN AIRLIFT PHOTOBIOREACTORS

Two replicate AL-PBRs were used. The total volume of each was 1.5 L. The complete reactor design is described in detail in Chapter 5. The medium used was MLA (Bolch & Blackburn 1996) (Table 5.1). Seed inoculum was prepared as explained in section 5.2.2

An assessment was made of the influence of temperatures (5, 10, 15, 20, 25, and 30ºC) on μ, and PUFA and ALA concentrations at different growth phases. Reactor temperature was maintained by recirculating water from a controlled-temperature water-bath (TX150 - R4, Grant Instruments Cambridge Ltd, UK) through the external jackets of the reactors. Samples from the reactors were collected, using a sterile syringe, at 24 hour intervals after inoculation, for both cell counting and FA analysis. Cell counts were made using a haemocytometer. Samples for FA analysis were frozen prior to freeze-drying for transport to the laboratories of Callaghan Innovation Ltd, Wellington, New Zealand, where they were processed. Fatty acid analysis was

carried out for samples from both reactors for the exponential phase and at the start and end of stationary phase.

7.2.2 CELL COUNTS

Sample collections and cell counts were performed as explained in section 5.2.3.

7.2.3 MAXIMUM SPECIFIC GROWTH VELOCITY

Calculation of μmax (section 5.2.4) was undertaken using cell concentration spanning the period of exponential cell growth for each condition tested, as explained in Chapters 5 and 6. These times were between 24 and 72 hours for the 20, 25 and 30^{o}C experiments and 24 to 384 hours for 5^{o}C, 24 to 264 hours for 10^{o}C and 24 to 144 hours for the 15^{o}C experiments.

7.2.4 FREEZE DRYING

Freeze drying was performed as described in section 6.2.4.

7.2.5 FATTY ACID ANALYSIS

FA analysis was performed as explained in section 4.2.2.

7.2.6 STATISTICAL ANALYSIS

Statistical analysis was carried out as outlined in section 5.2.5.

7.3 RESULTS

7.3.1 EFFECT OF TEMPERATURE ON ALGAL GROWTH

Growth curves and kinetic patterns differed at different culture temperatures (Figure 7.1). Table 7.3 shows the value of μmax corresponding to each temperature, calculated from crude curves fitted to means of the experimental data. The values of μmax recorded from experiments carried out below 15ºC were very low (μmax at 5ºC and 10ºC were $8.94x10^{-3}$ h^{-1} and $1.40x10^{-2}$ h^{-1} respectively) compared to those from experiments at 15ºC and above ($3.17x10^{-2}$ h^{-1}, $6.54x10^{-2}$ h^{-1}, $6.17x10^{-2}$ h^{-1}, and $4.97 x10^{-2}$ h^{-1}). The highest μmax of $6.54x10^{-2}$ h^{-1} was at 20ºC, above which it dropped progressively ($6.17x10^{-2}$ and $4.97x10^{-2}$ h^{-1} at 25 and 30°C respectively).

Means of cell concentration replicates differ from each other as functions of both time and temperature, and in their interaction, according to ANOVA results and Tukey tests (Table 7.4). The logistic models fitted to the experimental data are shown in Figure 5.7. According to these models, both maximum estimated population size (Φ_1; Figure 7.3) and maximum cell production rate (Φ_3; Figure 7.4) display unimodal responses to temperature at the PFD used in these experiments. However, the temperatures at which the peaks occur differ. Φ_1 peaks at 10°C ($4.70x10^6$ cells mL^{-1}), after which a slow decline occurs up to 25°C, followed by a sharp drop at 30°C to the lowest estimate recorded ($2.56x10^6$ cells mL^{-1}). Φ_3, on the other hand, peaks at 20°C ($2.00x10^5$ cells mL^{-1} h^{-1}), although errors around the means at this temperature and at 25°C overlap.

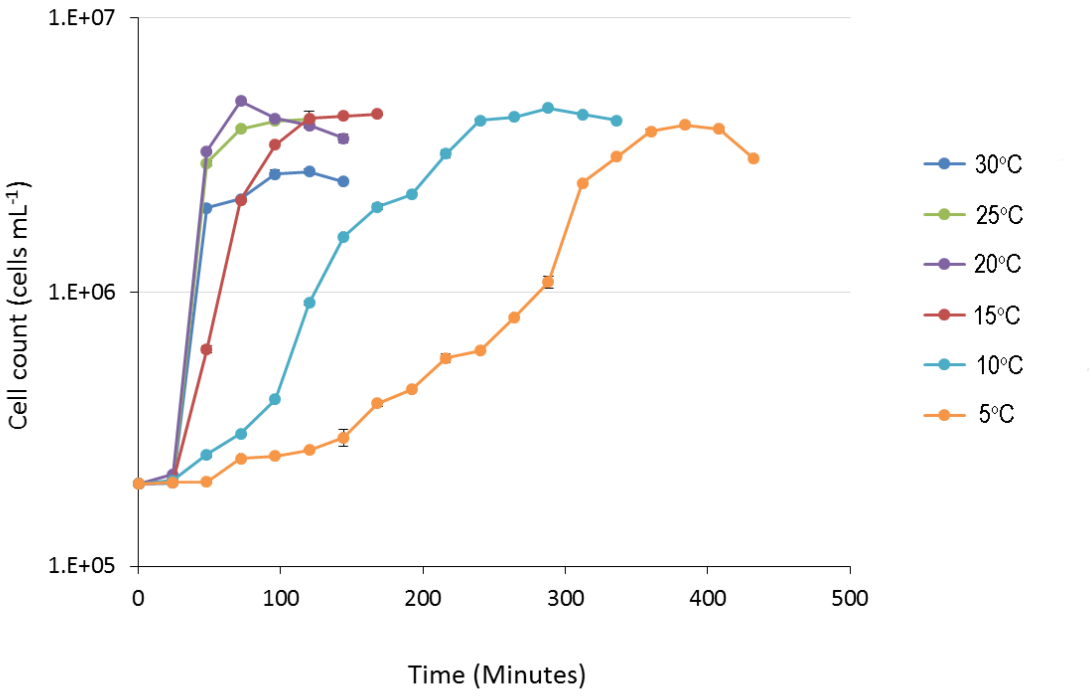

Figure 7.1 Growth curves of *Lobochlamys segnis* LCR-CC-5-1a at six temperatures. Error bars indicate standard deviation from the mean. Error bars indicate standard deviation from the mean.

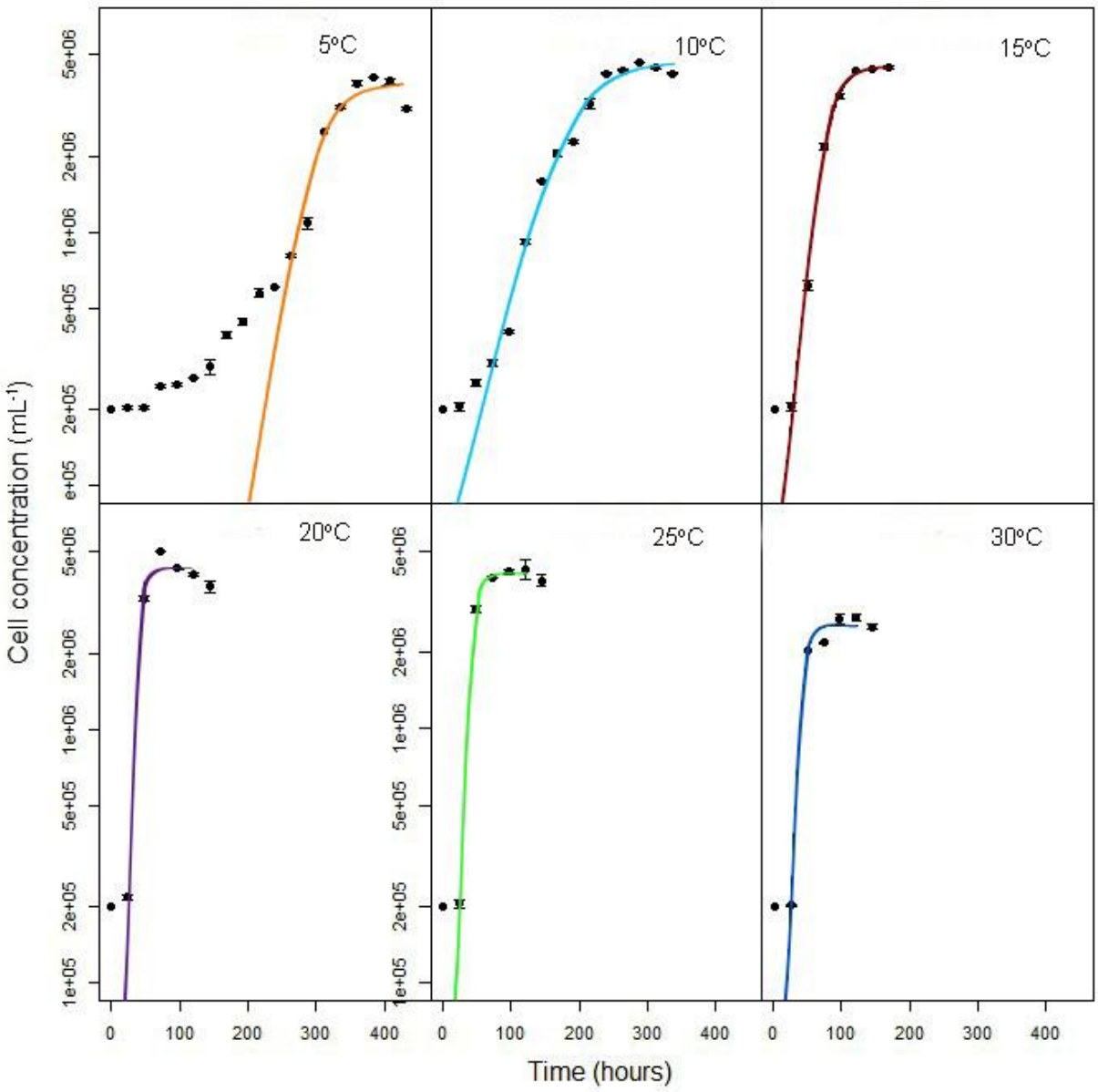

Figure 7.2. Logistic growth curves fitted to experimental data (symbols; means ± SE) of *Lobochlamys segnis* cell concentrations over time at different temperatures. Curves were fitted using the nonlinear least squares (nls) function in R.

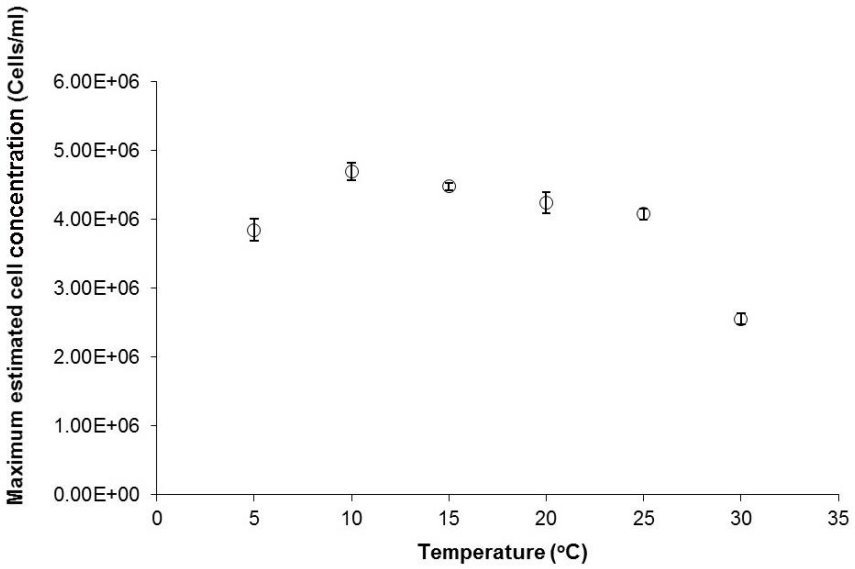

Figure 7.3 Maximum estimated population sizes (Φ_1) from logistic growth models fitted to cell count data over time, related to temperature under which the populations were grown. Error bars indicate standard error from the mean.

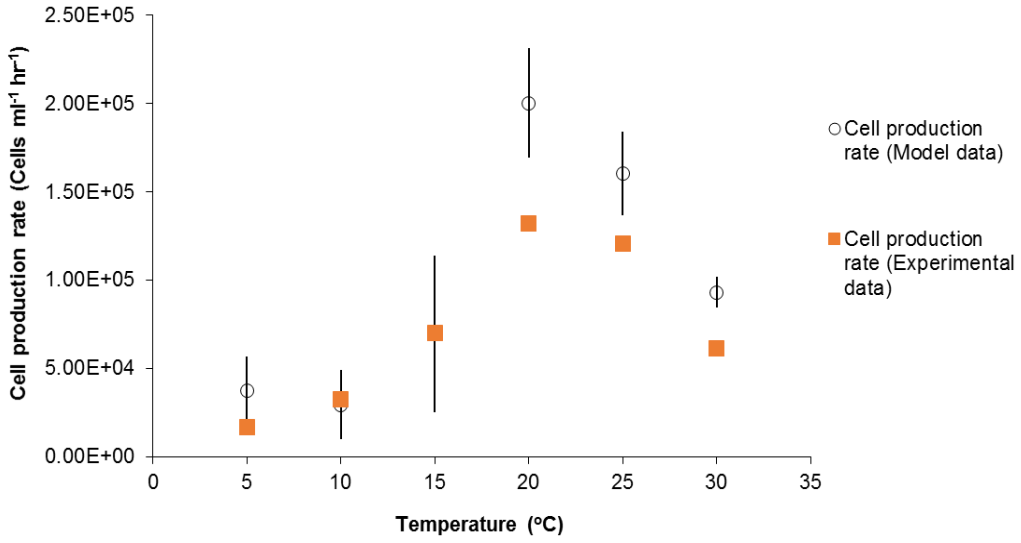

Figure 7.4 Maximum cell production rates (Φ_3) estimated from logistic growth models and from converted μmax values from crude curves fitted to experimental data at the different temperatures tested. Error bars indicate standard error from the mean.

Table 7.3. Values of μmax corresponding to cell concentrations spanning the period of exponential cell growth for each temperature

Temperature (^{o}C)	Maximum specific growth velocity (μmax) (h^{-1})
5	$8.94x10^{-3}$
10	$1.40x10^{-2}$
15	$3.17x10^{-2}$
20	$6.54x10^{-2}$
25	$6.17x10^{-2}$
30	$4.97\ x10^{-2}$

As in Chapter 6, Tukey tests showed that a high number of combinations of cell counts at different times and temperatures were significantly different, but again many of these are trivial (e.g. between the start and end of the same or different experiments). Notable significant differences are as follows.

- At 5^{o}C the maximum cell concentration was reached at 384 hours and this combination was significantly different from that at 10^{o}C at 288 hours, 20^{o}C at 72 hours and 30^{o}C at 120 hours (when those experiments also reached stationary phase).
- At 15^{o}C the maximum cell concentration was reached at 168 hours and this combination was significantly different from that at 20 ^{o}C at 72 hours and 30^{o}C at 120 hours. Also, 25^{o}C at 120 hours was significantly different that that at 20^{o}C at 72 hours.

- At 30ºC the maximum cell concentration was reached at 120 hours and this combination is significantly different than that at 20ºC at 72 hours and 25ºC at 120 hours.

Table 7.4 Results of two way ANOVA in which cell concentration data were modelled as a function of temperature and time.

	Df	Sum square	Mean square	F value	Pr (>F)
Temperature	5	5072383	1014477	2350.8	< 2e-16 ***
Hours	18	41281119	2293395	5314.5	< 2e-16 ***
Temperature: Hours	39	10382877	266228	616.9	< 2e-16 ***
Residuals	63	27187	432		

Signif. codes: <0.001 '***' 0.001 '**' 0.01 '*' 0.05 '.' 0.1 ' ' 1

Figure 7.4 compares maximum cell production rates estimated directly from the logistic growth models with those converted from maximum specific growth velocities calculated from crude curves fitted to the experimental data. The two methods agree (i.e. the converted μmax value falls within the standard errors of the modelled estimates) for experiments run at 5, 10 and 15ºC. However, at 20, 25 and 30ºC the cell production rates converted from the crude curves are less than the modelled estimates (with the caveat that errors in the converted experimental data may well overlap with those of the modelled estimates, if they could be calculated).

7.3.2 INFLUENCE OF TEMPERATURE ON PUFA PROFILES AND PRODUCTION

7.3.2.1 PUFA concentration in *Lobochlamys segnis* LCR-CC-5-1a at different growth phases under different temperatures

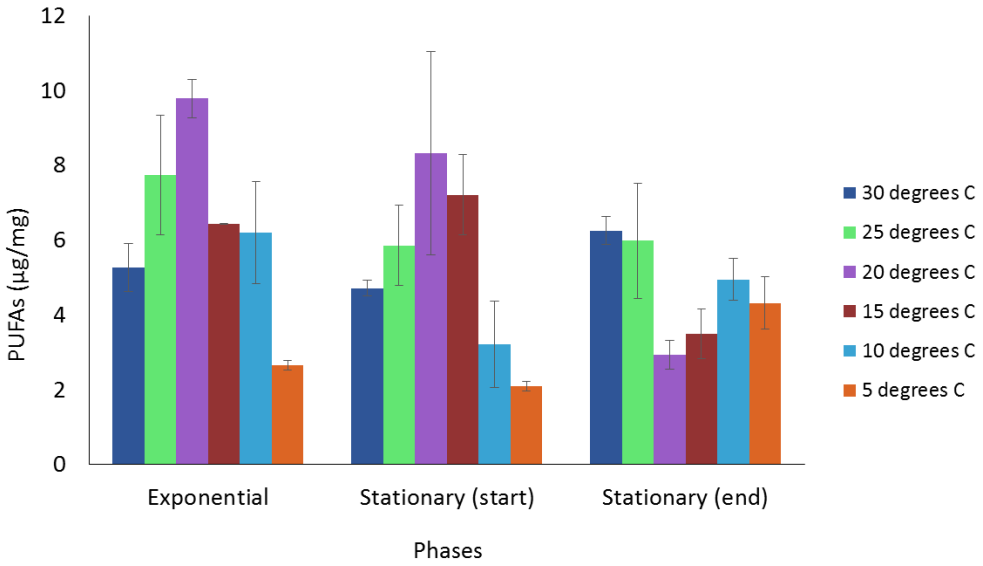

Figure 7.5 Relationship between PUFA concentrations (µg/mg of biomass) at different temperatures and during exponential phase and at start and end of stationary phase. Data points represent means ± standard errors.

Figure 7.5 shows the PUFA concentrations in *L. segnis* LCR-CC-5-1a at different temperatures and at the exponential growth phase, and at the beginning and end of the stationary phase. Means of PUFA concentrations differ from each other as functions of both growth phase and temperature, according to ANOVA results and Tukey tests (Table 7.5; Figure 7.6). However,

the interaction effect between different PFD and growth phases was significant (Table. 7.5): the mean PUFA concentration at 20°C is significantly higher than that at 5°C in the first two phases, but not the third (Figure 7.6).

Table 7.5 Results of two way ANOVA in which polyunsaturated fatty acid concentrations were modelled as a function of temperature and time.

	Df	Sum square	Mean square	F value	Pr(>F)	
Temperature	5	59.99	11.999	5.382	0.00337	**
Phase	2	17.76	8.880	3.983	0.03696	*
Temperature: Phase	10	71.00	7.100	3.185	0.01573	*
Residuals	18	40.13	2.229			

Signif. codes: <0.001 '***' 0.001 '**' 0.01 '*' 0.05 '.' 0.1 ' ' 1

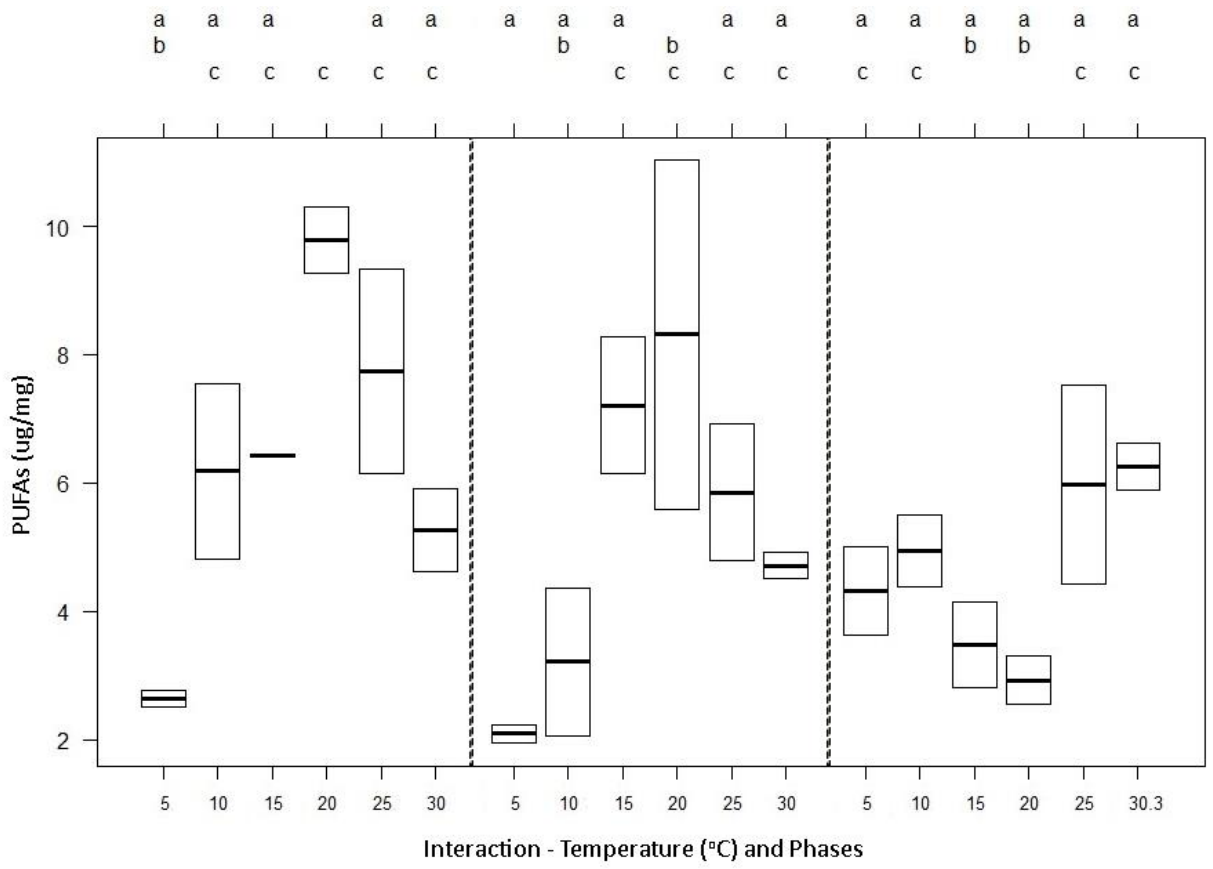

Figure 7.6 Results of Tukey tests on the ANOVA model from Table 7.5. The values on the X axis are experimental temperatures (exponential phase on the left hand side, start of stationary phase in the middle and the end of stationary phase on the right hand side). The numbers on the Y axis represent µg of PUFAs per mg of algae biomass dry weight. The line in the box plots represent the means of the PUFAs concentration and the boxes represent the quartiles. The letters above the plot indicate significant differences between means according to Tukey test results; treatments sharing the same letters are not significantly different.

7.3.2.2 Omega 3 FA accumulation in *Lobochlamys segnis* LCR-CC-5-1a different growth phases under different temperatures

Figure 7.7 shows the relationship between omega 3 FA concentrations in *L. segnis* LCR-CC-5-1a at different temperatures during the exponential, and at the start and end of stationary phase. Omega 3 FA concentrations differ from each other as functions of both growth phase and temperature (see ANOVA results and Tukey tests in Table 7.6 and Figure 7.8). The interaction effect between different temperature and growth phases was significant (Table. 7.6). The combinations contributing to the significant differences are shown in Figure 7.8. These were:

- 20ºC at exponential phase with 5, 10 and 20ºC at start of stationary phase and 20ºC at end of stationary phase;
- 15ºC at start of stationary phase with 20ºC at end of stationary phase.

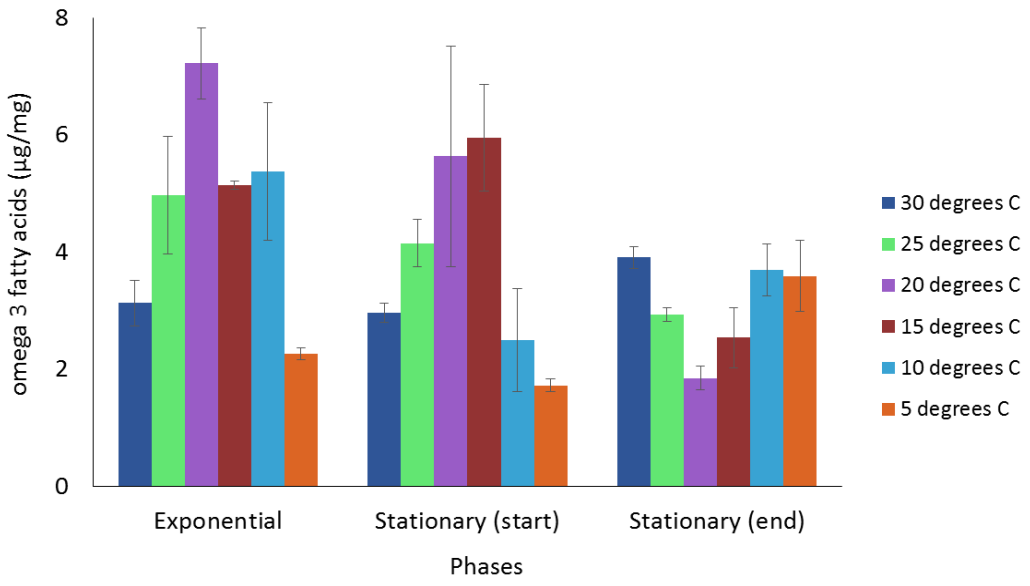

Figure 7.7. Relationship between omega 3 FA concentrations at different temperatures and during exponential, and at start and end of stationary phase. Data points represent means ± standard errors.

Table 7.6 Results of two way ANOVA in which omega 3 FA concentrations were modelled as a function of temperature and time.

	Df	Sum square	Mean square	F value	Pr(>F)	
Temperature	5	21.81	4.362	4.281	0.00967	**
Phase	2	15.33	7.663	7.520	0.00423	**
Temperature: Phase	10	45.09	4.509	4.425	0.00305	**
Residuals	18	18.34	1.019			

Signif. codes: <0.001 '***' 0.001 '**' 0.01 '*' 0.05 '.' 0.1 ' ' 1

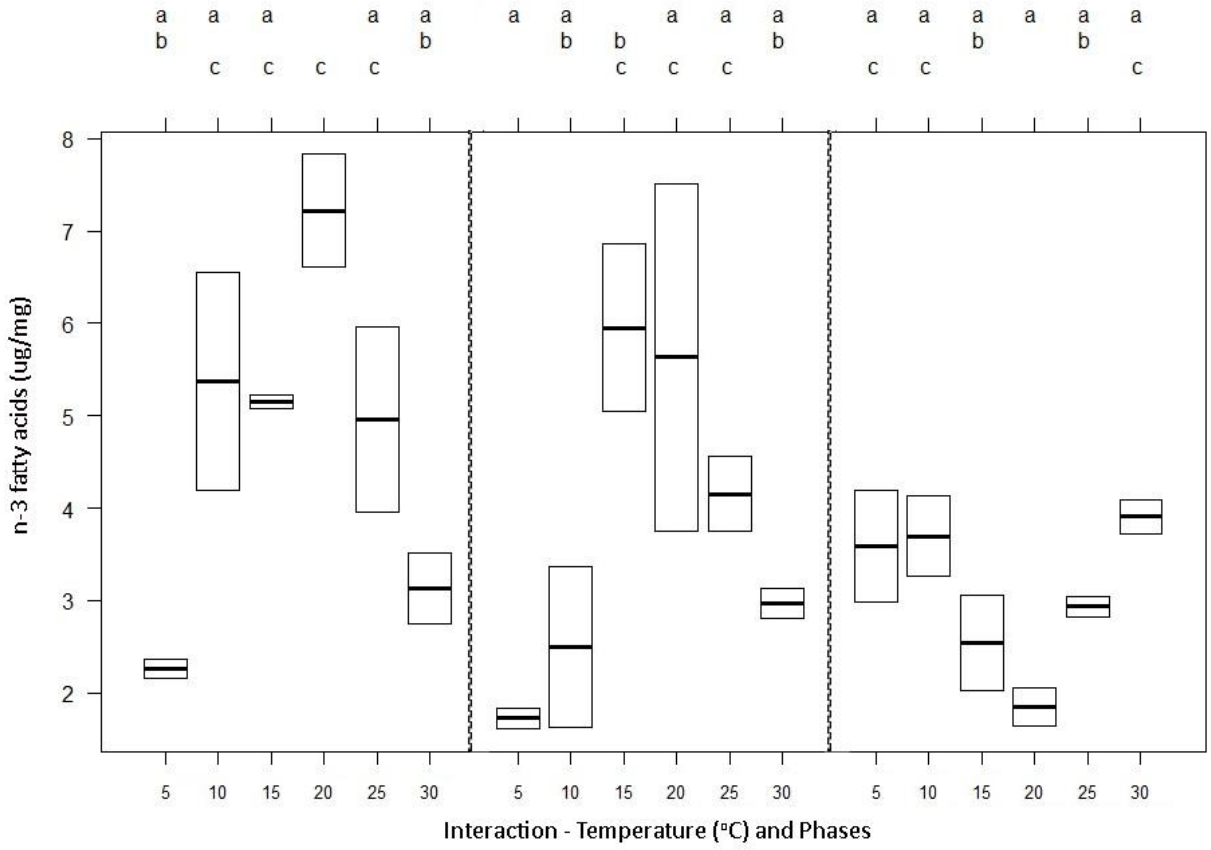

Figure 7.8 Results of Tukey tests on the ANOVA model from Table 7.6. The values on the X axis are the different experimental temperatures (on left, exponential phase; middle, start of stationary phase; right, end of stationary phase). The numbers on the Y axis represent µg of omega 3 fatty acids per mg of algae biomass. The line in the box plots represent the means of the omega 3 fatty acids concentration and the boxes represent the quartiles. The letters above the plot indicate significant differences between means according to Tukey test results; treatments sharing the same letters are not significantly different.

7.3.2.3. α-linolenic acid accumulation in *Lobochlamys segnis* LCR-CC-5-1a at different temperatures at different growth phases

Figure 7.9 shows the relationship between the means of the ALA concentrations in *Lobochlamys segnis* LCR-CC-5-1a at different temperature at the exponential, start of the stationary and at the end of the stationary phase. Means of ALA concentration replicates differ from each other as functions of growth phases and temperature, according to ANOVA results and Tukey tests (Table 7.7; Figure 7.10). The interaction effect between different temperature and growth phases was significant (Table. 7.7). The combinations contributing to the significant differences are shown in Figure 7.10. These were:

- 20ºC at exponential phase with all temperatures at start and end of stationary phase except 15, 20 and 25ºC at the start of stationary phase.
- 15ºC at start of stationary phase with 20ºC at end of stationary phase.

Table 7.7 Results of two way ANOVA in which ALA concentrations were modelled as a function of temperature and time.

	Df	Sum square	Mean square	F value	Pr(>F)	
Temperature	5	9.970	1.994	5.000	0.00479	**
Phase	2	6.900	3.450	8.652	0.00233	**
Temperature: Phase	10	19.694	1.969	4.939	0.00166	**
Residuals	18	7.177	0.399			

Signif. codes: <0.001 '***' 0.001 '**' 0.01 '*' 0.05 '.' 0.1 ' ' 1

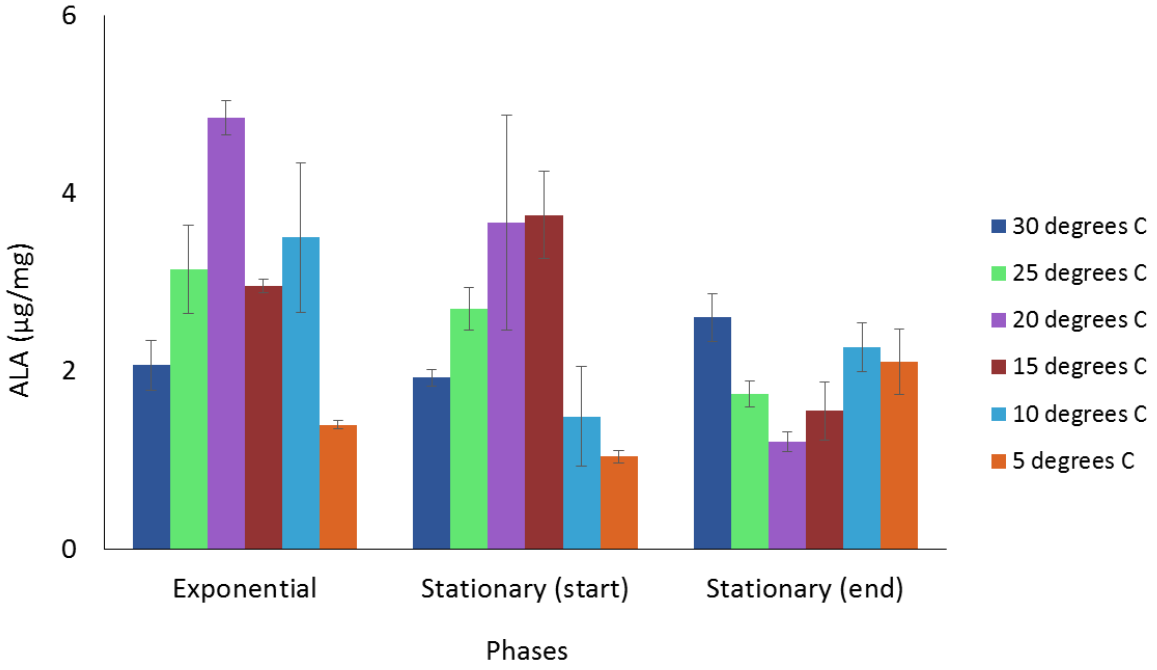

Figure 7.9 Relationship between ALA concentrations at different temperature at exponential, start of stationary and at the end of stationary phase. Data points represent means ± standard errors.

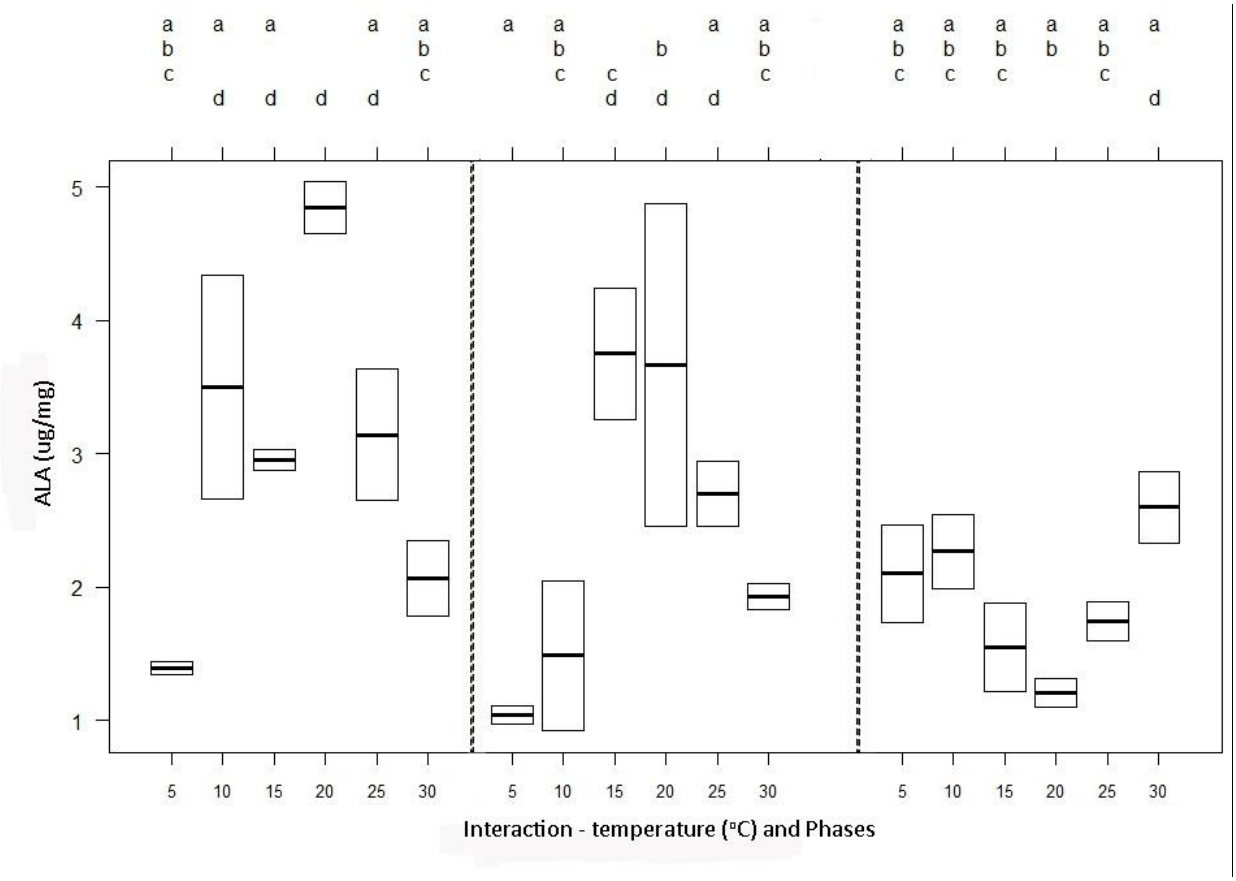

Figure 7.10 Results of Tukey tests on the ANOVA model from Table 7.7. The values on the X axis are different temperatures under which experiments were carried out (exponential phase on the left hand side, start of stationary phase in the middle and the end of stationary phase on the right hand side). The numbers on the Y axis represent µg of ALA per mg of algae biomass. The line in the box plots represent the means of the ALA concentration and the boxes represent the quartiles. The letters above the plot indicate significant differences

7.4 DISCUSSION

7.4.1 OPTIMUM TEMPERATURE FOR AIRLIFT PHOTOBIOREACTOR

The alpine strain *Lobochlamys segnis* LCR-CC-5-1a showed different growth responses in experiments conducted at different temperatures. This was evident in different measures of growth rate; both μ calculated from means of the experimental data (Figure 7.1 & Table 7.3) and cell production rate from the modelled estimates, and when converted from μmax calculated from the experimental data (Figure 7.4) and the maximum cell concentration from the modelled estimates (Figure 7.3).

According to the modelled estimates and the experimental data the optimum temperature for cell production rate is at 20°C (Figure 7.4). Thus, this strain has an optimum temperature for growth much greater than the average temperature in its habitat of isolation (4.7°C; Table 3.2, Chapter 3). This is not unexpected. For instance, according to Teoh *et al.* (2004), Antarctic algae are psychrotrophs rather than psychrophilic organisms. Most of the strains isolated from Antarctica could grow up to at least 15°C (Teoh *et al.* 2004). *Navicula* UMACC 231 and two *Chlorella* isolates (UMACC 234 and UMACC 237), all cultured from Antarctic samples, could survive up to 30°C. Similarly, cyanobacteria from polar regions are psychrotrophs rather than psychrophiles. At the opposite extreme, algae from hot environments such as thermal springs are known to have growth optima at approximately 20°C (Marre 1962). Thus the optimum temperature for the cultivation of an alga does not always depend on the environment from which it is isolated.

Cell production rates as calculated from crude curves fitted to the experimental data strongly agree with the fitted models (Figure 7.4). Both methods suggest an optimum temperature of 20°C. However, there are differences between the cell production rates calculated from the crude curves and the modelled estimates at 20, 25 and 30°C. It is worth noting that calculations from the crude curves do not allow estimation of errors; if this was done, the errors inherent in these estimates could well overlap.

7.4.2 CHANGE IN PUFA CONCENTRATIONS WITH TEMPERATURE

Lobochlamys segnis LCR-CC-5-1a showed changes in μ (Figure 7.4) and FA profile at different temperatures (Figure 7.5). According to Mansour *et al.* (2005) the accumulation of PUFAs at stationary phase in culture is generally high, but in my case the optimum temperature for growth produced maximum PUFA accumulation during the exponential phase, not during the stationary phase (hence, ANOVA interaction terms for temperature and phase with respect to PUFAs were all significant). A general decrease in PUFA production in the stationary phase is evident (Figures 7.5–7.10), although significant differences generally occurred only between the maxima in the exponential phase and the lower values in the stationary phase. Similar results showing reduction in FA concentration from the exponential to the stationary phase were reported by Volkman *et al.* (1991) and Tonon *et al.* (2002). The same pattern was evident in concentrations of overall PUFAs, omega 3 FAs, and ALA. Overall, the maximum PUFA accumulation was achieved during the exponential phase of the 20°C experiment, which is also the temperature resulting in the highest cell production rate (Figure 7.4 and 7.5).

7.5 CONCLUSION

The maximum value of μmax ($6.54x10^{-2}$ h^{-1}) was recorded at 20ºC. The maximum cell production rate of $4.70x10^{6}$ cells mL^{-1} h^{-1} estimated by logistic growth modelling and the cell production rate converted from μmax ($1.32x10^{5}$ cells mL^{-1} h^{-1}) were also at 20ºC. If the aim is to maximize the production of biomass, this value is therefore recommended for growing the strain LCR-CC-5-1a. While it could theoretically be possible for the optimum production of secondary metabolites to occur at a different value, there was no significant increase in concentration of PUFAs, omega 3 FAs, or ALA at the other temperatures tested in my experiments (and these were significantly lower at some temperatures). Therefore, in this case, maximizing biomass production has the effect of maximizing PUFA production. However, the age of the culture has an impact on PUFA accumulation in the cells. At 20ºC the maximum PUFA accumulation was achieved at exponential phase, in comparison to lower values obtained at the start and end of stationary phase. In conclusion, 20ºC is the optimum for mass growth of this organism, in which exponential phase harvesting is recommended for obtaining the maximum production of PUFAs.

.

CHAPTER 8

CONCLUSIONS

CONCLUSIONS

8.1 SUMMARY OF RESULTS

8.1.1 DIVERSITY OF ALGAE AT THE NEW SITE

The study of algal distribution at Canyon Creek, Canterbury, New Zealand revealed ten distinct taxa (Chapters 2 and 3), of which two belong to Trebouxiophyceae and eight belong to Chlorophyceae. *Coelastrella multistriata* var. *grandicosta* is a newly discovered variety of Scenedesmaceae (Gopalakrishnan *et al*. 2014) and two other taxa, *Variochloris* sp. and *Ettlia* sp., differ from all published species and will be proposed as new in future work according to the requirements of the International Code of Nomenclature for algae, fungi, and plants (McNeill *et al.* 2012).

This study has added 1 new variety of a species, 1 new record, and 1 new combination to the list of 26 Scenedesmaceae already described from New Zealand, of which some are still considered provisional (Broady *et al*. 2012). The scenedesmacean species *Desmodesmus abundans*, which is common in New Zealand and worldwide, is identified from Canyon Creek. Another species of Scenedesmaceae, *Desmodesmus granulatus*, which is already identified in Britain, Portugal and Romania, is identified for the first time in New Zealand. *Pseudococcomyxa simplex* and *Oocystis minuta* from Canyon Creek were recorded previously from Mt. Philistine (approximately 200 km further northwest). *Diplosphaera mucosa* and *Chloromonas palmelloides*, which have already been identified from Antarctica (Broady 1983), were identified for the first time in New Zealand.

At Canyon Creek some taxa were recognized that were identified from other alpine and polar zones, non-alpine zones, relatives of species from deserts and isolates that await formal classification and naming. Novis (2001) suggested a biogeographic overlap between the New Zealand alpine zone and Antarctica. For instance, *Raphidonema nivale, Botrydiopsis constricta*, *Pseudococcomyxa simplex* and *Chloromonas rubroleosa* (Ling & Seppelt 1993) identified on Mt. Philistine were also identified from Antarctica. The species *Cryptodesmus ellipsoideus, Pseudococcomyxa simplex* and *Oocystis minuta* identified from Canyon Creek are also known from Mt. Philistine, another alpine location in New Zealand. This demonstrates that the communities of alpine algae at sites separated by some distance (and with differing environments) are not unique. However, knowledge of the distribution of algae in these areas is far from complete, and many species no doubt await discovery.

8.1.2 FATTY ACIDS PRODUCED BY CANYON CREEK STRAINS

According to Lang *et al* (2011) it is quite common to have a small amount of PUFAs in green algae. However, it is known that stress such as low temperature increases PUFA concentrations in cultured strains (Renaud *et al*. 1995, Thompson Jr 1996). Environmental factors have distinct roles in defining the FA profile composition (Piorreck *et al*. 1984, Roessler 1990), and at very low temperatures the production of PUFAs helps organisms to survive and adapt (Murata *et al*. 1975, Sato & Murata 1980, Lynch & Thompson 1982, Renaud *et al*. 2002). Consequently, it was proposed in the present work that strains from alpine regions should have a higher content of PUFAs than strains from warmer regions. In this study, eight among the ten species investigated have proportions of PUFAs higher than that of monounsaturated fatty acids (MUFAs) and saturated FAs.

8.1.3 *LOBOCHLAMYS SEGNIS* LCR-CC-5-1A AS THE SELECTED STRAIN FOR GROWTH OPTIMIZATION

Among the ten strains chosen for the FA analysis on the basis of growth kinetics and response to temperature, *Lobochlamys segnis* (LCR-CC-5-1A) has been selected for its potential to be scaled-up at industrial level. Specifically, this algal strain showed higher specific growth velocity when compared to the other strains, and tolerance to a wider temperature range. Furthermore, in the screening analysis *Lobochlamys segnis* (LCR-CC-5-1A) contained 60% of its total FAs as PUFAs, and in that 60% the ALA content was 46% (Chapter 4).

8.1.4 IMPACT OF CHANGING PARAMETERS ON GROWTH AND METABOLITE PRODUCTION IN CULTURE

The effect of changes in carbon supply, photon flux density (PFD) and temperature on growth and PUFA production were investigated in *L. segnis* LCR-CC-5-1A. Carbon was supplied as CO_2. The results of this study, demonstrate that increasing the biomass is the only way to increase the production of PUFAs from *L. segnis.* The results obtained in experiments with different concentrations of CO_2 show that an increase in the CO_2 concentration had a positive impact on the alga's growth rate, but only up to 3.0%. Increasing the CO_2 concentration above 3.0% showed no further improvements in μ, the specific growth velocity. This result strongly suggests that the cells are saturated by 3.0% CO_2. Thus, the optimum CO_2 concentration required for the maximum production of biomass, PUFAs and ALA that potentially could be used in industrial scale production is 3.0% (Chapter 5).

Although optimum production of secondary metabolites could occur under different conditions than the optimum μ, there was no significant increase in concentration of PUFAs, omega-3 FAs, or ALA under such conditions in the experiments carried out. Therefore, in this case, maximizing biomass production has the effect of maximizing PUFA production. In experiments trialling different PFDs at 20°C, the maximum cell production rate of $1.5x10^5$ cells mL^{-1} h^{-1} occurred at a PFD of 178 μmol $m^{-2}s^{-1}$. In experiments trialling different temperatures at this PFD value, the maximum cell production rate of $2x10^5$ cells mL^{-1} h^{-1} occurred at a temperature of 20°C. In conclusion, a temperature of 20°C and PFD of 178 μmol m^{-2} s^{-1} is appropriate for mass growth of this organism, in which exponential phase harvesting is recommended to obtain maximum PUFA yield in industrial large scale production (Chapters 6 and 7).

The response of PUFAs to changes in PFD and temperature with respect to growth phase appears different. In experiments in which the former was varied, ANOVA interaction terms were never significant. By contrast, they were always significant when temperature was varied. This is partly explained by sampling a different number of phases in the temperature experiments – in the PFD experiments there was no equivalent of the late stationary phase sampling. So it is possible that PFD would show the same pattern if such samples were taken. However, the main reason for this disparity is likely to be the degree of variation in the PFD responses. Unless a strategy could be formulated that reduces this variation – such as controlling the production of EPS – it seems unlikely that significant patterns would emerge. However, levels of both temperature and PFD distant from their optimal values stress the cells, and secondary metabolites (including PUFAs) are often produced in response to stress (see section 1.4.1).

8.2 FURTHER WORK

Optimal values of some remaining parameters required to develop this strain to commercial production in large scale need to be determined.

Suggested future work is as follows:

1. Optimizing the nutrient composition of the culture medium for the production of maximum biomass of *L. segnis* LCR-CC-5-1a to yield the maximum production of PUFAs, specifically ALA.
2. Studying the effect of change in pH and optimizing it for the maximum production of PUFAs, specifically ALA.
3. At high PFD, some difficulties in cultivating this algal strain were experienced. These were most likely due to the production of extracellular polysaccharide (EPS), which hindered proper mixing and sampling. It is strongly recommend to study the properties of the EPS with the aim of reducing its production by modifying other parameters involved in the fermentation process. This could increase the biomass and the product yield.
4. CO_2 could be replaced with an organic carbon source to study the difference in growth conditions and production of secondary metabolites. In the AL-PBR the mixing could be achieved by supplying atmospheric air (not mixing with CO_2). The aim would be to determine which carbon source produces highest growth rates and product yield, and potentially reducing the time, cost and materials needed for the fermentation.
5. The strains isolated from Canyon Creek were examined for FA production, however, there are other isolated and characterized alpine strains, for instance *Ettlia* sp. LCR-CC-26-1f, which is rich in astaxanthine, and may also be suitable for production at large

scale. Parameters which are required for maximum production of pigments can be optimized in the AL-PBRs, using experiments analogous to those reported here.

6. Experiments that could be carried out over the course of this project were restricted to two AL-PBRs. This limited the treatment combinations that could be explored. Consequently, the conclusions regarding optimum conditions assume additivity – that the effect of temperature is not influenced by PFD, for example. Although an exhaustive combination of treatments would be prohibitively time-consuming, it would be possible to test a few selected combinations to verify that growth curves conform to predictions from the relationships already established here.

REFERENCES

Aaronson, S. 1973. Effect of incubation temperature on the macromolecular and lipid content of the phytoflagellate *Ochromonas danica*. *Journal of Phycology* **9**:111-13.

Abedi, E. & Sahari, M. A. 2014. Long-chain polyunsaturated fatty acid sources and evaluation of their nutritional and functional properties. *Food Science & Nutrition* **2**:443-63.

Ackman, R. G., Jangaard, P., Hoyle, R. & Brockerhoff, H. 1964. Origin of marine fatty acids. I. Analyses of the fatty acids produced by the diatom *Skeletonema costatum*. *Journal of the Fisheries Board of Canada* **21**:747-56.

Admiraal, W. 1976. Influence of light and temperature on the growth rate of estuarine benthic diatoms in culture. *Marine Biology* **39**:1-9.

Aizawa, K. & Miyachi, S. 1986. Carbonic anhydrase and CO_2 concentrating mechanisms in microalgae and cyanobacteria. *FEMS Microbiology Letters* **39**:215-33.

Akiyama, M. 1979. Some ecological and taxonomic observations on the colored snow algae found in Rumpa and Skarvsnes, Antarctica. *Memoirs of National Institute of Polar Research. Special issue* **11**:27-34.

An, J. Y. & Kim, B. W. 2000. Biological desulfurization in an optical-fiber photobioreactor using an automatic sunlight collection system. *Journal of Biotechnology* **80**:35-44.

Andersen, P. & Throndsen, J. 2003. Estimating cell numbers. *In* Hallegraeff, G. M., Anderson, D. M. and Cembella, A. D [Eds.] *Monographs on Oceanographic Methodology*. UNESCO, Paris. pp. 99–129.

Armstrong, G. A. & Hearst, J. E. 1996. Carotenoids 2: Genetics and molecular biology of carotenoid pigment biosynthesis. *The FASEB Journal* **10**:228-37.

Arrigo, K. R. & Sullivan, C. W. 1992. The influence of salinity and temperature covariation on the photophysiological characteristics of Antarctic sea ice microalgae. *Journal of Phycology* **28**:746-56.

Asada, Y., Miyake, M. & Miyake, J. 1998. Production of bioplastics and hydrogen gas by photosynthetic microorganisms. *Chinese Journal of Oceanology and Limnology* **16**:91-104.

Auestad, N., Halter, R., Hall, R. T., Blatter, M., Bogle, M. L., Burks, W., Erickson, J. R., Fitzgerald, K. M., Dobson, V. & Innis, S. M. 2001. Growth and development in term infants fed long-chain polyunsaturated fatty acids: a double-masked, randomized, parallel, prospective, multivariate study. *Pediatrics* **108**:372-81.

Auestad, N., Scott, D. T., Janowsky, J. S., Jacobsen, C., Carroll, R. E., Montalto, M. B., Halter, R., Qiu, W., Jacobs, J. R. & Connor, W. E. 2003. Visual, cognitive, and language assessments at 39 months: a follow-up study of children fed formulas containing long-chain polyunsaturated fatty acids to 1 year of age. *Pediatrics* **112**:e177-e83.

Aunins, J., Croughan, M., Wang, D. & Goldstein, J. 1986. Engineering developments in homogeneous culture of animal cells: oxygenation of reactors and scale up. *Biotechnology and Bioengineering Symposium.* pp. 699-723.

Babcock, R. W., Malda, J. & Radway, J. C. 2002. Hydrodynamics and mass transfer in a tubular airlift photobioreactor. *Journal of Applied Phycology* **14**:169-84.

Barclay, W., Meager, K. & Abril, J. 1994. Heterotrophic production of long chain omega-3 fatty acids utilizing algae and algae-like microorganisms. *Journal of Applied Phycology* **6**:123-29.

Bandarra, N. M., Pereira, P. A., Batista, I. & Vilela, M. H. 2003. Fatty acids, sterols and α-tocopherol in *Isochrysis galbana*. *Journal of Food Lipids* **10**:25-34.

Barahona, L. F. & Rorrer, G. L. 2003. Isolation of halogenated monoterpenes from bioreactor-cultured microplantlets of the macrophytic red algae *Ochtodes secundiramea* and *Portieria hornemannii*. *Journal of Natural Products* **66**:743-51.

Barbosa, M. J. & Wijffels, R. H. 2004. Overcoming shear stress of microalgae cultures in sparged photobioreactors. *Biotechnology and Bioengineering* **85**:78-85.

Becker, E. 2007. Micro-algae as a source of protein. *Biotechnology Advances* **25**:207-10.

Behrens, P., Hoeksema, S., Arnett, K., Cole, M., Heubner, T., Rutten, J. & Kyle, D. 1989. Eicosapentaenoic acid from microalgae. *Novel Microbial Products for Medicine and Agriculture. Elsevier Science Publishers, Amsterdam*. pp. 253-59.

Behrens, P. W. 1992. Microalgae as a source of bioactive products. *In*: Coombes, J. D. [Ed.] *New Drugs from Natural Sources.* pp. 166-75.

Behrens, P. W. & Kyle, D. J. 1996. Microalgae as a source of fatty acids. *Journal of Food Lipids* **3**:259-72.

Behrens, P. W., Sicotte, V. J. & Delente, J. 1994. Microalgae as a source of stable isotopically labeled compounds. *Journal of Applied Phycology* **6**:113-21.

Bell, R. A. 1993. Cryptoendolithic algae of hot semiarid lands and deserts. *Journal of Phycology* **29**:133-39.

Benemann, J. R. 1979. Production of nitrogen fertilizer with nitrogen-fixing blue-green algae. *Enzyme and Microbial Technology* **1**:83-90.

Berenbaum, M. R. 1995. The chemistry of defense: theory and practice. *Proceedings of the National Academy of Sciences USA* **92**:2-8.

Bigogno, C., Khozin-Goldberg, I., Boussiba, S., Vonshak, A. & Cohen, Z. 2002. Lipid and fatty acid composition of the green oleaginous alga *Parietochloris incisa*, the richest plant source of arachidonic acid. *Phytochemistry* **60**:497-503.

Bogen, C., Klassen, V., Wichmann, J., Russa, M. L., Doebbe, A., Grundmann, M., Uronen, P., Kruse, O. & Mussgnug, J. H. 2013. Identification of *Monoraphidium contortum* as a promising species for liquid biofuel production. *Bioresource Technology* **133**:622-26.

Bolch, C. J. & Blackburn, S. I. 1996. Isolation and purification of Australian isolates of the toxic cyanobacterium *Microcystis aeruginosa* Kütz. *Journal of Applied Phycology* **8**:5-13.

Borowitzka, M. A. 1992. Algal biotechnology products and processes—matching science and economics. *Journal of Applied Phycology* **4**:267-79.

Borowitzka, M. A. 1999. Commercial production of microalgae: ponds, tanks, and fermenters. *Progress in Industrial Microbiology* **35**:313-21.

Boschker, H. & Middelburg, J. 2002. Stable isotopes and biomarkers in microbial ecology. *FEMS Microbiology Ecology* **40**:85-95.

Boswell, K., Gladue, R., Prima, B. & Kyle, D. 1992. SCO production by fermentative microalgae. *In* Kyle, D.J & Ratledge, C. [Eds] *Industrial Applications of Single Cell Oils, American Oil Chemists Society. Champaign*: IL, pp. 274-86.

Boussiba, S. & Vonshak, A. 1991. Astaxanthin accumulation in the green alga *Haematococcus pluvialis*. *Plant and Cell Physiology* **32**:1077-82.

Boussiba, S., Vonshak, A., Cohen, Z., Avissar, Y. & Richmond, A. 1987. Lipid and biomass production by the halotolerant microalga *Nannochloropsis salina. Biomass* **12**:37-47.

Brasaemle, D. L. 2007. Thematic review series: adipocyte biology. The perilipin family of structural lipid droplet proteins: stabilization of lipid droplets and control of lipolysis. *Journal of Lipid Research* **48**:2547-59.

Brenna, J. T. 2002. Efficiency of conversion of α-linolenic acid to long chain n-3 fatty acids in man. *Current Opinion in Clinical Nutrition & Metabolic Care* **5**:127-32.

Brennan, L. & Owende, P. 2010. Biofuels from microalgae—a review of technologies for production, processing, and extractions of biofuels and co-products. *Renewable and Sustainable Energy Reviews* **14**:557-77.

British Nutrition Foundation. 1992. Unsaturated Fatty Acids: Nutritional and Physiological Significance: the Report of the British Nutrition Foundation's Task Force. London, England: Chapman & Hall 152-163

Britton, G. 1988. Biosynthesis of carotenoids. *In* Goodwin, T.[Eds] *Plant Pigments.* Academic press, London: pp. 133-82.

Broady, P. 1977. A new genus and two new species of terrestrial chlorophycean algae from Signy Island, South Orkney Islands, Antarctica. *British Phycological Journal* **12**:7-15.

Broady, P. 1983. New records of Chlorophycean micro-algae cultured from Antartic terrestrial habitats. *Nova Hedwigia* **36**:445-84.

Broady, P. 1996. Diversity, distribution and dispersal of Antarctic terrestrial algae. *Biodiversity & Conservation* **5**:1307-35.

Broady, P., Flint, E. A., Nelson., W. A., Cooper., V. C., Winton., M. D. D. & Novis., P. M. 2012. Phyla Chlorophyta and Charophyta: green algae. *In* D.P. Gordon [Ed.], *New Zealand Inventory of Biodiversity Vol 3: Kingdoms Bacteria, Protozoa, Chromista, Plantae, Fungi*, Christchurch: Canterbury University Press, pp. 347-381.

Broady, P. A. 1987. The morphology, distribution and ecology of *Pseudococcomyxa simplex* (Mainx) Fott (Chlorophyta, Chlorellaceae), a widespread terrestrial Antarctic alga. *Polar Biology* **7**:25-30.

Brown, M., Jeffrey, S., Volkman, J. & Dunstan, G. 1997. Nutritional properties of microalgae for mariculture. *Aquaculture* **151**:315-31.

Brown, M. R., Dunstan, G. A., Norwood, S. & Miller, K. A. 1996. Effects of harvest stage and light on the biochemical composition of the diatom *Thalassiosira pseudonana*. *Journal of Phycology* **32**:64-73.

Bryant, D. A. & Frigaard, N.-U. 2006. Prokaryotic photosynthesis and phototrophy illuminated. *Trends in Microbiology* **14**:488-96.

Burge, S. W., Daub, J., Eberhardt, R., Tate, J., Barquist, L., Nawrocki, E. P., Eddy, S. R., Gardner, P. P. & Bateman, A. 2013. Rfam 11.0: 10 years of RNA families. D226-D232.

Camarasa, E., Carvalho, E., Meleiro, L., Maciel Filho, R., Domingues, A., Wild, G., Poncin, S., Midoux, N. & Bouillard, J. 2001. A hydrodynamic model for air-lift reactors. *Chemical Engineering and Processing: Process Intensification* **40**:121-28.

Cărăuş, I. 2012. Algae of Romania. *Studii şi Cercetări, Universitatea Bacau, Biologie* **7**:1-694.

Carvalho, A. P. & Malcata, F. X. 2005. Optimization of ω-3 fatty acid production by microalgae: crossover effects of CO2 and light intensity under batch and continuous cultivation modes. *Marine Biotechnology* **7**:381-88.

Carvalho, A. P., Meireles, L. A. & Malcata, F. X. 2006. Microalgal reactors: a review of enclosed system designs and performances. *Biotechnology Progress* **22**:1490-506.

Castenholz, R. W. 1977. The effect of sulfide on the blue-green algae of hot springs II. Yellowstone National Park. *Microbial Ecology* **3**:79-105.

Changnon, S. A. & Jones, D. 1972. Review of the influences of the Great Lakes on weather. *Water Resources Research* **8**:360-71.

Chaumont, D. 1993. Biotechnology of algal biomass production: a review of systems for outdoor mass culture. *Journal of Applied Phycology* **5**:593-604.

Chen, C.-H. & Berns, D. S. 1980. Thermotropic properties of thermophilic, mesophilic, and psychrophilic blue-green algae. *Plant Physiology* **66**:596-99.

Chillakuru, R. A., Ryu, D. D. & Yilma, T. 1991. Propagation of recombinant vaccinia virus in HeLa cells: adsorption kinetics and replication in batch cultures. *Biotechnology Progress* **7**:85-92.

Chisti, M. & Moo-Young, M. 1987. Airlift reactors: characteristics, applications and design considerations. *Chemical Engineering Communications* **60**:195-242.

Chodat, R. 1913. Monographies d'algues en culture pure. Materiaux Pour la Flore Cryptogamique Suisse. **42**:1–266.

Chodat, R. 1926. *Scenedesmus*. *Aquatic Sciences-Research Across Boundaries* **3**:71–258.

Chrismadha, T. & Borowitzka, M. A. 1994. Effect of cell density and irradiance on growth, proximate composition and eicosapentaenoic acid production of *Phaeodactylum tricornutum* grown in a tubular photobioreactor. *Journal of Applied Phycology* **6**:67-74.

Clandinin, M. T., Jumpsen, J. & Suh, M. 1994. Relationship between fatty acid accretion, membrane composition and biological functions. *Journal of Pediatrics* **125**:25-32.

CliFlo: NIWA's National Climate Database on the Web, Retrieved 26-October-2014. http://cliflo.niwa.co.nz/

Cohen, Z. 1990. The production potential of eicosapentaenoic and arachidonic acids by the red alga *Porphyridium cruentum*. *Journal of the American Oil Chemists' Society* **67**:916-20.

Cohen, Z., Norman, H. & Heimer, Y. 1995. Microalgae as a source of omega 3 fatty acids. *World Review of Nutrition and Dietetics* **77**:1-31.

Converti, A., Casazza, A. A., Ortiz, E. Y., Perego, P. & Del Borghi, M. 2009. Effect of temperature and nitrogen concentration on the growth and lipid content of *Nannochloropsis oculata* and *Chlorella vulgaris* for biodiesel production. *Chemical Engineering and Processing: Process Intensification* **48**:1146-51.

Cordero, B., Otero, A., Patiño, M., Arredondo, B. O. & Fabregas, J. 1996. Astaxanthin production from the green alga *Haematococcus pluvialis* with different stress conditions. *Biotechnology Letters* **18**:213-18.

Courties, C., Vaquer, A., Troussellier, M., Lautier, J., Chrétiennot-Dinet, M. J., Neveux, J., Machado, C. & Claustre, H. 1994. Smallest eukaryotic organism. *Nature* **370**:255.

Couvert, A., Bastoul, D., Roustan, M., Line, A. & Chatellier, P. 2001. Prediction of liquid velocity and gas hold-up in rectangular air-lift reactors of different scales. *Chemical Engineering and Processing: Process Intensification* **40**:113-19.

Craggs, R., Heubeck, S., Lundquist, T. & Benemann, J. 2011. Algal biofuels from wastewater treatment high rate algal ponds. *Water Science & Technology* **63**:660-65.

Cresswell, R., Rees, T. & Shah, N. 1989. Algal and cyanobacterial biotechnology. Longman's Scientific and Technical Press, Harlow, 341 pp.

Cuaresma, M., Janssen, M., Vílchez, C. & Wijffels, R. H. 2009. Productivity of *Chlorella sorokiniana* in a short light-path (SLP) panel photobioreactor under high irradiance. *Biotechnology and Bioengineering* **104**:352-59.

Cuaresma, M., Janssen, M., Vílchez, C. & Wijffels, R. H. 2011. Horizontal or vertical photobioreactors? How to improve microalgae photosynthetic efficiency. *Bioresource Technology* **102**:5129-37.

Czygan, F. C. 1968. Sekundär-Carotinoide in Grünalgen. *Archives of Microbiology* **62**:209-36.

Da John, W. & Patel, Y. R. 1985. Variations in the volumes of microbial cells with change in the agitation rates of chemostat cultures. *Journal of General Microbiology* **131**:725-36.

Daniel, S., Cornelia, S. & Fred, Z. 2004. UV-A sunscreen from red algae for protection against premature skin aging. *Cosmet Toiletries Manufacture Worldwide* **2004**:139-43.

Davison, I. R. 1991. Environmental effects on algal photosynthesis: temperature. *Journal of Phycology* **27**:2-8.

De Wit, R. & Bouvier, T. 2006. 'Everything is everywhere, but, the environment selects'; what did Baas Becking and Beijerinck really say? *Environmental Microbiology* **8**:755-58.

Degen, J., Uebele, A., Retze, A., Schmid-Staiger, U. & Trösch, W. 2001. A novel airlift photobioreactor with baffles for improved light utilization through the flashing light effect. *Journal of Biotechnology* **92**:89-94.

Delente, J. J., Behrens, P. W. & Hoeksema, S. D. 1992. Closed photobioreactor and method of use. Google Patents, United States Patent, pp. 5, 151, 347.

Delepine, M. 1951. Joseph Pelletier and Joseph Caventou. *Journal of Chemical Education* **28**:454-461.

DeLong, E. F. & Yayanos, A. A. 1986. Biochemical function and ecological significance of novel bacterial lipids in deep-sea procaryotes. *Applied and Environmental Microbiology* **51**:730-37.

Delucia, E. H., Sasek, T. W. & Strain, B. R. 1985. Photosynthetic inhibition after long-term exposure to elevated levels of atmospheric carbon dioxide. *Photosynthesis Research* **7**:175-84.

Department of Health. 1991. Dietary reference values for food energy and nutrients for the United Kingdom. *Committee on Medical Aspects of Food Policy. Report on Health and Social Subjects 41*. HSMO: London, UK.

Doughman, S. D., Krupanidhi, S. & Sanjeevi, C. B. 2007. Omega-3 fatty acids for nutrition and medicine: considering microalgae oil as a vegetarian source of EPA and DHA. *Current Diabetes Reviews* **3**:198-203.

Draget, K. I., Smidsrød, O. & Skjåk-Bræk, G. 2005. Alginates from algae. *In* Steinbüchel, A. & Rhee, S. K. [Eds.] *Polysaccharide and Polyamides in the food Industry*. Wiley-VCH Verlag GmbH & Co, Weinheim, pp. 1-30.

Duong, V. T., Li, Y., Nowak, E. & Schenk, P. M. 2012. Microalgae isolation and selection for prospective biodiesel production. *Energies* **5**:1835-49.

Duval, B., Duval, E. & Hoham, R. W. 2010. Snow algae of the Sierra Nevada, Spain, and high Atlas mountains of Morocco. *International Microbiology* **2**:39-42.

Erwin, J. & Bloch, K. 1964. Biosynthesis of unsaturated fatty acids in microorganisms. *Science* **143**:1006-12.

Etheridge, M. K. 1983. The seasonal biology of the phytoplankton in Lake Maratoto and Lake Rotomahana. Unpublished MSc thesis. Hamilton, New Zealand, University of Waikato. 264 p.

Ettl, H. & Gärtner, G. 1995. Syllabus der Boden-, Luft- und Flechtenalgen. Gustav Fischer Verlag, Stuttgart. 721 pp.

Ettl, H. & Komárek, J. 1982. Was versteht man unter dem Begriff coccale Grünalgen?(Systematische Bemerkungen zu den Grünalgen II). *Algological Studies/Archiv für Hydrobiologie, Supplement Volume*:345-74.

Falk-Petersen, S., Sargent, J., Henderson, J., Hegseth, E., Hop, H. & Okolodkov, Y. 1998. Lipids and fatty acids in ice algae and phytoplankton from the Marginal Ice Zone in the Barents Sea. *Polar Biology* **20**:41-47.

Feller, U., Anders, I. & Mae, T. 2008. Rubiscolytics: fate of Rubisco after its enzymatic function in a cell is terminated. *Journal of Experimental Botany* **59**:1615-24.

Felsenstein, J. 2004. *Inferring phylogenies.* Sunderland: Sinauer Associates, 664 pp.

Fidalgo, J., Cid, A., Torres, E., Sukenik, A. & Herrero, C. 1998. Effects of nitrogen source and growth phase on proximate biochemical composition, lipid classes and fatty acid profile of the marine microalga *Isochrysis galbana*. *Aquaculture* **166**:105-16.

Findlay, R. H., Trexler, M. B., Guckert, J. & White, D. C. 1990. Laboratory study of disturbance in marine sediments: response of a microbial community. *Marine Ecology Progress Series. Oldendorf* **62**:121-33.

Foissner, W. 2006. Biogeography and dispersal of micro-organisms: a review emphasizing protists. *Acta Protozoologica* **45**:111-36.

Scientific Committee for Food. 1993. Essential fatty acids. Reports of the Scientific Committee for Food. *Nutrient and Energy Intakes for the European Community.* pp. 52-59.

Forján, E., Garbayo, I., Henriques, M., Rocha, J., Vega, J. M. & Vílchez, C. 2011. UV-A mediated modulation of photosynthetic efficiency, xanthophyll cycle and fatty acid production of *Nannochloropsis*. *Marine Biotechnology* **13**:366-75.

Fox, J. & Weisberg, S. 2011. An {R} Companion to Applied Regression. *In*: 2 [Ed.]. Sage, Thousand Oaks CA

Fraenkel, G. S. 1959. The raison d'etre of secondary plant substances. *Science* **129**:1466-70.

Fujimoto, N., Sudo, R., Sugiura, N. & Inamori, Y. 1997. Nutrient-limited growth of *Microcystis aeruginosa* and *Phormidium tenue* and competition under various N:P supply ratios and temperatures. *Limnology and Oceanography* **42**:250-56.

Gaffney, A. M., Markov, S. A. & Gunasekaran, M. 2001. Utilization of cyanobacteria in photobioreactors for orthophosphate removal from water. *Applied Biochemistry and Biotechnology* **91**:185-93.

Gandarra, N. M., Pereira, P. A., Batista, I. & Vilela, M. H. 2003. Fatty acids, sterols and α-tocopherol in *Isochrysis galbana*. *Journal of Food Lipids* **10**:25-34.

García-González, M., Moreno, J., Manzano, J. C., Florencio, F. J. & Guerrero, M. G. 2005. Production of *Dunaliella salina* biomass rich in 9-*cis*-β-carotene and lutein in a closed tubular photobioreactor. *Journal of Biotechnology* **115**:81-90.

Ghildyal, N., Lonsane, B. & Karanth, N. 1988. Foam control in submerged fermentation: state of the art. *Advances in Applied Microbiology* **33**:173-222.

Gill, I. & Valivety, R. 1997. Polyunsaturated fatty acids, Part 1: Occurrence, biological activities and applications. *Trends in Biotechnology* **15**:401-409.

Goes, J. I., Handa, N., Taguchi, S., Hama, T. & Saito, H. 1995. Impact of UV radiation on the production patterns and composition of dissolved free and combined amino acids in marine phytoplankton. *Journal of Plankton Research* **17**:1337-62.

Goldman, J. C. & Carpenter, E. J. 1974. A kinetic approach to the effect of temperature on algal growth. *Limnology and Oceanography* **19**:756-66.

Gopalakrishnan, K., Novis, P. & Visnovsky, G. 2014. Alpine Scenedesmaceae from New Zealand: new taxonomy. *New Zealand Journal of Botany* 52:84-99.

Graeve, M., Kattner, G. & Hagen, W. 1994. Diet-induced changes in the fatty acid composition of Arctic herbivorous copepods: experimental evidence of trophic markers. *Journal of Experimental Marine Biology and Ecology* **182**:97-110.

Graham, L., Graham, J. & Wilcox, L. W. 2009. Algae. San Francisco, CA: Pearson Benjamin Cummings, 616p.

Graham, L. & Wilcox, L. 2000. Algae. Upper Saddle River, NJ: Prentice-Hall, 640 pp..

Grama, B. S., Stenuit, B., Jeffryes, C. & Agathos, S. N. 2014. Characterization of fatty acid and carotenoid production in an *Acutodesmus* microalga isolated from the Algerian Sahara. *Environmental Sciences, Technologies and Management* **69**:265-75.

Grung, M., Metzger, P. & Liaaen-Jensen, S. 1989. Primary and secondary carotenoids in two races of the green alga *Botryococcus braunii*. *Biochemical Systematics and Ecology* **17**:263-69.

Guillard, R. R., Bold, H. C. & MacEntee, F. J. 1975. Four new unicellular chlorophycean algae from mixohaline habitats. *Phycologia* **14**:13-24.

Guillard, R. R. L. 1975. Culture of phytoplankton for feeding marine invertebrates. In: Smith, W.L. & Chanley, M. H [Eds.] *Culture of Marine Invertebrate Animals.* Plenum Publication. Corporation, New York, pp. 29-60.

Guiry, M. D. & Guiry, G. 2013. AlgaeBase World-wide electronic publication, National University of Ireland, Galway, Retrieved 1 April 2013, from http://www.algaebase.org.

Guschina, I. A. & Harwood, J. L. 2006. Lipids and lipid metabolism in eukaryotic algae. *Progress in Lipid Research* **45**:160-86.

Hall, D. O., Acién Fernández, F., Guerrero, E. C., Rao, K. K. & Grima, E. M. 2003. Outdoor helical tubular photobioreactors for microalgal production: modeling of fluid-dynamics and mass transfer and assessment of biomass productivity. *Biotechnology and Bioengineering* **82**:62-73.

Hallegraeff, G. M., Anderson, D. M., Cembella, A. D. & Enevoldsen, H. O. 2003. *Manual on harmful marine microalgae.* IOC-UNESCO, Paris, 551 pp.

Hanagata, N. 1998. Phylogeny of the subfamily Scotiellocystoideae (Chlorophyceae, Chlorophyta) and related taxa inferred from 18S ribosomal RNA gene sequence data. *Journal of Phycology* **34**:1049–54.

Hanagata, N., Takeuchi, T., Fukuju, Y., Barnes, D. J. & Karube, I. 1992. Tolerance of microalgae to high CO2 and high temperature. *Phytochemistry* **31**:3345-48.

Hansson, G. 1983. Methane production from marine, green macro-algae. *Resources and Conservation* **8**:185-94.

Happey-Wood, C. M. 1988. *Ecology of freshwater planktonic green algae.* Cambridge University Press, Cambridge, 175-226.

Harwood, J. L. 1998. Membrane lipids in algae. *In*: Siegenthaler, P.-A., Murata, N., [Ed.] *Lipids in Photosynthesis: Structure, Fuction and Genetics.* Kluwer Academic Publishers, Kluwer, The Netherlands, pp. 53–64.

Hegewald, E., Hindák, F. & Schnepf, E. 1990. Studies on the genus *Scenedesmus* Meyen (Chlorophyceae, Chlorococcales) from South India, with special reference to the cell wall ultrastructure. Schweizerbart Science Publishers, Johannesstr, pp. 1-75.

Hegewald, E. & Schnepf, E. 1991. *Scenedesmus abundans* (Kirchn.) Chod., an older name for *Chlorella fusca* Shih. et Krauss. *Archiv für Protistenkunde* **140**:133-76.

Hegewald, E. & Silva, P. C. 1988. Annotated catalogue of *Scenedesmus* and nomenclaturally related genera, including original descriptions and figures. *In*: J. Cramer, S. [Ed.]. Bibliotheca Phycologica, Johannesstr, pp. 1–75.

Hegewald, E., Wolf, M., Keller, A., Friedl, T. & Krienitz, L. 2010. ITS2 sequence-structure phylogeny in the Scenedesmaceae with special reference to *Coelastrum* (Chlorophyta, Chlorophyceae), including the new genera *Comasiella* and *Pectinodesmus*. *Phycologia* **49**:325–35.

Heinz, E. 1996. Plant glycolipids: structure, isolation and analysis. *In*: Christie, W. W. [Ed.] *Advances in Lipid Methodology*. Oily Press, Dundee, pp. 211-332.

Henrikson, R. 1989. Earth food spirulina. *Laguna Beach, CA: Ronore Enterprises, Inc*, 187 pp.

Hessen, D. O. & Van Donk, E. 1993. Morphological changes in *Scenedesmus* induced by substances released from *Daphnia*. *Archiv fur Hydrobiologie* **127:** 129-140.

Hoham, R. & Duval, B. 2001. Microbial ecology of snow and freshwater ice with emphasis on snow algae. *Snow ecology: an interdisciplinary examination of snow-covered ecosystems. Cambridge University Press, Cambridge*: 168-228.

Hoham, R. W. 1975. Optimum temperatures and temperature ranges for growth of snow algae. *Arctic and Alpine Research*:**7**:13-24.

Hoham, R. W., Bonome, T. A., Martin, C. W. & Leebens-Mack, J. H. 2002. A combined 18s rDNA and *rbc*L phylogenetic analysis of *Chloromonas* and *Chlamydomonas* (Chlorophyceae, Volvocales) emphasizing snow and other cold-temperature habitats. *Journal of Phycology* **38**:1051–64.

Holtmann, T. & Hegewald, E. 1986. The influence of nutrient solutions on the variability of the genus *Scenedesmus* subgenus *Acutodesmus*. *Archiv fur Hydrobiologie* **73**:365–80.

Holton, R. W., Blecker, H. H. & Stevens, T. S. 1968. Fatty acids in blue-green algae: possible relation to phylogenetic position. *Science* **160**:545-47.

Horodyski, R. J. & Knauth, L. P. 1994. Life on land in the precambrian. *Science* **263**:494-498.

Horrocks, L. A. & Yeo, Y. K. 1999. Health benefits of docosahexaenoic acid (DHA). *Pharmacological Research* **40**:211-25.

Hortobágyi, T. 1969. Phytoplankton organisms from three reservoirs on the Jamuna River, India. Akadémiai Kiadó, Hungary, pp. 1-80.

Huang, J., Aki, T., Hachida, K., Yokochi, T., Kawamoto, S., Shigeta, S., Ono, K. & Suzuki, O. 2001. Profile of polyunsaturated fatty acids produced by *Thraustochytrium* sp. KK17-3. *Journal of the American Oil Chemists' Society* **78**:605-10.

Huang, Y. & Rorrer, G. L. 2002. Optimal temperature and photoperiod for the cultivation of *Agardhiella subulata* microplantlets in a bubble-column photobioreactor. *Biotechnology and Bioengineering* **79**:135-44.

Huss, V. A., Frank, C., Hartmann, E. C., Hirmer, M., Kloboucek, A., Seidel, B. M., Wenzeler, P. & Kessler, E. 1999. Biochemical taxonomy and molecular phylogeny of the genus *Chlorella* sensu lato (Chlorophyta). *Journal of Phycology* **35**:587-98.

Janssen, M., Tramper, J., Mur, L. R. & Wijffels, R. H. 2003. Enclosed outdoor photobioreactors: light regime, photosynthetic efficiency, scale-up, and future prospects. *Biotechnology and Bioengineering* **81**:193-210.

Javornický, P. & Hindák, F. 1969. *Cryptomonas frigoris* spec. nova (Cryptophyceae), the new cyst-forming flagellate from the snow of the High Tatras. *Biologia* **25**:241-50.

Jiang, H. & Gao, K. 2004. Effects of lowering temperature during culture on the production of polyunsaturated fatty acids in the marine diatom *Phaeodactylum tricornutum* (Bacillariophyceae). *Journal of Phycology* **40**:651-54.

Jiang, Y. & Chen, F. 1999. Effects of salinity on cell growth and docosahexaenoic acid content of the heterotrophic marine microalga *Crypthecodinium cohnii*. *Journal of Industrial Microbiology and Biotechnology* **23**:508-13.

Jiang, Y., Fan, K. W., Wong, R. T. Y. & Chen, F. 2004. Fatty acid composition and squalene content of the marine microalga *Schizochytrium mangrovei*. *Journal of Agricultural and Food Chemistry* **52**:1196-200.

Jiménez, C., Cossío, B. R., Labella, D. & Xavier Niell, F. 2003. The feasibility of industrial production of *Spirulina* (*Arthrospira*) in Southern Spain. *Aquaculture* **217**:179-90.

Johns, R., Nichols, P. & Perry, G. 1979. Fatty acid composition of ten marine algae from Australian waters. *Phytochemistry* **18**:799-802.

Jonker, J. & Faaij, A. 2013. Techno-economic assessment of micro-algae as feedstock for renewable bio-energy production. *Applied Energy* **102**:461-75.

Jordan, D. B. & Ogren, W. L. 1984. The CO_2/O_2 specificity of ribulose 1, 5-bisphosphate carboxylase/oxygenase. *Planta* **161**:308-13.

Jukes, T. H. & Cantor, C. R. 1969. Evolution of Protein Molecules. New York: Academic Press. pp. 21–132.

Kadam, K. 2002. Environmental implications of power generation via coal-microalgae cofiring. *Energy* **27**:905-22.

Kalina, T. 1987. Taxonomy of the subfamily Scotiellocystoideae Fott 1976 (Chlorellaceae, Chlorophyceae). *Algological Studies/Archiv für Hydrobiologie Suppl.* **45**:473–521.

Kasting, J. F. & Siefert, J. L. 2002. Life and the evolution of Earth's atmosphere. *Science* **296**:1066-68.

Kaur, A., Chaudhary, A., Kaur, A., Choudhary, R. & Kaushik, R. 2005. Phospholipid fatty acid-A bioindicator of environment monitoring and assessment in soil ecosystem. *Current Science Bangalore* **89**:1103-1112.

Keeling, P. J. 2004. Diversity and evolutionary history of plastids and their hosts. *American Journal of Botany* **91**:1481-93.

Keffer, J. & Kleinheinz, G. 2002. Use of *Chlorella vulgaris* for CO_2 mitigation in a photobioreactor. *Journal of Industrial Microbiology & Biotechnology* **29**:275-80.

Kessler, E., Schafer, M., Hummer, C., Kloboucek, A. & Huss, V. 1997. Physiological, biochemical, and molecular characters for the taxonomy of the subgenera of *Scenedesmus* (Chlorococcales, Chlorophyta). *Botanica Acta* **110**:244–50.

Kessler, W. R., Popović, M. K. & Robinson, C. W. 1993. Xanthan production in an external-circulation-loop airlift fermenter. *The Canadian Journal of Chemical Engineering* **71**:101-06.

Khotimchenko, S. V. & Yakovleva, I. M. 2005. Lipid composition of the red alga *Tichocarpus crinitus* exposed to different levels of photon irradiance. *Phytochemistry* **66**:73-79.

Kieselbach, T., Hagman, Å., Andersson, B. & Schröder, W. P. 1998. The thylakoid lumen of chloroplasts: isolation and characterization. *Journal of Biological Chemistry* **273**:6710-16.

Kim, Z. H., Kim, S. H., Lee, H. S. & Lee, C. G. 2006. Enhanced production of astaxanthin by flashing light using *Haematococcus pluvialis*. *Enzyme and Microbial Technology* **39**:414-19.

Kleinig, H. & Czygan, F. 1969. Lipids of *Protosiphon* (Chlorophyta). I. Carotenoids and carotenoid esters of five strains of *Protosiphon botryoides* (Kütz.) Klebs. *Zeitschrift für Naturforschung. Teil B: Chemie, Biochemie, Biophysik, Biologie* **24**:927-30.

Kodama, M., Iremoto, H. & Miyachi, S. A. 1993. New species of highly CO_2-tolerant fast growing marine microalga suitable for high density culture. *Journal of Marine Biotechnology* **1**:21–25.

Kol, E. 1968. Kryobiologie: Biologie und Limnologie des Schnees und Eises. *In*: Elster, H. J. & Ohle, W. [Eds.]. E. Schweizerbart, Stuttgart: 216 pp.

Kunihiro, T., Takasu, H., Miyazaki, T., Uramoto, Y., Kinoshita, K., Yodnarasri, S., Hama, D., Wada, M., Kogure, K. & Ohwada, K. 2011. Increase in alphaproteobacteria in association with a polychaete, *Capitella* sp. I, in the organically enriched sediment. *The ISME Journal* **5**:1818-31.

Kyle, D., Behrens, P., Bingham, S., Arnett, K. & Lieberman, D. 1988. Microalgae as a source of EPA-containing oils *In*: Applewhite, T. H. [Ed.] *Biotechnology for the Fats and Oils Industry.* AOCS Press, Champaign, pp. 117–22.

Lamont, A. 1958. Air agitation and pachuca tanks. *The Canadian Journal of Chemical Engineering* **36**:153-60.

Lang, I., Hodac, L., Friedl, T. & Feussner, I. 2011. Fatty acid profiles and their distribution patterns in microalgae: a comprehensive analysis of more than 2000 strains from the SAG culture collection. *BMC Plant Biology* **11**:124.

Leathwick J. R, W. G., Stephens R. T. T. 2002. Climate Surfaces for New Zealand. Landcare Research contract report: LC9798/126, New Zealand

Lee, Y. K. & Soh, C. W. 2004. Accumulation of astaxanthin in *Haematococcus lacustris* (Chlorophyta). *Journal of Phycology* **27**:575-77.

Leflaive, J. & Ten-Hage, L. 2007. Algal and cyanobacterial secondary metabolites in freshwaters: a comparison of allelopathic compounds and toxins. *Freshwater Biology* **52**:199-214.

Lefrancois, M. L., Mariller, C.C., Mejane, J.V. 1955. Effectionnements aux procedes de cultures forgiques et de fermentations industrielles. Brevet d'Invention. France, no 1, 102, 200, Delivree le 4 Mai.

Legrys, G. 1978. Power demand and mass transfer capability of mechanically agitated gas-liquid contactors and their relationship to air-lift fermenters. *Chemical Engineering Science* **33**:83-86.

Leliaert, F., Smith, D. R., Moreau, H., Herron, M. D., Verbruggen, H., Delwiche, C. F. & De Clerck, O. 2012. Phylogeny and molecular evolution of the green algae. *Critical Reviews in Plant Sciences* **31**:1-46.

Lesser, M. P., Barry, T. M. & Banaszak, A. T. 2002. Effects of UV radiation on a Chlorophyte alga (*Scenedesmus* sp.) isolated from the fumarole fields of Mt. Erebus, Antarctica. *Journal of Phycology* **38**:473–81.

Lewis, L. A. & Flechtner, V. R. 2002. Green algae (Chlorophyta) of desert microbiotic crusts: diversity of North American taxa. *Taxon* **51**:443–51.

Lewis, L. A. & Flechtner, V. R. 2004. Cryptic species of *Scenedesmus* (Chlorophyta) from desert soil communities of Western North America. *Journal of Phycology* **40**:1127–37.

Li, Y., Horsman, M., Wang, B., Wu, N. & Lan, C. Q. 2008. Effects of nitrogen sources on cell growth and lipid accumulation of green alga *Neochloris oleoabundans*. *Applied Microbiology and Biotechnology* **81**:629-36.

Liang, Y., Beardall, J. & Heraud, P. 2006. Effects of nitrogen source and UV radiation on the growth, chlorophyll fluorescence and fatty acid composition of *Phaeodactylum tricornutum* and *Chaetoceros muelleri* (Bacillariophyceae). *Journal of Photochemistry and Photobiology B: Biology* **82**:161-72.

Ling, H. & Seppelt, R. 1990. Snow algae of the Windmill Islands, continental Antarctica. *Mesotaenium berggrenii* (Zygnematales, Chlorophyta) the alga of grey snow. *Antarctic Science* **2**:143-48.

Ling, H. & Seppelt, R. 1993. Snow algae of the Windmill Islands, continental Antarctica. 2. *Chloromonas rubroleosa* sp. nov.(Volvocales, Chlorophyta), an alga of red snow. *European Journal of Phycology* **28**:77-84.

Liu, J., Huang, J., Sun, Z., Zhong, Y., Jiang, Y. & Chen, F. 2011. Differential lipid and fatty acid profiles of photoautotrophic and heterotrophic *Chlorella zofingiensis*. Assessment of algal oils for biodiesel production. *Bioresource Technology* **102**:106-10.

Lorenz, R. T. & Cysewski, G. R. 2000. Commercial potential for *Haematococcus* microalgae as a natural source of astaxanthin. *Trends in Biotechnology* **18**:160-67.

Loubiere, K., Olivo, E., Bougaran, G., Pruvost, J., Robert, R. & Legrand, J. 2008. A new photobioreactor for continuous microalgal production in hatcheries based on external-loop airlift and swirling flow. *Biotechnology and Bioengineering* **102**:132-47.

Lu, C., Fernández, F. A., Guerrero, E. C., Hall, D. & Grima, E. M. 2002. Overall assessment of *Monodus subterraneus* cultivation and EPA production in outdoor helical and bubble column reactors. *Journal of Applied Phycology* **14**:331-42.

Lüder, U. H., Knoetzel, J. & Wiencke, C. 2002. Acclimation of photosynthesis and pigments to seasonally changing light conditions in the endemic Antarctic red macroalga *Palmaria decipiens*. **24**:598-603.

Luo, X., Lee, D., Lau, R., Yang, G. & Fan, L. S. 1999. Maximum stable bubble size and gas holdup in high-pressure slurry bubble columns. *AIChE Journal* **45**:665-80.

Lynch, D. V. & Thompson, G. A. 1982. Low temperature-induced alterations in the chloroplast and microsomal membranes of *Dunaliella salina*. *Plant Physiology* **69**:1369-75.

Lyons, W. A. 1997. *The handy weather answer book.* Visible Ink Press, Detroit, Michigan, USA, 397 pp.

Mann, J. E. & Schlichting Jr, H. E. 1967. Benthic algae of selected thermal springs in Yellowstone National Park. *Transactions of the American Microscopical Society* **86**:2-9.

Mansour, M. P., Frampton, D. M., Nichols, P. D., Volkman, J. K. & Blackburn, S. I. 2005. Lipid and fatty acid yield of nine stationary-phase microalgae: applications and unusual C24–C28 polyunsaturated fatty acids. *Journal of Applied Phycology* **17**:287-300.

Mantzouridou, F., Roukas, T. & Kotzekidou, P. 2002. Effect of the aeration rate and agitation speed on β-carotene production and morphology of *Blakeslea trispora* in a stirred tank reactor: mathematical modeling. *Biochemical Engineering Journal* **10**:123-35.

Marre, E. 1962. Temperature. *In*: Lewin, R. A. [Ed.] *Physiology and biochemistry of algae.* Academic Press Inc, New York, pp. 541-50.

Martínez-Fernández, E., Acosta-Salmón, H. & Southgate, P. C. 2006. The nutritional value of seven species of tropical microalgae for black-lip pearl oyster (*Pinctada margaritifera*, L.) larvae. *Aquaculture* **257**:491-503.

McLarnon-Riches, C. J., Rolph, C. E., Greenway, D. L. & Robinson, P. K. 1998. Effects of environmental factors and metals on *Selenastrum capricornutum* lipids. *Phytochemistry* **49**:1241-47.

McNeill, J., Barrie, F. R., Buck, W. R., Demoulin, V., Greuter, W., Hawksworth, D. L., Herendeen, P. S., Knapp, S., Marhold, K., Prado, J., Prud'homme van Reine, W. F., Smith, G. F., Wiersma, J. H, & Turland, N. 2012. International Code of Nomenclature for algae, fungi and plants (Melbourne Code) adopted by the Eighteenth International Botanical Congress Melbourne, Australia, July 2011. Koenigstein, Koeltz Scientific Books. 240 p.

Melis, A. & Happe, T. 2001. Hydrogen production. Green algae as a source of energy. *Plant Physiology* **127**:740-48.

Mensens, C., De Laender, F., Janssen, C. R., Sabbe, K. & De Troch, M. 2014. Stressor-induced biodiversity gradients: revisiting biodiversity–ecosystem functioning relationships. *Oikos*. **124(6)**:677-84.

Merchuk, J. 1990. Why use air-lift bioreactors? *Trends in Biotechnology* **8**:66-71.

Merchuk, J. & Berzin, I. 1995. Distribution of energy dissipation in airlift reactors. *Chemical Engineering Science* **50**:2225-33.

Merchuk, J., Ladwa, N., Cameron, A., Bulmer, M. & Pickett, A. 1994. Concentric-tube airlift reactors: Effects of geometrical design on performance. *American Institute of Chemical Engineers Journal* **40**:1105-17.

Merchuk, J., Ronen, M., Giris, S. & Arad, S. M. 1998. Light/dark cycles in the growth of the red microalga *Porphyridium* sp. *Biotechnology and Bioengineering* **59**:705-13.

Merchuk, J. C. 1991a. Shear effects on animal cells. *In*: M.D. White, S. R. a. A. S. [Ed.] *Biologicals from Recombinant and Microorganisms and Animal Cells. Production and Recovery.* VCH Publication,, Weinheim, Germany, 199 pp.

Merchuk, J. C. 1991b. Shear effects on suspended cells. *Advances Biochemical Engineering / Biotechnology* 44:65-95.

Merchuk, J. C. & Gluz, M. 1999. Bioreactors, airlift reactors. *In*: Flickinger, M.C. & Drew, S.W. [Ed.] *Encyclopedia of Bioprocess Technology: Fermentation, Biocatalysis and Bioseparation.* Wiley, New York, USA, pp. 320-353.

Merchuk, J. C. & Siegel, M. H. 1988. Air-lift reactors in chemical and biological technology. *Journal of Chemical Technology and Biotechnology* **41**:105-20.

Meyen, F. J. F. 1829. *Beobachtungen über einige niedere Algenformen.* Geologica Bavarica. pp. 100–128.

Miyachi, S., Tsuzuki, M., Maruyama, I., Gantar, M., Miyachi, S. & Matsushima, H. 1986. Effects of CO_2 concentration during growth on the intracellular structure of *Chlorella* and *Scenedesmus* (Chlorophyta). *Journal of Phycology* **22**:313-19.

Mock, T. & Kroon, B. 2002. Photosynthetic energy conversion under extreme conditions—II: the significance of lipids under light limited growth in Antarctic sea ice diatoms. *Phytochemistry* **61**:53-60.

Molina, E., Fernández, J., Acién, F. & Chisti, Y. 2001. Tubular photobioreactor design for algal cultures. *Journal of Biotechnology* **92**:113-31.

Moore, L. R. & Chisholm, S. W. 1999. Photophysiology of the marine cyanobacterium *Prochlorococcus*: Ecotypic differences among cultured isolates. *Limnology and Oceanography* **44**:628-38.

Moore, L. R., Goericke, R. & Chisholm, S. W. 1995. Comparative physiology of *Synechococcus* and *Prochlorococcus*: influence of light and temperature on growth, pigments, fluorescence and absorptive properties. *Marine Ecology Progress Series.* **116**:259-75.

Morel, F. M. M., Westall, J. C., Rueter, J. G. & Chaplick, J. P. 1975. *Description of the algal growth media" Aquil" and" Fraquil" ;* R. M. Parsons Laboratory for Water Resources and Hydrodynamics, Massachusetts Institute of Technology, Cambridge, MA. 33 pp.

Moreno, J., Vargas, M., Olivares, H., Rivas, J. N. & Guerrero, M. G. 1998. Exopolysaccharide production by the cyanobacterium *Anabaena* sp. ATCC 33047 in batch and continuous culture. *Journal of Biotechnology* **60**:175-82.

Morgan-Kiss, R. M., Priscu, J. C., Pocock, T., Gudynaite-Savitch, L. & Huner, N. P. 2006. Adaptation and acclimation of photosynthetic microorganisms to permanently cold environments. *Microbiology and Molecular Biology Reviews* **70**:222-52.

Morita, M., Watanabe, Y., Okawa, T. & Saiki, H. 2001a. Photosynthetic productivity of conical helical tubular photobioreactors incorporating *Chlorella* sp. under various culture medium flow conditions. *Biotechnology and Bioengineering* **74**:136-44.

Morita, M., Watanabe, Y. & Saiki, H. 2001b. Evaluation of photobioreactor heat balance for predicting changes in culture medium temperature due to light irradiation. *Biotechnology and Bioengineering* **74**:466-75.

Murata, N., Takahashi, S., Nishiyama, Y. & Allakhverdiev, S. I. 2007. Photoinhibition of photosystem II under environmental stress. *Biochimica et Biophysica Acta Bioenergetics* **1767**:414-21.

Murata, N., Troughton, J. H. & Fork, D. C. 1975. Relationships between the transition of the physical phase of membrane lipids and photosynthetic parameters in *Anacystis nidulans* and lettuce and spinach chloroplasts. *Plant Physiology* **56**:508-17.

Myers, R. A. & Worm, B. 2003. Rapid worldwide depletion of predatory fish communities. *Nature* **423**:280-83.

Nakano, Y., Miyatake, K., Okuno, H., Hamazaki, K., Takenaka, S., Honami, N., Kiyota, M., Aiga, I. & Kondo, J. 1996. Growth of photosynthetic algae *Euglena* in high CO_2 conditions and its photosynthetic characteristics. *International Symposium on Plant Production in Closed Ecosystems 440.* pp. 49-54.

Napolitano, G. E. 1994. The relationship of lipids with light and chlorophyll measurements in freshwater algae and periphyton. *Journal of Phycology* **30**:943-50.

Neustupa, J., Eliáš, M., Škaloud, P., Němcová, Y. & Šejnohová, L. 2011. *Xylochloris irregularis* gen. et sp. nov. (Trebouxiophyceae, Chlorophyta), a novel subaerial coccoid green alga. *Phycologia* **50**:57-66.

Nichols, D. S., Nichols, P. D. & McMeekin, T. A. 1993. Polyunsaturated fatty acids in Antarctic bacteria. *Antarctic Science* **5**:149-60.

Novis, P. M. 2001. *Ecology and taxonomy of alpine algae, Mt. Philistine, Arthur's Pass National Park, New Zealand.* University of Canterbury, Christchurch, New Zealand, 217 pp.

Novis, P. M. 2002a. Ecology of the snow alga *Chlainomonas kolii* (Chlamydomonadales, Chlorophyta) in New Zealand. *Phycologia* **41**:280-92.

Novis, P. M. 2002b. New records of snow algae for New Zealand, from Mt Philistine, Arthur's Pass National Park. *New Zealand Journal of Botany* **40**:297-312.

Novis, P. M. 2006. Taxonomy of *Klebsormidium* (Klebsormidiales, Charophyceae) in New Zealand streams and the significance of low-pH habitats. *Phycologia* **45**:293-301.

Novis, P. M., Whitehead, D., Gregorich, E. G., Hunt, J. E., Sparrow, A. D., Hopkins, D. W., Elberling, B. & Greenfield, L. G. 2007. Annual carbon fixation in terrestrial populations of *Nostoc commune* (Cyanobacteria) from an Antarctic dry valley is driven by temperature regime. *Global Change Biology* **13**:1224-37.

Novis, P. M., Beer, T. & Vallance, J. 2008a. New records of microalgae from the New Zealand alpine zone, and their distribution and dispersal. *New Zealand Journal of Botany* **46**:347-66.

Novis, P. M., Hoham, R. W., Beer, T. & Dawson, M. 2008b. Two snow species of the quadriflagellate green alga *Chlainomonas* (Chlorophyta, Volvocales): ultrastructure and phylogenetic position within the *Chloromonas* clade. *Journal of Phycology* **44**:1001-12.

Novis, P. M. & Visnovsky, G. 2011a. Novel alpine algae for New Zealand: Klebsormidiales. *New Zealand Journal of Botany* **49**:339-49.

Novis, P. M. & Visnovsky, G. 2011b. Novel alpine algae from New Zealand: Cyanobacteria. Phytotaxa **22**: 1–24.

Novis, P. M. & Visnovsky, G. 2012. Novel alpine algae from New Zealand: Chlorophyta. *Phytotaxa* **39**:1–30.

Nozaki, H., Itoh, M., Sano, R., Uchida, H., Watanabe, M. M. & Kuroiwa, T. 1995. Phylogenetic relationships within the colonial Volvocales (Chlorophyta) inferred from *rbc*L gene sequence data. *Journal of Phycology* **31**:970-79.

Nyholm, N. & Källqvist, T. 1989. Methods for growth inhibition toxicity tests with freshwater algae. *Environmental Toxicology and Chemistry* **8**:689-703.

Ogbonna, J. C. & Tanaka, H. 2000. Light requirement and photosynthetic cell cultivation–Development of processes for efficient light utilization in photobioreactors. *Journal of Applied Phycology* **12**:207-18.

Olaizola, M. 2000. Commercial production of astaxanthin from *Haematococcus pluvialis* using 25,000-liter outdoor photobioreactors. *Journal of Applied Phycology* **12**:499-506.

Orcutt, D. M. & Patterson, G. W. 1974. Effect of light intensity upon lipid composition of *Nitzschia closterium* (*Cylindrotheca fusiformis*). *Lipids* **9**:1000-03.

Ortega-Calvo, J., Mazuelos, C., Hermosin, B. & Sáiz-Jiménez, C. 1993. Chemical composition of *Spirulina* and eukaryotic algae food products marketed in Spain. *Journal of Applied Phycology* **5**:425-35.

Palmqvist, K., Ögren, E. & Lernmark, U. 1994. The CO_2-concentrating mechanism is absent in the green alga *Coccomyxa*: a comparative study of photosynthetic CO_2 and light responses of *Coccomyxa,*, *Chlamydomonas reinhardtii* and barley protoplasts. *Plant, Cell & Environment* **17**:65-72.

Partensky, F., Hess, W. & Vaulot, D. 1999. *Prochlorococcus*, a marine photosynthetic prokaryote of global significance. *Microbiology and Molecular Biology Reviews* **63**:106-27.

Piorreck, M., Baasch, K.-H. & Pohl, P. 1984. Biomass production, total protein, chlorophylls, lipids and fatty acids of freshwater green and blue-green algae under different nitrogen regimes. *Phytochemistry* **23**:207-16.

Polymenakou, P., Bertilsson, S., Tselepides, A. & Stephanou, E. 2005a. Links between geographic location, environmental factors, and microbial community composition in sediments of the Eastern Mediterranean Sea. *Microbial Ecology* **49**:367-78.

Polymenakou, P. N., Bertilsson, S., Tselepides, A. & Stephanou, E. G. 2005b. Bacterial community composition in different sediments from the Eastern Mediterranean Sea: a comparison of four 16S ribosomal DNA clone libraries. *Microbial Ecology* **50**:447-62.

Polzin, J. P. & Rorrer, G. L. 2003. Halogenated monoterpene production by microplantlets of the marine red alga *Ochtodes secundiramea* within an airlift photobioreactor under nutrient medium perfusion. *Biotechnology and Bioengineering* **82**:415-28.

Prescott, G. W. 1962. *Algae of the Western Great Lakes Area.* W. C. Brown Coompany ,Dubuque, Iowa, 977 pp.

Přibyl, P., Eliaš, M., Cepak, V., Lukavský, J. & Kaštanek, P. 2012. Zoosporogenesis, morphology, ultrastructure, pigment composition, and phylogenetic position of *Trachydiscus minutus* (Eustigmatophyceae, Heterokontophyta). *Journal of Phycology* **48**:231-42.

Pröschold, T., Marin, B., Schlösser, U. G. & Melkonian, M. 2001. Molecular phylogeny and taxonomic revision of *Chlamydomonas* (Chlorophyta). I. Emendation of *Chlamydomonas* Ehrenberg and *Chloromonas* Gobi, and Description of *Oogamochlamys* gen. nov. and *Lobochlamys* gen. nov. *Protist* **152**:265-300.

Provasoli, L. & Carlucci, A. 1974. Vitamins and growth regulators. *In*: Stewart, W. D. P. [Ed.] *Algal Physiology and Biochemistry (Botanical Monographs).* Blackwell Scientific, Oxford, pp. 741-87.

Pulz, O. 2001. Photobioreactors: production systems for phototrophic microorganisms. *Applied Microbiology and Biotechnology* **57**:287-93.

Pushkar, Y., Yano, J., Sauer, K., Boussac, A. & Yachandra, V. K. 2008. Structural changes in the Mn4Ca cluster and the mechanism of photosynthetic water splitting. *Proceedings of the National Academy of Sciences USA* **105**:1879-84.

Qiang, H. & Richmond, A. 1996. Productivity and photosynthetic efficiency of *Spirulina platensis* as affected by light intensity, algal density and rate of mixing in a flat plate photobioreactor. *Journal of Applied Phycology* **8**:139-45.

R Devolopment Core Team 2014. R: A language and environment for statistical computing. R Foundation for Statistical Computing, Vienna, Austria.

Ramawat, K. & Merillon, J. 1999. *Biotechnology: secondary metabolites.* Oxford and IBH publishing, Delhi, India, 565 pp.

Ratledge, C. 2004. Fatty acid biosynthesis in microorganisms being used for single cell oil production. *Biochimie* **86**:807-15.

Ratledge, C. & Wilkinson, S. G. 1988. An overview of microbial lipids. *In*: Wilkinson, S. G. [Ed.] *Microbial Lipids.* Academic Press, London, U.K, pp. 3-22.

Raven, J. A. & Geider, R. J. 1988. Temperature and algal growth. *New Phytologist* **110**:441-61.

Raven, P. H., Evert, R. F. & Eichhorn, S. E. 2005. *Biology of plants.* Macmillan, New York. pp. 124-27.

Reay, D. S., Nedwell, D. B., Priddle, J. & Ellis-Evans, J. C. 1999. Temperature dependence of inorganic nitrogen uptake: reduced affinity for nitrate at suboptimal temperatures in both algae and bacteria. *Applied and Environmental Microbiology* **65**:2577-84.

Renaud, S., Zhou, H., Parry, D., Thinh, L.-V. & Woo, K. 1995. Effect of temperature on the growth, total lipid content and fatty acid composition of recently isolated tropical microalgae Isochrysis sp., Nitzschia closterium, Nitzschia paleacea, and commercial species Isochrysis sp.(clone T. ISO). *Journal of Applied Phycology* **7**:595-602.

Renaud, S. M., Thinh, L.-V., Lambrinidis, G. & Parry, D. L. 2002. Effect of temperature on growth, chemical composition and fatty acid composition of tropical Australian microalgae grown in batch cultures. *Aquaculture* **211**:195-214.

Rhodes, M., Gardiner, S. and Broad, D. 1991. Animal Cell Bioreactors 3. *In*: Ho, Ch & Wang, D. [Eds.]. Butterworth-Heinemann, Boston, 5 pp.

Richardson, K., Beardall, J. & Raven, J. 1983. Adaptation of unicellular algae to irradiance: an analysis of strategies. *New Phytologist* **93**:157-91.

Richmond, A. 2000. Microalgal biotechnology at the turn of the millennium: a personal view. *Journal of Applied Phycology* **12**:441-51.

Richmond, A. 2008. *Handbook of microalgal culture: biotechnology and applied phycology.* Wiley-Blackwell, Oxford, 545 pp.

Rindi, F., Guiry, M. D. & López-Bautista, J. M. 2008. Distribution, morphology, and phylogeny of *Klebsormidium* (Klebsormidiales, Charophyceae) in urban environments in Europe. *Journal of Phycology* **44**:1529-40.

Rippka, R., Deruelles, J., Waterbury, J. B., Herdman, M. & Stanier, R. Y. 1979. Generic assignments, strain histories and properties of pure cultures of cyanobacteria. *Journal of General Microbiology* **111**:1–61.

Rodolfi, L., Chini Zittelli, G., Bassi, N., Padovani, G., Biondi, N., Bonini, G. & Tredici, M. R. 2009. Microalgae for oil: Strain selection, induction of lipid synthesis and outdoor mass cultivation in a low-cost photobioreactor. *Biotechnology and Bioengineering* **102**:100-12.

Roessler, P. G. 1990. Environmental control of glycerolipid metabolism in microalgae: commercial implications and future research directions. *Journal of Phycology* **26**:393-99.

Ronquist, F. & Huelsenbeck, J. P. 2003. MrBayes 3: Bayesian phylogenetic inference under mixed models. *Bioinformatics* **19**:1572–74.

Rubin, D. 1991. 4,7,10,13,16,19-Docosahexaenoic acid and 5,8,11,14,17-eicosapentaenoic acid or their salts, immunoglobulins, protein, carbohydrate, water; microencapsulation; concentrates. U.S Patent No. 5,013,569. Washington, DC: U.S Patent and Trademark Office.

Rubio, F. C., Fernandez, F., Perez, J., Camacho, F. G. & Grima, E. M. 1999. Prediction of dissolved oxygen and carbon dioxide concentration profiles in tubular photobioreactors for microalgal culture. *Biotechnology and Bioengineering* **62**:71-86.

Sahu, A., Pancha, I., Jain, D., Paliwal, C., Ghosh, T., Patidar, S., Bhattacharya, S. & Mishra, S. 2013. Fatty acids as biomarkers of microalgae. *Phytochemistry* **89**:53-58.

Samson, R. & Leduy, A. 2009. Multistage continuous cultivation of blue-green alga *Spirulina maxima* in the flat tank photobioreactors with recycle. *The Canadian Journal of Chemical Engineering* **63**:105-12.

Sánchez Mirón, A., Contreras Gómez, A., García Camacho, F., Molina Grima, E. & Chisti, Y. 1999. Comparative evaluation of compact photobioreactors for large-scale monoculture of microalgae. *Journal of Biotechnology* **70**:249-70.

Sánchez Mirón, A., Garcia Camacho, F., Contreras Gomez, A., Grima, E. M. & Chisti, Y. 2000. Bubble-column and airlift photobioreactors for algal culture. *American Institute of Chemical Engineers Journal* **46**:1872-87.

Sandesh Kamath, B., Vidhyavathi, R., Sarada, R. & Ravishankar, G. 2008. Enhancement of carotenoids by mutation and stress induced carotenogenic genes in *Haematococcus pluvialis* mutants. *Bioresource Technology* **99**:8667-73.

Sato, N. & Murata, N. 1980. Temperature shift-induced responses in lipids in the blue-green alga, *Anabaena variabilis*: The central role of diacylmonogalactosylglycerol in thermo-adaptation. *Biochimica et Biophysica Acta Lipids and Lipid Metabolism* **619**:353-66.

Schlegel, I., Krienitz, L. & Hepperle, D. 2000. Variability of calcification of *Phacotus lenticularis* (Chlorophyta, Chlamydomonadales) in nature and culture. *Phycologia* **39**:318-22.

Schlichting Jr, H. E. 1974. Survival of some fresh-water algae under extreme environmental conditions. *Transactions of the American Microscopical Society*:610-13.

Schwimmer, M. & Schwimmer, D. 1955. The role of algae and plankton in medicine. *The role of algae and plankton in medicine* Grune and Stratton, Inc., New York. 88 pp.

Seaburg, K. G., Parked, B. C., Wharton, R. A. & Simmons, G. M. 1981. Temperature-growth responses of algal isolates from Antarctic oases. *Journal of Phycology* **17**:353-60.

Semenenko, V. E., Vladimirova, M. G., Tsoglin, L. N. & Popova, M. A. 1966. Growth, productivity, and the photosynthesis rate of *Chlorella* culture as dependent on the CO_2 concentration in gas mixture and on the specific. *In*: Ierusalimskii, N. D. & Kovrov, B. G. [Eds.] *Controlled Biosynthesis.* Nauka, Moscow, pp. 128–36.

Seo, Y.-B., Lee, Y.-W., Lee, C.-H. & You, H.-C. 2010. Red algae and their use in papermaking. *Bioresource Technology* **101**:2549-53.

Sergeenko, T. V., Muradyan, E. A., Pronina, N. A., Klyachko-Gurvich, G. L., Mishina, I. M. & Tsoglin, L. N. 2000. The effect of extremely high CO_2 concentration on the growth and biochemical composition of microalgae. *Russian Journal Plant Physiology* **47**:722–29.

Šetlík, I., Šust, V. & Málek, I. 1970. Dual purpose open circulation units for large scale culture of algae in temperate zones. I. Basic design considerations and scheme of a pilot plant. *Algological Studies/Archiv für Hydrobiologie, Supplement Volumes* **1**:111-64.

Shahidi, F. & Miraliakbari, H. 2005. Omega-3 fatty acids in health and disease: part 2-health effects of omega-3 fatty acids in autoimmune diseases, mental health, and gene expression. *Journal of Medicinal Food* **8**:133-48.

Sharma, K. K., Schuhmann, H. & Schenk, P. M. 2012. High lipid induction in microalgae for biodiesel production. *Energies* **5**:1532-53.

Shifrin, N. S. & Chisholm, S. W. 1981. Phytoplankton lipids: interspecific differences and effects of nitrate, silicate and light-dark cycles. *Journal of Phycology* **17**:374-84.

Siegel, M. H. & Merchuk, J. C. 1988. Mass transfer in a rectangular air-lift reactor: Effects of geometry and gas recirculation. *Biotechnology and Bioengineering* **32**:1128-37.

Sierra, E., Acien, F., Fernandez, J., Garcia, J., Gonzalez, C. & Molina, E. 2008. Characterization of a flat plate photobioreactor for the production of microalgae. *Chemical Engineering Journal* **138**:136-47.

Silvera, A. B. & Cortina, A. 2013. Comparison of two different vertical column photobioreactors for the cultivation of *Nannochloropsis* sp. *Journal of Energy Resources and Technology.* **135**:011201 (1-7).

Singh, M. 2005. Essential fatty acids, DHA and human brain. *The Indian Journal of Pediatrics* **72**:239-42.

Singh, R. & Sharma, S. 2012. Development of suitable photobioreactor for algae production–A review. *Renewable and Sustainable Energy Reviews* **16**:2347-53.

Solovchenko, A., Khozin-Goldberg, I., Didi-Cohen, S., Cohen, Z. & Merzlyak, M. 2008. Effects of light intensity and nitrogen starvation on growth, total fatty acids and arachidonic acid in the green microalga *Parietochloris incisa*. *Journal of Applied Phycology* **20**:245-51.

Somerville, C. 1995. Direct tests of the role of membrane lipid composition in low-temperature-induced photoinhibition and chilling sensitivity in plants and cyanobacteria. *Proceedings of the National Academy of Sciences USA* **92**:6215.

Sorokin, C. & Krauss, R. W. 1958. The effects of light intensity on the growth rates of green algae. *Plant Physiology* **33**:109-113.

Spolaore, P., Joannis-Cassan, C., Duran, E. & Isambert, A. 2006. Commercial applications of microalgae. *Journal of Bioscience and Bioengineering* **101**:87-96.

Spurr, A. R. 1969. A low-viscosity epoxy resin embedding medium for electron microscopy. *Journal of Ultrastructure Research* **26**:31–43.

Srinivas, R. & Ochs, C. 2012. Effect of UV-A irradiance on lipid accumulation in *Nannochloropsis oculata*. *Photochemistry and Photobiology* **88**:684-89.

Stein, J. R. 1963. A *Chromulina* (Chrysophyceae) from snow. *Canadian Journal of Botany* **41**:1367-70.

Stein, J. R. 1973. *Handbook of phycological methods: culture methods and growth measurements*. Cambridge University Press, 448 pp.

Stránsky, K., Jursík, T. & Vítek, A. 1997. Standard equivalent chain length values of monoenic and polyenic (methylene interrupted) fatty acids. *Journal of High Resolution Chromatography* **20**:143-58.

Suh, I. S. & Lee, C. G. 2003. Photobioreactor engineering: design and performance. *Biotechnology and Bioprocess Engineering* **8**:313-21.

Sushchik, N., Kalacheva, G., Zhila, N., Gladyshev, M. & Volova, T. 2003. A temperature dependence of the intra-and extracellular fatty-acid composition of green algae and cyanobacterium. *Russian Journal of Plant Physiology* **50**:374-80.

Svetashev, V. I., Vysotskii, M. V., Ivanova, E. P. & Mikhailov, V. V. 1995. Cellular fatty acids of *Alteromonas* species. *Systematic and Applied Microbiology* **18**:37-43.

Swofford, D. 2002. Phylogenetic analysis using parsimony (PAUP) v. 4.0 b10. Sunderland, MA, Sinauer.

Szabó, I., Bergantino, E. & Giacometti, G. M. 2005. Light and oxygenic photosynthesis: energy dissipation as a protection mechanism against photo-oxidation. *EMBO reports* **6**:629-34.

Tamura, K., Peterson, D., Peterson, N., Stecher, G., Nei, M. & Kumar, S. 2011. MEGA5: molecular evolutionary genetics analysis using maximum likelihood, evolutionary distance, and maximum parsimony methods. *Molecular Biology and Evolution* **28**:2731–39.

Tamura, K., Stecher, G., Peterson, D., Filipski, A. & Kumar, S. 2013. MEGA6: molecular evolutionary genetics analysis version 6.0. *Molecular Biology and Evolution* **30**:2725-29.

Tan, H. 2008. Algae-to-biodiesel at least five to 10 years away. Energy Current: News for the Business of Energy, Singapore.

Tan, W., Dai, G., Ye, W. & Shen, J. 1995. Local flow behavior of the liquid phase in an airlift bioreactor for potential use in animal cell suspension cultures. *The Chemical Engineering Journal and The Biochemical Engineering Journal* **57**:B31-B36.

Tanaka, H. 1987. Large-scale cultivation of plant cells at high density: a review. *Process Biochemistry* **22**:106-13.

Tang, E. P., Tremblay, R. & Vincent, W. F. 1997. Cyanobacterial dominance of polar freshwater ecosystems: are high-latitude mat-formers adapted to low temperature? *Journal of Phycology* **33**:171-81.

Tatsuzawa, H. & Takizawa, E. 1995. Changes in lipid and fatty acid composition of *Pavlova lutheri*. *Phytochemistry* **40**:397-400.

Teoh, M.-L., Chu, W.-L., Marchant, H. & Phang, S.-M. 2004. Influence of culture temperature on the growth, biochemical composition and fatty acid profiles of six Antarctic microalgae. *Journal of Applied Phycology* **16**:421-30.

Thimijan, R. W. & Heins, R. D. 1983. Photometric, radiometric, and quantum light units of measure: a review of procedures for interconversion. *HortScience* **18**:818-22.

Thompson, J. D., Gibson, T. J., Plewniak, F., Jeanmougin, F. & Higgins, D. G. 1997. The CLUSTAL_X windows interface: flexible strategies for multiple sequence alignment aided by quality analysis tools. *Nucleic Acids Research* **25**:4876–82.

Thompson Jr, G. A. 1996. Lipids and membrane function in green algae. *Biochimica et Biophysica Acta (BBA)-Lipids and Lipid Metabolism* **1302**:17-45.

Throndsen, J. 1995. Estimating cell numbers. *In* Hallegraeff, G. M., Anderson, D. M. & Cembella, A. D. [Eds.] *Manual on Harmful Marine Microalgae*, UNESCO, Paris. pp. 63-80.

Tonon, T., Harvey, D., Larson, T. R. & Graham, I. A. 2002. Long chain polyunsaturated fatty acid production and partitioning to triacylglycerols in four microalgae. *Phytochemistry* **61**:15-24.

Trainor, F. R. 1998. Biological aspects of *Scenedesmus* (Chlorophyceae)-phenotypic plasticity. Berlin, J. Cramer, 367 pp.

Trainor, F. R. & Hilton, R. L. 1963. Identification of species of *Scenedesmus*. *Nature* **200**: 800 pp.

Tredici, M., 1999. Photobioreactors. *In* Flickinger, M.C & Drew, S.W [Eds.] Encyclopedia of Bioprocess Technology: Fermentation, Biocatalysis, and Bioseparation, Wiley, New York. pp. 395-419.

Tsarenko, P. & John, D. M. 2002. Order Sphaeropleales. *In*: John D.M, Whitton B.A & Brook A.J [Eds.] *The freshwater algal flora of the British Isles: an identification guide to freshwater and terrestrial algae.* Cambridge, Cambridge University Press, pp. 420–44.

Tsuzuki, M., Gantar, M., Aizawa, K. & Miyachi, S. 1986. Ultrastructure of *Dunaliella tertiolecta* cells grown under low and high CO_2 concentrations. *Plant and Cell Physiology* **27**:737-39.

Tsuzuki, M. & Miyachi, S. 1989. The function of carbonic anhydrase in aquatic photosynthesis. *Aquatic Botany* **34**:85-104.

Turpin, D. H., Miller, A. & Canvin, D. T. 1984. Carboxysome content of *Synechococcus leopoliensis* (Cyanophyta) in response to inorganic carbon. *Journal of Phycology* **20**:249-53.

Tzen, J. T., Cao, Y., Laurent, P., Ratnayake, C. & Huang, A. H. 1993. Lipids, proteins, and structure of seed oil bodies from diverse species. *Plant Physiology* **101**:267-76.

Ueno, Y., Kurano, N. & Miyachi, S. 1998. Ethanol production by dark fermentation in the marine green alga, *Chlorococcum littorale*. *Journal of Fermentation and Bioengineering* **86**:38-43.

Ugwu, C., Aoyagi, H. & Uchiyama, H. 2008. Photobioreactors for mass cultivation of algae. *Bioresource Technology* **99**:4021-28.

Urakawa, H., Yoshida, T., Nishimura, M. & Ohwada, K. 2001. Characterization of microbial communities in marine surface sediments by terminal-restriction fragment length polymorphism (T-RFLP) analysis and quinone profiling. *Marine Ecology Progress Series* **220**:47-57.

Vaishnav, P. & Demain, A. L. 2011. Unexpected applications of secondary metabolites. *Biotechnology Advances* **29**:223-29.

Van den Hoek, C., Mann, D. & Jahns, H. M. 1996. *Algae: an introduction to phycology.* Cambridge University Press, Cambridge, 623 pp.

Van Der Pol, L. A., Bonarius, D., Van De Wouw, G. & Tramper, J. 1993. Effect of silicone antifoam on shear sensitivity of hybridoma cells in sparged cultures. *Biotechnology Progress* **9**:504-09.

Venkataraman, L. V. & Becker, E. W. 1985. *Biotechnology and utilization of algae: the Indian experience.* Department of Science & Technology and Central Food Technological Research Institute, Mysore, India,

Vioque, A. 2007. Transformation of cyanobacteria. In: León R, Galván A, Fernández E (eds) *Transgenic microalgae as green cell factories. Advances in Experimental Medicine and Biolology* Springer, New York, pp. 12-22.

Volkman, J., Jeffrey, S., Nichols, P., Rogers, G. & Garland, C. 1989. Fatty acid and lipid composition of 10 species of microalgae used in mariculture. *Journal of Experimental Marine Biology and Ecology* **128**:219-40.

Volkman, J. K., Dunstan, G. A., Jeffrey, S. & Kearney, P. S. 1991. Fatty acids from microalgae of the genus *Pavlova*. *Phytochemistry* **30**:1855-59.

Volkman, J. K., Barrett, S. M., Blackburn, S. I., Mansour, M. P., Sikes, E. L. & Gelin, F. 1998. Microalgal biomarkers: a review of recent research developments. *Organic Geochemistry* **29**:1163-79.

Vonshak, A. & Richmond, A. 1988. Mass production of the blue-green alga *Spirulina*: An overview. *Biomass* **15**:233-47.

Wang, X. 2004. Lipid signalling. *Current Opinion in Plant Biology* **7**:329-36.

Ward, O. P. & Singh, A. 2005. Omega-3/6 fatty acids: alternative sources of production. *Process Biochemistry* **40**:3627-52.

Weinberg, E. D. 1970. Biosynthesis of secondary metabolites: roles of trace metals. *Adv. Microb. Physiol* **4**:1-44.

Weiss, R. L. 1983. Fine structure of the snow alga *Chlamydomonas nivalis* and associated bacteria. *Journal of Phycology* **19**:200-04.

White, C. & Costello, C. 2014. Close the high seas to fishing? *PLoS Biology* **12**:e1001826.

Whitelam, G. & Codd, G. 1986. Damaging effects of light on microorganisms. In: Herbert, R. A. & Codd, G. A. (Eds.) *Microbes in Extreme Environments*: Academic, London, pp.129-69.

Wilson, H. D. 1976. Vegetation of Mount Cook National Park, New Zealand. Wellington: Department of Lands and Survey.

World Health Organization. 1998. *Fats and oils in human nutrition: report of a joint expert consultation.* WHO: ROME.

Wu, J. 1995. Mechanisms of animal cell damage associated with gas bubbles and cell protection by medium additives. *Journal of Biotechnology* **43**:81-94.

Wu, S. T., Yu, S. T. & Lin, L. P. 2005. Effect of culture conditions on docosahexaenoic acid production by *Schizochytrium* sp. S31. *Process Biochemistry* **40**:3103-08.

Xu, L., Weathers, P. J., Xiong, X. R. & Liu, C. Z. 2009. Microalgal bioreactors: Challenges and opportunities. *Engineering in Life Sciences* **9**:178-89.

Yano, Y., Nakayama, A. & Yoshida, K. 1997. Distribution of polyunsaturated fatty acids in bacteria present in intestines of deep-sea fish and shallow-sea poikilothermic animals. *Applied and Environmental Microbiology* **63**:2572-77.

Yonfmanitchai, W. & Ward, O. 1989. Omega-3 fatty acids: alternative sources of production. *Process Biochemistry* **24**:117-25.

Yong, Y. & Lee, Y. K. 1991. Do carotenoids play a photoprotective role in the cytoplasm of *Haematococcus lacustris* (Chlorophyta)? *Phycologia* **30**:257-61.

Yoshimura, Y., Kohshima, S. & Ohtani, S. 1997. A community of snow algae on a Himalayan glacier: change of algal biomass and community structure with altitude. *Arctic and Alpine Research.* **29**:126-37.

You, T. & Barnett, S. M. 2004. Effect of light quality on production of extracellular polysaccharides and growth rate of *Porphyridium cruentum*. *Biochemical Engineering Journal* **19**:251-58.

Zhang, J., Huss, V. A., Sun, X., Chang, K. & Pang, D. 2008. Morphology and phylogenetic position of a trebouxiophycean green alga (Chlorophyta) growing on the rubber tree,

Hevea brasiliensis, with the description of a new genus and species. *European Journal of Phycology* **43**:185-93.

Zhu, C., Lee, Y. & Chao, T. 1997. Effects of temperature and growth phase on lipid and biochemical composition of *Isochrysis galbana* TK1. *Journal of Applied Phycology* **9**:451-57.

APPENDIX

A1. Cell concentration of *Lobochlamys segnis* at different carbon dioxide concentration experiments

1.5%					3.0%				4.5%		
Hours	Reactor 1	Reactor 2	Average		Reactor 1	Reactor 2	Average		Reactor 1	Reactor 2	Average
0	2.00E+05	2.00E+05	2.00E+05		2.00E+05	2.00E+05	2.00E+05		2.00E+05	2.00E+05	2.00E+05
24	2.20E+05	2.10E+05	2.15E+05		2.10E+05	2.10E+05	2.10E+05		2.21E+05	2.12E+05	2.17E+05
48	1.10E+06	1.05E+06	1.08E+06		3.20E+06	3.05E+06	3.13E+06		3.31E+06	3.22E+06	3.27E+06
72	2.70E+06	2.58E+06	2.64E+06		4.50E+06	4.90E+06	4.70E+06		5.00E+06	4.98E+06	4.99E+06
96	3.54E+06	3.30E+06	3.42E+06		5.00E+06	5.10E+06	5.05E+06		4.30E+06	4.31E+06	4.31E+06
120	3.91E+06	4.00E+06	3.96E+06		5.00E+06	5.30E+06	5.15E+06		4.12E+06	4.00E+06	4.06E+06
144	4.10E+06	4.20E+06	4.15E+06		4.70E+06	5.00E+06	4.85E+06		3.78E+06	3.49E+06	3.64E+06
168	3.32E+06	3.41E+06	3.37E+06								

A2. Cell concentration of *Lobochlamys segnis* at different temperature experiments

	30 degree C			20 degree C			20 degree C		
hours	Reactor 1	Reactor 2	Average	Reactor 1	Reactor 2	Average	Reactor 1	Reactor 2	Average
0	2.00E+05	2.00E+05	2.00E+05	2.00E+05	2.00E+05	2.00E+05	2.00E+05	2.00E+05	2.00E+05
24	2.00E+05	2.02E+05	2.01E+05	2.10E+05	1.99E+05	2.05E+05	2.21E+05	2.12E+05	2.17E+05
48	2.03E+06	2.03E+06	2.03E+06	3.02E+06	2.89E+06	2.96E+06	3.31E+06	3.22E+06	3.27E+06
72	2.17E+06	2.20E+06	2.19E+06	3.96E+06	3.93E+06	3.95E+06	5.00E+06	4.98E+06	4.99E+06
96	2.61E+06	2.79E+06	2.70E+06	4.26E+06	4.17E+06	4.22E+06	4.30E+06	4.31E+06	4.31E+06
120	2.70E+06	2.81E+06	2.76E+06	3.98E+06	4.56E+06	4.27E+06	4.12E+06	4.00E+06	4.06E+06
144	2.56E+06	2.50E+06	2.53E+06	3.70E+06	4.00E+06	3.85E+06	3.78E+06	3.49E+06	3.64E+06

Table A2 (Continued)

	15 degree C			10 degree C			5 degree C		
hours	Reactor 1	Reactor 2	Average	Reactor 1	Reactor 2	Average	Reactor 1	Reactor 2	Average
0	2.00E+05	2.00E+05	2.00E+05	2.00E+05	2.00E+05	2.00E+05	2.00E+05	2.00E+05	2.00E+05
24	2.00E+05	2.10E+05	2.05E+05	2.00E+05	2.11E+05	2.06E+05	2.00E+05	2.05E+05	2.03E+05
48	6.00E+05	6.35E+05	6.18E+05	2.50E+05	2.60E+05	2.55E+05	2.01E+05	2.05E+05	2.03E+05
72	2.13E+06	2.21E+06	2.17E+06	2.99E+05	3.10E+05	3.05E+05	2.50E+05	2.45E+05	2.48E+05
96	3.40E+06	3.51E+06	3.46E+06	4.00E+05	4.12E+05	4.06E+05	2.55E+05	2.50E+05	2.53E+05
120	4.30E+06	4.31E+06	4.31E+06	9.00E+05	9.30E+05	9.15E+05	2.65E+05	2.66E+05	2.66E+05
144	4.41E+06	4.39E+06	4.40E+06	1.60E+06	1.59E+06	1.60E+06	3.10E+05	2.80E+05	2.95E+05
168	4.51E+06	4.41E+06	4.46E+06	2.00E+06	2.10E+06	2.05E+06	4.00E+05	3.86E+05	3.93E+05
192				2.25E+06	2.30E+06	2.28E+06	4.50E+05	4.32E+05	4.41E+05
216				3.10E+06	3.30E+06	3.20E+06	5.90E+05	5.59E+05	5.75E+05
240				4.20E+06	4.26E+06	4.23E+06	6.10E+05	6.11E+05	6.11E+05
264				4.33E+06	4.40E+06	4.37E+06	8.00E+05	8.21E+05	8.11E+05
288				4.70E+06	4.69E+06	4.70E+06	1.13E+06	1.05E+06	1.09E+06
312				4.40E+06	4.51E+06	4.46E+06	2.50E+06	2.50E+06	2.50E+06
336				4.21E+06	4.25E+06	4.23E+06	3.10E+06	3.15E+06	3.13E+06
360							3.80E+06	3.91E+06	3.86E+06
384							4.06E+06	4.10E+06	4.08E+06
408							3.99E+06	3.89E+06	3.94E+06
432							3.05E+06	3.12E+06	3.09E+06

A3. Alpha linolenic acid (µg/mg) produced by *Lobochlamys segnis* at different temperature experiments

		Reactor1	Reactor2	Mean	SD
30 degree C	Exponential phase	2.347113	1.785098	2.07	0.4
	Stationary phase (start)	1.83623	2.023938	1.93	0.13
	Stationary phase (end)	2.87241	2.332465	2.6	0.38
25 degree C	Exponential phase	3.638131	2.648461	3.14	0.7
	Stationary phase (start)	2.944589	2.459228	2.7	0.34
	Stationary phase (end)	1.887296	1.598533	1.74	0.2
20 degree C	Exponential phase	4.655626	5.040131	4.85	0.27
	Stationary phase (start)	2.457049	4.8747	3.67	1.71
	Stationary phase (end)	1.100907	1.315908	1.21	0.15
15 degree C	Exponential phase	2.878324	3.029195	2.95	0.11
	Stationary phase (start)	4.24119	3.262433	3.75	0.69
	Stationary phase (end)	1.220721	1.883748	1.55	0.47
10 degree C	Exponential phase	2.664109	4.342278	3.5	1.19
	Stationary phase (start)	0.929368	2.050264	1.49	0.79
	Stationary phase (end)	1.989873	2.546936	2.27	0.39
5 degree C	Exponential phase	1.348491	1.445874	1.4	0.07
	Stationary phase (start)	0.970982	1.113674	1.04	0.1
	Stationary phase (end)	1.735972	2.471886	2.1	0.52

A4. Alpha linolenic acid (µg/mg) produced by *Lobochlamys segnis* at different temperature experiments

		Reactor1	Reactor2	Mean	SD
30 degree C	Exponential phase	3.520929	2.740739	3.13	0.55
	Stationary phase (start)	2.803534	3.131994	2.97	0.23
	Stationary phase (end)	4.090937	3.722189	3.91	0.26
25 degree C	Exponential phase	5.966589	3.962363	4.96	1.42
	Stationary phase (start)	4.559727	3.746599	4.15	0.57
	Stationary phase (end)	3.047424	2.82016	2.93	0.16
20 degree C	Exponential phase	6.607588	7.828318	7.22	0.86
	Stationary phase (start)	3.75488	7.51435	5.63	2.66
	Stationary phase (end)	1.642734	2.056449	1.85	0.29
15 degree C	Exponential phase	5.218114	5.070662	5.14	0.1
	Stationary phase (start)	6.861016	5.045759	5.95	1.28
	Stationary phase (end)	2.019933	3.052948	2.54	0.73
10 degree C	Exponential phase	4.197488	6.550359	5.37	1.66
	Stationary phase (start)	1.620902	3.372034	2.5	1.24
	Stationary phase (end)	3.258026	4.131047	3.69	0.62
5 degree C	Exponential phase	2.15942	2.357626	2.26	0.14
	Stationary phase (start)	1.616793	1.836217	1.73	0.16
	Stationary phase (end)	2.983878	4.195143	3.59	0.86

A5. PUFAs (µg/mg) produced by *Lobochlamys segnis* at different temperature experiments

		Reactor1	Reactor2	Mean	SD
30 degree C	Exponential phase	5.908161	4.615176	5.26	0.91
	Stationary phase (start)	4.509157	4.914276	4.71	0.29
	Stationary phase (end)	6.615281	5.878837	6.25	0.52
25 degree C	Exponential phase	9.332288	6.144579	7.74	2.25
	Stationary phase (start)	6.920514	4.78207	5.85	1.51
	Stationary phase (end)	7.524355	4.425117	5.97	2.19
20 degree C	Exponential phase	9.269185	10.29857	9.78	0.73
	Stationary phase (start)	5.598331	11.02615	8.31	3.84
	Stationary phase (end)	2.544985	3.307319	2.93	0.54
15 degree C	Exponential phase	6.441412	6.416249	6.43	0.02
	Stationary phase (start)	8.272677	6.145459	7.21	1.5
	Stationary phase (end)	2.81213	4.15056	3.48	0.95
10 degree C	Exponential phase	4.820525	7.557251	6.19	1.94
	Stationary phase (start)	2.064064	4.366994	3.22	1.63
	Stationary phase (end)	4.377811	5.502567	4.94	0.8
5 degree C	Exponential phase	2.518861	2.769659	2.64	0.18
	Stationary phase (start)	1.957387	2.222822	2.09	0.19
	Stationary phase (end)	3.620216	5.009757	4.31	0.98

A6. Cell concentration of *Lobochlamys segnis* at different photon flux density experiments

Light intensities		115 µmol m-2 s-1			178 µmol m-2 s-1			210 µmol m-2 s-1	
hours	Reactor 1	Reactor 2	Average	Reactor 1	Reactor 2	Average	Reactor 1	Reactor 2	Average
0	200000	200000	2.00E+05	200000	200000	2.00E+05	200000	200000	2.00E+05
24	290000	220000	2.55E+05	310000	290000	3.00E+05	390000	360000	3.75E+05
48	1600000	1300000	1.45E+06	2300000	2100000	2.20E+06	3000000	2800000	2.90E+06
72	4300000	4700000	4.50E+06	5100000	5000000	5.05E+06	5900000	5700000	5.80E+06
96	6800000	6200000	6.50E+06	4800000	4400000	4.60E+06	5000000	4800000	4.90E+06
120	5300000	5300000	5.30E+06	3900000	3600000	3.75E+06	4700000	4500000	4.60E+06

Table A6 (Continued)

Light intensity (µE)		236 µmol m-2 s-1			77 µmol m-2 s-1			38 µmol m-2 s-1			253 µmol m-2 s-1	
hours	Reactor 1	Reactor 2	Average	Reactor 1	Reactor 2	Average	Reactor 1	Reactor 2	Average	Reactor 1	Reactor 2	Average
0	200000	200000	2.00E+05	200000	200000	2.00E+05	200000	200000	2.00E+05	200000	200000	2.00E+05
24	300000	310000	3.05E+05	210000	230000	2.20E+05	210000	200000	2.05E+05	220000	220000	2.20E+05
48	2200000	2400000	2.30E+06	1100000	1300000	1.20E+06	700000	850000	7.75E+05	1200000	1400000	1.30E+06
72	4000000	4300000	4.15E+06	3500000	3900000	3.70E+06	1300000	1500000	1.40E+06	3300000	3500000	3.40E+06
96	4100000	4100000	4.10E+06	3900000	4000000	3.95E+06	3400000	3500000	3.45E+06	4500000	4700000	4.60E+06
120							3600000	3900000	3.75E+06	4900000	4900000	4.90E+06
144							4000000	3900000	3.95E+06	5200000	5100000	5.15E+06
168							4100000	3900000	4.00E+06	4900000	5100000	5.00E+06
192							3000000	3400000	3.20E+06	4400000	4800000	4.60E+06
216							2900000	3000000	2.95E+06	4300000	4500000	4.40E+06
240							2300000	2700000	2.50E+06	4300000	4400000	4.35E+06
264							1500000	1300000	1.40E+06			
288							1000000	1300000	1.15E+06			
312							900000	800000	8.50E+05			

A7. Alpha linolenic acid (µg/mg) produced at different photon flux density experiments

µmol m^{-2} s^{-1}	Phase	Reactor1	Reactor2	Mean	SD
38	Exponential	3.41	3.22	3.32	0.13
	Stationary	1.27	0.79	1.03	0.34
77	Exponential	4.10	7.72	5.91	2.56
	Stationary	6.15	5.14	5.64	0.71
115	Exponential	3.66	2.26	2.96	0.98
	Stationary	3.43	3.80	3.62	0.26
178	Exponential	5.28	5.92	5.60	0.45
	Stationary	5.03	5.76	5.39	0.52
210	Exponential	3.72	4.71	4.21	0.70
	Stationary	0.84	2.05	1.44	0.85
236	Exponential	10.11	7.18	8.64	2.07
	Stationary	3.60	4.56	4.08	0.68

A8. Omega 3 fatty acids (µg/mg) produced at different photon flux density experiments

µmol m^{-2} s^{-1}	Phases			Reactor1	Reactor2	Mean	SD	SE
38	Exponential	38	3	4.66	4.64	4.65	0.02	0.01
	Stationary		9	1.63	1.09	1.36	0.38	0.27
77	Exponential	77	5	6.49	11.90	9.19	3.83	2.71
	Stationary		6	9.39	7.45	8.42	1.37	0.97
115	Exponential	115	3	4.61	3.01	3.81	1.14	0.80
	Stationary		6	3.01	5.15	4.08	1.51	1.07
178	Exponential	178	3	7.86	8.90	8.38	0.74	0.52
	Stationary		6	7.50	8.55	8.03	0.74	0.53
210	Exponential	210	3	5.77	7.25	6.51	1.05	0.74
	Stationary		6	1.30	3.09	2.20	1.27	0.89
236	Exponential	236	3	15.06	11.08	13.07	2.81	1.99
	Stationary		5	5.31	6.76	6.04	1.02	0.72

A9. Polyunsaturated fatty acids (µg/mg) produced t at different photon flux density experiments

µmol m^{-2} s^{-1}	Phase			Reactor1	Reactor2	Mean	SD	SE
38	Exponential	38	3	11.40	11.80	11.60	0.28	0.20
	Stationary	38	9	4.90	3.50	4.20	0.99	0.70
77	Exponential	77	5	9.86	19.60	14.73	6.88	4.87
	Stationary	77	6	15.04	11.89	13.46	2.23	1.58
115	Exponential	115	3	9.38	6.23	7.80	2.23	1.58
	Stationary	115	6	8.17	9.06	8.62	0.63	0.45
178	Exponential	178	3	12.21	14.15	13.18	1.38	0.97
	Stationary	178	6	12.32	14.48	13.40	1.53	1.08
210	Exponential	210	3	8.84	11.18	10.01	1.65	1.17
	Stationary	210	6	2.68	6.04	4.36	2.38	1.68
236	Exponential	236	3	20.36	14.56	17.46	4.10	2.90
	Stationary	236	5	8.63	10.66	9.64	1.44	1.02

Percentage of saturated fatty acids produced by different strains										
FA	26-1F-A	18-1A	6-1B	5-1A	13-1C	11-1D	11-1C-1A	15-1B-1A	28-1A-1A	12-1D
14:0			1.3%							
16:0	14.9%	8.0%	20.6%	13.1%	13.0%	22.4%	21.8%	13.6%	14.3%	10.4%
17:0	0.7%		0.2%			1.4%	1.0%	0.7%	1.3%	0.7%
18:0	5.3%	2.0%	4.5%	1.2%	4.9%	5.3%	2.3%	2.0%	2.5%	3.0%
19:0	1.0%			1.2%				0.5%		
20:0		0.2%	0.7%		0.3%			5.0%	0.3%	0.4%
22:0	0.9%	0.4%	1.8%	5.7%						
24:0	4.3%	0.9%	2.7%	1.3%	4.7%	1.9%	1.6%	1.8%	3.1%	5.2%
Percentage of monounsaturated fatty acids produced by different strains										
17:1	5.9%	5.4%	4.7%	0.0%	3.8%	2.8%	8.9%	6.2%	8.1%	4.9%
18:1	18.2%	63.9%	21.8%	10.9%	16.6%	18.8%	25.6%	34.7%	24.8%	22.8%
20:1		0.1%	0.3%		0.4%			0.9%	0.5%	0.4%
Percentage of polyunsaturated fatty acids produced by different strains										
18:2 (n-6)	31.3%	1.6%	12.4%	18.2%	28.3%	18.4%	9.8%	16.2%	11.5%	29.5%
18:3 (n-3)	7.7%	12.9%	21.8%	31.2%	22.9%	11.0%	20.7%	11.4%	27.2%	17.6%
18:4 (n-3)	1.1%	0.1%		1.4%		5.1%	0.9%			
20:2(n-6)					1.5%			1.3%		
20:3 (n-3)	1.0%	0.2%	0.9%	0.0%	0.0%	0.0%	0.0%	2.1%	0.6%	0.6%
20:4 (n-6)		0.2%	0.7%							
22:3	2.0%	0.3%	1.9%	16.1%		2.3%	1.5%		1.0%	1.0%
21:5 n-3	0.8%				1.1%	1.7%			2.0%	
22:5 n-6	1.9%	1.1%					1.9%	0.6%		1.2%